e-ISSN:2602-2079

Volume 5
Issue 12
2021

JOURNAL of Surgery and Medicine

International Medical Journal

JOSAM

Journal of Surgery and Medicine

Journal Boards

Editor-in-Chief

Editors & Editorial Board

Subjects: Cardiology, Medical science

Language Editor

Subjects: Surgical Science, Medical Science

Advisory Board

Journal of Surgery and Medicine

LAST ISSUE

Volume: 5 - Issue: 12

YEAR: 2021

Research article

Research Article

1. The effect of platelet-rich plasma on chondrocyte healing in traumatic dislocation of the hip in a rat model

Toktamış SAVAŞ Orhan BUYUKBEBECİ Erman ÖĞÜMSÖĞÜTLÜ Ahmet Sarper BOZKURT Ömer ERONAT

Page: 1159-1163 PDF

Research Article

2. The effect of Ginkgo biloba EGb 761 on intestinal anastomotic healing in rats with ischemia-reperfusion induced in the lower extremities

Serdar BASİM Pelin BASİM Okan DEMİRAY

Page: 1164-1169 PDF

Research Article

3. Fragmented QRS and blood pressure pattern in normotensive individuals with a history of preeclampsia

Kemal GÖÇER Ekrem AKSU Ugurkan ERKAYIRAN

Page: 1170-1173 PDF

Research Article

4. YouTube as a source of information on the radiologic approach to COVID-19

Zeynep Nilüfer TEKİN Canan SATIR ÖZEL

Page: 1174-1178 PDF

Research Article

5. Maternal amylase, lipase, lactate dehydrogenase, creatine kinase levels at preterm delivery, and the effect of tocolysis

Simten GENÇ Melike EREN Sadık KÜKRER Arzu YURCİ Başak CINGILLIOĞLU Elif Dilasa KÖSE Orhan SAHIN Hicran ŞİRİNOĞLU Veli MİHMANLI

Page: 1179-1183 PDF

Research Article

6. Neck circumference - A simple and valid screening tool for obesity in school children

Sreelatha P R Chinchilu R V

Page: 1184-1187 PDF

Research Article

Download Cover Image

167 195 0

Archive

Volume: 5 Issue: 10

Volume: 5 Issue: 11

Volume: 5 Issue: 12

Volume: 6 Issue: 1

7. Radiologic and clinical features of infection related cytotoxic lesions of corpus callosum splenium in adults

Mehmet Ali İKİDAĞ

Page: 1188-1192 PDF

Research Article

8. Epidemiological factors associated with colorectal cancer in north-east India: A hospital-based descriptive cross-sectional study

Zothansanga RALTE Venu Gopala Reddy PALETİ Vimal KUMAR

Page: 1193-1197 PDF

Research Article

9. A comparison of the harmonic scalpel, coblation, bipolar, and cold knife tonsillectomy methods in adult patients

Buğra SUBAŞI Fatih OĞHAN Hamdi TAŞLI Nesibe Esra KARAMAN Seçkin AKBAL

Page: 1198-1201 PDF

Research Article

10. The predictive role of neutrophil-lymphocyte ratio, platelet lymphocyte ratio, and other complete blood count parameters in eclampsia and HELLP syndrome

Feyza BAYRAM Süleyman Serkan KARAŞİN

Page: 1202-1205 PDF

Research Article

11. Smartphones for evaluation of computerized tomography scan of patients with suspected skull fractures and intracranial hemorrhage in emergency medicine

Hasan ALDİNC Cem GUN

Page: 1206-1209 PDF

Research Article

12. The effect of Covid-19 pandemic on gastric cancer surgery

Nidal İFLAZOĞLU Ömer YALKIN

Page: 1210-1213 PDF

Review

Review

1. Acute and chronic invasive fungal sinusitis and imaging features: A review

Hacı Taner BULUT Ela KAPLAN Mahmut ÇORAPLI

Page: 1214-1217 PDF

Review

2. An overview about galectin-3 and its relationship with cardiovascular diseases

Lütfü AŞKIN Hüsna AŞKIN Okan TANRIVERDİ Ali Gökhan ÖZYILDIZ Şıho HİDAYET

Page: 1218-1220 PDF

Case report

Case Report

1. Closed reduction with external fixation and percutaneous screwing in talus neck fractures with severe soft tissue edema: A case report

Emre TEKŞAN Sercan KARADENİZ

Page: 1221-1223 PDF

Case Report

2. Phalloplasty – Sensate radial forearm free flap for creation of neourethra and neophallus in gender affirmation surgery: A case report

George TALİAT Kumaraswamy MOHAN KUMAR Arjun NAGARAJ

Page: 1224-1226 PDF

Case Report

3. Intravenous regional anesthesia (IVRA) with forearm tourniquet for short-term hand surgery: A case report

Huseyin GOCERGİL Elzem SEN Mehmet CESUR Ergun MENDES

Page: 1227-1229 PDF

Case Report

4. A rare cause of upper extremity deep venous thrombosis: Paget Schroetter syndrome

Fatih ERDEM Bahar KEYİK Bahadır ÇAĞLAR Süha SERİN Erdoğan BÜLBÜL

Page: 1230-1232 PDF

J Surg Med. 2021;5(12):1159-1163.
DOI: 10.28982/josam.1005052

Journal of Surgery and Medicine
e-ISSN=2602-2079

The effect of platelet-rich plasma on chondrocyte healing in traumatic dislocation of the hip in a rat model

Toktamış Savaş [1], Orhan Büyükbebeci [2], Erman Öğümsöğütlü [2], Ahmet Sarper Bozkurt [3], Ömer Eronat [4]

[1] Department of Orthopedics and Traumatology, Ceylanpinar State Hospital, Ceylanpinar, Sanliurfa, Turkey
[2] Department of Orthopedics and Traumatology, Gaziantep University Sahinbey Research and Practice Hospital, Gaziantep, Turkey
[3] Department of Physiology, Gaziantep University Medical Faculty, Institute of Health Science, Gaziantep, Turkey
[4] Department of Pathology, Gaziantep University Sahinbey Research and Practice Hospital, Gaziantep, Turkey

ORCID ID of the author(s)

TS: 0000-0003-2670-4738
OB: 0000-0001-9565-6739
EÖ: 0000-0002-1835-323X
ASB: 0000-0002-7293-0974
ÖE: 0000-0001-6768-9998

Corresponding Author
Toktamış Savaş
Ceylanpinar State Hospital Polyclinic of Orthopedics and Traumatology, Sanliurfa, Turkey
E-mail: toktamms@gmail.com

Ethics Committee Approval
The study was approved by the University of Gaziantep local ethics committee of animal experiments (Approval number: 2019/20), Turkey.
All institutional and national guidelines for the care and use of laboratory animals were followed.

Conflict of Interest
No conflict of interest was declared by the authors.

Financial Disclosure
The authors declared that this study has received no financial support.

Published
2021 November 28

Abstract

Background/Aim: Traumatic hip dislocations (THD) are orthopedic emergencies and significant complications such as cartilage degeneration can be reduced with early reduction. This study aimed to examine the effect of platelet-rich plasma (PRP) on cartilage cells in one-, two- or 8-hours prolonged hip dislocation.

Methods: We used 24 Sprague-Dawley rats in this study and divided them into three main groups based on whether their hips were in the protruding position for one, two, or eight hours. Each main group was further divided into two subgroups, with the right hips constituting the experimental group and the left hips, the control group. Traumatic hip dislocation modeling was performed surgically on both hips of the rats under anesthesia in the same session. After both dislocated joints were reduced and the hip capsules were sutured, platelet-rich plasma was administered to the right hips. After 1 week, all rats were sacrificed, their femoral heads were excised and subjected to histopathological examination. Terminal deoxynucleotidyl transferase-mediated dUTP nick-end labeling (TUNEL) testing was used to show chondrocyte apoptosis in the femoral head. The apoptotic index (AI) showing the ratio of cartilage cells to apoptosis was calculated histopathologically. A comparison of apoptotic indices was made between the groups.

Results: The AIs of the one-, two- and eight hours-long hip dislocation groups were 0.012 (0.005), 0.023 (0.011), 0.046 (0.012), respectively ($P<0.001$), while those of the control groups were 0.028 (0.010), 0.077 (0.015), 0.100 (0.016), respectively ($P<0.001$).

Conclusion: In traumatic hip dislocation known to cause chondrocyte apoptosis, PRP provides a significant reduction in the apoptotic index.

Keywords: Apoptosis, Cartilage, Traumatic joint dislocation, Apoptotic index, Platelet-rich plasma (PRP)

How to cite: Savaş T, Büyükbebeci O, Öğümsöğütlü E, Bozkurt AS, Eronat Ö. The effect of platelet-rich plasma on chondrocyte healing in traumatic dislocation of the hip in a rat model. J Surg Med. 2021;5(12):1159-1163.

Introduction

Traumatic hip dislocation (THD) leads to pathological sequelae due to both the mechanism of dislocation and the lack of necessary intervention. Conditions such as cartilage damage during trauma to the hip and malnutrition of the femoral head are beyond the control of the surgeon. Other factors, such as the timing and accuracy of the reduction, are positively influenced by the correct evaluation of dislocation as an emergency. Although complications can be reduced with early reduction, and good or excellent results can be seen, long-term complications after hip trauma, such as avascular necrosis (AVN), arthrosis, nerve injury, heterotopic ossification, and re-dislocation [1-4], are common.

PRP can be defined as an autologous platelet concentrate compacted into a small volume of plasma [5, 6]. There are cellular mitogens such as platelet-derived growth factor (PDGF), transforming growth factor-β (TGF-β), endothelial cell growth factor (ECGF), epidermal growth factor (EGF), vascular endothelial growth factor (VEGF), insulin-like growth factor (IGFs), and Interleukin-β in the α granules of the thrombocytes. Of these mitogens, IGF-1 is one of the major growth factors associated with cartilage matrix synthesis and cartilage repair. Type 2 collagen regulates the synthesis of proteoglycan and other matrix components [7]. Another growth factor TGF-β1, which is a subgroup of TGF-β, plays a role in bone morphogenic protein-2 (BMP-2) chondrocyte differentiation and matrix maturation. BMP-7, also known as osteogenic protein-1 (OP-1), stimulates type 2 and 4 collagen, aggrecan [ACAN: Cartilage specific proteoglycan core protein (CSPCP) or chondroitin sulfate proteoglycan 1], decorin, fibronectin, hyaluronate, etc., which are cartilage-specific extracellular proteins in chondrocytes [8, 9]. In the light of all these data, we planned our study hypothesizing that externally administered PRP will function as a stimulating factor and reduce chondrocyte apoptosis in chondrocytes with a physiologically low division capacity.

Materials and methods

The animals in this study were obtained from Gaziantep University Experimental Animals Research Center, where all operations except the preparation of specimens were performed.

Twenty-four male Sprague-Dawley rats, 20-24 weeks old and weighing 324-617 grams, were divided into three main groups and randomly assigned to cages in groups of eight, based on whether their hips were in the protruding position for one, two, or eight hours. Each main group was further divided into two subgroups, with the right hips constituting the experimental group and the left hips, the control group. All rats were numbered with ear tags. Both hips of the animals were surgically removed in the same session and reduced after remaining dislocated for the specified periods. Hip capsules were sutured. Thirty µl PRP and twenty µl of phosphate-buffered saline (PBS) were injected into the right capsule after suturing, and only 50 µl of PBS was injected into the left capsule with a Hamilton injector.

Anesthetic technique

After induction anesthesia with 5% isoflurane (Isoflurane-USP, Piramal Critical Care Inc.™, Bethlehem, Pennsylvania, USA), a 1-2% maintenance dose of inhaler anesthesia was administered during the operation with a mask. The respiratory rates and body temperatures of the animals were monitored during surgery. Depth of anesthesia was assessed by the toe pinch test.

PRP preparation technique

Approximately 1 ml of blood was drawn by cannulation from the preoperative right femoral vein of each rat to obtain PRP. The blood samples were placed into a tube containing 2 ml of trisodium citrate to prevent coagulation. PRP was obtained from the collected blood per the 2-stage centrifuge protocol [10].

Surgical technique

A posterior approach was used for access to both hip joints. After incising the skin bilaterally, subcutaneous tissues, and gluteal muscles were divided while protecting both sciatic nerves, and the hip capsule was revealed (Figure 1). Following capsulotomy performed parallel to the coronal plane of the acetabulum and division of *ligamentum teres*, the hip was dislocated posteriorly to prevent spontaneous reduction (Figure 2). Both knees were fixed in extension, and the hips were fixed in internal rotation and adduction to prevent spontaneous reduction. Care was taken to exclude the effects of mechanical trauma on the cartilage during hip dislocation (Figure 3). After hip capsule suturing, 30 µl PRP and 20 µl PBS were injected into the right capsule, and only 50 µl of PBS was injected into the left capsule with a Hamilton injector. The layers were closed properly. After 1 week, both femoral head samples were taken from the old incision line.

Figure 1: Right hip dissection image of the rat a: Marking the skin incision line with a surgical pen, b: Demonstration of the gluteus superficialis muscle, c: Division of the gluteus superficialis muscle, d: The space between piriformis and gluteus medius muscle, e: Demonstration of the sciatic nerve and piriformis after the division of this space

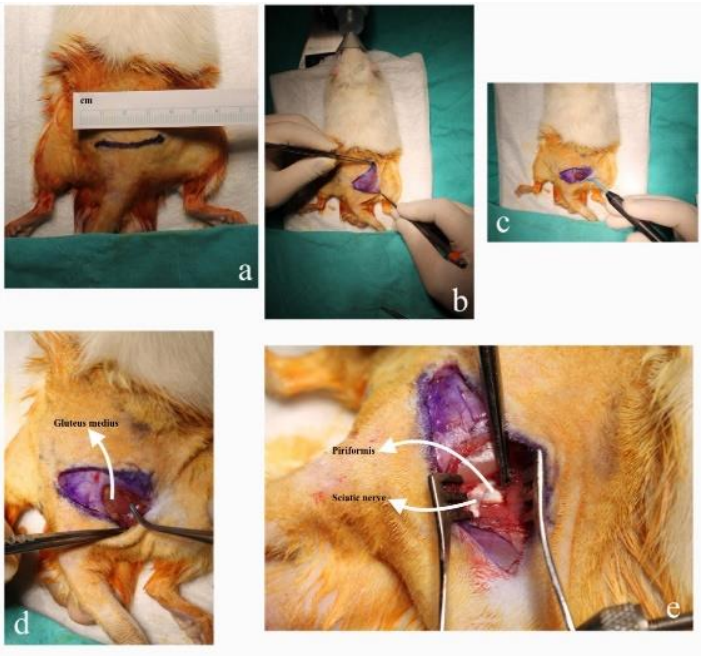

Figure 2: Dissection of rat femoroacetabular capsule. a: Hip capsule after dividing the insertion site of the piriformis muscle from the musculotendinous junction, b: Capsulotomy, c: Distraction of hip joint and demonstration of the femoral head, d: Demonstration of ligamentum teres

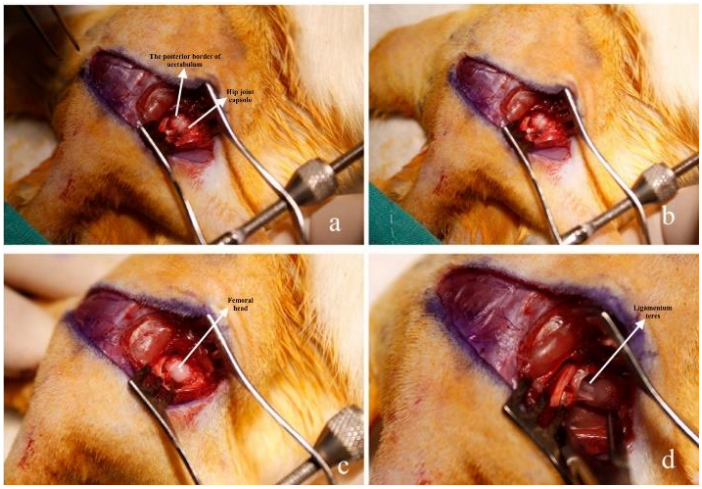

Figure 3: Demonstration of the hip dislocation. a: Right hip dislocated, b: Bilateral hip dislocated

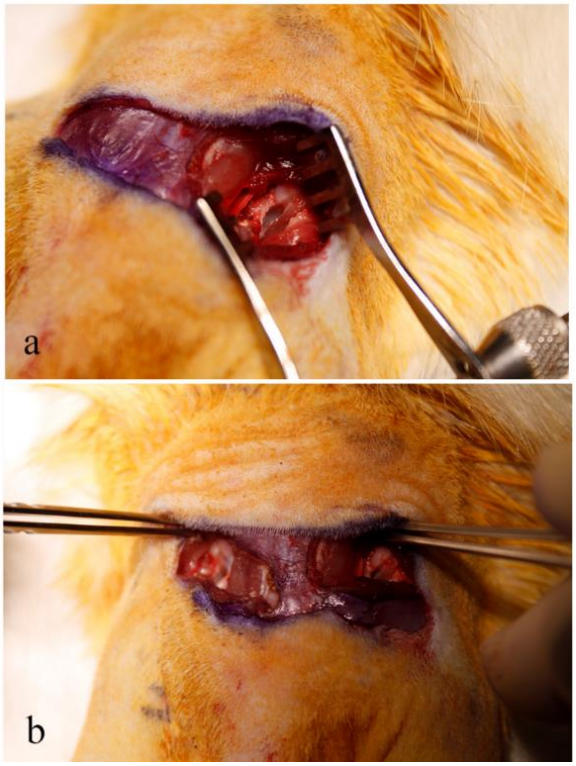

Preoperative and postoperative care

Standard room conditions were provided for all experimental animals, with 12 hours of dark and light cycles. The room temperature was kept between 18-20°C. To prevent hypothermia, the rats were operated under both a light source and a heater, and they were warmed up during recovery. In the postoperative period, the rats were followed up in single cages for 7 days and fed ad libitum.

Histopathological evaluation

The specimens were prepared in Gaziantep University, Department of Pathology.

After both femoral heads of each rat were stored in 10% buffered formaldehyde solution at 4 °C for 7-10 days, the samples were kept in 20% formic acid solution for 2-3 weeks at 4°C for decalcification. The decalcification solution was changed twice a week. The samples were then embedded in paraffin and blocked. The prepared paraffin blocks were sectioned with a 5µm-thickness and stained with hematoxylin-eosin. For the terminal deoxynucleotidyl transferase-mediated dUTP nick-end labeling (TUNEL) test**,** apoptosis was demonstrated with the TUNEL Chromogenic Apoptosis Detection Kit (ABP Biosciences ™, MD, USA, A049). Apoptosis was determined by observing the change in the nuclear chromatin nuclei (Figure 4). When calculating the apoptotic index (AI), the ratio of all chondrocytes to apoptotic cells at ×100 magnifications was considered, and 829-840 cells were counted for each section.

Figure 4: Chondrocytes undergoing apoptosis with TUNEL stain. There is an increased number of apoptotic nuclei in the 1-h and 8-h experimental groups compared with the control groups (All histopathological slides ×100 magnification). TUNEL, terminal deoxynucleotidyl transferase-mediated dUTP nick-end labeling

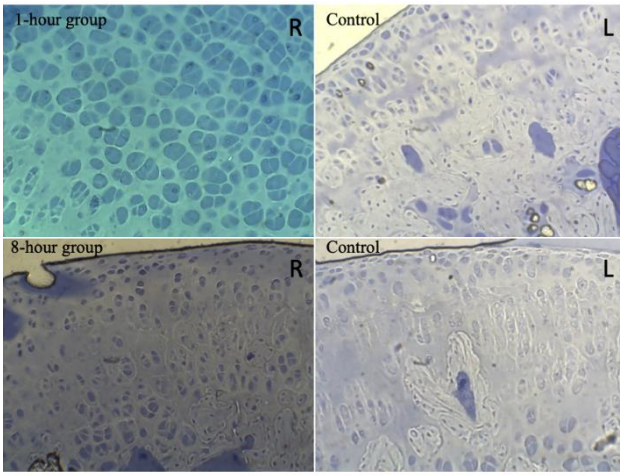

Statistical analysis

The compliance of the data to normal distribution was assessed with the Shapiro Wilk test, and one-way ANOVA-LSD multiple comparison tests were used to compare normally distributed variables in more than two independent groups. The paired t-test was used in the evaluation of normally distributed measurements at two different times. Pearson's correlation coefficient was used to test the relationships between numerical variables.

The minimum required number of animals in each group was five. Power analysis was performed using GPower version 3.1.

Results

In this study, only the cartilage tissues of the femoral heads, not the acetabular cartilages, were evaluated. The AIs of the one-, two- and eight hours-long hip dislocation groups were 0.012 (0.005), 0.023 (0.011), 0.046 (0.012), respectively (P<0.001), while those of the control groups were 0.028 (0.010), 0.077 (0.015), 0.100 (0.016), respectively (P<0.001) (Figure 5). The AIs of the experimental and control groups were similar in the 1-hour hip dislocation group (P=0.056), while those of the two- and eight-hour hip dislocation groups significantly differed (P<0.001 for both). There was no significant difference between the one- and two-hour hip dislocation experimental groups in terms of AI (P=0.066), but their control subgroups significantly differed (Table 1).

Table 1: Comparison between the experimental and control group in terms of AI and among themselves. AI, apoptotic index

	1-h group	2-h group	8-h group	*P*-value between main groups
Experimental group	0.01 (0.01)	0.02 (0.01)	0.05 (0.01)	0.001
Control group	0.03 (0.01)	0.08 (0.02)	0.1 (0.02)	0.001
P-value between subgroups	0.056	0.001	0.001	

Figure 5: Graph showing femoral head apoptotic indices between the experimental and control groups

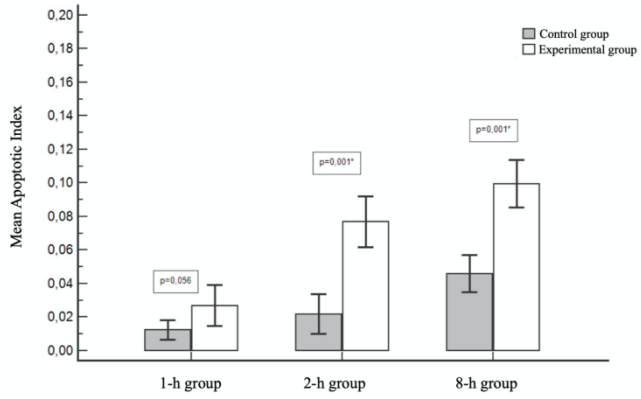

Discussion

THD may occur due to cartilage damage caused by mechanical action during dislocation and decreased blood flow in the vessels feeding the subchondral bone [11]. AVN of the femoral head develops because of damage to the vessels feeding the femoral head during dislocation [12]. In addition to all these pathophysiological reasons, the healing process in cartilage limits the classical healing response progressing with bleeding-dependent inflammation and repair due to the avascular structure of the tissue, [13] and progenitor cells in the blood cannot reach the damaged area due to the avascular structure of the cartilage tissue [14]. Apoptosis occurs in the chondrocytes of the femoral head due to the combination of various factors such as the limited number of cells in cartilage tissue and physiologically low division capacity (mitotic activity) of adult chondrocytes [14]. Consequently, the development of osteoarthritis of the hip joint, called coxarthrosis, becomes inevitable.

Chondrocyte apoptosis is clinically important as it occurs in humans and experimentally induced osteoarthritis [14-16] and it has been suggested that chondrocyte death may contribute to the pathogenesis of osteoarthritis [17]. Hashimoto et al. [17] showed that chondrocyte apoptosis increased in the osteoarthritic human joint cartilage, that it may occur even before osteoarthritis becomes evident, and may be related to the severity of cartilage deterioration.

PRP, used in patients with osteoarthritis due to degenerative or secondary reasons, gained increasing popularity in orthopedics [18]. We showed that prolonged dislocation of the joint caused the death of chondrocytes in the form of apoptosis and that PRP given after 1 hour in rats caused a significant decrease in AI and may reduce the long-term complications of concentric reduction.

Although clinical studies are stating that early reduction in hip dislocations should be performed within the first 12-24 hours [19-22], Hougaard et al. [23] and Jasulka et al. [24] stated that it should be performed within the first 6 hours. However, Dreinhofer et al. [3] showed that even if the hip reduction was achieved within the first 6 hours, AVN developed in the femoral head in the long term. In the animal study conducted by Elliot et al. [25], dislocation of the rat hip joint for more than 1 hour caused a significant increase in the apoptotic index. In our study, the apoptotic index significantly increased with the duration of dislocation in both the experimental and the control groups. The mean apoptotic index of the control groups in this study was between 0.04 and 0.12. The femoral head apoptotic index rates in other studies ranged from 0.01 to 0.23 [25-27]. D'Lima thought that this was related to the artifacts in the culture and cutting technique of the pathological specimens [26-28].

Many studies are conducted on PRP and there is no full consensus on this issue among the orthopedic community. Some studies argue that this treatment method does not affect diseases related to orthopedics [18], while others find it effective [29, 30]. In our study, only the experimental group of the 1-hour group did not show a statistically significant decrease compared to the control group. The experimental group of the other groups exhibited a significant reduction in AI ratios compared to the control group.

Limitations

The limitations of our study are the small number of subjects and the lack of a follow-up of long-term traumatic hip dislocation complications. We think that if the financial and ethical problems are overcome, there is a need for further, multicenter studies regarding the effect of platelet-rich plasma on the apoptotic index in humans, with more extensive case series which also evaluate the interobserver and intraobserver variability and reliability.

Conclusion

In the light of all these data, while early reduction is an indispensable treatment method in a patient admitted with THD, the dislocation of the rat hip joint for more than 1 hour significantly increases AI, and PRP application decreases joint degeneration provides a clinically significant improvement by decreasing AI. PRP is a glimmer of hope for the treatment of many diseases in orthopedics and traumatology, but only PRP should not be seen as a definite treatment method.

References

1. Armstrong JR. Traumatic dislocation of the hip joint; review of 101 dislocations. The Journal of bone and joint surgery British volume. 1948;30b(3):430-45.
2. DeLee JC. Fractures and dislocations of the hip. In: Rockwood CA, Bucholz RW, Green DP, Court-Brown CM, Heckman JD, Tornetta P, editors. Rockwood and Green's Fractures in Adults. Philadelphia, PA: Lippincott-Raven; 1996. p. 1756-803.
3. Dreinhofer KE, Schwarzkopf SR, Haas NP, Tscherne H. Isolated traumatic dislocation of the hip. Long-term results in 50 patients. The Journal of bone and joint surgery British volume. 1994;76(1):6-12.
4. Yang RS, Tsuang YH, Hang YS, Liu TK. Traumatic dislocation of the hip. Clinical orthopedics and related research. 1991(265):218-27.
5. Middleton KK, Barro V, Muller B, Terada S, Fu FH. Evaluation of the effects of platelet-rich plasma (PRP) therapy involved in the healing of sports-related soft tissue injuries. The Iowa orthopaedic journal. 2012;32:150-63.
6. Sunitha RV, Munirathnam NE. Platelet-rich fibrin: Evolution of a second-generation platelet concentrate. Indian Journal of Dental Research. 2008;19(1):42-6.
7. Loeser RF. Growth factor regulation of chondrocyte integrins. Differential effects of insulin-like growth factor 1 and transforming growth factor beta on alpha 1 beta 1 integrin expression and chondrocyte adhesion to type VI collagen. Arthritis and rheumatism. 1997;40(2):270-6.
8. Chubinskaya S, Malfait AM, Wimmer MA. Form and function of articular cartilage. In: O'Keefe RJ, editor. Orthopaedic basic science: foundations of clinical practice American Academy of Orthopaedic Surgeons. 4th ed ed. Rosemont, IL2013. p. 183-97.
9. Nishida Y, Knudson CB, Eger W, Kuettner KE, Knudson W. Osteogenic protein 1 stimulates cells-associated matrix assembly by normal human articular chondrocytes: up-regulation of hyaluronan synthase, CD44, and aggrecan. Arthritis and rheumatism. 2000;43(1):206-14.
10. Dhurat R, Sukesh M. Principles and Methods of Preparation of Platelet-Rich Plasma: A Review and Author's Perspective. Journal of cutaneous and aesthetic surgery. 2014;7(4):189-97.
11. Papavasiliou VA. The fate of articular cartilage in traumatic dislocation of the hip. Clinical orthopaedics and related research. 1982(171):287-9.
12. Mehlman CT, Hubbard GW, Crawford AH, Roy DR, Wall EJ. Traumatic hip dislocation in children. Long-term followup of 42 patients. Clinical orthopaedics and related research. 2000(376):68-79.
13. Colwell CW, Jr., D'Lima DD, Hoenecke HR, Fronek J, Pulido P, Morris BA, et al. In vivo changes after mechanical injury. Clinical orthopaedics and related research. 2001(391 Suppl):S116-23.
14. Lotz M, Hashimoto S, Kühn K. Mechanisms of chondrocyte apoptosis. Osteoarthritis Cartilage. 1999;7(4):389-91.
15. Hashimoto S, Takahashi K, Amiel D, Coutts RD, Lotz M. Chondrocyte apoptosis and nitric oxide production during experimentally induced osteoarthritis. Arthritis and rheumatism. 1998;41(7):1266-74.
16. Kourí JB, Aguilera JM, Reyes J, Lozoya KA, González S. Apoptotic chondrocytes from osteoarthrotic human articular cartilage and abnormal calcification of subchondral bone. J Rheumatol. 2000;27(4):1005-19.
17. Hashimoto S, Ochs RL, Komiya S, Lotz M. Linkage of chondrocyte apoptosis and cartilage degradation in human osteoarthritis. Arthritis and rheumatism. 1998;41(9):1632-8.

18. Guner S, Buyukbebeci O. Analyzing the effects of platelet gel on knee osteoarthritis in the rat model. Clin Appl Thromb Hemost. 2013;19(5):494-8.
19. Brav EA. Traumatic dislocation of the hip: army experience and results over a twelve-year period. J Bone Joint Surg Am. 1962;44(6):1115-34.
20. Epstein HC. Posterior fracture-dislocations of the hip; long-term follow-up. The Journal of bone and joint surgery American volume. 1974;56(6):1103-27.
21. Pietrafesa CA, Hoffman JR. Traumatic dislocation of the hip. Jama. 1983;249(24):3342-6.
22. Stewart MJ, McCarroll HR, Jr., Mulhollan JS. Fracture-dislocation of the hip. Acta orthopaedica Scandinavica. 1975;46(3):507-25.
23. Hougaard K, Thomsen PB. Traumatic posterior dislocation of the hip--prognostic factors influencing the incidence of avascular necrosis of the femoral head. Arch Orthop Trauma Surg. 1986;106(1):32-5.
24. Jaskulka RA, Fischer G, Fenzl G. Dislocation and fracture-dislocation of the hip. The Journal of bone and joint surgery British volume. 1991;73(3):465-9.
25. Elliott J, Ng de J, Tham SK. Chondrocyte apoptosis in response to dislocation of the hip in the rat model. ANZ journal of surgery. 2006;76(5):398-402.
26. D'Lima DD, Hashimoto S, Chen PC, Colwell CW, Jr., Lotz MK. Impact of mechanical trauma on matrix and cells. Clinical orthopaedics and related research. 2001(391 Suppl):S90-9.
27. D'Lima DD, Hashimoto S, Chen PC, Lotz MK, Colwell CW, Jr. Cartilage injury induces chondrocyte apoptosis. The Journal of bone and joint surgery American volume. 2001;83-A Suppl 2(Pt 1):19-21.
28. D'Lima DD, Hashimoto S, Chen PC, Lotz MK, Colwell CW, Jr. In vitro and in vivo models of cartilage injury. The Journal of bone and joint surgery American volume. 2001;83-A Suppl 2(Pt 1):22-4.
29. Kon E, Mandelbaum B, Buda R, Filardo G, Delcogliano M, Timoncini A, et al. Platelet-rich plasma intra-articular injection versus hyaluronic acid viscosupplementation as treatments for cartilage pathology: from early degeneration to osteoarthritis. Arthroscopy. 2011;27(11):1490-501.
30. Peerbooms JC, Sluimer J, Bruijn DJ, Gosens T. Positive effect of an autologous platelet concentrate in lateral epicondylitis in a double-blind randomized controlled trial: platelet-rich plasma versus corticosteroid injection with a 1-year follow-up. Am J Sports Med. 2010;38(2):255-62.

This paper has been checked for language accuracy by JOSAM editors.
The National Library of Medicine (NLM) citation style guide has been used in this paper.

J Surg Med. 2021;5(12):1164-1169.
DOI: 10.28982/josam.890700

Journal of Surgery and Medicine
e-ISSN=2602-2079

The effect of *Ginkgo biloba* EGb 761 on intestinal anastomotic healing in rats with ischemia-reperfusion induced in the lower extremities

Serdar Basım [1], Pelin Basım [2], Okan Demiray [3]

[1] Department of General Surgery, Başakşehir State Hospital, Istanbul, Turkey
[2] Department of General Surgery, Medical Faculty, Istanbul Medipol University, Istanbul, Turkey
[3] Department of General Surgery, Gaziosmanpaşa Taksim Training and Research Hospital, Istanbul, Turkey

ORCID ID of the author(s)

SB: 0000-0002-3072-9260
PB: 0000-0002-9452-9276
OD: 0000-0001-6920-7585

Corresponding Author
Pelin Basım
Medipol Universitesi Tip Fakultesi Genel Cerrahi Ana Bilim Dali. TEM Avrupa Otoyolu Goztepe Cikisi No: 1 Bagcilar/İstanbul, Turkey
E-mail: pelinakbaba@gmail.com

Ethics Committee Approval
Ethical approval was obtained from the Local Ethics Committee of the Turkish Ministry of Health Haydarpaşa Research and Teaching Hospital (date: 26.08.2004 number: 840098-604.01.01-E.3767)

Conflict of Interest
No conflict of interest was declared by the authors.

Financial Disclosure
The authors declared that this study has received no financial support.

Published
2021 December 15

Abstract

Background/Aim: Remote ischemia-reperfusion (I-R) injury for anastomotic healing is a newly identified risk factor and there is a wide array of studies being conducted. This study aimed to reveal the negative effects of lower I-R on the colonic anastomotic healing process and examine the effects of *Ginkgo biloba* EGb 761 treatment, a platelet activating factor (PAF) antagonist, on anastomotic healing through the inhibition of pathological mechanisms of mediators causing these negative effects.

Methods: Thirty-six Wistar-Albino rats were divided into sham, I-R and I-R+EGb 761 groups, each consisting of 12 rats. In the subjects in the sham group, an end-to-end anastomosis was performed by transecting the descending colon following midline laparotomy. In the I-R group, unilateral lower extremity ischemia was created by occluding the femoral artery and collaterals using a tourniquet from the most proximal segment of the left extremity. Then, the descending colon was transected, anastomosis was performed, and reperfusion was created by a tourniquet application at the 30th minute of ischemia. Different from the I-R (control) group, the subjects in the I-R+EGb 761 group were given two equal doses of 64 mg/kg/d *Ginkgo biloba* EGb 761 by the orogastric route until 10 days after surgery. After all subjects were sacrificed on the 10th day of surgery, the descending colon segment containing the anastomosis area was resected and samples were taken for bursting pressure and hydroxyproline measurements.

Results: In the I-R group, anastomotic bursting pressure and perianastomotic hydroxyproline values were significantly lower compared to the sham group and the I-R+EGb 761 group. However, there was no statistically significant difference in these parameters between the sham and the I-R+EGb 761 groups.

Conclusion: Colonic anastomotic bursting pressure and peri-anastomotic hydroxyproline values in the sham group were significantly decreased by lower extremity I-R, and this change was prevented with the use of EGb 761.

Keywords: Remote ischemia-reperfusion, Ginkgo biloba EGb 761, PAF antagonist

How to cite: Basım S, Basım P, Demiray O. Effect of Ginkgo biloba EGb 761 on intestinal anastomotic healing in rats with ischemia-reperfusion induced in the lower extremities. J Surg Med. 2021;5(12):1164-1169.

Introduction

Among the factors responsible for mortality and morbidity after gastrointestinal system surgery, anastomotic leaks have a leading role [1, 2]. A successful anastomotic healing process depends on many factors. Intestinal anastomoses should be performed to healthy bowel ends, without tension, with appropriate suture materials and technique, causing minimal tissue damage, clear of contaminated material, fibrin, etc., and should be reinforced with a serosal patch or omentum, when necessary. There should be no distal obstruction and the patient should be nutritionally prepared to decrease post-operative anastomotic complications. Blood supply and oxygenation of anastomosis are the most important factors for successful anastomotic healing. Although the negative effects of tissue ischemia on wound healing are well known, the role of reperfusion in anastomotic healing has not yet been explained in detail [2].

When a tissue in an organism undergoes ischemia, a series of chemical events occur, leading to cellular dysfunction and necrosis. It is especially important to ensure the blood supply in ischemic tissues to provide sufficient energy for the cell and remove toxic metabolites. Reperfusion is the reorganization of blood flow to the tissue by eliminating the factor causing ischemia. Reperfusion has two positive effects on ischemic tissue: Meeting the energy needs and removing toxic metabolites [2-4].

However, this 'inevitable re-flow' (reperfusion) phenomenon paradoxically triggers a series of metabolic events that cause further damage to tissues [2,4-5]. Reperfusion injury occurs through a complex mechanism accompanied by free oxygen radicals, endothelial factors, and neutrophils. The release of many vasoactive mediators, cytokines, endothelin, and free toxic oxygen radicals leads to leukocyte activation, endothelial dysfunction, and tissue edema in the reperfused tissue. The cardiovascular and pulmonary systems are also affected after ischemia-reperfusion (I-R). All these factors can disrupt anastomotic perfusion, and the released mediators can cause adverse effects around the anastomosis [2, 6-8].

Although many mediators have been defined in intestinal and distal organ dysfunction related to I-R, it is known that platelet activating factor (PAF) and free toxic oxygen radicals play a particularly important role in this process [3, 5, 9]. Many experimental studies have shown that *Ginkgo biloba* extract EGb 761 and other PAF antagonists can reduce or even prevent a possible injury in local and remote organ systems due to intestinal I-R [5-7, 9-12]. As a *Ginkgo biloba* extract, EGb 761, prepared in a form suitable for experimental use, is a PAF antagonist with strong effects that scavenges toxic free radical activity [13]. While providing vascular relaxation, it prevents platelet aggregation and stabilizes lysosomal membranes. This extract is used for therapeutic purposes in many ischemic events, including cerebrovascular and peripheral vascular insufficiency. EGb 761 has different effect potentials in different organs and systems and exhibits protective effects in neurodegenerative, sensory and vascular diseases [13, 14]. This molecule, which can act systemically at molecular, cellular, and textural levels or in the whole organism, has no particular one-way (activator or inhibitory) effect; rather, it is a regulatory compound that helps the adaptation of an organism to the current environment [10, 13, 15].

Considering the positive effects of EGb 761 on various pathophysiological mechanisms in remote organ I-R injury, the current study aimed to analyze the effects of this compound on intestinal anastomosis healing in rats with I-R injury induced in the lower extremity.

Materials and methods

Materials

Ethics approval was obtained from the Local Ethics Committee of the Turkish Ministry of Health Haydarpaşa Research and Teaching Hospital (date: 26.08.2004 number: 840098-604.01.01-E.3767), and the study was conducted at the Experimental Research Center (TADEM) of Taksim Training and Research Hospital between January 2005 and June 2005. Thirty-six male Wistar-Albino rats, weighing between 250-300 grams, raised in the Experimental Animal Production and Research Laboratory of Taksim Training and Research Hospital were used. The rats were housed in appropriate cages in the animal laboratory at a temperature of 22 ± 2 °C, a humidity of 50-60% and under 12 hours of light and dark cycles by turning the lights on at 8 a.m. and turning them off at 8 p.m. The rats were fed a standard commercial pellet diet and provided tap water. All rats were handled according to the 'Care Principles of Experimental Animals' specified by the National Association of Medical Research and the 'Guidelines for the Care and Use of Laboratory Animals' revised by the Institute of Laboratory Animal Resources.

Ginkgo biloba extract EGb 761 (Tebokan® Fort Damla) was purchased from Abdi İbrahim Pharmaceuticals and kept under suitable conditions. Biochemical measurements were performed at the Biochemistry Clinic of Taksim Training and Research Hospital. Surgical instruments of the hospital were used after completing routine sterilization procedures. Intestinal samples were stored at -20°C in a deep freezer until biochemical evaluations.

Methods

All rats used in the study were kept in the same laboratory environment for a week before the experiment. They were fed standard laboratory diet and water. The rats to be operated were fasted with only water intake on the night before surgery.

For anesthesia, following ether induction, 65 mg/kg sodium pentothal (Pental® 1gr, İbrahim Etem Ulagay Pharmaceuticals, İstanbul, Turkey) was intraperitoneally administered. One-third of this dose was repeated intramuscularly when necessary. The surgery and injections were performed under general anesthesia. During the anesthesia, the subjects were monitored under room air conditions without the need for respiratory support. Surgery was performed under a heating lamp in order to prevent hypothermia that may develop during the experiment.

Care was taken to perform standard surgical procedures and follow sterilization rules. To perform the surgical procedure under ideal conditions, fixing boards were used. All surgical procedures were performed with a loop. Laparotomies were

performed with a 3.5-4 cm midline incision after the abdominal skin was shaved, cleaned, and covered with povidone iodine. To reduce heat loss from the tissues, the intestines were covered with gauze pads soaked in warm and sterile saline. Five milliliters of Ringer's lactate were subcutaneously administered to all subjects following the surgical procedure to prevent dehydration.

Experimental models

Sham model: No procedure was performed to cause ischemia in this group, and it was taken as the basis for pathological evaluations and bursting pressure. Colon anastomosis was performed following a 4 cm midline incision after anesthesia induction to create the control group model.

I-R model: To create the remote I-R model, after anesthesia induction, unilateral lower extremity ischemia (LEI) was created by compressing the femoral artery and collaterals with a tourniquet from the upper third of the left thigh. The lack of distal pulses and pale leg color indicated ischemia. Following an ischemia period of 20 minutes, a full-thickness incision and anastomosis were made on the descending colon with a 3.5-4 cm midline incision. At the end of the 30th minute, the tourniquet compressing the femoral artery was loosened and reperfusion was achieved. The return of leg color to normal and the ability to record distal pulses with a manual Doppler device were considered reperfusion.

Bowel anastomosis model: Following a midline laparotomy, the descending colon was prepared and cut, and anastomosis was performed with 6/0 propylene (Prolene, Ethicon UK®) over a single layer using an average of 8-10 sutures over one layer. The abdomen was covered with 3/0 silk material over two layers.

Experimental groups

A total of 36 subjects were included in the study and divided into three groups of 12 rats each.

Group 1 (Sham group): In this group, anastomotic healing was investigated without an ischemia model. Intestinal anastomosis was performed and the abdomen was closed after laparotomy.

Group 2 (I-R group): In this group, the effects of remote I-R injury on anastomotic healing were investigated. LEI was induced with a tourniquet, and intestinal anastomosis was performed following laparotomy. After the 30-minute ischemia period, reperfusion was created by loosening the tourniquet.

Group 3 (I-R + EGb 761 group): In this group, the effects of *Ginkgo biloba* EGb 761 on anastomosis healing were investigated. Different from the I-R group, this group was administered two equal doses of 64 mg/kg/d *Ginkgo biloba* EGb 761 through the orogastric route until 10 days after surgery.

In all three groups, on the 10th day of surgery, laparotomy was performed again and the colon segment covering the anastomosis area was resected for bursting pressure measurements and biochemical examinations (hydroxyproline level). Subsequently, the subjects were sacrificed.

Sampling

In all groups, 10 days after the operation, the descending colon segment that was anastomosed was identified by a re-laparotomy after ether induction. A large segment of the colon including the anastomosis line was resected without damaging the anastomotic line, preserving the surrounding adhesions. Feces in the colon segment was cleared by administering physiological saline from the proximal end. Subsequently, the removed segment was cut at 2 cm proximal and distal of the anastomotic line to obtain a standard bowel length for bursting pressure measurements and biochemical examinations (hydroxyproline level).

Measurements

Anastomotic bursting pressure measurements were performed with the modification of a technique previously described in the literature in detail [2]. Accordingly, an 18-F plastic catheter was placed at the proximal end of the anastomosis line and tied over the catheter with 2/0 silk, ensuring no leakage. At the distal end, it was tied with 2/0 silk sutures so that the fluid would not leak. The catheter placed at the proximal end was connected to the infusion pump (Abbott Lifecare 5000®) set to deliver 2 ml of fluid per minute via a three-way tap. Another catheter placed in the three-way tap was connected to the mercury manometer instrument. In all subjects, bursting pressures were recorded in mmHg by observing fluid leakage from the anastomotic line or pressure drop on the manometer. The measurement of hydroxyproline was carried out in the biochemistry laboratory of Taksim Education and Research Hospital using a model based on the principle of the hydrolysis of this substance from collagen, its oxidization with chloramine T, and then the reaction with the Erlich reagent to form colored chromophore compounds.

Statistical analysis

Data were analyzed using the IBM-SPSS for Windows version 20.0 software package (IBM Corp., Armonk, NY, USA). The mean bursting pressures and tissue hydroxyproline concentrations of the corresponding groups were calculated and expressed as median (SD) (Figure 1 and Figure 2). One-way analysis of variance (ANOVA) and Tukey's multiple comparison test were used for the statistical analysis of the results. $P<0.05$ was considered significant.

Figure 1: Comparison of anastomotic bursting pressure between the groups

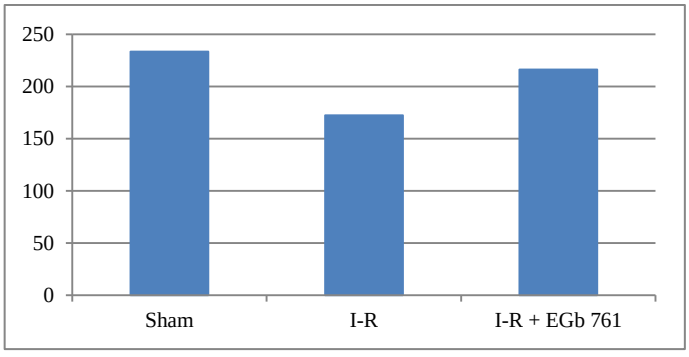

Figure 2: Comparison of anastomotic hydroxyproline level between the groups

Results

The bursting pressures and hydroxyproline levels of the materials obtained from the subjects are shown in Table 1. The one-way ANOVA was performed for both parameters. A statistically significant difference was found between the three groups (P<0.001). Tukey's multiple comparison test was conducted to determine which group caused the significant difference.

Table 1: Bursting pressures (mm HG) and hydroxyproline (µmol/g) levels of the groups

Subject number	Sham group		I-R group		I-R + EGb 761 group	
	HP	BP	HP	BP	HP	BP
1	5.56	240	4.18	132	5.34	194
2	6.11	280	4.67	192	5.22	200
3	6.47	210	4.56	108	5.89	300
4	6.91	260	3.78	168	5.56	232
5	6.23	198	4.89	140	6.45	262
6	5.11	190	4.18	240	6.89	248
7	6.78	190	4.33	110	6.23	220
8	6.34	300	5.11	236	5.56	194
9	6.56	240	3.56	182	5.34	206
10	7.56	222	3.80	152	7.34	168
11	5.89	200	4.16	202	5.34	180
12	7.34	270	4.22	206	5.40	190

I-R: ischemia-reperfusion, HP: hydroxyproline, BP: bursting pressure

The mean anastomotic bursting pressures of the three groups are shown in Table 2, and their mean anastomotic hydroxyproline levels are given in Table 3. According to the results of ANOVA and Tukey's multiple comparison test in the intergroup evaluations of anastomotic bursting pressures, there was a significant difference between the sham group and the I-R group and between the I-R group and the I-R + EGb 761 group (P<0.001 and P<0.01 respectively) while no statistically significant difference was observed between the sham group and the I-R + EGB 761 group in terms of bursting pressure (P>0.05). Similarly, the statistical analysis of the hydroxyproline level measurements performed in the samples taken from the anastomosis line revealed was a statistically significant difference between the sham group and the I-R group and between the I-R group and the I-R + EGb 761 group (P<0.001 and P<0.01, respectively); however, the values of the sham group and the I-R + EGb 761 group were similar (P>0.05).

Table 2: Mean values of anastomotic bursting pressure

Groups	Median (SD) mm Hg	*P*-value
Sham	233.333 (37.60)	<0.001
I-R	172.333 (44.97)	
I-R+ EGb 761	216.166 (38.21)	

I-R: ischemia-reperfusion

Table 3: Mean values of anastomotic hydroxyproline levels

Groups	Median (SD) µmol/g
Sham	6.405 (0.70)
I-R	4.28 (0.46)
I-R + EGb 761	5.88 (0.69)

I-R: ischemia-reperfusion

In light of these values, it was concluded that the anastomotic bursting pressure and anastomotic line hydroxyproline level values showed significant changes due to the I-R process, but they returned to normal with the use of EGb 761.

Discussion

LEI is an arterial pathology which can present with acute and chronic forms, both with high morbidity. Acute LEI, which is less common, continues to be one of the major circulatory disorders of the arterial system despite the progress in diagnostic and therapeutic modalities, and maintains its importance in clinical practice with its high morbidity and mortality rates [2]. Cardiac arrhythmias, advanced age, low cardiac output, severe heart valve diseases, recent myocardial infarction, and cardiac surgery are clinically defined risk factors for LEI [15]. In LEI, the contemporary approach aimed at reducing mortality is the continuation of aggressive diagnosis and treatment protocols [17].

The duration of ischemia directly affects the prognosis of the patient; therefore, early diagnosis and treatment are vital. However, the resulting injury is of biphasic nature and has an important share in reperfusion, as well as ischemia [2, 15, 18]. Parks and Granger showed that in the I-R process, the intestinal mucosa was damaged less in the ischemic period, and most of the injury actually occurred in the reperfusion period [19]. In addition, the idea that reperfusion is responsible for the injury seen in the intestinal models of I-R was supported by the significant reduction in mucosal damage with agents administered before ischemia [3, 5]. Especially after acute LEI, the sudden reversal of blood supply paradoxically results in systemic complications and unexpected mortality [20, 21]. It is assumed that lower extremity I-R (LEI-R) causes damage to the intestinal mucosa and permeability disorders through various mediators [22]. Although it is predicted that ischemic injury can be reduced with early diagnosis, reperfusion injury and its consequences are still inevitable in this approach. Therefore, molecular studies to prevent injury caused by reperfusion, regardless of local or remote ischemia, remain popular and are conducted extensively.

LEI-R causes dysfunction in various organs, such as the liver, lung, and cardiovascular and hematopoietic systems [23]. Pulmonary injury is characterized by the accumulation of neutrophils in the lung tissue as a result of increased microvascular permeability and the activation of agents released from the tissue exposed to I-R. Some of the systemic consequences of LEI occur through neural pathways. Although the underlying mechanism is not yet fully known, metabolites such as PAF, bradykinin, lactic acid, and prostaglandins promote a cardiovascular response and stimulate abdominal sensory nerves. In two similar studies conducted on the I-R injuries of different organs, Grace [3] and Stammberger et al. [23] mentioned that reactive oxygen metabolites, especially hydrogen peroxide and hydroxyl radicals, activated abdominal visceral C fibers, and thus affected systemic vascular tone.

In addition to LEI due to acute embolization, procedures such as kidney transplantation and less frequently liver transplantation, aortic surgery, and traumatic vascular surgery may provide a basis for the development of LEI in clinical surgery practice. In all these clinical situations, especially in the presence of traumatic LEI and multiorgan injury, intestinal anastomoses may be required if there is intestinal injury in the abdomen. There are many studies in the literature suggesting that in such cases, systemic and local injury caused by I-R have negative effects on anastomotic perfusion and the released mediators increase anastomotic complications by causing adverse effects around the anastomosis. Therefore, researchers aim to examine anastomotic healing during the reperfusion period and compare the injury caused by the severity of the

systemic effect with that which occurs during reperfusion [2, 15, 24].

In their consecutive studies, Kologlu et al. [20, 25] investigated the effects of remote organ ischemia on colonic anastomosis and found that the group exposed to LEI-R had a significant decrease in bursting pressure and mean tissue hydroxyproline level compared to the control group. Similarly, the authors showed the negative effects of 60-minute segmental small intestine I-R, unilateral lower extremity reperfusion, and renal I-R on healing in anastomoses in the right colon. In light of all these data, it can be stated that I-R injury is a systemic phenomenon, and remote I-R has a significant negative effect on intestinal anastomotic healing.

LEI-R injury is difficult to examine in clinical settings; therefore, animal models are used in studies. However, the selected model and the depth and duration of ischemia are particularly important for evaluating the results. The prevention of reperfusion injury will also not be meaningful in the absence of a sufficiently deep ischemia. In our rat model, we induced deep LEI over 30 minutes and investigated the effects of reperfusion following ischemia on the anastomotic healing process based on bursting pressure and hydroxyproline level, which are defined as the two most important parameters indicating anastomotic healing in the literature. The anastomotic bursting pressure and hydroxyproline levels being significantly lower in the I-R group compared to the sham group suggests that LEI-R negatively affected the anastomotic healing process, which supports the literature data.

There are experimental studies in the literature to prevent remote organ injury caused by LEI-R. Although various pharmacological agents can be used in animal experiments to reverse the injury caused by free oxygen radicals, most are not applicable in clinical practice. PAF is one of the most effective proinflammatory agents released in I-R, and it is known to play an important role in I-R-related intestinal dysfunction and remote organ dysfunction. In pharmacological strategies to prevent I-R injury, considering these effects of PAF, many studies have shown that different PAF antagonists can be used to partially eliminate pathophysiological mechanisms that play a role in I-R-related local and remote organ injury. Wehrens et al. [16] and Ateş et al. [18] showed that the increase in PAF levels after intestinal I-R and the resulting leukocyte adhesion and extravasation can be prevented by PAF antagonists. Similarly, in a study conducted with lexipafant, a PAF antagonist, the rats exposed to intestinal I-R were found to have significantly increased mucosal endothelial and epithelial permeability, improvement in mucosal barrier function, and decreased bacterial translocation rates after lexipafant treatment [9].

In addition to PAF antagonists mentioned above, *Ginkgo biloba* extract EGb 761, a new PAF antagonist with vascular relaxation properties and free radical scavenging effects, has also been used in some I-R models. EGb 761 has the effect of reducing mucosal injury associated with small bowel ischemia. The use of EGb 761 in rats where I-R was formed by the occlusion of the superior mesenteric artery was reported to reduce mucosal injury and significantly increase free oxygen radical levels in the intestinal mucosa compared to the control group [10]. At the same time, through the effects of the downregulation of TLR4/NF-κB and inhibition of inflammatory response, EGb 761 was shown to reduce the rate of ventricular fibrillation, the most common cause of sudden cardiac death due to myocardial I-R [26].

In light of the literature data, we further investigated EGB 761, which has the potential to prevent or regress various pathophysiological mechanisms through its role in I-R injury, in terms of its effects on anastomotic healing.

Limitations

The most important strength of this study is that it is the first and most comprehensive study on the remote effects of lower I-R on intestinal anastomotic healing conducted in an animal model, offering an alternative comparable treatment modality. The sole and only limitation of the study is that the subjects of the study population have not been assessed about an already present ischemic pathology in their lower extremities. However, there is a need for further studies on this subject, including other remote I-R models of various organs or systems of human anatomy.

Conclusions

We evaluated changes in anastomotic healing based on bursting pressure and perianastomotic hydroxyproline level measurements to determine the strength of colonic anastomosis. When the results were evaluated, anastomotic bursting pressure and hydroxyproline values were significantly lower in the LEI-R-induced rats compared to the other groups. In the group in which EGb 761 was used, there was a significant improvement, reversing the negative effects of I-R injury. In brief, bursting pressure and hydroxyproline values in the sham group significantly decreased with I-R, and returned to normal with the use of EGb 761. These results were attributed to the effects of the ability of EGb 761 to partially recover intestinal, cardiovascular and pulmonary injury by preventing endothelial and epithelial injury caused by I-R. Based on these findings, we consider that EGb 761 may become a treatment modality in anastomotic healing, especially in cases negatively affected by remote I-R in the presence of multitrauma, which is difficult to treat and has its paradoxical course.

References

1. Dietz UA, Debus E-S. Intestinal anastomoses prior to 1882; a legacy of ingenuity, persistence, and research form a foundation for modern gastrointestinal surgery. World J Surg. 2005;29:396-401.
2. Kuzu MA, Köksoy C, Kale IT, Tanik A, Terzi C, Elhan AH. Reperfusion injury delays healing of intestinal anastomosis in a rat. Am J Surg. 1998;176:348-51.
3. Grace PA. Ischaemia-reperfusion injury. Br J Surg. 1994;81:637-47.
4. Kartal H, Büyük B. Effects of alpha-lipoic acid on skeletal muscle ischemia-reperfusion injury in mice. J Surg Med. 2020; 4(7): 567-572.
5. Zimmerman BJ, Granger DN. Reperfusion injury. Surg Clin North Am. 1992;72:65-83.
6. Souza DG, Cara DC, Cassali GD, Coutinho SF, Silveira MR, Andrade SP, et al. Effects of the PAF receptor antagonist UK74505 on local and remote reperfusion injuries following ischaemia of the superior mesenteric artery in the rat. Br J Pharmacol. 2000;131:1800-8.
7. Carter MB, Wilson MA, Wead WB, Garrison RN. Platelet-activating factor mediates pulmonary macromolecular leak following intestinal ischemia-reperfusion. J Surg Res. 1996;60:403-8.
8. Börjesson A, Wang X, Sun Z, Inghammar M, Truedsson L, Andersson R. Early treatment with lexipafant, a platelet-activating factor-receptor antagonist, is not sufficient to prevent pulmonary endothelial damage after intestinal ischaemia and reperfusion in rats. Dig Liver Dis. 2002;34:190-6.
9. Sun Z, Wang X, Deng X, Lasson A, Soltesz V, Börjesson A, et al. Beneficial effects of lexipafant, a PAF antagonist on gut barrier dysfunction caused by intestinal ischemia and reperfusion in rats. Dig Surg. 2000;17:57-65.
10. Pehlivan M, Dalbeler Y, Hazinedaroglu S, Arikan Y, Erkek AB, Günal O, et al. An assessment of the effect of Ginkgo Biloba EGb 761 on ischemia reperfusion injury of intestine. Hepatogastroenterology. 2002;49:201-4.
11. Noel AA, Hobson RW 2nd, Durán WN. Platelet-activating factor and nitric oxide mediate microvascular permeability in ischemia-reperfusion injury. Microvasc Res. 1996;52:210-20.
12. Louajri A, Harraga S, Godot V, Toubin G, Kantelip JP, Magnin P. The effect of ginkgo biloba extract on free radical production in hypoxic rats. Biol Pharm Bull. 2001;24:710-2.
13. Schutte A, Topp SA, Knoefel WT, Brilloff S, Mueller L, Rogiers X, et al. Influence of Ginkgo Biloba extract (EGB 761) on expression of EGR-1 mRNA and HSP-70 mRNA after warm ischemia in the rat liver. Transplant Proc. 2001;33:3724-5.
14. Christen Y, Maixent JM. What is Ginkgo biloba extract EGb 761? An overview--from molecular biology to clinical medicine. Cell Mol Biol (Noisy-le-grand). 2002;48:601-11.

15. Kecskeméti V, Balogh I. The role of platelet-activating factor (PAF) antagonists and nitric oxide in cardiac actions of PAF. Electrophysiological and morphological study. J Physiol Pharmacol. 2000;51:723-35.
16. Kohlman-Trigoboff D, Gongora E, Stanford J, Smith BM. Risk factors associated with acute lower extremity ischemia after coronary revascularization. J Vasc Nurs. 2002;20:78-83.
17. Wehrens XH, Rouwet EV, oude Egbrink MG, Slaaf DW, Ramsay G. Effects of experimental lower-limb ischaemia-reperfusion injury on the mesenteric microcirculation. Br J Surg. 2002;89:185-91.
18. Ateş M, Köksal MH, Celayir MF, Baykan A. Prophylactic and therapeutic effect of ginko biloba extract (Egb761) on mortality of intestinal deep ischemia-reperfusion model in rats. Dicle Medical Journal. 2010;37:199-203.
19. Parks DA, Granger DN. Contributions of ischemia and reperfusion to mucosal lesion formation. Am J Physiol. 1986;250:G749-53.
20. Kologlu M, Yorganci K, Renda N, Sayek I. Effect of local and remote ischemia-reperfusion injury on healing of colonic anastomoses. Surgery. 2000;128:99-104.
21. Mansour Z, Charles AL, Kindo M, Pottecher J, Chamaraux-Tran TN, Lejay A, et al. Remote effects of lower limb ischemia-reperfusion: impaired lung, unchanged liver, and stimulated kidney oxidative capacities. Biomed Res Int. 2014;2014:392390.
22. Yassin MM, Barros D'Sa AA, Parks G, Abdulkadir AS, Halliday I, Rowlands BJ. Mortality following lower limb ischemia-reperfusion: a systemic inflammatory response? World J Surg. 1996;20:961-7.
23. Stammberger U, Carboni GL, Hillinger S, Schneiter D, Weder W, Schmid RA. Combined treatment with endothelin- and PAF-antagonists reduces posttransplant lung ischemia/reperfusion injury. J Heart Lung Transplant. 1999;18:862-8.
24. Tekin K, Aytekin F, Ozden A, Bilgihan A, Erdem E, Sungurtekin U, et al. Antithrombin III prevents deleterious effects of remote ischemia-reperfusion injury on healing of colonic anastomoses. Am J Surg. 2002;184:160-5.
25. Kologlu M, Sayek I, Kologlu LB, Onat D. Effect of persistently elevated intraabdominal pressure on healing of colonic anastomoses. Am J Surg. 1999;178:293-7.
26. Tang Y, Zhou G, Yao L, Xue P, Yu D, Xu R, et al. Protective effect of Ginkgo biloba leaves extract, EGb761, on myocardium injury in ischemia reperfusion rats via regulation of TLR-4/NF-κB signaling pathway. Oncotarget. 2017;8:86671-80.

This paper has been checked for language accuracy by JOSAM editors.
The National Library of Medicine (NLM) citation style guide has been used in this paper.

J Surg Med. 2021;5(12):1170-1173.
DOI: 10.28982/josam.1002516

Journal of Surgery and Medicine
e-ISSN=2602-2079

Fragmented QRS and blood pressure pattern in normotensive individuals with a history of preeclampsia

Kemal Göçer [1], Ekrem Aksu [2], Uğurkan Erkayıran [3]

[1] Department of Cardiology, Necip Fazıl State Hospital, Kahramanmaras, Turkey
[2] Department of Cardiology, Kahramanmaras Sutcu Imam University Faculty of Medicine, Kahramanmaras, Turkey
[3] Department of Obstetrics and Gynecology, Necip Fazıl State Hospital, Kahramanmaras, Turkey

ORCID ID of the author(s)

KG: 0000-0003-2673-1971
EA: 0000-0003-1939-1008
UE: 0000-0002-8519-1883

Corresponding Author
Kemal GÖÇER
Department of Cardiology, Necip Fazıl State Hospital, Dulkadiroglu, Kahramanmaras, Turkey
E-mail: k.gocer01@hotmail.com

Ethics Committee Approval
The ethics committee of Kahramanmaras Sutcu Imam University Faculty of Medicine approved the study on 22.07.2020 with decision number 3. All procedures in this study involving human participants were performed in accordance with the 1964 Helsinki Declaration and its later amendments.

Conflict of Interest
No conflict of interest was declared by the authors.

Financial Disclosure
The authors declared that this study has received no financial support.

Published
2021 December 20

Abstract

Background/Aim: Hypertension is well defined in preeclamptic individuals and those with a history of preeclampsia. However, the relationship between blood pressure pattern and fragmented QRS on electrocardiography (ECG) has not been elucidated in normotensive patients with a history of preeclampsia. This study aimed to investigate the frequency of non-dipper blood pressure (BP) patterns in normotensive individuals with a history of preeclampsia and to evaluate the relevance of this pattern to fragmented QRS (fQRS).

Methods: Sixty-three normotensive (office BP measurement) patients with a history of preeclampsia were included in this study between August 2020 and January 2021. These individuals underwent 24-hour ambulatory BP monitoring. The patients were divided into two groups as dipper and non-dipper, according to their BP patterns. The two groups were compared in terms of echocardiographic parameters, laboratory values, and QRS fragmentation on ECG.

Results: Left ventricular diastolic dysfunction (LVDD) diagnosed by echocardiography (P= 0.015) and fQRS on ECG (P=0.002) were significantly higher in the non-dipper group than in the dipper group. Tricuspid regurgitation velocity (P=0.004) and average E/e' ratio (P<0.001) were higher in the non-dipper group. Mitral E/A ratio (P=0.437) and left atrial volume index (P=0.439) were similar between the two groups in echocardiography. The fQRS, LVDD, triglyceride, and low-density lipoprotein were subjected to multivariate logistic regression analysis, and fQRS was found to be an independent predictor of the non-dipper BP pattern in women with a history of preeclampsia (P=0.023, OR=4.951, 95% CI:1.245-19.688).

Conclusion: The presence of an fQRS pattern on the ECG is associated with a non-dipper BP pattern in normotensive individuals with a history of preeclampsia.

Keywords: Preeclampsia, Fragmentation, Electrocardiography, Holter, Blood pressure

How to cite: Göçer K, Aksu E, Erkayıran U. Fragmented QRS and blood pressure pattern in normotensive individuals with a history of preeclampsia. J Surg Med. 2021;5(12):1170-1173.

Introduction

Preeclampsia is a multisystemic disease that occurs in women after the 20th week of pregnancy, characterized by new-onset hypertension and proteinuria or hypertension and multi-organ dysfunction [1]. The incidence of preeclampsia is 3-5% in all pregnancies [2]. The disease usually resolves after birth. However, even after delivery, an increased risk of developing cardiovascular (CV) events despite a normotensive course exists in individuals with a history of preeclampsia [3]. This suggests that it might be related to the blood pressure (BP) pattern. The BP is usually the highest during the daytime and lowest at night. A decrease of less than 10% in nighttime BP levels in 24-hour ambulatory blood pressure monitoring (ABPM) is defined as a non-dipper BP pattern. This pattern is associated with increased CV mortality [4]. Adverse cardiac outcomes caused by preeclampsia do not end with delivery and left ventricular diastolic dysfunction (LVDD), endothelial dysfunction, and atherosclerosis can be observed. It is reported that these adverse cardiac effects seen after preeclampsia is resolved [5]. This process, which is not precisely known, may be related to myocardial and vascular remodeling [6].

Fragmented QRS (fQRS) pattern on electrocardiography (ECG), which is an indicator of delayed and inhomogeneous ventricular conduction, was associated with myocardial fibrosis, scarring, and numerous CV diseases [7]. The fQRS, observed in approximately one-third of hypertensive patients, has a higher incidence than in normotensives even in the absence of left ventricular hypertrophy (LVH) [8]. Various studies consider the relationship between fQRS and non-dipper BP in hypertensive patients [9].

In this study, we investigated the frequency and relationship of non-dipper BP pattern and fQRS in normotensive individuals with a history of preeclampsia.

Materials and methods

Study design

This prospective cross-sectional study was conducted between August 2020 and January 2021 at the cardiology, obstetrics, and gynecology clinic. A total of 63 normotensives (according to office BP) consecutive individuals with a history of preeclampsia were included. Written informed consent was obtained from all individuals. The study was conducted per the principles of the Helsinki declaration and approved by the Ethics Committee of Kahramanmaras Sutcu Imam University Faculty of Medicine (22.07.2020, decision no:3).

Eighty-one individuals were examined. Ten smokers, two individuals with LVH, one individual with left bundle branch block, two individuals with diabetes mellitus (DM), one individual with collagen connective tissue disease, and two individuals with hypertension at 24-hour ABPM were excluded. The remaining 63 individuals constituted our study population (Figure 1). They were divided into two groups as dipper and non-dipper, according to their BP patterns. Demographic data and medical histories of all patients were recorded. Electrocardiography, echocardiography, and 24-hour ABPM were performed for all participants. The fQRS and echocardiographic measurements were blindly evaluated to prevent operator-induced bias without knowing the clinical status of the individuals. Laboratory routines consisting of glucose, blood urea nitrogen, creatinine, total cholesterol, low-density lipoprotein (LDL), high-density lipoprotein (HDL), triglyceride (TG), and hemoglobin were noted.

Figure 1: Flow chart of the study protocol

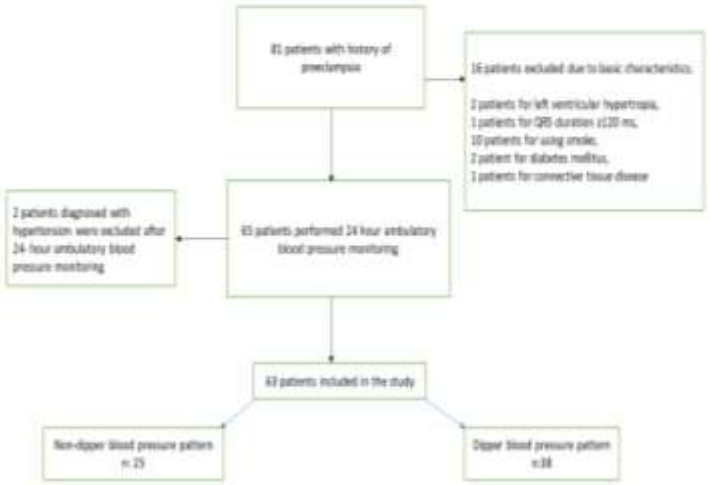

Definition of preeclampsia

Preeclampsia was defined according to criteria issued by The American College of Obstetricians and Gynecologists in 2017, which include new-onset hypertension after 20 weeks of gestation (systolic ≥ 140 mmHg and/or ≥90 mmHg diastolic BP on two occasions at least 4 hours apart) in addition to proteinuria (≥300 mg in a 24-hour urine or spot urine protein/creatinine ≥30 mg/mmol or at least +1 in stick test), in the absence of proteinuria, new-onset hypertension with any complications, a platelet count of less than 100.000/microliter, pulmonary edema, cerebral or visual symptoms, elevated serum liver enzymes to twice of the normal range, and a serum creatinine concentration of greater than 1.1 mg/dL in the absence of other renal diseases.

Blood pressure measurements

The blood pressure of participants was measured at the time of admission to the hospital. The average office BP values were recorded by calculating the average of the last two BP values measured 2-3 times with an automatic BP measuring device, 1-2 minutes apart after a 5-minute rest. Hypertension and normal BP were determined by the office BP and 24-hour ABPM based on 2020 International Society of Hypertension Global Hypertension Practice guidelines. Normal BP, high-normal BP, and hypertension were defined as <130 and <85 mmHg, 130-140 and/or 85-90 mmHg, ≥140 and/or ≥90 mmHg for systolic and diastolic pressures, respectively.

A 24-hour ambulatory BP device (Mobil-O-Graph NG (I.E.M. Stolberg Germany)) was placed in all individuals to determine BP level and pattern. The cuff of the BP device was placed on the non-dominant arm and the blood pressure was measured automatically every 30 minutes. Participants were asked to continue their daily activities. ABPM was re-performed to individuals with more than 20 percent invalid registration. Mean daily (24 hours), daytime, and nighttime BP records were obtained from ABPM based on the sleep and waking periods. No change was observed in the sleep and wake-up periods while the device was attached. Dipper BP pattern was defined as a more than 10% decrease in systolic and diastolic BP at nighttime,

while the non-dipper pattern indicated less than 10% reduction at nighttime in systolic and diastolic BP.

Electrocardiography

Standard 12-lead surface ECG (filter range, 0.15-100 Hz; AC filter, 60 Hz, 25 mm/s, 10 mm/Mv) was performed to all participants. ECGs were blindly interpreted by two independent cardiologists and fQRS morphology defined by Das was examined on the ECG. The fQRS was defined as the presence of various RSR' patterns or notching of the R or S waves in at least two consecutive leads corresponding to a major coronary artery region when the QRS duration was <120 ms.

Echocardiographic parameters

All measurements were performed with the Philips EPIQ 7C (Philips Healthcare, MA, USA) ECHO device in the left lateral decubitus position. Doppler echocardiography and m-mode parameters in two-dimensions were measured per the guidelines of the American Society of Echocardiology (ASE) and the European Association of Cardiovascular Imaging (EACVI). The ejection fraction (EF) was calculated with M-mode imaging. Peak early transmitral flow velocity (E), peak late transmitral flow velocity (A), isovolumic relaxation time (IVRT), and deceleration time (DT) were measured through pulsed doppler in all individuals. Pulsed-wave tissue doppler imaging recordings were obtained through a view of the lateral and septal sections of the mitral annulus from the apical four-chamber after the measurements of conventional echocardiography were completed. Normal diastolic function of LV (EF >50) was defined as the presence of only one or the absence of these parameters: Septal e' velocity < 7 cm/s or lateral e' velocity <10 cm/s, average E/e' >14, Left atrial volume index (LAVI) >34ml/m², tricuspid regurgitation (TR) velocity >2.8 m/s. The presence of two or more of these parameters was defined as LVDD.

Statistical analysis

The effect size (0.492) was calculated with the power analysis program according to the reference study at a test power of 0.80 and a significance level of 0.05. The minimum number of patients was determined as 53 before the study began. Statistical Package for Social Sciences (SPSS) for Windows 21 was used to analyze the data. Continuous variables were expressed as mean (standard deviation) and categorical variables, as a percentage. The participants were divided into two groups as non-dipper and dipper. Kolmogorov-Smirnov test, skewness, and kurtosis were used for the assessment of normal distribution. Independent Student's t-test was used for continuous variables with normal distribution. The Chi-square test was performed on categorical variables. Fragmented QRS, LVDD, TG, and LDL were entered into a multivariate logistic regression analysis. A 2-sided *P*-value of <0.05 was considered significant.

Results

Sixty-three individuals with a history of preeclampsia were included in the study. These individuals were divided into two groups as non-dipper (n=25) and dipper (n=38) according to their 24-hour ABPM. The two groups were compared in terms of basic characteristics (Table 1). There was no significant difference between the two groups' mean body mass indexes (*P*=0.841) and ages (*P*=0.731).

Table 1: Baseline characteristics and clinical findings of study groups

	Dipper (n=38)	Non-dipper (n=25)	*P*-value
Age, years	29.81 (4.63)	30.20 (3.78)	0.731
Body mass index (kg/m2)	36.42 (3.41)	36.27 (2.36)	0.841
Creatinine (mg/dl)	0.80 (0.14)	0.75 (0.14)	0.185
LDL (mg/dl)	108.13 (28.27)	116.51 (26.74)	0.244
HDL (mg/dl)	51.35 (6.33)	49.57 (7.30)	0.307
Triglycerides (mg/dl)	174.76 (64.87)	169.32 (64.33)	0.745
Blood pressure (mm Hg)			
Systolic			
Office	115.25 (10.19)	115.40 (9.67)	0.958
Daytime	115.13 (8.52)	111.24 (9.78)	0.1
Night-time	100.26 (7.99)	106.16 (8.35)	0.007
24-h	111.10 (8.19)	109.72 (9.19)	0.534
Night–day ratio	0.87 (0.02)	0.95 (0.03)	<0.001
Diastolic			
Office	75 (5.32)	72 (6.77)	0.054
Daytime	72.52 (8.33)	68.28 (6.73)	0.037
Night-time	61.97 (8.07)	63.20 (6.48)	0.527
24-h	67.92 (8.27)	66.56 (6.52)	0.491
Night–day ratio	0.85 (0.03)	0.92 (0.06)	<0.001
Fragmented QRS, n (%)	4 (10.5)	11 (44)	0,002
Diastolic dysfunction, n (%)	4 (10.5)	9 (36)	0,015

Abbreviations: LDL: low-density lipoprotein, HDL: high-density lipoprotein

Echocardiographic parameters of all individuals were noted and compared. There was no difference between the two groups in terms of mitral E/A ratio (*P*=0.437) and LAVI (*P*=0.439). TR velocity (*P*=0.004) and average E/e' ratio (*P*<0.001) were significantly higher in the non-dipper group. Table 2 shows the parameters in detail. fQRS (*P*=0.002) and LVDD (*P*=0.015) significantly differed between the two groups.

The presence of LVDD, TG, LDL, and having fQRS were included in the multivariate regression analysis (Table 3). We found that fQRS was an independent predictor of the non-dipper BP pattern (*P*=0.023, OR=4.951, 95%CI 1.245-19.688).

Table 2: Echocardiographic findings of dipper and non-dipper groups

	Dipper	Non-dipper	*P*-value
LVEF (%)	63.76 (2.86)	63.56 (2.46)	0.772
IVST, mm	9.68 (0.66)	9.68 (0.69)	0.981
Mitral E velocity, cm/s	87.81 (7.19)	92.36 (9.49)	0.035
Mitral A velocity, cm/s	73.23 (10.45)	81.08 (12.69)	0.010
Mitral E/A ratio	1.23 (0.25)	1.17 (0.28)	0.437
DT, ms	170.13 (7.51)	166.48 (6.97)	0.057
IVCT, ms	33.68 (2.89)	32.04 (3.85)	0.058
ET, ms	291 (7.95)	286.24 (8.68)	0.029
IVRT, ms	70.60 (5.92)	73.04 (6.49)	0.130
LAVI, mL/m2	20.34 (3.29)	21.08 (4.20)	0.439
TR velocity, cm/s	1.97 (0.15)	2.17 (0.28)	0.004
Tissue Doppler parameters			
Septal e′, cm/s	10.55 (2.03)	8.44 (2.78)	0.002
Lateral e', cm/s	12.31 (2.66)	9.36 (3.20)	<0.001
Average e', cm/s	11.43 (2.17)	8.90 (2.85)	<0.001
Septal A', cm/s	9.02 (1.44)	8.44 (1.73)	0.150
Lateral A', cm/s	10.57 (2.18)	9.12 (2.20)	0.012
Average E/e' ratio	8 (2)	11.29 (3.31)	<0.001

DT: Deceleration Time, ET: Ejection Time, IVCT: Isovolumetric Contraction Time, IVRT: Isovolumetric Relaxation Time, IVST: Interventricular Septal Thickness, LAVI: Left Atrial Volume Index, TR: Tricuspid Regurgitation

Table 3: Independent predictors of non-dipper blood pressure pattern

	B	OR	*P*-value	95%CI
Diastolic dysfunction	1.115	3.049	0.140	0.683-13.409
Triglycerides	-0,004	0.996	0.430	0.987-1.006
Low-density lipoprotein	0.004	1.004	0.727	0.983-1.025
Fragmented QRS, n (%)	1.600	4.951	0.023	1.245-19.688

Discussion

Preeclampsia occurs after the 20th week of pregnancy and is accompanied by organ dysfunctions. The condition regresses with delivery and BP returns to normal levels. However, individuals with a history of preeclampsia have been associated with CV mortality in the future despite the disappearance of the disease [10]. This is the first study on the non-dipper BP pattern, which we think will cause adverse CV events in normotensive individuals with a history of preeclampsia. We investigated fQRS and echocardiographic parameters, which we assumed to affect this pattern.

Blood pressure follows a circadian rhythm throughout the day. Nighttime BP levels decrease more than 10% compared to daytime BP. A less than %10 decrease in BP at nighttime is defined as the non-dipper pattern. Individuals with non-dipper BP patterns had three times more adverse CV events than dipper individuals [11]. Non-dipper normotensive individuals have been associated with a decrease in LVDD and an increase in left ventricular mass. In addition, a few studies report that the non-dipper normotensive pattern was related to chronic kidney disease, high creatinine levels, DM, and metabolic syndrome, which are CV risk factors [12, 13]. In our study, no difference was found between creatinine values, body mass index, and lipid profiles in the non-dipper group compared to the dipper group. The emergence of CV adverse events takes a long time due to the low average age of these individuals. In addition, these patients were not compared with a healthy group and both groups had a history of preeclampsia.

Fragmented QRS is an indicator of ventricular conduction caused by myocardial scarring, ischemia, or fibrosis [14]. Eyuboglu et al. [15] reported that fQRS could be associated with impaired circadian BP changes in prehypertensive patients. The fQRS is more common in hypertensive patients compared to normotensives. In addition, the frequency of fQRS was increased in hypertensive individuals with non-dipper BP patterns compared to individuals with dipper BP patterns [8]. The fQRS pattern was also detected on ECG in normotensive healthy individuals, but the reason for this could not be revealed. It was observed that the frequency of fQRS increased in preeclampsia. In our study, the fQRS pattern was higher in non-dipper BP pattern in normotensive individuals with a history of preeclampsia compared to those with a dipper BP pattern. The increased sympathetic activity due to nighttime autonomic dysfunction in hypertensive patients may have a similar underlying mechanism in normotensive non-dipper individuals. The incidence of ventricular arrhythmia was increased in individuals with non-dipper hypertension and sudden death was observed. The fQRS, which affects the non-dipper BP pattern in our study, may be an indicator of ventricular arrhythmia. Individuals should be followed closely in terms of the fQRS pattern.

Left ventricular diastolic dysfunction often precedes deterioration in systolic function in hypertension and can lead to heart failure or pulmonary edema, both of which are highly common in patients with preeclampsia [16]. In a study, LVDD was seen in 1 out of 5 cases of preeclampsia and in 38.9% of individuals with severe preeclampsia. Muthyala et al. [17] reported that stage 2 LVDD was observed in two-thirds of the severe preeclampsia group. Left ventricular diastolic dysfunction, which is frequent in preeclampsia, was significantly higher in the non-dipper group. In our study, no difference was observed between dipper and non-dipper groups in terms of systolic dysfunction. There were numerically more significant differences in tissue Doppler parameters between the two groups compared to pulsed Doppler parameters. Tissue Doppler imaging may be a sensitive echocardiographic technique to detect diastolic dysfunction. In our study, the effect of diastolic dysfunction on non-dipper BP could not be demonstrated. This may be because our patients were normotensive or not hypertensive enough.

There were some limitations to our study. First, this study was small and scaled. Second, a filter setting of 40 or 60 Hz was not optimal to evaluate fQRS on ECG compared to a low-pass filter setting (100 or 150 Hz). Additionally, the effects of wearing the 24-hour ambulatory BP device on the emotional state, hence their reflection of the BP records, were not known.

Conclusion

The fQRS pattern may be a simple and reliable test for predicting future cardiovascular adverse events in individuals with a history of preeclampsia.

References

1. Atadağ Y, Aydın A, Kaya D, Öksüz A, Köşker HD. Risk assessments, pregnancy and birth processes of pregnant women at primary health care center: A retrospective study. J Surg Med. 2017;1(1):5-8.
2. Filipek A, Jurewicz E. Preeklampsja – choroba kobiet w ciąży [Preeclampsia - a disease of pregnant women]. Postepy Biochem. 2018 Dec 29;64(4):232-29. doi: 10.18388/pb.2018_146
3. McDonald SD, Malinowski A, Zhou Q, Yusuf S, Devereaux PJ. Cardiovascular sequelae of preeclampsia/eclampsia: a systematic review and meta-analyses. Am Heart J. 2008 Nov;156(5):918-30.
4. Tigen K, Karaahmet T, Fotbolcu H, Gürel E, Cevik C, Gecmen C, et al. The influence of dipper and nondipper blood pressure patterns on left ventricular functions in hypertensive patients: a tissue Doppler study. Turk Kardiyol Dern Ars. 2009;37(2):101-6. PMID: 19404031
5. Sánchez-Aranguren LC, Prada CE, Riaño-Medina CE, Lopez M. Endothelial dysfunction and preeclampsia: role of oxidative stress. Front Physiol. 2014 Oct 10;5:372.
6. Staff AC, Dechend R, Pijnenborg R. Learning from the placenta: acute atherosis and vascular remodeling in preeclampsia-novel aspects for atherosclerosis and future cardiovascular health. Hypertension. 2010 Dec;56(6):1026-34.
7. Eyuboglu M. Fragmented QRS as a Marker of Myocardial Fibrosis in Hypertension: a Systematic Review. Curr Hypertens Rep. 2019 Aug 26;21(10):73.
8. Tanriverdi Z, Eyuboglu M, Bingol Tanriverdi T, Nurdag A, Demirbag R. The relationship between fragmented QRS and non-dipper status in hypertensive patients without left ventricular hypertrophy. Clin Exp Hypertens. 2017;39(7):680-4.
9. Zhang R, Chen S, Zhao Q, Sun M, Yu B, Hou J. Fragmented QRS complex is a prognostic marker of microvascular reperfusion and changes in LV function occur in patients with ST elevation myocardial infarction who underwent primary percutaneous coronary intervention. Exp Ther Med. 2017 Jun;13(6):3231-3238.
10. Diehl CL, Brost BC, Hogan MC, Elesber AA, Offord KP, Turner ST, Garovic VD. Preeclampsia as a risk factor for cardiovascular disease later in life: validation of a preeclampsia questionnaire. Am J Obstet Gynecol. 2008 May;198(5):e11-3.
11. Verdecchia P, Porcellati C, Schillaci G, Borgioni C, Ciucci A, Battistelli M, et al. Ambulatory blood pressure. An independent predictor of prognosis in essential hypertension. Hypertension. 1994 Dec;24(6):793-801.
12. Hoshide S, Kario K, Hoshide Y, Umeda Y, Hashimoto T, Kunii O, et al. Associations between nondipping of nocturnal blood pressure decrease and cardiovascular target organ damage in strictly selected community-dwelling normotensives. Am J Hypertens. 2003 Jun;16(6):434-8.
13. Rodrigues TC, Canani LH, Viatroski RS, Hoffmann LH, Esteves JF, Gross JL. Masked hypertension, nocturnal blood pressure and retinopathy in normotensive patients with type 1 diabetes. Diabetes Res Clin Pract. 2010 Feb;87(2):240-5.
14. Das MK, Khan B, Jacob S, Kumar A, Mahenthiran J. Significance of a fragmented QRS complex versus a Q wave in patients with coronary artery disease. Circulation. 2006 May 30;113(21):2495-501.
15. Eyuboglu M, Akdeniz B. Association Between Non-Dipping and Fragmented QRS Complexes in Prehypertensive Patients. Arq Bras Cardiol. 2019 Jan;112(1):59-64.
16. Maurer MS, Spevack D, Burkhoff D, Kronzon I. Diastolic dysfunction: can it be diagnosed by Doppler echocardiography? J Am Coll Cardiol. 2004 Oct 19;44(8):1543-9.
17. Muthyala T, Mehrotra S, Sikka P, Suri V. Maternal Cardiac Diastolic Dysfunction by Doppler Echocardiography in Women with Preeclampsia. J Clin Diagn Res. 2016 Aug;10(8):QC01-3.

This paper has been checked for language accuracy by JOSAM editors.
The National Library of Medicine (NLM) citation style guide has been used in this paper.

J Surg Med. 2021;5(12):1174-1178.
DOI: 10.28982/josam.1023148

Journal of Surgery and Medicine
e-ISSN=2602-2079

YouTube as a source of information on the radiologic approach to COVID-19

Zeynep Nilüfer Tekin [1], Canan Satır Özel [2]

[1] Department of Radiology, Medeniyet University Göztepe Prof Dr Süleyman Yalçın City Hospital, Istanbul, Turkey
[2] Department of Obstetrics and Gynecology, Medeniyet University Göztepe Prof Dr Süleyman Yalçın City Hospital, Istanbul, Turkey

ORCID ID of the author(s)
ZNT: 0000-0002-8209-0331
CSÖ: 0000-0001-5287-5114

Corresponding Author
Zeynep Nilüfer Tekin
Department of Radiology, Medeniyet University, Göztepe Prof Dr Süleyman Yalçın City Hospital, Dr. Erkin Street 34720 Istanbul, Turkey
E-mail: drnilufer@gmail.com

Ethics Committee Approval
Ethics committee approval was not required because the study data was obtained from YouTube, a public website, and did not contain any animal and patient data.

Conflict of Interest
No conflict of interest was declared by the authors.

Financial Disclosure
The authors declared that this study has received no financial support.

Published
2021 December 20

Abstract

Background/Aim: Since YouTube videos do not have accuracy filters, there are concerns about the information content. There are no studies specifically addressing the link between “Covid-19" and "radiology" in terms of content, reliability, and efficacy. The study aims to analyze videos posted on YouTube concerning Covid-19 and imaging in English.

Methods: The parameters of 120 most viewed videos on YouTube were recorded with the search of keywords "Covid-19 radiology" and "Covid-19 imaging". Quality Criteria for Consumer Health Information (DISCERN) and medical information and content index (MICI) scores were used to assess the reliability and medical content quality, respectively. The content was evaluated by types of radiological modalities and the patient groups included. Efficacy classification was conducted to assess "informative," "misleading," "individual experience" and "news update" groups. Video sources and target audience were analyzed.

Results: After the exclusion criteria, 55 videos were examined. The informative group (n=49) had a higher MICI score (MICI=8) when compared to the other groups (individual experience: 1 (n=3), news update: 1 (n=3), $P<0.001$). Among the informative ones, 25 videos (51%) were from radiology-related YouTube channels (YC). The MICI and DISCERN scores of the videos, where “radiologists” and “clinicians” make explanations, were significantly higher compared to the “others” group ($P=0.001$, and $P=0.005$, respectively). Computed tomography (CT) was the most frequently mentioned radiologic modality (n=49.84%). Pediatric and pregnant population videos were comparatively rarely offered (n=4.7% and n=3.4%).

Conclusion: The most viewed videos on YouTube about Covid-19 and radiology are reliable and informative videos narrated by radiologists and published by radiology-related channels and radiology societies. Accurate and scientific evidence-based information sharing is important on online social and scientific platforms.

Keywords: COVID-19, Pandemic, Radiology, Imaging, YouTube

How to cite: Tekin ZN, Özel CS. YouTube as a source of information on the radiologic approach to COVID-19. J Surg Med. 2021;5(12):1174-1178.

Introduction

Covid-19, an infectious disease caused by the SARS-COV2 virus causing serious pneumonia, first appeared in Wuhan, Hubei Province, China [1]. The World Health Organization officially declared it a pandemic on March 11, 2020. To this date, the total infected cases detected worldwide reached over 83 million, while the number of deaths is over 1.8 million [2]. The controversy in the literature and the social media covers a wide spectrum from the comparison of screening/testing accuracy of PCR versus radiological imaging to increased radiation exposure due to excessive imaging [3, 4].

Restrictions imposed since the beginning of the pandemic increased the consumption of visual media [5]. Video sharing is a rising trend today [6] and YouTube is the main social online platform [7]. YouTube is also used by both patients and healthcare professionals as a source of obtaining and sharing medical information [8]. Health-related information spreads rapidly on the Internet, especially during pandemic periods [9, 10]. However, since there are no filtering criteria on YouTube according to information quality, a large number of videos with low reliability and usefulness are shared along with informative videos without any labeling differences [11].

The study aims to examine the most viewed YouTube videos related to Covid-19 and imaging and to analyze their content during the current pandemic.

Materials and methods

This descriptive study was carried out using YouTube (www.youtube.com) data on 01.01.2021. Ethics committee approval was not required because the study data was obtained from YouTube, a public website and does not contain any animal or patient data.

Selection of the study material

A new YouTube account was created to minimize the effect of search history, cache, and cookies on the search results. “COVID-19 imaging” and “COVID-19 radiology” were used as keywords. Based on view counts on YouTube, the top 60 most frequently viewed videos on the first 3 pages for each keyword were determined to have high relevance [12, 13] and included in the study. Some studies show that YouTube users do not tend to watch videos listed after the first few pages, and over 90% of Internet users look at the first 3 pages of search results [14, 15]. Due to YouTube's continuous variable flow, 120 search results covering the keywords were recorded on a separate list.

Duplicated or irrelevant videos, those without audio and in non-English languages were eliminated. The selection criteria and stages of the study materials are shown in Figure 1.

Assessment of video parameters

Video length, and uploading date, the duration of the video on the site, the number of views, the number of likes and dislikes, and the number of comments of all data were noted. Views per day were calculated as total view/duration, and the like ratio was calculated as (the number of likes x100) / (number of likes + number of dislikes). The video power index (VPI), which shows the popularity of the video, and is calculated as (view ratio x like ratio/100), was also assessed [16].

Assessment of reliability and efficacy

Modified DISCERN score was adapted by Singh et al. from the original 16-question DISCERN tool [17]. Scoring is between 0-5 points and reliability increases as the scores rise.

The efficacy of video content was evaluated under the headings “informative,” “misleading,” “individual experience,” and “news update” [18]. Videos with reliable information based on scientific evidence, those compatible with the title, and that include treatment and prevention techniques, videos addressing the epidemiology, etiology, clinical course, diagnostic methods, and tests, especially the radiological features of the disease, are considered "informative". "Misleading", on the contrary, indicates false, biased, and non-scientific, manipulative videos. "Individual experience" is for videos that cover personal experiences. Videos updated in the light of new information, namely, the demographic characteristics of the pandemic published by news agencies, were evaluated in the category of "news update". Each video was addressed in one category.

Evaluation of video contents and sources

The content of the videos was evaluated by MICI scores [9, 10, 18]. This scoring was performed in five sections: Prevalence, transmission, signs/symptoms, screening/testing and, treatment/outcome. Each section contained 5 different components scored as 0-1, and the total score ranged between 0-25.

Video content was evaluated according to the mentioned imaging methods and the patient groups. Imaging methods were categorized as X-Ray, computerized tomography (CT), ultrasonography (US), magnetic resonance imaging (MRI), and Positron Emission Tomography - Computed Tomography (PET/CT), and patient groups were categorized as adult, elderly, pediatric, and pregnant.

Video sources were evaluated under the headings “radiology-related YC,” “radiology society educational YC”, “radiology department educational YC”, “clinicians,” “commercial,” “news agencies,” and “independent users” according to the posting channels. The narrators of radiology-related YC, radiology society educational YC, radiology department educational YC were listed as a solitary group under the title of "radiologists", while commercial, news agency, and independent user-sourced videos were grouped into "others". Narrators were compared in three categories (radiologists, clinicians, and others)

All videos were evaluated according to the principles mentioned by two independent physicians (ZNT, CSÖ) and interobserver agreement was assessed. In case of inconsistency in the mDISCERN scores and evaluation of efficacy, the videos were re-assessed, and a consensus was reached.

Statistical analysis

All statistical tests were conducted using the Statistical Package for the Social Sciences 21.0 for Windows (SPSS Inc., Chicago, IL, USA). The Kolmogorov-Smirnov test was used to analyze the normality of the data. Continuous data were expressed as mean (SD) and categorical data were expressed as percentages. The student’s t-test or Mann Whitney U test was used to compare unpaired samples as needed. Among groups of radiologists, clinicians, and others, ANOVA was used for primary analysis to compare the data containing parametric

variables, while the Kruskal-Wallis test was used for nonparametric variables. The agreement between the two physicians was assessed using the Kappa coefficient. Statistical significance was assumed if $P<0.05$ for two-sided.

Results

Fifty-five videos were included in the study after the implementation of the exclusion criteria (Figure 1). At the time of analysis, the mean (SD) video upload duration was 242 (67) days, and the median video length was 848 seconds (65-5,808). The median view count was 8,648 (range: 1,719-290,183), and the median view count per day was 36 (0-195). The median likes, dislikes, and comment numbers were 120 (0-4,975), 3 (0-346), and 8 (0-924), respectively. The median VPI of the videos was 31 (0-1,024).

Figure 1: Flowchart of the study

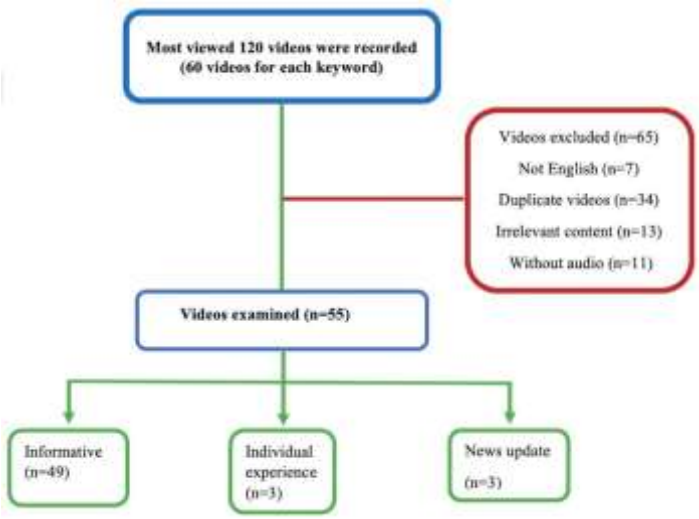

The source of 25 videos (45%) was radiology-related YC, 7 videos (13%) were from radiology society educational YC, 2 videos (4%), from radiology department educational YC, 9 videos (16%) belonged to clinicians, 7 videos (13%) were commercial, 3 videos (5%) were posted by news agencies and 2 videos (4%), by independent users. The distribution of videos by source category is shown in Figure 2.

Figure 2: Distribution of the videos based on source channel category

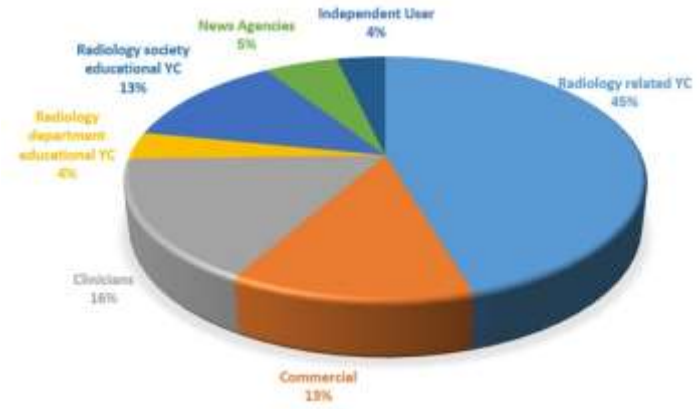

The median DISCERN score was 4 (0-5), and the median MICI score was 6 (1-19). The target audience in 49 videos (89%) were physicians, whereas it was radiology technicians in 4 videos (7%), and patients in 2 videos (4%).

MICI scale showed that 55 (100%) videos mentioned screening/testing, 8 (14%) mentioned prevalence, 20 (36%) mentioned transmission, 35 (64%), signs and symptoms, and 22 (40%) mentioned treatment/outcome.

Thirty-seven videos (67%) mentioned X-ray, 49 videos (84%) mentioned CT, 12 videos (22%) mentioned ultrasonography, 3 videos (6%) mentioned MRI and 2 videos (4%) mentioned PET-CT as radiological assessment tools. Forty-eight videos (87%) revealed information regarding adult patients, 8 videos (14%), regarding elderly patients, 4 videos (7%), regarding pediatrics, and 2 videos (4%), regarding pregnant patients. Video content based on imaging methods and patient groups is given in Table 1.

Table 1: Video contents according to imaging modalities and patient groups

Contents of videos	n (%)
X-ray	37 (67%)
CT	46 (84%)
US	12 (22%)
MRI	3 (6%)
PET-CT	2 (4%)
Adult	48 (87%)
Elderly	8 (14%)
Pediatric	4 (7%)
Pregnant	2 (4%)

* More than one topic can be mentioned in a video, n number, % percentage

Forty-nine (90%) videos were in the "informative" category, 3 (5%) videos regarded "individual experience," and 3 (5%) videos belonged to the "news update" category. The median DISCERN score was 4 in the "informative" category, 2 in the "individual experience" category, and 3 in the "news update" category. The features of videos and scoring results according to efficacy category are also shown in Table 2.

Table 2: Features of videos by efficacy classification

	Informative	Individual experience	News update
Number of videos (%)	49 (90%)	3 (5%)	3 (5%)
Length of videos (sec)	870 (120-4,240)	1,451 (97-5,808)	135 (65-169)
Video duration (days)	269 (54-365)	249 (184-276)	277 (68-284)
View count	9,984(1,719-290,183)	8648 (5,824-30,279)	5,223 (3,176-55,854)
Views per day	36 (0-1,095)	31 (31-122)	76 (11-202)
Total likes	120 (0-4,975)	251 (113-737)	58 (21-143)
Total dislikes	3 (0-346)	4 (1-20)	4 (4-31)
Comments	8 (0-924)	25 (11-77)	14 (0-14)
VPI	29 (0-1,024)	31 (31-118)	64 (10-166)
DISCERN score	4 (1-5)	2 (2-2)	3 (0-4)
MICI score	8 (1-19)	1 (1-1)	1 (1-4)

The median MICI score was 8 in the "informative" category compared to 1 in the "individual experience" and "news update" categories ($P<0.001$).

Twenty-five informative videos (51%) were posted by radiology-related YC, 7 videos (14%), by radiology society educational YC, 2 videos (4%), by radiology department educational YC, and 9 videos (18%), by clinicians. Four videos (12%) were commercials and two videos (4%) belonged to independent users. The "individual experience" category was entirely sourced commercially, and the videos in the "news update" category were procured from news agencies. The video characteristics (view count, likes, etc.) were distributed comparably when grouped for the narrators' backgrounds (radiologist, clinician, others) (Table 3). The DISCERN and MICI scores of physician-narrated videos were higher ($P=0.001$ and $P=0.005$, respectively) (Figure 3).

Table 3: Features and scoring of videos by narrator classification

	Radiologists	Clinicians	Others	*P*-value
Number of videos (%)	34 (62%)	9 (16%)	12 (22%)	
Length of videos(sec)	1,042 (120-4,240)	848 (252-2,511)	286 (65-5,808)	0.051
Video duration (days)	266 (54-303)	269 (143-366)	276 (68-292)	0.906
View count	10,428 (3,122-290,183)	15,840(1,719-94,280)	6,054(3,005-148,176)	0.516
Views per day	38(11-1,095)	50(7-350)	30(11-515)	0.569
Like Ratio	98(0-100)	97(0-99)	96(82-100)	0.322
Comments	14(0-924)	5(0-132)	8(0-105)	0.244
VPI	36(0-1,024)	42(0-344)	30(10-511)	0.672
DISCERN Score	4(3-5) [a]	5(4-5) [e]	2(0-5) [a e]	0.001
MICI Score	9(1-19) [a]	6(2-11) [e]	1(1-14) [a e]	0.005

[*] $P<0.05$ between "radiologists" and "clinicians" categories, [a] $P<0.05$ between "radiologists" and "others" categories, [e] $P<0.05$ between "clinicians" and "others" categories

Figure 3: DISCERN and MICI score comparison according to video narrators

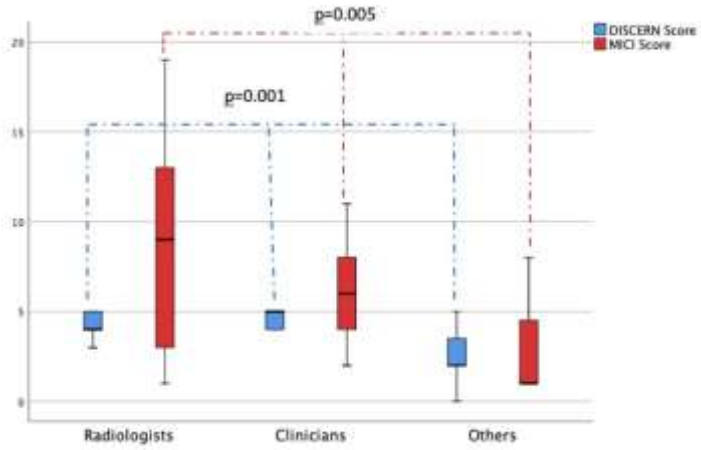

Compatibility of efficacy and DISCERN scores were calculated using inter-observer variability analysis. A 100% inter-observer agreement was found during efficacy assessment. Kappa coefficient of agreement for DISCERN was 0.87 ($P<0.001$).

Discussion

Both physicians and patients look for sources where they can access more practical, easily accessible, and comprehensive information on the imaging of Covid-19 disease as the pandemic goes on. Certain groups like pregnant and pediatric patients have somewhat limited options for imaging, as there are limitations due to radiation exposure. Elderly patients with comorbidities and other risk factors may have atypical/different findings and a more challenging differential diagnosis list when being evaluated for possible COVID-19. COVID-19 also introduces considerable stress to the patients' families who in turn may increase their research, especially in times of increased workload and social distancing, which both limit face-to-face time with the physicians. Therefore, patients/families and healthcare professionals frequently use YouTube, which has become an important source of online medical information research and sharing [8].

Lack of peer review before posting and easy access without any credential check frequently results in sub-par information quality in YouTube videos [19] with documentation of misleading, non-evidence-based information postings [20].

Social media is one of the main channels where Covid-19 information is updated [21]. Some of the effects were measured in Zhang et al.'s study, showing a strong correlation between worsening depression and anxiety during the Covid-19 pandemic and behavioral changes in YouTube use [22]. Another study found a comparable correlation between mental health problems in the Covid-19 pandemic and frequent social media exposure [23].

Since social media use is associated with measurable mental health and behavioral changes, accurate information sharing from social media becomes more important. Most studies focused on the social media aspects of prevention and treatment of COVID-19 [12, 24]. To the best of our knowledge, this is the first study reporting on the social media aspects of Covid-19 radiology, which has its controversies.

The majority of the most viewed YouTube videos included in this study were informative, and their DISCERN scores were quite high. The MICI score was significantly higher in the informative group compared to the non-informative group. While MICI scores in the informative group ranged between 6-7 in similar studies, DISCERN scores were in the range of 2-3.5 [9, 25]. In our study, the median scores were 8 and 4, respectively. The videos in our study were partly more comprehensive in terms of medical content and had high reliability compared to those previously discussed in the literature. We think that the fact that most informative videos in the study target physicians and that the videos are narrated by radiologists and clinicians resulted in comparatively higher scores. The main channels of informative videos in the study were radiology-related YC, radiology society educational YC, and clinicians' YC.

The video contents were comparable to regular medical literature, with CT, X-ray, and the US being the most frequently mentioned modalities, and MRI and PET-CT being the least mentioned [26, 27]. Adult and elderly patients with comorbidities were the most common patient groups to be discussed, followed by pediatric and pregnant patients, respectively.

While general COVID-19 discussion for pregnant patients is very prevalent in social media [28], such media consumption is shown to increase anxiety and depression symptoms and the tendency to seek out even more information among pregnant women [29]. These facts show that more accessible and high-quality/informative content should be shared on COVID-19, pregnant women, and imaging. We believe that videos narrated by radiologists, containing simple but comprehensible information about the role of radiation-based methods and alternative imaging modalities such as ultrasonography in COVID-19 will be beneficial for these patients.

Our study shows that the YouTube discussion of COVID-19 radiology is comparatively rare, but the information quality is higher with the most content being posted by physicians and radiology channels. The small sample size, the dynamic nature of the content, and single language choice limit the generalizability of our results. Further studies should focus on the dynamics of discussion and the development of accessible quality control methods when seeking medical information on social media.

Conclusion

The most viewed videos about Covid-19 and radiology on YouTube are highly reliable and informative videos posted by radiology-related channels and societies and narrated by

physicians. It is also important that fast, easily accessible information based on scientific evidence can reach both the patients and the physicians through online social platforms. Therefore, universities, societies established by healthcare professionals, and academicians should continue to deliver accurate and effective information to Internet users as they do on scientific platforms.

Acknowledgments

The authors would like to thank all YouTubers for inspiring them to carry out this study. The authors also thank Assoc. Prof. Mehmet Şenel Bademci and Ass. Prof. Zeynep Bilgi for their advice and support.

References

1. Coronaviridae Study Group of the International Committee on Taxonomy of Viruses. The species Severe acute respiratory syndrome-related coronavirus: classifying 2019-nCoV and naming it SARS-CoV-2. Nat Microbiol. 2020;5:536-44. doi: 10.1038/s41564-020-0695-z.
2. World Health Organization, Coronavirus disease 2019 (COVID-19) situation report (2020), https://www.who.int/publications/m/item/weekly-epidemiological-update---29-december-2020; [accessed 29 December 2020].
3. Tofighi S, Najafi S, Johnston SK, Gholamrezanezhad A. Low-dose CT in COVID-19 outbreak: radiation safety, image wisely, and image gently pledge. Emerg Radiol. 2020;27:601-5. doi: 10.1007/s10140-020-01784-3.
4. Long C, Xu H, Shen Q, Zhang X, Fan B, Wang C, et al. Diagnosis of the Coronavirus disease (COVID-19): rRT-PCR or CT? Eur J Radiol. 2020;126:108961. doi: 10.1016/j.ejrad.2020.108961.
5. Lemenager T, Neissner M, Koopmann A, Reinhard I, Georgiadou E, Müller A, et al. COVID-19 Lockdown Restrictions and Online Media Consumption in Germany. Int J Environ Res Public Health. 2021;18:14.
6. Freeman B, Chapman S. Is "YouTube" telling or selling you something? Tobacco content on the YouTube video-sharing website. Tob Control. 2007;16:207-10. doi:10.1136/tc.2007.020024.
7. Top 15 Most Popular Websites (ebizma website). 2020, http://www. ebizmba.com/articles/most-popular-websites; [accessed 15 May 2020].
8. Basnet B, Bhattarai S, Khanal A, Upadhyay M, Baruwal A. Quality of YouTube patient information on prostate cancer screening. Proc (Bayl Univ Med Cent). 2019;32:361-3. doi: 10.1080/08998280.2019.1594493.
9. Khatri P, Singh SR, Belani NK, Yeong YL, Lohan R, Lim YW, et al. YouTube as source of information on 2019 novel coronavirus outbreak: a cross sectional study of English and Mandarin content. Travel Med Infect Dis. 2020;35:101636. doi: 10.1016/j.tmaid.2020.101636.
10. Nagpal SJ, Karimianpour A, Mukhija D, Mohan D, Brateanu A. YouTube videos as a source of medical information during the Ebola hemorrhagic fever epidemic. Springer plus. 2015;4:457. doi: 10.1186/s40064-015-1251-9.
11. Youtube Policies and Security. (Youtube Website), https://www. Youtube.com/about/policies/#community-guidelines; [accessed 15 May 2020].
12. Kocyigit BF, Akaltun MS, Sahin AR. YouTube as a source of information on COVID-19 and rheumatic disease link. Clin Rheumatol. 2020;39:2049-54. doi: 10.1007/s10067-020-05176-3.
13. Sampson M, Cumber J, Li C, Pound CM, Fuller A, Harrison D. A systematic review of methods for studying consumer health YouTube videos, with implications for systematic reviews. Peer J. 2013;1:e147. doi: 10.7717/peerj.147.
14. Ataç Ö, Özalp YC, Kurnaz R, Güler OM, İnamlık M, Hayran O. Youtube as an Information Source During the Coronavirus Disease (COVID-19) Pandemic: Evaluation of the Turkish and English Content. Cureus. 2020;12:e10795. doi: 10.7759/cureus.10795.
15. Desai T, Shariff A, Dhingra V, Minhas D, Eure M, Kats M. Is content really king? An objective analysis of the public's response to medical videos on YouTube. PLoS One. 2013;8:e82469. doi: 10.1371/journal.pone.0082469.
16. Erdem MN, Karaca S. Evaluating the Accuracy and Quality of the Information in Kyphosis Videos Shared on YouTube. Spine. 2018;43:E1334-e1339. doi: 10.1097/brs.0000000000002691.
17. Singh AG, Singh S, Singh PP. YouTube for information on rheumatoid arthritis--a wakeup call? J Rheumatol. 2012;39:899-903. doi: 10.3899/jrheum.111114.
18. Yuksel B, Cakmak K. Healthcare information on YouTube: Pregnancy and COVID-19. Int J Gynaecol Obstet. 2020;150:189-93. doi: 10.1002/ijgo.13246.
19. Aydin MA, Akyol H. Quality of Information Available on YouTube Videos Pertaining to Thyroid Cancer. J Cancer Educ. 2020;35:599-605. doi: 10.1002/ijgo.13246.
20. Madathil KC, Rivera-Rodriguez AJ, Greenstein JS, Gramopadhye AK. Healthcare information on YouTube: A systematic review. Health Informatics J. 2015;21:173-94. doi: 10.1177/1460458213512220.
21. Bao Y, Sun Y, Meng S, Shi J, Lu L. 2019-nCoV epidemic: address mental health care to empower society. Lancet. 2020;395:e37-e38. doi: 10.1016/s0140-6736(20)30309-3.
22. Zhang B, Zaman A, Silenzio V, Kautz H, Hoque E. The Relationships of Deteriorating Depression and Anxiety With Longitudinal Behavioral Changes in Google and YouTube Use During COVID-19: Observational Study. JMIR Ment Health. 2020;7:e24012. doi: 10.2196/24012.
23. Gao J, Zheng P, Jia Y, Chen H, Mao Y, Chen S, et al. Mental health problems and social media exposure during COVID-19 outbreak. PLoS One. 2020;15:e0231924. doi: 10.1371/journal.pone.0231924.
24. Hernández-García I, Giménez-Júlvez T. Characteristics of YouTube Videos in Spanish on How to Prevent COVID-19. Int J Environ Res Public Health. 2020;17. doi: 10.3390/ijerph17134671.
25. Dutta A, Beriwal N, Van Breugel LM, Sachdeva S, Barman B, Saikia H, et al. YouTube as a Source of Medical and Epidemiological Information During COVID-19 Pandemic: A Cross-Sectional Study of Content Across Six Languages Around the Globe. Cureus. 2020;12:e8622. doi: 10.7759/cureus.8622.
26. Aljondi R, Alghamdi S. Diagnostic Value of Imaging Modalities for COVID-19: Scoping Review. J Med Internet Res. 2020;22:e19673. doi: 10.2196/19673.
27. Fields BKK, Demirjian NL, Dadgar H, Gholamrezanezhad A. Imaging of COVID-19: CT, MRI, and PET. Semin Nucl Med. 2020. doi: 10.1053/j.semnuclmed.2020.11.003.
28. Kawchuk G, Hartvigsen J, Innes S, Simpson JK, Gushaty B. The use of internet analytics by a Canadian provincial chiropractic regulator to monitor, evaluate and remediate misleading claims regarding specific health conditions, pregnancy, and COVID-19. Chiropr Man Therap. 2020;28:24. doi: 10.1186/s12998-020-00314-9.
29. Ayaz R, Hocaoğlu M, Günay T, Yardımcı OD, Turgut A, Karateke A. Anxiety and depression symptoms in the same pregnant women before and during the COVID-19 pandemic. J Perinat Med. 2020;48:965-70. doi: 10.1515/jpm-2020-0380.

This paper has been checked for language accuracy by JOSAM editors.
The National Library of Medicine (NLM) citation style guide has been used in this paper.

J Surg Med. 2021;5(12):1179-1183.
DOI: 10.28982/josam.980386

Journal of Surgery and Medicine
e-ISSN=2602-2079

Maternal amylase, lipase, lactate dehydrogenase, creatine kinase levels at preterm delivery, and the effect of tocolysis

Simten Genc [1], Melike Eren [1], Sadik Kukrer [2], Arzu Yurci [3], Basak Cingillioglu [1], Elif Dilasa Pala Kose [1], Orhan Sahin [1], Hicran Acar Sirinoglu [1], Veli Mihmanli [1]

[1] Obstetrics and Gynecology Department Okmeydani Training and Research Hospital Istanbul, Turkey
[2] Obstetrics and Gynecology Department, University of Health Sciences Adana City Training and Research Hospital
[3] Memorial Kayseri Hospital IVF Center, Gynecology Obstetrics & Reproductive Medicine, Kayseri, Turkey

ORCID ID of the author(s)

SG: 0000-0003-4446-4467
ME: 0000-0002-5134-6082
SK: 0000-0001-8465-3225
AY: 0000-0003-4808-9019
BC: 0000-0002-1666-8588
EDPK: 0000-0003-2898-5430
OS: 0000-0002-7216-3816
HAS: 0000-0003-4100-3868
VM: 0000-0001-8701-8462

Corresponding Author
Simten Genc
Darulaceze Cad. No:25, Okmeydani, Sisli, 34384, Istanbul, Turkey
E-mail: simtengenc@yahoo.com.tr

Ethics Committee Approval
Approval was granted by the Ethics Committee of the University of Health Sciences, Okmeydani Training and Research Hospital (Date 15/02/2021, No:48670771-514.10/16).
All procedures in this study involving human participants were performed in accordance with the 1964 Helsinki Declaration and its later amendments.

Conflict of Interest
No conflict of interest was declared by the authors.

Financial Disclosure
The authors declared that this study has received no financial support.

Published
2021 December 23

Abstract

Background/Aim: Preterm labor is one of the main obstetric problems and the leading cause of neonatal mortality and morbidity. Some pregnant women at risk of preterm labor receive tocolytic therapy, but the agents used can affect maternal blood parameters and enzyme levels. Physiological changes that occur during pregnancy may cause changes in enzymatic activities. Maternal amylase, lipase, lactate dehydrogenase (LDH), and creatine kinase (CK) levels should be followed throughout pregnancy to assess any increase. This study aimed to examine maternal amylase, lipase, creatine kinase, and lactate dehydrogenase levels in pregnant women who gave term and preterm birth and determine the physiological changes that may occur with gestational age and tocolysis.

Methods: The records of patients over their 24th gestational week who gave birth at the Gynecology and Obstetrics Department of Okmeydani Training and Research Hospital between July-December 2018 were reviewed in this retrospective cohort study. Their clinical findings, maternal and obstetric outcomes were noted. A total of 548 pregnant women were included in the study, who were divided into three groups: Group 1- Preterm delivery without tocolysis, Group 2- Preterm delivery with tocolysis, Group 3- Term delivery

Results: The maternal age, gravidity, history of abortion, fetal gender, amylase, and lipase values were similar between the groups (P>0.05 for all), while delivery types and cesarean section indications significantly differed (P=0.009, and P<0.001 respectively). The mean LDH value of Group 2 was significantly higher than those of Groups 1 and 3 (P=0.006, and P=0.024, respectively). The mean CK value of Group 3 was also higher than those of Groups 1 and 2 (P=0.021, and P<0.001, respectively), and that of Group 1 was significantly higher than that of Group 2 (P=0.021). LDH, amylase, lipase, and CK levels were not correlated with gestational age and fetal weight in the premature birth groups. In Group 3, a significant negative correlation was observed between fetal weight and amylase (r=-0.136 P=0.02). Among all patients, gestational week and LDH (r=-0.117, P=0.006) and fetal weight and LDH (r=-0.107, P=0.012) were negatively correlated, while fetal weight and lipase (r=0.095 P=0.027) and gestational week and CK were positively correlated (r=0.085 P=0.047) (Table 2, Figures 2 and 3).

Conclusion: Maternal enzyme levels may change with gestational week and as fetal weight increases. It is necessary to differentiate between pathological and physiological changes. These enzymes are also affected by tocolytic agents. Since our study was conducted in a healthy pregnant group without any systemic diseases, we think that the changes caused by gestational age and fetal weight gain are physiologically acceptable. However, any sudden elevation in these enzymes should be thoroughly investigated throughout pregnancy.

Keywords: Amylase, Creatine kinase, Lactate dehydrogenase, Lipase, Nifedipine, Tocolysis

How to cite: Genc S, Eren M, Kukrer S, Yurci A, Cingillioglu B, Kose EDP, Sahin O, Sirinoglu HA, Mihmanli V. Maternal amylase, lipase, lactate dehydrogenase, creatine kinase levels at preterm delivery and the effect of tocolysis. J Surg Med. 2021;5(12):1179-1183.

Introduction

Physiological changes that occur during pregnancy may alter enzymatic activities. Amylase is mostly secreted from the pancreas and salivary glands. Lipase, on the other hand, is mainly found in the pancreas, with small amounts in the stomach, liver, and intestinal mucosa. Its serum level stays higher for longer periods. However, in conditions such as acute pancreatitis, which is rare and may progress with maternal and fetal mortality and morbidity, a significant increase is observed in both amylase and lipase values [1].

Lactate dehydrogenase (LDH) is found in various tissues such as the heart, the liver, skeletal muscle, and the kidney, and elevated values have nonspecific clinical significance [2]. Creatine kinase (CK) is important in the regulation of high-energy phosphate metabolism [3]. The changes which may occur in these enzymatic activities during normal pregnancy have not been fully elucidated. Maternal enzyme activities should be thoroughly assessed in healthy pregnant women, and their elevations should be investigated, just as in non-pregnant women.

Preterm labor, one of the main problems of obstetrics, is the leading cause of neonatal mortality and morbidity. The respiratory, gastrointestinal, renal, and neurological systems of preterm babies are at elevated risk for various complications. Some pregnant women at risk of preterm labor receive tocolytic therapy [4]. However, the agents used can affect maternal blood parameters and enzyme levels.

This study aimed to examine the maternal amylase, lipase, creatine kinase, and lactate dehydrogenase levels in pregnant women who gave term and preterm birth and to determine the physiological changes that may occur with gestational age and tocolysis.

Materials and methods

The records of the patients over their 24th gestational week who were admitted to the Gynecology and Obstetrics Department of Okmeydani Training and Research Hospital to deliver a baby between July and December 2018 were retrospectively analyzed, and clinical findings and maternal and obstetric outcomes were noted. A total of 548 pregnant women were included in the study. Pregnant women under 18 years of age, smokers, those with systemic diseases, gestational diabetes, preeclampsia, multiple pregnancy, maternal TORCH group infections, chorioamnionitis, fetal death, and fetal anomaly were not included in the study.

Vaginal examinations were performed in all patients at the time of their admission to the hospital, and the presence of cervical effacement and dilatation were recorded. Uterine contractions were followed with external monitoring, and obstetric ultrasonography was performed to observe fetal development. Transvaginal ultrasonography was performed to determine the length of the cervical canal in the preterm delivery group. The gestational age was calculated per the last menstrual date or the ultrasonographic findings obtained before 20 weeks of gestation. Age, gravida, parity, number of miscarriages, gestational age, birth weight, fetal sex, and the delivery type were noted. The patients were divided into 3 groups: Group 1 included the patients who had preterm delivery without tocolysis (n=199), Group 2 patients had preterm delivery and received tocolysis (n=56), and Group 3 included those who gave term deliveries (n=293).

Preterm delivery is defined as the progressive dilatation of the cervix before 37 weeks of gestation with uterine contractions. In our study, the diagnostic criteria of preterm labor were the presence of effective (45-50 mmHg) uterine contractions, occurring 4 times in 20 minutes or 6 times in 60 minutes, as well as a cervical dilation of 2 cm or observation of cervical changes during physical examination. All pregnant women between their 24th-34th gestational weeks received 12 mg of betamethasone at their time of admission and an additional dose after 24 hours for fetal lung maturation.

The nifedipine tocolysis protocol was started on the pregnant women whose contractions persisted despite bed rest and hydration. For tocolysis, the American College of Obstetricians and Gynecologists (ACOG) recommends a loading dose of 30 mg of nifedipine administered orally, followed by 10 mg to 20 mg every 4 to 6 hours [5], which we followed. In our clinic, nifedipine 10 mg capsule was administered orally for a loading dose, repeated every 20 minutes for 3 doses. The maintenance treatment was continued with 10 mg of nifedipine administered in the form of 2 capsules, 4 times in 48 hours. The treatment was discontinued after 48 hours in pregnant women without uterine contractions. In those whose contractions continued after 48 hours, maintenance treatment was continued until the contractions ceased. We observed no side effects, such as maternal tachycardia, hypotension, or chest pain, therefore, did not need to cease treatment early. Pregnant women giving preterm labor over their 34th gestational week or giving birth immediately did not receive tocolysis. Maternal amylase, lipase, creatine kinase, and lactate dehydrogenase levels were studied by obtaining blood samples from all pregnant women before delivery. The normal range for these enzymes in our hospital is as follows: Amylase: 28-100 U/L, lipase: <67 U/L, creatine kinase: 0-145 U/L, and LDH: <248 U/L.

Statistical analysis

All statistical analyses were performed using the Number Cruncher Statistical System (NCSS) 2007 Statistical Software (Utah, USA) package program. Data were presented with descriptive statistical methods (mean, standard deviation, median, interquartile range), and the distribution of variables was examined with the Shapiro-Wilk normality test. One-way analysis of variance (ANOVA) and Tukey multiple comparison tests were used to compare normally distributed groups and subgroups, respectively. Non-normally distributed groups and subgroups were compared with the Kruskal-Wallis test and Dunn's multiple comparison test, respectively. The chi-square test was used for the comparison of qualitative data, and the Pearson correlation test was employed to determine the relationships between the variables. A *P*-value of <0.05 was considered significant.

Ethics approval

This study was performed per the principles of the Declaration of Helsinki. Approval was granted by the Ethics Committee of the University of Health Sciences, Okmeydani

Training and Research Hospital (Date 15/02/2021 No:48670771-514.10/16).

Results

The maternal age, gravidity, history of abortion, fetal gender, amylase, and lipase values were similar between the groups (P>0.05 for all) (Table 1), while delivery types and cesarean section indications significantly differed (P=0.009, and P<0.001 respectively). The rates of failure to progress, cephalopelvic disproportion, and macrosomia were higher in Group 3, while malpresentation and placental disorders were more frequent in Group 2.

Table 1: Demographic characteristics, obstetric outcomes, and maternal enzyme levels

		Group 1 Tocolysis (-) n=99	Group 2 Tocolysis (+) n=56	Group 3 ≥37 weeks n=293	*P*-value
Age (years)	Mean(SD)	27.63 (6.66)	28.2 (7.3)	27.17 (5.54)	0.449[a]
Delivery	Vaginal	96 48.24%	24 42.86%	175 59.73%	0.009[b]*
	Cesarean	103 51.76%	32 57.14%	118 40.27%	
Gender	Female	84 42.21%	28 50.00%	151 51.54%	0.121[b]
	Male	115 57.79%	28 50.00%	142 48.46%	
Gravida	Mean(SD)	2.9 (1.79)	2.61 (1.79)	2.51 (1.18)	0.074[c]
	Median (IQR)	3 (2-4)	2 (1-3)	2 (2-3)	
Parity	Mean(SD)	1.6 (1.53)	1.29 (1.52)	1.25 (1.01)	0.022[c]*
	Median (IQR)	1 (1-2)	1 (0-2)	1 (0.5-2)	
Abortus	Mean(SD)	0.3 (0.75)	0.32 (0.66)	0.26 (0.61)	0.540[c]
	Median (IQR)	0 (0-0)	0 (0-0.75)	0 (0-0)	
Gestational age (weeks)	Mean(SD)	35.62 (1.13)	32.11 (2.65)	39.12 (1.2)	<0.001[a]*
Fetal weight (g)	Mean(SD)	2734.65 (456.41)	1967.16 (648.13)	3311.14 (555.3)	<0.001[a]*
Maternal lactate dehydrogenase (U/L)	Mean(SD)	257.18 (86.88)	310.93 (127.6)	261.49 (73.9)	0.019[c]*
	Median (IQR)	239 (206-288)	264 (216.25-359.5)	249 (213-292.5)	
Maternal amylase (U/L)	Mean(SD)	70.72 (24.97)	67.73 (30.16)	70.91 (24.88)	0.428[c]
	Median (IQR)	68.85 (50.36-83.46)	63.4 (48.54-80.68)	66.85 (53.60-84.27)	
Maternal lipase (U/L)	Mean(SD)	18.99 (11.9)	17.72 (9.64)	20.61 (15.01)	0.279[c]
	Median (IQR)	16.78 (11.44-24.5)	16.42 (10.38-24.17)	17.14 (12.35-24.64)	
Maternal creatine kinase (U/L)	Mean(SD)	94.27 (72.64)	75.98 (54.66)	109.24 (121.54)	<0.001[c]*
	Median (IQR)	68 (50-115)	53.5 (37.25-100.25)	82 (59.5-115.5)	

a One-way analysis of variance, b Chi-square test c Kruskal Wallis test *Statistically significant

The three groups had comparable amylase and lipase values (P=0.428, and P=0.279, respectively). The mean LDH value of Group 2 was significantly higher than those of Groups 1 and 3 (P=0.006, and P=0.024, respectively). The mean CK value of Group 3 was also higher than those of Groups 1 and 2 (P=0.021, and P<0.001, respectively), and that of Group 1 was significantly higher than that of Group 2 (P=0.021).

LDH, amylase, lipase, and CK levels were not correlated with gestational age and fetal weight in the premature birth groups. In Group 3, a significant negative correlation was observed between fetal weight and amylase (r=-0.136 P=0.02) (Figure 1). Among all patients, gestational week and LDH (r=-0.117 P=0.006) and fetal weight and LDH (r=-0.107 P=0.012) were negatively correlated, while fetal weight and lipase (r=0.095 P=0.027) and gestational week and CK were positively correlated (r=0.085 P=0.047) (Table 2, Figures 2 and 3).

Table 2: Correlation of gestational age and fetal weight with maternal enzymes

			Gestational age	Fetal weight
Group 1, Tocolysis (-)	LDH	r	-0.055	-0.120
		p	0.442	0.09
	Amylase	r	0.066	0.093
		p	0.357	0.190
	Lipase	r	0.001	0.103
		p	0.992	0.149
	CK	r	0.024	-0.106
		p	0.740	0.138
Group 2, Tocolysis (+)	LDH	r	0.017	-0.045
		p	0.902	0.740
	Amylase	r	0.038	0.087
		p	0.782	0.523
	Lipase	r	0.101	0.122
		p	0.458	0.369
	CK	r	0.034	0.084
		p	0.804	0.538
Group 3, Term	LDH	r	-0.068	0.021
		p	0.249	0.720
	Amylase	r	-0.033	-0.136
		p	0.569	0.02
	Lipase	r	0.001	0.036
		p	0.992	0.534
	CK	r	-0.04	-0.005
		p	0.496	0.928
All groups	LDH	r	-0.117	-0.107
		p	0.006	0.012
	Amylase	r	0.031	-0.006
		p	0.464	0.883
	Lipase	r	0.072	0.095
		p	0.093	0.027
	CK	r	0.085	0.052
		p	0.047	0.238

Pearson correlation test

Figure 1: Correlation between amylase level and fetal weight

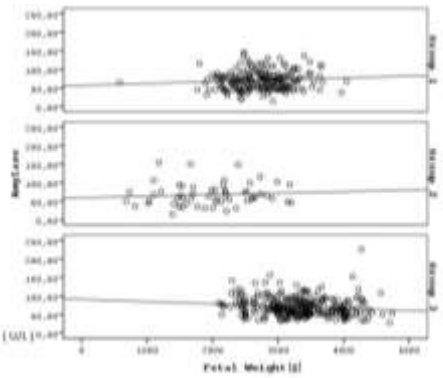

Figure 2: Correlation between maternal enzyme levels and gestational age

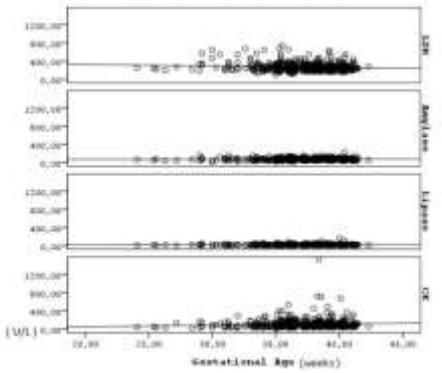

Figure 3: Correlation between maternal enzyme levels and fetal weight

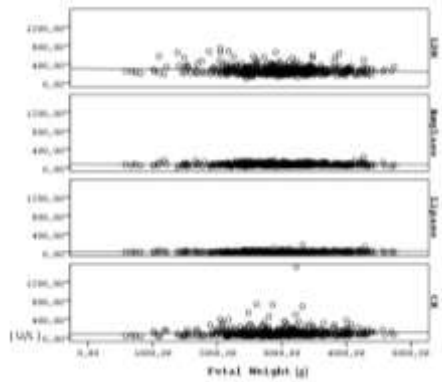

Discussion

Physiological changes can occur in maternal enzyme levels throughout the pregnancy. Since our hospital is a reference center, many patients are admitted to the emergency department to give birth. Therefore, unlike many studies, our study group consisted of a large number of patients. We think that we can better understand the changes that may occur with the advancing gestational weeks and the effects of tocolysis since healthy pregnant women without any systemic disease were included as a control group in our study.

Amylase is produced mainly by the pancreas and salivary glands and is one of the main enzymes of the digestive system. Salivary alpha-amylase is an indicator of sympathetic nervous system activity [6]. Today, salivary and serum amylase tests are widely used in obstetrics and gynecology. Cases of ruptured ectopic pregnancy can also lead to an increase in serum lipase and amylase levels, mimicking acute pancreatitis [7]. Psychological or physical stress, and acute stress conditions during delivery, such as spinal anesthesia in cesarean section, may increase α-amylase levels [8, 9]. As our patient group was treated under observation in the hospital, these patients may have been exposed to stress. In the study of Nava et al., the authors stated that amylase levels did not change with gestational age [10], similar to our results.

Prematurity is one of the leading causes of neonatal mortality and morbidity. Various agents are used for tocolytic therapy. Many centers aim to postpone the delivery with tocolytic agents for 48 hours to ensure the maximum effectiveness of corticosteroids and the transfer of the pregnant women to reference centers. There is no consensus on the first-line agents [11]. Ritodrine has been used for many years as a beta-agonist for tocolysis, but it may cause hyperamylasemia. Although the effect of this agent on serum amylase activity is not fully known, it was shown to cause excessive secretion of salivary type amylase in approximately one-third of pregnant women [12]. In the study of Nakajima et al. on the analysis of the umbilical cord of premature fetuses, amylase levels did not differ between the group receiving and not receiving ritodrine and did not change with birthweight and gestational age [13]. In our study, we used nifedipine as a tocolytic agent. Nifedipine is a calcium channel blocker globally administered via the oral or sublingual route for tocolysis [4]. It exerts its activity by preventing the free calcium ion from entering the cell through the calcium channels in the plasma membrane. It decreases uterine vascular resistance, contractile activity, and the basal tonus of myometrium, as well as the amplitude, and tonus of contractions. In a meta-analysis in which nifedipine was compared with β adrenergic agents, nifedipine was more effective and better tolerated [14]. In our study, no significant difference was found in the amylase values of the pregnant women who gave premature birth when compared with those that did and did not receive tocolytic therapy. However, in women with term pregnancies, fetal weights increased, and amylase values decreased. Xydas et al. [15] obtained several blood samples from healthy pregnant women who did not receive tocolytic therapy to determine whether a change occurred in their serum amylase and lipase values, but no significant change was found in amylase and lipase values with advancing gestational weeks, similar to our results. Tocolytic therapy did not affect these enzymes, also. Acute pancreatitis during pregnancy is a rare condition that can lead to maternal and fetal mortality and high serum amylase and lipase levels are just as important findings in pregnant women as in non-pregnant women. However, a thorough knowledge of the physiological changes during pregnancy in detail will prevent delays in diagnoses [16]. Serum lipase is a better biomarker than serum amylase to evaluate a diagnosis of acute pancreatitis [17]. In a prospective study by Karsentine et al. [18], pregnant women were examined in all three trimesters and compared with the non-pregnant group with no differences found in amylase levels. However, significantly lower serum lipase activity was observed in the first trimester compared to the third trimester and non-pregnant women. The serum lipase activity of pregnant women in their second and third trimesters and non-pregnant women were similar. Lipase levels remained below the normal upper limit. While diagnosing acute pancreatitis, these physiological modifications during pregnancy should also be considered. In our study, lipase levels increased with fetal weight. However, tocolytic therapy did not play a role in this increase.

There was no significant difference between serum amylase and lipase levels and amylase-creatinine clearance ratio (Cam: Ccr%) in pregnant and non-pregnant women. There is no published data regarding the effect of tocolytic therapy on serum lipase activity, which is considered one of the most sensitive, and specific indicators of pregnancy, and pancreatitis [19]. Under normal conditions, moderate increases in Lactate dehydrogenase (LDH) are observed in cord blood associated with the onset of labor and changes in acid-base status. Its levels also increase in advancing gestation. The increase in LDH levels with pregnancy is more dependent on pH values than on gestational age [20]. In a study conducted with pregnant women who had a preterm delivery, blood samples taken during the 2nd trimester were examined and the average maternal LDH levels were insignificantly higher [21]. In our study, LDH values of the tocolysis group were significantly higher than the LDH values of the preterm group that did not receive tocolytic therapy and the term group. In another study, LDH levels measured in mid-trimester amniocentesis material and preterm delivery were significantly related [22]. One of the most interesting results in our study was that in all patient groups, LDH levels decreased with advancing gestational weeks.

Plasma creatine kinase (CK) activity measured in early pregnancy was associated with blood pressure during pregnancy and severe gestational hypertension diagnosed before 34 weeks of gestation, but no relationship was found between creatine kinase levels and other hypertensive diseases [23]. In the study conducted on women who gave preterm deliveries and received tocolytic therapy with ritodrine for more than 1 week, the cord blood CK concentration was significantly higher than the group that did not receive tocolytic therapy. Additionally, CK was significantly associated with gestational age and birth weight. However, in the same study, no change was detected in LDH levels associated with tocolysis, and tocolytic therapy was not significantly associated with gestational age and birth weight [13]. In another study, if tocolytic therapy was continued for longer than a week, CK levels rose above the normal range in nearly a quarter of these patients [24]. Adamcov et al. [25]

reported that CK levels correlated with gestational age or birth weight. In our study, as the gestational week increased, CK levels also significantly increased.

Maternal enzyme values may vary during pregnancy. In most studies, ritodrine and magnesium sulfate were used for tocolysis. In our study, tocolysis was performed with nifedipine, and we observed that LDH values were higher in the preterm group that underwent tocolytic therapy. However, CK values were higher in the preterm delivery group that did not receive tocolytic therapy. No significant difference was found between these groups in terms of amylase and lipase values. There was no significant correlation between LDH, amylase, lipase, and creatine kinase values, gestational week, and fetal weight in the premature delivery groups. Besides, tocolytic therapy did not change the levels of these enzymes. In pregnant women with term deliveries, as fetal weight increased, amylase values decreased. In the entire patient group, as the gestational week advanced, LDH decreased, but CK increased. As fetal weight increased, LDH decreased, but lipase increased.

Conclusion

Maternal enzyme levels may change with gestational week and as fetal weight increases. It is necessary to distinguish between pathological and physiological changes. Enzymes are also affected by the agents used in tocolysis. Since our study was conducted in a healthy pregnant group without any systemic diseases, we think that the changes caused by gestational age and fetal weight gain can be physiologically acceptable. However, multicentered prospective studies with a greater number of patients are needed to distinguish between the pathological and physiological values accurately.

References

1. Mali P. Pancreatitis in pregnancy: etiology, diagnosis, treatment, and outcomes. Hepatobiliary Pancreat Dis Int. 2016 Aug;15(4):434-8. doi: 10.1016/s1499-3872(16)60075-9.
2. Mongelli M, Kwan Y, Kay LL, Hjelm M, Rogers MS. Effect of labour and delivery on plasma hepatic enzymes in the newborn. J Obstet Gynaecol Res. 2000 Feb;26(1):61-3. doi: 10.1111/j.1447-0756.2000.tb01203.x.
3. De Guingand DL, Ellery SJ, Davies-Tuck ML, Dickinson H. Creatine and pregnancy outcomes, a prospective cohort study in low-risk pregnant women: study protocol. BMJ Open. 2019 Jan 15;9(1):e026756. doi: 10.1136/bmjopen-2018-026756.
4. Leal-Júnior CC, Amorim MMR, Souza GFA, Lima AKS, Souza ASR. Effectiveness of an oral versus sublingual loading dose of nifedipine for tocolysis. Int J Gynaecol Obstet. 2020 Mar;148(3):310-315. doi: 10.1002/ijgo.13067. Epub 2019 Dec 11.
5. ACOG Committee on Practice Bulletins. American College of Obstetricians and Gynecologist. ACOG Practice Bulletin. Clinical management guidelines for obstetrician-gynecologist. Number 43, May 2003. Management of preterm labor. Obstet Gynecol. 2003 May;101(5 Pt 1):1039-47. doi: 10.1016/s0029-7844(03)00395-8.
6. Rohleder N, Nater UM. Determinants of salivary alpha-amylase in humans and methodological considerations. Psychoneuroendocrinology. 2009 May;34(4):469-85. doi: 10.1016/j.psyneuen.2008.12.004. Epub 2009 Jan 19.
7. Mitura K, Romanczuk M. Ruptured ectopic pregnancy mimicking acute pancreatitis. Ginekol Pol. 2009 May;80(5):383-5.
8. Nater UM, Rohleder N. Salivary alpha-amylase as a non-invasive biomarker for the sympathetic nervous system: current state of research. Psychoneuroendocrinology. 2009 May;34(4):486-96. doi: 10.1016/j.psyneuen.2009.01.014. Epub 2009 Feb 26.
9. Guglielminotti J, Dehoux M, Mentré F, Bedairia E, Montravers P, Desmonts JM, et al. Assessment of salivary amylase as a stress biomarker in pregnant patients. Int J Obstet Anesth. 2012 Jan;21(1):35-9. doi: 10.1016/j.ijoa.2011.09.008. Epub 2011 Nov 26.
10. Nava S, Bocconi L, Zuliani G, Kustermann A, Nicolini U. Aspects of fetal physiology from 18 to 37 weeks' gestation as assessed by blood sampling. Obstet Gynecol. 1996 Jun;87(6):975-80. doi: 10.1016/0029-7844(96)00056-7.
11. van Vliet EO, Schuit E, Heida KY, Opmeer BC, Kok M, Gyselaers W, et al. Nifedipine versus atosiban in the treatment of threatened preterm labour (Assessment of Perinatal Outcome after Specific Tocolysis in Early Labour: APOSTEL III-Trial). BMC Pregnancy Childbirth. 2014 Mar 3;14:93. doi: 10.1186/1471-2393-14-93.
12. Takahashi T, Minakami H, Tamada T, Sato I. Hyperamylasemia in response to ritodrine or ephedrine administered to pregnant women. J Am Coll Surg. 1997 Jan;184(1):31-6.
13. Nakajima Y, Masaoka N. Evaluation of creatine kinase, lactate dehydrogenase, and amylase concentrations in umbilical blood of preterm infants after long-term tocolysis. Obstet Gynecol Int. 2014;2014:278379. doi: 10.1155/2014/278379.
14. Tsatsaris V, Papatsonis D, Goffinet F, Dekker G, Carbonne B. Tocolysis with nifedipine or beta-adrenergic agonists: a meta-analysis. Obstet Gynecol. 2001 May;97(5 Pt 2):840-7. doi: 10.1016/s0029-7844(00)01212-6.
15. Xydas NP, May JH, Henson MC. Maternal serum amylase and lipase profiles in pregnancy: determinations in both once-sampled and multisampled patient cohorts. South Med J. 1996 Feb;89(2):199-203. doi: 10.1097/00007611-199602000-00008.
16. Cruciat G, Nemeti G, Goidescu I, Anitan S, Florian A. Hypertriglyceridemia triggered acute pancreatitis in pregnancy - diagnostic approach, management and follow-up care. Lipids Health Dis. 2020 Jan 4;19(1):2. doi: 10.1186/s12944-019-1180-7.
17. Chase CW, Barker DE, Russell WL, Burns RP. Serum amylase and lipase in the evaluation of acute abdominal pain. Am Surg. 1996 Dec;62(12):1028-33.
18. Karsenti D, Bacq Y, Bréchot JF, Mariotte N, Vol S, Tichet J. Serum amylase and lipase activities in normal pregnancy: a prospective case-control study. Am J Gastroenterol. 2001 Mar;96(3):697-9. doi: 10.1111/j.1572-0241.2001.03607.x.
19. Ordorica SA, Frieden FJ, Marks F, Hoskins IA, Young BK. Pancreatic enzyme activity in pregnancy. J Reprod Med. 1991 May;36(5):359-62.
20. Weiner CP, Sipes SL, Wenstrom K. The effect of fetal age upon normal fetal laboratory values and venous pressure. Obstet Gynecol. 1992 May;79(5(Pt 1)):713-8.
21. Ozgu-Erdinc AS, Cavkaytar S, Aktulay A, Buyukkagnici U, Erkaya S, Danisman N. Mid-trimester maternal serum and amniotic fluid biomarkers for the prediction of preterm delivery and intrauterine growth retardation. J Obstet Gynaecol Res. 2014 Jun;40(6):1540-6. doi: 10.1111/jog.12371.
22. Borna S, Mirzaie F, Abdollahi A. Mid-trimester amniotic fluid C-reactive protein, ferritin and lactate dehydrogenase concentrations and subsequent risk of spontaneous preterm labour. Aust N Z J Obstet Gynaecol. 2009 Aug;49(4):400-3. doi: 10.1111/j.1479-828X.2009.01019.x.
23. Horjus DL, Bokslag A, Hutten BA, van den Born BH, Middeldorp S, Vrijkotte TGM. Creatine kinase is associated with blood pressure during pregnancy. J Hypertens. 2019 Jul;37(7):1467-1474. doi: 10.1097/HJH.0000000000001900.
24. Matsuda Y, Nagayoshi Y, Kirihara N. Evaluation of creatine kinase level during long-term tocolysis. J Perinat Med. 2002;30(6):476-9. doi: 10.1515/JPM.2002.074.
25. Adamcová M, Kokstein Z, Palicka V, Vávrová J, Podholová M, Kost'ál M. Cardiac troponin T in neonates after acute and long-term tocolysis. Biol Neonate. 2000 Nov;78(4):288-92. doi: 10.1159/000014281.

This paper has been checked for language accuracy by JOSAM editors.
The National Library of Medicine (NLM) citation style guide has been used in this paper.

J Surg Med. 2021;5(12):1184-1187.
DOI: 10.28982/josam.899255

Journal of Surgery and Medicine
e-ISSN=2602-2079

Neck circumference - A simple and valid screening tool for obesity in school children

Sreelatha P. R., Chinchilu R.V.

Additional Professor of Pediatrics, GTDMC, Alappuzha, Kerala, India

ORCID ID of the author(s)
SPR: 0000-0002-5702-4412
CRV: 0000-0002-4725-2403

Corresponding Author
Chinchilu R.V.
GTDMC, Alappuzha, Kerala, 688005, India
E-mail: rvchinchilu@gmail.com

Ethics Committee Approval
The institutional ethics committee of TD medical college, Alappuzha. EC27/2017- 19-06-2017. All procedures in this study involving human participants were performed in accordance with the 1964 Helsinki Declaration and its later amendments.

Conflict of Interest
No conflict of interest was declared by the authors.

Financial Disclosure
The authors declared that this study has received no financial support.

Published
2021 November 25

Abstract

Background/Aim: Childhood obesity is on a rise worldwide with an estimated prevalence of over 8% and 6% in boys and girls, respectively. Being a forerunner of adult obesity and its consequences, this has to be detected earlier and appropriate interventions instituted timely for better health outcomes. Neck Circumference is a simple screening tool for detecting obesity. This study aimed to find out the correlation between neck circumference and body mass index (BMI) and measures of central obesity like waist circumference (WC), hip circumference (HC), and waist-hip ratio (WHR). It also tried to find out the age and gender-specific cut-off values for overweight and obesity in schoolchildren aged 6 to 16 years.

Methods: This was a cross-sectional observational study conducted in the primary and secondary schools of a sub-urban region of south Kerala, India. The anthropometric measurements, including weight, height, neck circumference, waist and hip circumferences of children aged 6-16 years who satisfied the inclusion criteria were obtained by health professionals, and their BMIs were compared with WHO standards to detect overweight and obesity. The correlation between BMI and NC, sensitivity, and specificity of NC in detecting overweight and obesity, and age-related cut-off values of NC were calculated using appropriate statistical methods. The correlation of NC with indicators of central obesity like waist circumference, hip circumference, and waist-hip ratio were also determined.

Results: A total of 1797 students were studied. Neck circumference showed a significant positive correlation (r = +0.6 to +0.8, P<0.001) with body mass index, waist circumference, and hip circumference but not with waist-hip ratio (r =+.3 to -.2). In ROC analysis, age-specific cut-off values of NC for obesity and overweight were obtained age- and gender-wise, with sensitivities of 87.5% and 100%, and specificities of 52.2% - 88.9%, respectively.

Conclusion: Neck circumference is a valid and simple tool to detect overweight and obesity in schoolchildren. It is also an indicator of the central distribution of fat in children aged 6 to 16 years.

Keywords: Neck circumference, Body Mass Index, overweight, obesity, Waist circumference, Hip circumference

How to cite: Sreelatha PR, Chinchilu RV. Neck circumference – a simple and valid screening tool for obesity in school children. J Surg Med. 2021;5(12):1184-1187.

Introduction

Obesity is abnormal or excessive fat accumulation in the adipose tissue to the extent that health may be impaired [1]. The worldwide prevalence of overweight is on the rise. WHO estimates it to have tripled from 4% in 1975 to over 18% in 2016 in children aged 5-19 years [2]. Obesity increased from 1% in 1975 to 6% in girls and 8% in boys by 2016. If post-2000 trends continue, global levels of child and adolescent obesity will surpass those for moderately and severely underweight youth in the same age group by 2022 [4]. Childhood obesity is associated with a higher chance of obesity, premature death, and disability in adulthood, apart from the cardio-respiratory, osteoarticular and psycho-social morbidities in childhood itself [5]. It is observed that overweight and obesity are linked to more deaths worldwide than underweight. Hence, it is crucial to detect these conditions quite early in life and adopt timely interventions. For this, we need reliable and easy tools for their detection that can be utilized by health workers.

Body Mass Index (BMI) (weight (kilogram) / height $(m)^2$) provides the most useful albeit crude measurement of obesity. For children, there are age-specific WHO BMI centile charts for both boys and girls. A BMI $\geq 85^{th}$ centile is overweight, and $\geq 95^{th}$ centile is obesity [6].

Individuals with obesity and overweight differ in the extent of fat deposited as well as the regional distribution of that fat. Those with abdominal fat distribution (android obesity) are at increased risk for metabolic complications when compared to those with gynoid fat distribution in whom fat is more evenly and peripherally distributed [7]. Abdominal fat mass can vary dramatically within a narrow range of total body fat or BMI. BMI does not give any idea on the distribution of excess fat accumulation [8]. We need other measurements like waist circumference, waist-hip ratio, etc., or imaging modalities to identify patients at increased risk of obesity-related illnesses.

Waist Circumference (WC) is an indicator of fat accumulation that also correlates with abdominal fat distribution and is associated with ill health [9]. Hip circumference (HC) provides additional valuable information regarding gluteofemoral muscle mass and bone structure [10]. In adults, waist-hip ratio (WHR) >1 in males and >0.85 in females and waist circumference (WC) ≥94 in males and ≥80 in females indicates obesity [6]. WC can be influenced by food intake and cultural and social issues can interfere with getting an optimal WC and HC measured, especially in older female children. Thus, there is a need for more acceptable and reliable indicators of obesity and overweight.

Neck circumference is a novel anthropometric measurement that appears to be significantly correlated with indices of adiposity and abdominal obesity and hence is an indicator of metabolic risk in obese children [11]. If so, it can be used as a simple and time-saving tool for obesity detection in large population-based studies in both children and adults. Also, the practical and cultural issues met with measuring waist and hip circumference, especially in female adolescents, can be circumvented.

The present study intended to measure the neck circumference of school children aged 6 to 16 years and assess its correlation with BMI as well as waist circumference, hip circumference, and waist-hip ratio. We also tried to determine the age- and sex-specific optimal cutoff points for neck circumference in identifying obesity and overweight, using WHO BMI centile charts.

Materials and methods

This school-based cross-sectional study was performed on children aged 6-16 years studying in the primary and secondary schools within one educational zone, randomly selected from the district of Alappuzha, Kerala, South India. A minimum sample size of 1767 was required, after considering a 20% dropout. The subjects were selected by multistage random sampling. A prior sanction was obtained from the institutional ethics committee, concerned government authority, and school authorities. Informed consent from parents and assent from older children were also sought. Children with chronic systemic illnesses, skeletal abnormalities, and goiter were excluded from our study.

Study variables were weight, height, BMI, neck circumference**,** waist circumference (WC)**,** hip circumference (HC), waist-hip ratio (WHR). Trained interns were recruited for getting the measurements. Repeat measurements and cross-checking were randomly performed daily to ensure minimum intra- and interobserver variability. When variability was more than 0.5 CMs, reinforcement of training in performing the measurements was done. Weight was measured using a digital weighing machine corrected to the nearest 0.1kg. Height was measured using a portable stadiometer following the standard technique and the observed value was corrected to the nearest centimeter. BMI was calculated as weight in Kg/height in $metre^2$.WC was measured with a non-stretchable measuring tape horizontally connecting the midpoints between the lower costal margin and anterior superior iliac spine in the midaxillary line on each [12,13]. HC was measured along the levels of the greater trochanter [14]. Neck circumference was measured horizontally midway along the neck, horizontally connecting the mid-cervical spine and a point just below the cricoid cartilage with the person standing and looking straight forward [15,16]. BMI charts of WHO were used as standards for comparison.

Study setting

All primary and secondary schools under the jurisdiction of the local self-government of Ambalappuzha, who consented to the study, were selected.

Statistical analysis

Data were entered in MS EXCEL and analyzed with the SPSS software. Continuous variables were expressed in terms of mean and deviation for each age, separately for both genders [17]. Discrete variables were presented as a percentage [18]. Spearman's rho correlation coefficient was used to find the correlation between neck circumference and other variables and a *P*-value of less than 0.05 was considered significant [19]. Kendell's coefficient of concordance was determined for BMI, NC, and WC. ROC analysis was employed to obtain the cutoff values for NC in each age group [20].

Results

A total of 1797 students aged 6 to 16 years were included in the study. Among them, 50.9% (914) were males and 49.1% (883) were females (Table 1).

Table 1: Age- and gender-wise distribution of the study population

Age (yrs)	Male	Female	Total (%)	Age yrs.	Male	Female	Total (%)
6	37	30	67 (3.7)	12	75	94	169 (9.4)
7	85	93	178 (9.9)	13	74	72	146 (8.1)
8	100	85	185 (10.3)	14	90	99	189 (10.5)
9	105	83	188 (10.5)	15	94	73	167 (9.3)
10	120	118	238 (13.2)	16	39	19	58 (3.2)
11	95	117	212 (11.8)	Total	914	883	1797(100)

All age groups had a relatively uniform representation except for the extreme ones. In the older children, this was due to concerns of parents regarding loss of study time if participating in the study and some cases, religious reasons, which prevented them from giving consent. In the 6-year age group, this was because of the small number of students in the schools as many of this group were still in anganwadi or preprimary schools. Both genders were almost equally represented with a slight preponderance of males (Table 2).

Table 2: Age- and gender-wise mean (with standard deviation) of various anthropometric indices

Age (yrs)	Male					Female				
	BMI (SD)	WC,CM (SD)	HC,CM (SD)	NC,CM (SD)	WHR (SD)	BMI (SD)	WC,CM (SD)	HC,CM (SD)	NC,CM (SD)	WHR (SD)
6	14.8 (2.7)	52.8 (7.1)	61.3 (6.4)	25.1 (1.8)	0.86 (0.05)	14.2 (1.7)	53.2 (4.8)	61.5 (4.9)	25 (1.2)	0.87 (0.05)
7	15.0 (2.5)	54.8 (7.0)	63.3 (6.4)	26.0 (2.1)	0.87 (0.05)	14.5 (2.2)	53.9 (7.2)	62.8 (5.6)	24.8 (1.6)	0.86 (0.07)
8	15.3 (2.7)	55.8 (7.2)	64.8 (7.1)	26.1 (2.0)	0.86 (0.04)	15.3 (2.5)	56.2 (6.6)	67.0 (6.1)	25.3 (1.6)	0.84 (0.05)
9	15.7 (2.8)	57.4 (7.8)	67.7 (7.1)	26.6 (2.1)	0.85 (0.05)	15.2 (2.8)	57.2 (7.2)	69.0 (6.8)	26.0 (1.9)	0.83 (0.06)
10	16.1 (3.1)	58.8 (8.3)	69.7 (7.6)	27.6 (2.0)	0.84 (0.05)	15.8 (3.1)	57.7 (7.4)	71.5 (8.0)	26.6 (1.9)	0.81 (0.04)
11	16.5 (3.7)	61.4 (10.2)	71.8 (8.7)	27.9 (2.4)	0.85 (0.06)	16.1 (3.0)	59.2 (6.7)	73.6 (7.2)	27.2 (1.7)	0.81 (0.05)
12	17.1 (3.4)	63.4 (10.2)	74.7 (8.6)	28.6 (2.0)	0.85 (0.06)	16.9 (3.7)	61.9 (7.2)	77.5 (8.2)	27.9 (2.0)	0.80 (0.05)
13	16.7 (3.3)	63.5 (9.9)	86.0 (8.0)	29.1 (2.1)	0.82 (0.10)	18.3 (3.5)	64.3 (8.6)	82.2 (8.4)	28.9 (2.1)	0.78 (0.05)
14	17.6 (3.5)	66.3 (10.4)	81.1 (9.1)	30.6 (2.3)	0.82 (0.06)	18.0 (2.8)	62.5 (8.3)	81.3 (6.5)	28.7 (1.5)	0.77 (0.07)
15	18.0 (2.7)	66.7 (8.1)	83.6 (7.0)	31.8 (2.0)	0.80 (0.06)	19.3 (2.9)	66.2 (7.1)	84.0 (5.9)	29.4 (1.6)	0.79 (0.05)
16	18.2 (2.8)	67 (8.2)	85.2 (6.9)	32.2 (1.9)	0.79 (0.05)	18.9 (2.8)	63.4 (6.6)	82.4 (6.3)	29.3 (2.0)	0.77 (0.05)

Various anthropometric measurements showed varying trends across different ages and genders. BMI consistently increased with age in males. The mean BMI varied from 14.8 (2.7) kg/m^2 in 6-year-old males to 18.2 (2.8) kg/m^2 among the 16-year-old males. Among females, the corresponding values were 14.2 (1.7) kg/m^2 and 18.9 (2.8) kg/m^2, respectively. A consistent increase in BMI was seen with age in females until 13 years of age. Until 12 years of age, boys had higher BMIs, and after that, girls dominated.

WC, HC, and NC increased with age. While no relation to gender was noted in the case of WC, the HC was consistently higher in females and the NC was higher in males in all age groups. WHR remained almost the same (0.85) until 12 years of age, and then came down to 0.80. In girls, it steadily fell from 0.87 at 6 years of age to 0.77 at 16 years of age. The prevalence of obesity and overweight were 3.3 % (59) and 6.6% (119), respectively in our study population. Both were higher among boys than girls (4.4% vs. 2.2% and 8% vs. 5.2%, respectively).

The correlation of NC with BMI and other indices such as BMI percentiles, WC, HC, and WHR, as determined by Spearman's rho correlation for various ages and genders, is given in Table 3.

Table 3: Correlation between NC and other indices

Age	Male					Female				
	BMI (+)	WC (+)	HC (+)	WHR +/-	BMI Centile (+)	BMI (+)	WC (+)	HC (+)	WHR +/-	BMI Centile (+)
6	0.8 *	0.8 *	0.9 *	-0.2 *	0.4 *	0.8 *	0.5 *	0.4 **	0.32 ***	0.4 **
7	0.7 *	0.7*	0.8 *	0.02 ***	0.7 *	0.7 *	0.7 *	0.7 *	0.2 ***	0.7 *
8	0.7 *	0.7 *	0.7 *	0.3 **	0.7 *	0.7 *	0.6 *	0.6 *	0.2 ***	0.7 *
9	0.7 *	0.7 *	0.7 *	0.3 **	0.7 *	0.6 *	0.6 *	0.7 *	0.2 ***	0.6 *
10	0.7 *	0.7 *	0.7 *	0.3 **	0.7 *	0.7 *	0.8 *	0.8 *	0.2 ***	0.7 *
11	0.8*	0.8 *	0.8 *	0.3 *	0.8 *	0.7 *	0.6 *	0.7 *	-0.1 ***	0.7 *
12	0.8 *	0.8 *	0.8 *	0.3 ***	0.8 *	0.8 *	0.8 *	0.8 *	0.1 **	0.8 *
13	0.8 *	0.7 *	0.8 *	0.2 ***	0.8 *	0.6 *	0.7 *	0.7 *	0.2 **	0.6 *
14	0.7 *	0.7 *	0.8 *	0.1 ***	0.7 *	0.6 *	0.6 *	0.6 *	0.2 **	0.6 *
15	0.6 *	0.5 *	0.5 *	0.2 ***	0.5 *	0.7 *	0.6 *	0.7 *	0.3 **	0.7 *
16	0.6 *	0.6 *	0.7 *	-0.2 ***	0.6 *	0.7 *	0.7 *	0.8 *	0.1 ***	0.7 **

* P<0.001, ** P<0.05, *** P>0.05

NC showed a significant, positive correlation with BMI and BMI centiles as well as with WC and HC in all age groups of males and females. This was not the case with WHR.

Regarding BMI, the correlation coefficient varied from +0.6 to +0.8 with a P-value of <0.001 among both boys and girls. A similar observation could be made for WC and HC except in 15-year-old boys. WHR was not significantly positively correlated with NC in any of the age groups of boys or girls.

Using ROC, the age- and gender-specific neck circumference cutoffs were determined for both overweight and obesity per the WHO centile charts. Table 4 shows these values along with the sensitivity and specificity rates. A sensitivity between 87.5% and 100% was noted in all groups, except in 7-year-old boys (for whom it was only 70%). The specificity varied from 52.2% to 88.9% (Table 4).

Table 4: Neck circumference cutoffs for overweight and obesity

Age	Male				Female			
	Overweight		Obesity		Overweight		Obesity	
	Cutoff (cm)	Sensitivity / Specificity (%)	Cut Off (Cm)	Sensitivity / Specificity (%)	Cut Off (cm)	Sensitivity / Specificity (%)	Cut Off (cm)	
6	25.3	100/68.7	25.8	100/76.5	24.9	100/64.3	25.6	100/79.3
7	26.1	70/72.9	26.8	60/73.8	25.3	100/79.3	25.8	100/83.1
8	26.3	88.9/76.7	27.3	100/85.3	25.8	80/76.3	26.3	100/82.7
9	27.3	87.5/76.1	27.8	80/77	26.3	100/75.6	27.3	100/86.3
10	27.8	92.9/67	28.8	100/76.1	26.8	10065.1	27.8	100/74.4
11	28.3	100/77.5	29.3	83.3/82	27.3	100/65.1	28.3	100/78.4
12	29.3	100/71.2	29.8	100/82.6	28.8	100/75.3	28.8	66.7/73.6
13	29.8	100/73.8	30.3	100/77.8	29.3	87.5/71.4	29.8	100/74.6
14	30.8	100/58.7	31.3	75/66.3	29.8	100/78.1	30.3	100/87.8
15	31.8	100/52.2	32.2	100/64.5	30.1	100/79.4	Not possible	
16	32.8	100/56.8	Not possible		31.3	100/88.9	Not possible	

Kendall's coefficient of concordance (w) was calculated as 0.996 for BMI and NC (P<0.001) and 0.998 for NC and WC (P<0.001). Statistically, there was a very good agreement between NC, BMI, and WC.

Discussion

Malnutrition is a universal public health problem in both children and adults globally, categorized as over- and under-nutrition. United Nations (UN) General Assembly proclaimed 2016–2025 the United Nations Decade of Action on Nutrition. This decade holds an unprecedented opportunity for addressing all forms of malnutrition. To further tackle the double and triple burdens of malnutrition, early screening, and identification of at-risk children, including those already with malnutrition, is essential.

BMI is the widely used anthropometric index to identify overweight and obesity. Apart from the difficulties in calculating it, BMI does not give any indication of the distribution or amount

of fat in one's body. The amount of adipose tissue can vary considerably within a narrow range of BMI. Since the metabolic complications are directly related to upper body distribution of fat, we need better indicators of overall obesity and central obesity. Hydrostatic (underwater) weighing, air displacement plethysmography, imaging techniques like ultrasound, Dual-energy X-ray absorptiometry (DXA), near-infrared interactance are some of the more accurate methods for assessing total body fat and its distribution but cannot be used at population levels due to various reasons. For community-level screening, we need sensitive, reliable, easy, and acceptable screening tools. Neck circumference appears to be a promising one.

In our present study, a significant positive correlation was observed between neck circumference (NC) and BMI as well as waist circumference (WC) and hip circumference (HC) in schoolchildren aged 6 – 16 years of both genders. Age and gender-specific cut-off values could be obtained with a sensitivity of more than 80% in all the groups. No consistent correlation was noted between NC and WHR.

Nafiu et al. [20] studied 1102 children aged 6-18 years and found that NC was significantly correlated with indices of adiposity and can reliably identify children with high BMI. He could also determine NC cut-offs for obesity and overweight for different age groups and both genders. In their studies among Iranian schoolchildren, Taheril et al. [21], and on Indian children, Lipilekha et al. [22] made similar observations. Katz et al. [23] could provide age and sex standardized reference values of NC threshold for overweight and obesity for Canadian children [24]. Interestingly, Kim et al. [24] did not strongly support the use of NC measurement as a useful screening tool for classifying childhood overweight/obesity.

Hassan et al. [25] observed that NC is a reliable indicator of central obesity and it showed significantly positive correlations with BMI, WC, HC, and systolic and diastolic blood pressure, but not with dyslipidemia in children.

The cut-off values in our study differ from those of the above-mentioned studies indicating the need for establishing region-specific standards for better utilization of this screening tool.

Limitations

There is a fairly low representation of the ages of 6-16 years due to practical issues.

Recommendations

A single large cohort of children may be followed up over the years starting from their school entry to their leaving higher secondary school, to study the pattern of increase in NC. Thus, reference charts for NC for different ages could be prepared. Future research can be planned to assess the correlation of Neck Circumference with more objective measures of central obesity, such as ultrasound-guided visceral fat estimation.

Conclusions

Neck circumference is significantly correlated with measures of obesity, such as BMI, WC, and HC, and can be utilized as a screening tool for central obesity to detect children at high risk for metabolic complications of obesity and sleep apnea. Region-wise charts of NC for different ages and both genders should be made available.

References

1. Dietz WH, Robinson TN. Clinical practice. Overweight children and adolescents . N Engl J Med. 2005;352:2100–9.
2. Gill P, Baur LA, Bauman AE, Steinbeck KS. Establishing a standard definition for child overweight and obesity worldwide: International survey. Br Med J. 2000;320:1240–3.
3. Cornier, Marc-Andre, Despre´s, Jean-Pierre Davis N, Davis DA, Klein S, Lamarche B, Lopez-Jimenez, Francisco Rao G, St-Onge M-P, et al. Assessing Adiposity A Scientific Statement From the American Heart Association. Circulation. 2011;124:1996–2019.
4. Vucenik I, Stains JP. Obesity and cancer risk: Evidence, mechanisms, and recommendations. Ann N Y Acad Sci. 2012;1271:37–43.
5. Flodmark CE, Lissau I, Moreno LA, Pietrobelli A, Widhalm K. New insights into the field of children and adolescents' obesity: The European perspective. Int J Obes. 2004;28:1189–96.
6. Nelson text book of Paediatrics,21th edition. 2019. 345–346 p.
7. Gupta AK AA. Childhood obesity and hypertension. Indian Pediatr. 1990;27:333–7.
8. Laffel L SB. Epidemiology, presentations, and diagnosis of type 2 diabetes mellitus in children and adolescents. UpToDate. 2013;
9. Kasmini K, Idris MN, Fatimah A, Hanafiah S, Iran H, Asmah MN. Prevalence of overweight and obese school children aged between 7 to 16 years amongst the major 3 ethnic groups in Kuala Lumpur, Malaysia. Asia Pac J Clin Nutr. 1997;6:172–4.
10. Nafiu OO, Burke C, Lee J, Voepel-Lewis T, Malviya S, Tremper KK. Neck circumference as a screening measure for identifying children with high body mass index. Pediatrics. 2010;126.
11. Vedavati S, Jayashree R, Mohammad R. Erratum: Prevalence of overweight and obesity in affluent adolescent girls in Chennai in 1981 and 1998 (Indian Pediatrics (August 2003). Indian Pediatr [Internet]. 2003;40:926.
12. Aswathappa J, Garg S, Kutty K, Shankar V. Neck circumference as an anthropometric measure of obesity in diabetics. N Am J Med Sci. 2013;5:28–31.
13. Hassan Farman W, M Majeed H. Overweight and Obesity Among Children and Adolescents in Baladrouz City. Diyala J Med. 2019;16:31–8.
14. Cintra IP ; Passos MAZ ; Santos LC ; Machado HC and Fisberg M. Waist -to- Height Ratio Percentiles and Cutoffs for Obesity: A Cross-sectional Study in Brazilian Adolescents. J Heal Popul NUTR. 2014;32:411–9.
15. WHO. Obesity.Preventing and managing global epidemic. 2000;153–238. Available from: http://whqlibdoc.who.int/trs/WHO_TRS_894_(part4).pdf
16. Flynn JT, Daniels SR, Hayman LL, Maahs DM, McCrindle BW, Mitsnefes M, et al. American Heart Association Atherosclerosis, Hypertension and Obesity in Youth Committee of the Council on Cardiovascular Disease in the Young. Update: Ambulatory blood pressure monitoring in children and adolescents: A scientific statement from the Americ. Hypertension. 2014;63.
17. Algina J, Keselman HJ. Comparing squared multiple correlation coefficients: Examination of a confidence interval and a test significance. Psychol Methods. 1999;4:76–83.
18. Bonett DG. Meta-Analytic Interval Estimation for Bivariate Correlations. Psychol Methods. 2008;13:173–81.
19. Bobko P. Correlation and regression: Applications for industrial organizational psychology and management. Thousand Oaks, CA Sage Publ. 2001;5:200–1.
20. Nafiu OO, Burke C, Lee J, Voepel-Lewis T, Malviya S, Tremper KK. Neck circumference as a screening measure for identifying children with high body mass index. Pediatrics [Internet]. 2010;126. Available from:
21. Taheri M, Kajbaf TZ, Taheri MR, Aminzadeh M. Neck circumference as a useful marker for screening overweight and obesity in children and adolescents. Oman Med J. 2016;31:170–5.
22. Patnaik L, Pattnaik S, Rao EV, Sahu T. Validating neck circumference and waist circumference as anthropometric measures of overweight/obesity in adolescents. Indian Pediatr. 2017;54:377–80.
23. Katz SL, Vaccani JP, Clarke J, Hoey L, Colley RC, Barrowman NJ. Creation of a reference dataset of neck sizes in children: Standardizing a potential new tool for prediction of obesity-associated diseases? BMC Pediatr. 2014;14.
24. Kim Y, Lee J-M, Laurson K, Bai Y, Gaesser GA, Welk GJ. Accuracy of Neck Circumference in Classifying Overweight and Obese US Children. ISRN Obes. 2014;2014:1–6.
25. Hassan NE, Atef A, El-Masry SA, Ibrahim A, Al-Tohamy M, Rasheed EA, et al. Is neck circumference an indicator for metabolic complication of childhood obesity? Maced J Med Sci [Internet]. 2015;3:26–31.

This paper has been checked for language accuracy by JOSAM editors.
The National Library of Medicine (NLM) citation style guide has been used in this paper.

J Surg Med. 2021;5(12):1188-1192.
DOI: 10.28982/josam.945513

Research article

Journal of Surgery and Medicine
e-ISSN=2602-2079

Radiologic and clinical features of infection related cytotoxic lesions of corpus callosum splenium in adults

Mehmet Ali İkidağ

SANKO University Medical School, Department of Radiology, Gaziantep, Turkey

ORCID ID of the author(s)
MAİ: 0000-0003-4004-9645

Corresponding Author
Mehmet Ali İkidağ
SANKO Üniversitesi Sani Konukoğlu Uygulama ve Araştırma Hastanesi Radyoloji Bölümü, Ali Fuat Cebesoy 45, Şehitkamil, Gaziantep, Turkey
E-mail: mikidag@hotmail.com

Ethics Committee Approval
Ethical Committee of SANKO University, Gaziantep, approved this study (Date: 21.11.2018, Decision Number: 03).
All procedures in this study involving human participants were performed in accordance with the 1964 Helsinki Declaration and its later amendments.

Conflict of Interest
No conflict of interest was declared by the authors.

Financial Disclosure
The authors declared that this study has received no financial support.

Published
2021 November 20

Abstract

Background/Aim: The cytotoxic lesion of corpus callosum splenium (CLCCS) is a clinical-radiologic syndrome that typically manifests in children. It is characterized by restricted diffusion in the splenium of the corpus callosum on magnetic resonance imaging, and accompanying symptoms of encephalopathy. There are a few case reports regarding the adult population in the literature, and only a couple of these are related to febrile illness in adults. We aimed to evaluate the clinical and the radiologic characteristics of infections related to CLCCS in adults.

Methods: For this case series study, we reviewed the MRI examinations that were performed in our hospital between 2014 and 2019 to identify cases with corpus callosum splenium lesions related with febrile diseases in adults. We excluded the cases with demyelinating diseases, trauma, arterial or venous occlusive diseases, metabolic-toxic diseases, and posterior reversible encephalopathy syndrome (PRES), patients who had alcohol or drug abuse, or known malignancies. The admission dates, symptoms within the prodromal period, physical and laboratory findings, electroencephalograms, MRI features, medications and patient outcomes were recorded. Corpus callosum involvement on MRI was classified as Type 1 if lesions were limited to splenium, and Type 2 if pericallosal white matter extension was present.

Results: Seven patients (four males, three females, and ages ranging from 18 to 33 years with a mean of 26.4 years) were included in the study. All patients experienced prodromal symptoms such as fever (n=7), nausea (n=5), vomiting (n=4), diarrhea (n=4) and abdominal discomfort (n=3). Neurological symptoms included drowsiness (n=4), speech disorder (n=2), impairment of consciousness (n=4), lower extremity weakness (n=2), and seizures (n=1). Neurological examination revealed confusion (n=4), nuchal rigidity (n=2), and ataxia (n=2). In one patient, the blood culture was positive for *Staphylococcus epidermidis*, and the stool culture was positive for *Enterococcus species*. MRI findings of all patients revealed Type 1 oval (n=4) or round (n=3) shaped corpus callosum splenium lesions that appeared hyperintense on T2 and FLAIR images with diffusion restriction. None of our patients had band-like Type 1 or Type 2 lesions. Clinical relief was observed in 2 days in six patients, however, rapid clinical deterioration resulting in death occurred in one patient.

Conclusion: The leading symptoms in adults are fever and gastrointestinal disturbances including, nausea, vomiting, and diarrhea, while neurological examinations mostly reveal confusion, nuchal rigidity, and ataxia. In adult patients, restricted diffusion on MRI is usually limited to splenium, and pericallosal white matter is usually not involved. Mostly encountered in autumn and winter, encephalitis/encephalopathy with diffusion restriction in the splenium of corpus callosum in an adult febrile patient usually has a good prognosis, although it may lead to severe outcomes, and even result with death. Clinicians should be aware that, if even Type 1, isolated corpus callosum diffusion restriction on MRI may has catastrophic results in a febrile patient. Further studies may be useful to delineate the mechanism and its relationship with higher bilirubin levels in patients with CLCCS.

Keywords: Corpus callosum, Infection, MRI

How to cite: İkidağ MA. Radiologic and clinical features of infection related cytotoxic lesions of corpus callosum splenium in adults. J Surg Med. 2021;5(12):1188-1192.

Introduction

Cytotoxic lesion of corpus callosum splenium (CLCCS) is a clinical-radiologic syndrome that typically manifests in children. It is characterized by restricted diffusion in the splenium of the corpus callosum on magnetic resonance imaging (MRI), and accompanying symptoms of encephalopathy, ranging from headache to seizures. There is a wide spectrum of disorders responsible of CLCCS, including bacterial or viral infections, malignancies, drugs, and trauma, toxic or metabolic diseases. Though most of these conditions have favorable outcomes, some may have severe prognosis [1, 2].

Prior work in the literature consists of case studies for radiologic and clinical features of CLCCS in the adult population. Only a few of these are related to febrile illness in adults, as most focus on children. In this work, we aim to close this gap by evaluating the clinical and the radiologic characteristics of infections related to CLCCS in adults. We present our findings for adult febrile patients characterized by restricted diffusion in the splenium of the corpus callosum.

Materials and methods

We reviewed the brain MRI studies in our radiology database system to identify the cases with lesions of the corpus callosum from 2014 to 2019. The Ethics Committee of SANKO University, Gaziantep, approved this study (Date: 21.11.2018, Decision Number: 03).

We obtained patient demographics and clinical and laboratory data from the institutional database. We excluded the cases with known or new onset demyelinating diseases such as multiple sclerosis, patients with trauma, arterial or venous occlusive diseases, metabolic-toxic diseases, and posterior reversible encephalopathy syndrome (PRES), patients who had alcohol or drug abuse, or known malignancies. The admission dates, symptoms within the prodromal period, physical and laboratory findings including cerebrospinal fluid analysis if exists, electroencephalograms, MRI features, medications and patient outcomes were recorded.

All MRI studies were performed with a Siemens Magnetom Avanto, a 1.5 Tesla device, including vendor's preset T1 and T2 weighted sequences, fluid attenuated inversion recovery (FLAIR), and diffusion weighed imaging (DWI), apparent diffusion coefficient (ADC) map and post contrast T1 studies. All patients were given Dotarem (gadoterate meglumine, Guerbet) as a paramagnetic intravenous contrast agent. Radiological images were evaluated by two radiologists who were experienced in MRI for at least 15 years. The shape of the splenial lesion, other involved parts of the corpus callosum, pericallosal white matter, and additional findings on MRI were noted. Callosal lesions were classified as Type 1 if the lesion was limited to the splenium, including round, oval or band-like signal changes, and Type 2 if pericallosal white matter was involved.

Statistical analysis

The findings in the patient population were given in numbers and percentages.

Results

Seven patients were included in the study (four males (57%), three females (42%), and ages ranging from 18 to 33 years with a mean of 26.4 years). There were no notable diseases in any of the cases except for one. That patient was under treatment for hypothyroidism. Table 1 presents our findings.

All patients experienced prodromal symptoms. All had fever (axillary temperature >38ºC) within a week of hospital admission and their final diagnosis were acute encephalitis/encephalopathy. Prodromal symptoms were nausea (n=5, 71%), vomiting (n=4, 57%), diarrhea (n=3, 42%), abdominal discomfort (n=3, 42%), sore throat (n=2, 28%), muscle weakness (n=2, 28%), headache (n=2, 28%), and arthralgia (n=1, 14%). Neurological symptoms included drowsiness (n=4, 57%), speech disorder (n=2, 28%), impairment of consciousness (n=4, 57%), lower extremity weakness (n=2, 28%), and seizures (n=1, 14%). Neurological examination revealed confusion (n=5, 71%), nuchal rigidity (n=2, 28%), and ataxia (n=2, 28%). Laboratory findings revealed elevation in white blood cell count (n=6, 85%), C-reactive protein (n=4, 57%), erythrocyte sedimentation rate (n=3, 42%), liver function tests (n=5, 71%), fibrinogen (n=2, 28%), procalcitonin (n=1, 14%), and bilirubin (n=3, 42%). Electroencephalography was performed on four patients, and all were normal. Lumbar puncture and cerebrospinal fluid (CSF) analysis was performed on three patients. Two had slightly and the other had significantly elevated protein levels. Glucose levels and cell counts of cerebrospinal fluid were normal, and cultures were sterile.

One patient died (number 6). She was the only patient who had seizures on admission day and during hospitalization. Rapid clinical deterioration, status epilepticus, sepsis, acidosis, and respiratory failure occurred; she died on the fifth day of hospitalization following intubation. Her blood culture was positive for *Staphylococcus epidermidis*, and her stool culture was positive for *Enterococcus species*. No responsible pathogens were identified in the other patients. The patients were admitted to the hospital in September (n=2), November (n=1), December (n=2), June (n=1) and July (n=1). All initial MRI examinations were performed within the first two days of hospital admission, and the follow-up MRI exams were done after 19-38 days, except for the patient who died.

Corpus callosum involvement was limited to the splenium in all patients. All patients had Type 1 oval (n=4, 57%) or round (n=3, 42%) shaped corpus callosum splenium lesions that appeared hyperintense on T2 and FLAIR images with diffusion restriction (Figures 1 and 2). None of our patients had a band like Type 1 or Type 2 lesion. All patients underwent postcontrast T1 studies, but there was no contrast enhancement in any of the lesions. Lesions were completely resolved in six patients (85%) at control MRI studies.

All patients were treated with antibiotics and supportive care. Five patients received ceftriaxone, one received ampicillin/sulbactam. Patient 6 was treated with ceftriaxone, vancomycin, antiepileptic medication, and prednisolone. Acyclovir was also added to the therapy for patient 6 because she did not respond to antibiotics. Clinical relief was observed in two days in six patients, and full recovery was achieved.

Table 1: Demographics, clinical, radiologic and laboratory findings of patients with CLCC

	Age and Gender	Admission Month	Complaints	Neurological manifestations	Physical examination	Time of MRI (days)	Lesion Type	Laboratory	EEG	CSF Findings	Follow up MRI (days)	Outcome
1	28,M	November	Fever, nausea, vomiting,	Speech disorder, drowsiness	Confusion	1	1 round	Elevated WBC, CRP, Fibrinogen,	N	Slightly high protein	38	Complete Recovery
2	33,M	September	Fever, nausea, vomiting, diarrhea, abdominal pain	Drowsiness	Ataxia	2	1 oval	Elevated WBC, CRP, ALT, AST, Bilirubin	N	-	33	Complete Recovery
3	18,F	September	Fever, abdominal pain, nausea, diarrhea,	Impairment of consciousness, drowsiness, lower extremity weakness	Confusion, nuchal rigidity	1	1 round	Elevated WBC, CRP, ESR, ALT	N	Markedly high protein	19	Complete Recovery
4	27,F	December	Fever, sore throat, muscle weakness	Speech disorder	Ataxia	1	1 oval	Elevated ESR, LDH, Bilirubin	N	-	30	Complete Recovery
5	25,M	December	Fever, nausea, vomiting, arthralgia	Impairment of consciousness, lower extremity weakness	Confusion	1	1 round	Elevated WBC, ALT, AST, GGT, LDH, Bilirubin	-	-	27	Complete Recovery
6	33,F	July	Fever, abdominal pain, diarrhea, nausea, vomiting	Headache, impairment of consciousness, drowsiness, seizures	Confusion, nuchal rigidity + Extensor plantar reflex	1	1 oval	Elevated WBC, CRP, ESR, ALT, AST, Fibrinogen, Procalcitonin	-	Slightly high protein	-	Died
7	21,M	June	Fever, muscle weakness, sore throat	Headache, impairment of consciousness	Confusion	1	1 oval	Elevated WBC	-	-	33	Complete Recovery

CLCC: Cytotoxic lesion of corpus callosum, EEG: Electroencephalography, CSF: Cerebrospinal fluid, WBC: White blood cell count, CRP: C-reactive protein, ALT: Alanine transaminase, AST: aspartate transaminase, ESR: Erythrocyte sedimentation rate, LDH: Lactate dehydrogenase, GGT: Gamma-glutamyl transferase

Figure 1: Initial Diffusion MRI (a) and corresponding ADC map (b) of Patient 1. There is a round Type 1 splenial lesion in the center of corpus callosum splenium that shows diffusion restriction. Control Diffusion MRI (c) and ADC map (d) show normal signal

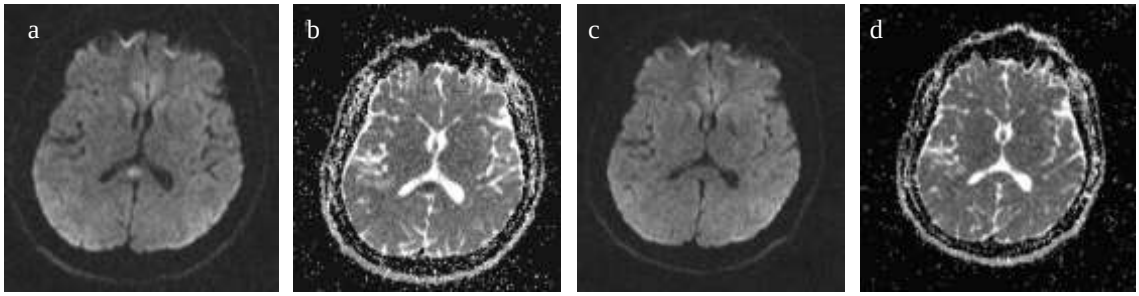

Figure 2: Diffusion weighted MRI and ADC maps of initial MRI examinations of Patient 2 (a, and b), Patient 3 (c and d), Patient 4 (e and f), Patient 5 (g and h), Patient 6 (i and j), and Patient 7 (k and l), respectively, that show diffusion restriction characterized by a high signal in DWI, and a low signal in ADC maps

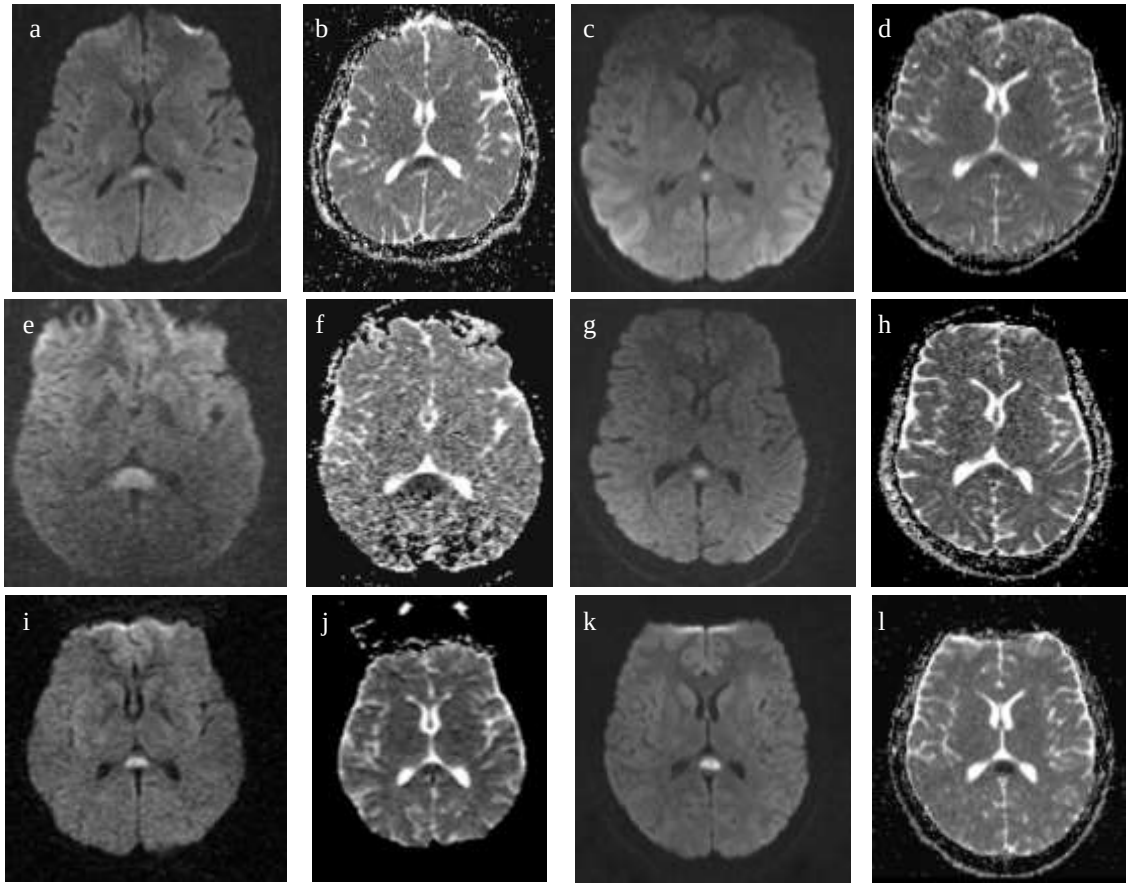

Discussion

Reversible splenial lesions were first described in patients under antiepileptic therapy. Then, an association with encephalitis/encephalopathy that were caused by a few pathogens, including rotavirus, influenza and *E. Coli* were reported [3-10]. In their study including 15 patients, most of which consisted of children, Tada et al. [11] reported that reversible splenial diffusion restriction might be observed together with mild encephalitis/encephalopathy, following an infection. The involvement of corpus callosum splenium and the presence of diffusion restriction was named as mild encephalitis/encephalopathy with reversible splenial lesion (MERS), reversible splenial lesion syndrome (RESLES) or reversible splenial lesion during febrile illness (RESLEF). Recently, it has been depicted that diffusion restriction in the splenium may be due to numerous bacterial or viral infections, malignancies, drugs, trauma, toxic or metabolic diseases, and it was proposed to name this entity as cytotoxic lesions of corpus callosum (CLCC), because not all these conditions have full clinical recovery [12-18]. Though the mechanism is not precisely depicted, cell-cytokine interactions leading to high extracellular glutamate, trapped water in the cells, and cytotoxic edema are held responsible [18].

In our study, fever and gastrointestinal symptoms were leading in the prodromal period, including nausea and vomiting, diarrhea, and abdominal discomfort. Prodromal symptoms, neurological evaluation and clinical outcomes in our patients did not differ from the previous studies at large [2, 10]. When compared with the children, these findings also show similarity, except for seizures, which is the most frequent admission reason in children [1]. Only one of our patients had seizures, and other initial clinical, laboratory and MRI findings were similar. Seizure is related to poor prognosis [2]. This finding correlates with our study, as the only patient presenting with seizure died. Also, none of our adult patients showed visual disturbances, although it is relatively common in children [1]. In a previous study, impairment of consciousness was correlated with poor prognosis [2]. Among four of our cases who had that symptom, three fully recovered and one died.

It is reported that nearly half of the patients showed diffuse slow waves on EEG studies and that this finding was correlated with poor prognosis [2]. In our study, four patients underwent EEG (all fully recovered cases) and all were reported as normal. This may be related with the spared pericallosal white matter in our patients.

Analysis of CSF was available in three patients, two had slightly and one had significantly elevated protein levels. One of the patients with slightly elevated protein levels died, the others survived without any sequelae. It is reported that CSF studies are nonspecific in this patient population, however, one study depicted high interleukin 6 levels and suggested that immunological response may be related with pathogenesis [19, 20].

Three of our patients had elevated serum bilirubin levels and one died. Apart from bilirubin encephalopathy that is encountered in the neonatal period, we have not been able to find any data about high serum bilirubin levels and encephalitis/encephalopathy. This subject may be delineated with further studies.

Previous studies reveal that Type 1 splenium lesions have favorable prognosis when compared with Type 2 lesions. In our study, all our patients had type 1 lesions, although one had a catastrophic outcome resulting with death. This finding suggests that not all Type 1 splenium lesions will recover completely, and clinicians should be aware of this entity. In their study consisting of three patients with reversible splenial lesions caused by antiepileptic treatment, da Rocha et al. [21] reported that one of the lesions showed contrast enhancement, and according to our knowledge, this is the only case in the literature that showed contrast enhancement. None of our patients had contrast enhancement in post-contrast studies. Previous studies reveal that normalization of pathologic signal changes in isolated splenial lesions occur within 1 week [10, 11]. The earliest control MRI in our group was on the 19th day, all surviving patients had normal signal intensity in the splenium in their control MRI examinations.

Patient 6 was a 33-year-old female, with the only one admitted with seizure. She was under treatment for hypothyroid for 3 years. She did not have any history of substance or alcohol use. Before the admission, she experienced stomachache, diarrhea, and fever for 3 days. She was brought to ER with confusion and developed seizures. After hospitalization, rapid clinical deterioration resulting with coma, acidosis, and sepsis occurred, leading to intubation, and a few days later, death. According to the clinical course, the findings could suggest acute disseminated encephalomyelitis (ADEM) or Marchiafava-Bignami disease (MBD), but MRI findings were unlikely, because MBD typically starts from the body of corpus callosum and extends towards genu and splenium, callosal necrosis is usually seen, and contrast enhancement occurs in acute presentations [22]. Also, our patient did not have alcohol use or malnutrition, and she had normal serum B_{12} levels. In ADEM, corpus callosum is usually involved by the extension of neighboring white matter lesions. Though corpus callosum involvement may be up to 15%, isolated splenial lesion in ADEM has not been reported before [23].

Most our patients were admitted to the hospital in autumn and winter. These are the seasons which most viral diseases are encountered, and MERS with seasonal influenza infection was previously reported [7, 24, 25]. We have been able to identify a responsible pathogen in only 1 of 7 patients.

This is the largest case series including the adult population with infection-related corpus callosum splenium lesions from Turkey. In their study that focused on the etiology of splenial lesions, Balcik et al. [26] reported 5 infection-related cases (3 tuberculosis meningitis and 2 viral encephalitis), where the outcomes of the patients were not stated. There are also a few case reports from our country on the adult population [27-29].

Also, according to our knowledge, this is the first study that involves a case who died with an isolated splenial lesion.

Limitations

Small sample size is the major limitation of the present study. Also, a responsible pathogen was identified in only one of the 7 patients. The study was undertaken in a local tertiary

center, and the results may not represent the entire condition in other districts of Turkey.

Conclusions

Mostly encountered in autumn and winter, encephalitis/encephalopathy with diffusion restriction in the splenium of corpus callosum in an adult febrile patient usually has a good prognosis, though it may lead to severe outcomes, even death. The leading symptoms are fever and gastrointestinal disturbances including, nausea, vomiting, and diarrhea, while neurological examinations mostly reveal confusion, nuchal rigidity, and ataxia. In adult patients, restricted diffusion is usually limited to splenium, and pericallosal white matter is usually not involved. Clinicians should be aware that, if even Type 1, isolated corpus callosum diffusion restriction on MRI may have catastrophic results in a febrile patient. Further studies may be useful to delineate the mechanism and relationship of higher bilirubin levels in patients with CLCCS.

References

1. Yıldız AE, Maraş Genç H, Gürkaş E, Akmaz Ünlü H, Öncel İH, Güven A. Mild encephalitis/encephalopathy with a reversible splenial lesion in children. Diagn Interv Radiol. 2018; 24(2):108-12. doi: 10.5152/dir.2018.17319
2. Zhang S, Ma Y, Feng J. Clinicoradiological spectrum of reversible splenial lesion syndrome (RESLES) in adults: a retrospective study of a rare entity. Medicine (Baltimore). 2015; 94(6):e512. doi: 10.1097/MD.0000000000000512
3. Kim SS, Chang KH, Kim ST, Suh DC, Cheon JE, Jeong SW, et al. Focal lesion in the splenium of the corpus callosum in epileptic patients: antiepileptic drug toxicity?Am J Neuroradiol. 1999;20:125–9.
4. Polster T, Hoppe M, Ebner A. Transient lesion in the splenium of the corpus callosum: three further cases in epileptic patients and a pathophysiological hypothesis. J Neurol Neurosurg Psychiatry. 2001;70:459–63.
5. Maeda M, Shiroyama T, Tsukahara H, Shimono T, Aoki S, Takeda K. Transient splenial lesion of the corpus callosum associated with antiepileptic drugs: evaluation by diffusion-weighted MR imaging. Eur Radiol 2003;13:1902–90.
6. Kobata R, Tsukahara H, Nakai A, Tanizawa A, Ishimori Y, Kawamura Y, et al. Transient MR Signal changes in the splenium of the corpus callosum in rotavirus encephalopathy: value of diffusion-weighted imaging. J Comput Assist Tomogr. 2002;26:825–8.
7. Takanashi J, Barkovich A, Yamaguchi K, Kohno Y. Influenza encephalopathy with a reversible lesion in the splenium of the corpus callosum. Am J Neuroradiol. 2004;25:798–802.
8. Ito S, Shima S, Ueda A, Kawamura N, Asakura K, Mutoh T. Transient splenial lesion of the corpus callosum in H1N1 influenza virus-associated encephalitis/encephalopathy. Intern Med. 2011;50(8):915-8.
9. Mazur-Melewska K, Jonczyk-Potoczna K, Szpura K, Biegański G, Mania A, Kemnitz P, et al. Transient lesion in the splenium of the corpus callosum due to rotavirus infection. Childs Nerv Syst. 2015;31(6):997-1000.
10. Lin D, Rheinboldt M. Reversible splenial lesions presenting in conjunction with febrile illness: a case series and literature review. Emerg Radiol. 2017;24(5):599-604.
11. Tada H, Takanashi J, Barkovich AJ, Oba H, Maeda M, Tsukahara H, et al. Clinically mild encephalitis/encephalopathy with a reversible splenial lesion. Neurology. 2004;63(10):1854-8. doi: 10.1212/01.wnl.0000144274.12174.cb
12. Takayama H, Kobayashi M, Sugishita M, Mihara B. Diffusion-weighted imaging demonstrates transient cytotoxic edema involving the corpus callosum in a patient with diffuse brain injury. Clin Neurol Neurosurg. 2000;102(3):135-9.
13. Cecil KM, Halsted MJ, Schapiro M, Dinopoulos A, Jones BV. Reversible MR imaging and MR spectroscopy abnormalities in association with metronidazole therapy. J Comput Assist Tomogr. 2002;26(6):948–51.
14. Tha KK, Terae S, Sugiura M, Nishioka T, Oka M, Kudoh K, et al. Diffusion-weighted magnetic resonance imaging in early stage of 5-flourouracil-induced leukoencephalopathy. Acta Neuro Scand. 2002;106(6):379–86.
15. Kim JH, Choi JY, Koh SB, Lee Y. Reversible splenial abnormality in hypoglycemic encephalopathy. Neuroradiology. 2007;49(3):217–22.
16. Rovira A, Alonso J, Cordoba J. MR imaging findings in hepatic encephalopathy. Am J Neuroradiol. 2008;29(9):1612–21.
17. Maeda M, Tsukahara H, Terada H, Nakaji S, Nakamura H, Oba H, et al. Reversible splenial lesion with restricted diffusion in a wide spectrum of diseases and conditions. J Neuroradiol. 2006;33(4):229–36.
18. Starkey J, Kobayashi N, Numaguchi Y, Moritani T. Cytotoxic Lesions of the Corpus Callosum That Show Restricted Diffusion: Mechanisms, Causes, and Manifestations. Radiographics. 2017;37(2):562-76.
19. Takanashi J. Two newly proposed infectious encephalitis/encephalopathy syndromes. Brain Dev. 2009;31(7):521-8.
20. Mao XJ, Zhu BC, Yu TM, Yao G. Adult severe encephalitis/encephalopathy with a reversible splenial lesion of the corpus callosum: A case report. Medicine (Baltimore). 2018;97(26):e11324.
21. da Rocha AJ, Reis F, Gama HP, da Silva CJ, Braga FT, Maia AC Jr, et al. Focal transient lesion in the splenium of the corpus callosum in three non-epileptic patients. Neuroradiology. 2006;48(10):731-5.
22. Arbelaez A, Pajon A, Castillo M. Acute Marchiafava-Bignami disease: MR findings in two patients. Am J Neuroradiol. 24(10):1955-7.
23. Tanaka Y, Nishida H, Hayashi R, Inuzuka T, Otsuki M. Callosal disconnection syndrome due to acute disseminated enchephalomyelitis. Rinsho Shinkeigaku. 2006;46:50-4.
24. Bulakbasi N, Kocaoglu M, Tayfun C, Ucoz T. Transient splenial lesion of the corpus callosum in clinically mild influenza-associated encephalitis/encephalopathy. Am J Neuroradiol. 2006;27:1983-6.
25. Kimura E, Okamoto S, Uchida Y, Hirahara T, Ikeda T, Hirano T, et al. A reversible lesion of the corpus callosum splenium with adult influenza-associated encephalitis/encephalopathy: a case report. J Med Case Rep. 2008;2:220.
26. Balcik ZE, Senadim S, Keskek A, Ozudogru A, Koksal A, Soysal A, et al. Does restricted diffusion in the splenium indicate an acute infarct? Neurol Belg. 2018 Jan 6. doi: 10.1007/s13760-017-0876-6
27. Gunaydin M, Ozsahin F. Transient visual loss: Transient lesion in the splenium of the corpus callosum. Turk J Emerg Med. 2017;18(3):128-30.
28. Altunkas A, Aktas F, Ozmen Z, Albayrak E, Almus F. MRI findings of a postpartum patient with reversible splenial lesion syndrome (RESLES). Acta Neurol Belg. 2016;116:347–9.
29. Eren F, Öngün G, Öztürk Ş. Clinical and Radiological Significance of Transient Brain Lesion in the Corpus Callosum Splenium: 2 Case Reports. Kafkas J Med Sci. 2018;8(2):133–6.

This paper has been checked for language accuracy by JOSAM editors.
The National Library of Medicine (NLM) citation style guide has been used in this paper.

J Surg Med. 2021;5(12):1193-1197.
DOI: 10.28982/josam.911871

Journal of Surgery and Medicine
e-ISSN=2602-2079

Epidemiological factors associated with colorectal cancer in north-east India: A hospital-based descriptive cross-sectional study

Zothansanga Ralte [1], Paleti Venu Gopala Reddy [2], Vimal Kumar [3]

[1] Department of General Surgery, Civil Hospital. Aizawl. Mizoram, India
[2] Department of General Surgery, Zoram Medical College. Falkawn, India
[3] Department of General Surgery, Mehta Surgical Hospital. Gandhidham. Gujarat, India

ORCID ID of the author(s)

ZR: 0000-0001-6601-0904
PVGR: 0000-0002-3191-0096
VK: 0000-0001-5046-2201

Corresponding Author
Paleti Venu Gopala Reddy
T -56, Saikhamakawn. Near To Sbi Atm Aizawl. Mizoram. India.796001
E-mail: drvenureddy143@gmail.com

Ethics Committee Approval
Institutional human ethics committee of the concerned tertiary care setting approved the study protocol, and all participants gave written informed consent before the study started (B.12018/1/13-CH(A)/IEC/72, Date:12-09-2016: Institutional ethics committee, civil hospital, Aizawl. Mizoram).
All procedures in this study involving human participants were performed in accordance with the 1964 Helsinki Declaration and its later amendments.

Conflict of Interest
No conflict of interest was declared by the authors.

Financial Disclosure
The authors declared that this study has received no financial support.

Published
2021 November 27

Abstract

Background/Aim: Identifying the epidemiological factors associated with the causation and development of colorectal cancer may help gain a better understanding of the disease to assist in screening and assessing the prognosis. This study aimed to determine and analyze the clinical-epidemiological profile of colorectal cancer.

Methods: A cross-sectional study was conducted at a tertiary teaching hospital on 138 colorectal cancer patients for 1.6 years (June 2017 to December 2018). The participants were examined clinically, and detailed history regarding demographic features, adverse habits, occupation, and family history was taken using a structured pro forma. The tumor stage and site of cancer were considered the primary outcomes. Descriptive and inferential analyses were carried out using coGuide software, V.1.03, and the *P*-value was set at <0.05.

Results: The mean age was 54.52 (15.9) years, and 86 (62.30%) patients were males. Twenty-seven (19.60%) had hypertension, 20 (14.50%) had fissures piles and 17 (12.30%) had Diabetes Mellitus. Ninety-seven (70.28%) had a history of smoking and alcohol consumption. Carcinoma cases were more common among patients with a history of non-vegetarian dietary intake, but it was not statistically significant. In our study, smoking and comorbidities like (hypertension, fissure piles) proved to be associated with stages of tumor ($P<0.05$).

Conclusion: The associated risk factors in our study were age >50 years, smoking, and hypertension. If controlled, these can help reduce the overall incidence of CRC in the Indian population.

Keywords: Colorectal cancer, Epidemiology, Smoking, Signs, and symptoms, Lifestyle factors

How to cite: Ralte Z, Reddy PVG, Kumar V. Epidemiological factors associated with colorectal cancer in north-east India: A hospital-based descriptive cross-sectional study. J Surg Med. 2021;5(12):1193-1197.

Introduction

The widely increasing number of cancer cases is perceived as an essential contributor to health ailments globally. Worldwide, approximately 13 million cancer cases are reported per year, among which almost 60% of patients die in developing countries. If not controlled, the number may increase to 10 million per year shortly [1]. According to the World Health Organization, colorectal cancer (CRC) is the third most common cancer diagnosed among men and the second most common in women [2]. Lung, prostate, colorectal, stomach, and liver cancers are the most common types of cancer in men, while breast, colorectal, lung, cervix, and stomach cancer are the most common among women (WHO, 2017) [3].

Over 1.8 million new colorectal cancer (CRC) cases and 881000 deaths were estimated to occur in 2018, accounting for approximately 1 in 10 cancer cases and deaths. Overall, CRC ranks third in terms of incidence but second in terms of mortality [4]. CRC incidence and mortality trends have evolved strikingly in recent decades. Despite significant declines in older populations, the incidence of CRC has nearly doubled among younger adults since the early 1990s [5]. In his systematic review (SR), Leddin [6] concluded that the risk of CRC increases in individuals with positive family history. The study showed that 3%-10% of subjects have one or more first-degree relatives (FDRs) diagnosed with CRC and 0.3%- 3% have two or more FDRs diagnosed with CRC.

The CRCs do not share similar driving mutations. They consist of a diversified group of a disease-driven array of modifications and mutagens. Hence, designing a "catch-all" molecular therapy for CRCs is troublesome. If CRC is diagnosed at an early stage, it can be treated surgically. Still, surgery remains ineffective if diagnosed in the advanced stage, as usually happens in 25% of cases where it has already metastasized to other areas. Drug resistance and cancer recurrence have restrained such patients for neoadjuvant and cytotoxic therapies. This deadly neoplasm can be prevented and treated when its development pattern, association with environmental and genetic factors, and molecular evolution are firmly understood by researchers and physicians [7].

CRCs' most crucial risk factors are industrialization and economic growth leading to a western dietary pattern, sedentary lifestyle, and increasing obesity [8]. In their study, Dos Santos Guedes MT et al. reported the interactions between lifestyle factors like tobacco usage and alcohol consumption, genetic factors, few environmental agents like ionizing radiation, chemical, and biological carcinogens as the possible factors for the development of most sporadic cancers [9]. Despite the awareness about CRC as a significant cause of mortality, the incidence of CRC is increasing. A review of the literature suggests a scarcity of data on factors associated with CRC. A previous study by Sharkas et al. [10] investigated the association between CRC and lifestyle factors. Based on the American Cancer Society (ACS, 2018), there is no proven way to prevent colorectal cancer. However, modifiable risk factors can be controlled to minimize the risk of developing the disease [11].

The first step in understanding cancer is to evaluate its local epidemiology. Identifying the epidemiological factors associated with the causation and development of the disease may help gain a better understanding of the disease to assist in screening and assessing the prognosis of the patients. Literature regarding the epidemiological factors associated with CRC in India is limited. Hence, we aimed to determine and analyze the clinical-epidemiological profile of colorectal cancer in East India.

Materials and methods

Study design: Descriptive cross-sectional study.

Study site: This study was conducted in the general surgery department at a tertiary care teaching hospital.

Source population: Subjects attending the department of general surgery at a tertiary care teaching hospital.

Study population: All the subjects diagnosed with colorectal cancer by either imaging or histopathological examination in the study setting were considered.

Sample size

The sample size was calculated assuming the expected proportion of colorectal cancer as 10% as per a previously published study by Bhattacharya et al. [12] with a 95% confidence level and 9% absolute precision. As recommended by Daniel et al. [13] for prevalence studies, the following formula was used for sample size calculation:

$n=Z2(1-P)/d2$

Where n = size of the sample

Z = level of confidence for Z

P = prevalence expected of proportion (If the expected prevalence is 36.53%, then P=0.365), and

d = Precision (If the precision is 9%, then d=0.09).

As per the parameters mentioned above, the required sample size would be 110.

To account for a non-participation rate of about 20%, a total of 132 subjects were needed for the study. One hundred and thirty-eight patients were recruited.

Sampling method: All study subjects were recruited sequentially by a convenient sampling method until the sample size was reached.

Study Duration: The data were collected between June 2017 and December 2018.

Inclusion criteria

Both genders, aged 18 years and above

Patients undergoing colorectal endoscopic biopsy during the study period for various clinical indications.

Exclusion criteria: Critically ill patients.

Ethical and informed consent: Institutional human ethics committee of the concerned tertiary care setting approved the study protocol, and all participants gave written informed consent before the study started (B.12018/1/13-CH(A)/IEC/72, Date:12-09-2016: Institutional ethics committee, civil hospital, Aizawl. Mizoram). The risks and benefits involved in the study were explained before obtaining consent. The confidentiality of the study participants was maintained throughout.

Epidemiological factors studied

Familial and hereditary factors: Relation- first-degree relative / cannot specify (second-degree relative)

Host factors: Age, gender, education, socioeconomic status, comorbidities

Lifestyle-related factors: Nutritional factors (a diet history), alcohol consumption, tobacco use in any form, etc.

Data collection

A detailed history was taken from the study participants using a structured pro forma, and data regarding demographic features, adverse habits, occupation, and family history were collected. All participants were clinically examined to document the relevant physical findings, and investigations like ultrasonography, CT abdomen, colonoscopy, etc., were performed. Biopsy of the identified lesions was done, and the tissue samples were sent for histopathology for the type and staging of colorectal cancer.

Statistical analysis

Tumor stage and site of cancer were considered as the primary outcomes. Other study variables were demographic parameters like age, gender, socioeconomic status, religion, education, comorbidity, surgical history, smoking and alcohol consumption, diet history, and signs and symptoms. Descriptive analyses were conducted by mean and standard deviation for quantitative variables like age and duration of tobacco usage and frequency and proportion for categorical variables like gender, comorbidities, adverse habits, family, and dietary history, etc. The chi-square test was used to compare demographic parameters and other relevant variables with stages of the tumor. *P*-value was set at <0.05 for significance. Data will be analyzed by using coGuide software, V.1.03 [14].

Results

A total of 138 subjects were included in the final analysis. In seven cases, the biopsy samples were inadequate and excluded from the study.

Table 1 shows the various demographic variables of colorectal cancer. There is an increased risk of colorectal carcinoma (CRC) with increasing age in our study population. The mean age was 54.52 (15.9) years, and 36 (26.10%) belonged to the age group of 41-50 years, and 27 (19.60%) belonged to above 60 years. There was an increased risk of colorectal carcinoma in males, as 86 (62.30%) were males, and the remaining 52 (37.70%) were females.

Table 1: Summary of demographic parameters (n=138)

Parameter	Summary
Age (Mean (SD))	54.52 (15.9)
Age group (in years)	
Less than 40 years	26(18.80%)
41 to 50 years	36 (26.10%)
51 to 60 years	23 (16.70%)
61 to 70 years	27 (19.60%)
71 to 80 years	20 (14.50%)
81 and above	6 (4.30%)
Gender	
Male	86 (62.30%)
Female	52 (37.70%)
Socioeconomic Status	
Low	36(26.10%)
Medium	80 (58.00%)
High	22 (15.90%)
Education	
Illiterate	5(3.60%)
Primary	26 (18.80%)
Secondary	46 (33.30%)
Diploma	30 (21.70%)
Graduate	20 (14.50%)
Postgraduate	11(8.00%)

Table 2 shows the associated comorbidities and past and adverse history. Among the study population, 27 (19.60%), had hypertension, 20 (14.50%) had fissure piles and 17 (12.30%) had diabetes mellitus. Ninety-seven (70.28%) had a positive history of smoking and alcohol consumption. The mean duration of tobacco use was 27.21 years in the study population.

Table 2: Summary of comorbidity, surgical history, and smoking and alcohol consumption (n=138)

Parameter	Summary (%)
Comorbidity	
Diabetes mellitus	17(12.30%)
Hypertension	27(19.60%)
Fusser piles	20(14.50%)
Tuberculosis	3(2.20%)
Asthma COPD	4(2.90%)
Chronic renal disease	3(2.20%)
Ulcerative Colitis	1(0.70%)
Surgical history	
Cholecystectomy	10(7.20%)
Ileal Resection	2(1.40%)
Smoking, using tobacco product	
Are you currently smoking	97(70.28%)
Using any other tobacco product	94(68.00%)
Type of tobacco product used	
Betel Nut	44(31.90%)
Khaine	24(17.40%)
Tuibur	12(8.70%)
No	58(42.00%)
Duration of smoking	27.21 (10.55) (range: 7 to 50)
Tobacco products usage	27.33 (9.66) (range: 6 to 52)
Alcohol consumption	
Males: Females	70:30

Table 3 shows the cancer site and family history. Fifty-six (40.57%) had a positive family history of cancer, and colorectal cancer was the most common site in 22 (15.94%) patients' family members. This was followed by seven (5.07%) lung cancers and six (4.35%) stomach cancer cases.

Table 3: Summary of the site of cancer and family history (n=138)

Parameter	Summary (%)
Cancer in family	56(40.57%)
Site of cancer	
Colorectal cancer	22(15.94%)
CA lung cancer	7(5.07%)
CA stomach cancer	6(4.35%)
CA breast cancer	5(3.62%)
Ovarian Cancer	4(2.90%)
CA Cervical cancer	3(2.17%)
Lymphoma cancer	3(2.17%)
Testicular cancer	2(1.45%)
Medullary ca thyroid	2(1.45%)
CA brain tumor	1(0.72%)
Bladder Cancer	1(0.72%)
No	82(59%)
Family history	
First-degree relative	
Brother	3(2.17%)
Sister	2(1.45%)
Father	3(2.17%)
Mom	4(2.90%)
No	126(91.30%)
Cannot specify (second-degree relative)	
Uncle	6(4.35%)
Aunty	7(5.07%)
Grandmother	8(5.80%)
Grandfather	9(6.52%)
Others	14(10.14%)
No	94(68.12%)

Diet history and signs and symptoms, and stages of cancer were reported in Table 4. Most patients (n=128, 92.80%) had a history of non-vegetarian dietary intake, followed by (n=108, 78.30%) smoked food intake. Out of 138 participants, 104 (75.04%) complained of occult blood per rectum as the main sign and symptom, followed by 71 (51.40%) who reported anorexia and weight loss. Diarrhea was reported in 36 (26.10%), and 36 (26.10%) complained of abdominal pain. Sixty-two (44.90%) had second-stage tumors, 39 (28.30%) had stage 1, 17 (12.30%) had stage 3 and the remaining 20 (14.50%) had stage 4 tumors.

Table 4: Summary of diet, signs and symptoms, and tumor stage (n=138)

Parameter	Summary
Diet history	
Animal proteins	128(92.80%)
Green vegetables and fruits	18(13.00%)
Smoked foods	108(78.30%)
High salt intake	74(53.60%)
Complex carbohydrates	18(13.00%)
Signs and symptoms	
Abdominal pain	36(26.10%)
Nausea and vomiting	27(19.60%)
Anorexia and Weight Loss	71(51.40%)
Diarrhea	49(35.50%)
Constipation	36(26.10%)
Urinary Symptoms	22(15.90%)
Occult Blood Per Rectum	104(75.40%)
Tenesmus	36(26.10%)
Pelvic pain	35(25.40%)
Mass Per Abdomen	27(19.60%)
Tumor stage	
Stage 1	39 (28.30%)
Stage 2	62 (44.90%)
Stage 3	17 (12.30%)
Stage 4	20 (14.50%)

Table 5 compared the demographic parameters and other relevant variables with stages of the tumor. No significant differences were observed in demographic parameters, comorbidities, smoking, or its duration (P>0.05). Carcinoma cases were insignificantly more common among patients with a history of non-vegetarian dietary intake. In our study, comorbidities (hypertension, fissure piles) proved to be risk factors, which were significant with regards to tumor stage (P<0.05).

Table 5: Comparison of demographic parameters, comorbidities, adverse habits, and diet history with stages of tumor (n=138)

Parameter	Tumor				*P*-value
	Stage I	Stage II	Stage III	Stage IV	
Age (in years)	54.46 (6.44)	55.56(14.85)	50 (19.02)	56.75(11.63)	0.549*
Gender					
Male (n=86)	24 (27.91%)	43 (50%)	6 (6.98%)	13 (15.12%)	0.083†
Female (n=52)	15 (28.85%)	19 (36.54%)	11 (21.15%)	7 (13.46%)	
Comorbidities					
Diabetic(n=17)	6 (35.29%)	3 (17.65%)	4 (23.53%)	4 (23.53%)	0.085†
Hypertension(n=27)	7 (25.93%)	6 (22.22%)	7 (25.93%)	7 (25.93%)	0.007†
Fusser Piles(n=20)	6 (30%)	4 (20%)	4 (20%)	6 (30%)	0.041†
Tuberculosis(n=3)	0 (0%)	2 (66.67%)	0 (0%)	1 (33.33%)	‡
Asthma COPD(n=4)	1 (25%)	1 (25%)	1 (25%)	1 (25%)	0.746†
Chronic renal disease (n=3)	2 (66.67%)	1 (33.33%)	0 (0%)	0 (0%)	‡
Ulcerative Colitis(n=1)	0 (0%)	0 (0%)	0 (0%)	1 (100%)	‡
Alcohol Consumption					
Males (n=70)	18 (25.71%)	37 (52.86%)	2 (2.86%)	13 (18.57%)	‡
Females (n=33)	8 (24.24%)	13 (39.39%)	7 (21.21%)	5 (15.15%)	
Smoking(n=97)	26 (26.8%)	45 (46.39%)	13 (13.4%)	13 (13.4%)	0.806†
Duration of smoking	27.51(11.53)	27.92(12.86)	29.35(13.1)	27.4(13.64)	0.961*
Tobacco product usage	25.92(11.88)	25.58(13.4)	29.71(10.2)	34.05(13.16)	0.051*
Diet history					
Animal Proteins(n=128)	37 (28.91%)	57 (44.53%)	16 (12.5%)	18 (14.06%)	0.898†
Green vegetables and fruits(n=18)	7 (38.89%)	7 (38.89%)	1 (5.56%)	3 (16.67%)	0.608†
Smoked Foods(n=108)	31 (28.7%)	47 (43.52%)	13 (12.04%)	17 (15.74%)	0.845†
High salt intake(n=74)	21 (28.38%)	30 (40.54%)	10 (13.51%)	13 (17.57%)	0.591†
Complex Carbohydrates(n=18)	7 (38.89%)	6 (33.33%)	3 (16.67%)	2 (11.11%)	0.588†

* One way ANOVA, † chi square test, ‡ No statistical test was applied- due to 0 subjects in the cells

Discussion

In the current cross-sectional study, 138 colorectal cancer patients were included. Our study population had an increased risk of colorectal carcinoma (CRC) due to increased age and male preponderance. Carcinoma cases were insignificantly more common among patients with a history of non-vegetarian dietary intake. In our study, smoking and comorbidities (hypertension, fissure piles) proved to be significantly related to tumor stage.

In the present study, 54.52 (15.9) years was the mean age. This finding is similar to a hospital-based analytical observational study by Bhattacharya et al. [12] where CRC was much more common in patients aged >50 years. CRCs are majorly diagnosed after 50 years of age in 90% of cases, and hence increasing age is considered the most significant factor associated with the risk of CRC development. In the United States, the incidence of CRC sharply increases after 40 years in males compared to females, as reported by Surveillance, Epidemiology and End Results Program from National Cancer Institute [15]. This gender difference could be attributed to varying levels of exposure to dietary and lifestyle risk factors. Our finding contrasts to a study by Siegel et al. [16] where subjects less than 50 years of age were diagnosed with CRC. In the mid-1990s, this was referred to as an early-onset disease. These young patients have multiple other challenges in continuing the cancer management as they are diagnosed at a very early stage with these rectal diseases compared to older patients.

In the present study, the majority, 56 (40.57%), had a positive family history of cancer, and colorectal cancer was the most common in 22 (15.94%) patients' family members. This finding is similar to the meta-analysis by Wong M et al. [17] conducted on 9.28 million individuals, reporting that the increase in the RR of CRC attributed to family history was higher in younger subjects. The possible explanations for family history related to CRC can be inherited risks, environmental factors, or a combination of both. Since aging is a global issue, the relationship between multimorbidity and CRC should not be ignored. The majority, 27 (19.60%), had hypertension as comorbidity, followed by 20 (14.50%) fissure pile and 17 (12.30%) diabetes mellitus patients. The finding is similar to a study by Shin CM et al. [18] where diabetes mellitus and hypertension were associated with the risk of CRC among men but not among women in Korea.

In the present study, 97 (70.28%) had a positive history of smoking. This finding was similar to an epidemiological analysis by Almatroudi et al. [19] They concluded that CRC cases among both genders in Saudi Arabia are mainly due to lifestyle factors such as the lack of physical exercise, increased BMI, and tobacco usage. The finding was in contrast to a case-control study by Mafiana et al. in Oman [20] that reported no significant association between smoking and the risk of CRC. In our study, 128 (92.80%) subjects had a history of non-vegetarian dietary intake, followed by 108 (78.30%) smoked food intake. This result is consistent with Sinha et al. [21] where fatty diet (60%), spicy food consumption (45%), and non-vegetarian diet (43%) were the most commonly observed lifestyle factors significantly affecting the disease and directly correlated with higher stage and tumor grade. A majority, 97 (70.00%), had a positive history of alcohol consumption. This finding is similar to a systematic review and meta-analysis by Chapelle et al. [22] where an increased incidence of CRC was observed with frequent alcohol or meat consumption. Stage II was the typical presentation of CRC in the majority 62 (44.90%), followed by 39 (28.30%) in stage I. This was in contrast to a study by Suryadevara et al. [23] where stage III was the most distinct presentation stage.

CRC has various risk factors, including age, sex, lifestyle, genetic factors, obesity, diabetes, gut microbiota status, and precancerous lesions. To restrict CRC, the preliminary step is limiting its incidence and mortality rates. To reduce the burden of CRC, public health officials should promote the prevention and management of modifiable risk factors through national policies. The increasing incidence and mortality rate of CRC

may be timely curbed by clarifying specific epidemiological characteristics, optimizing early screening strategies, and strictly implementing diagnosis and treatment guidelines [24].

Limitations

The study has some limitations: First, the study design is cross-sectional. The generalizability of the study findings to other settings is limited, as the profile and lifestyle practices of the study population appear to be completely different, with peculiar dietary patterns and a high prevalence of tobacco consumption. Obesity and physical activity, thought to be risk factors for CRC, were not reported in the present study, yielding biased results for modifiable risk factors. There is a need to conduct large-scale community-based, prospective longitudinal studies to understand the risk factors, their strength of association with colorectal cancer, and its outcomes to develop prevention strategies.

Conclusion

Hypertension, non-vegetarian diet, family history, and tobacco smoking are major contributing factors to CRC incidence in East India. Prevention is the primary strategy to reduce its incidence and mortality rates. Prevention can be achieved through lifestyle changes, a healthy diet, and early screening for high-risk individuals. Therefore, healthcare strategies should focus on enhancing prevention interventions and public health programs to reverse the increasing prevalence of CRC.

References

1. Gandhi AK, Kumar P, Bhandari M, Devnani B, Rath GK. The burden of preventable cancers in India: Time to strike the cancer epidemic. J Egypt Natl Canc Inst. 2017;29(1):11-8. doi: 10.1016/j.jnci.2016.08.002
2. Bnard F, Brkun AN, Martel M, Von Renteln D. Systematic review of colorectal cancer screening guidelines for average-risk adults: Summarizing the current global recommendations. World J Gastroenterol. 2018;24(1):124-38. doi: 10.3748/wjg.v24.i1.124
3. WHO. Cancer. World Health Organization [Internet].
4. Mannucci A, Zuppardo RA, Rosati R, Di Leo M, Perea J, Cavestro GM. Colorectal cancer screening from 45 years of age: Thesis, antithesis and synthesis. World J Gastroenterol. 2019;25(21):2565-80. doi: 10.3748/wjg.v25.i21.2565
5. Murphy CC. Colorectal Cancer in the Young: Does Screening Make Sense? Curr Gastroenterol Rep. 2019;21(7). doi: 10.1007/s11894-019-0695-4
6. Leddin D, Lieberman DA, Tse F, Barkun AN, Abou-Setta AM, Marshall JK, et al. Clinical Practice Guideline on Screening for Colorectal Cancer in Individuals With a Family History of Nonhereditary Colorectal Cancer or Adenoma: The Canadian Association of Gastroenterology Banff Consensus. Gastroenterology. 2018;155(5):1325-47. doi: 10.1053/j.gastro.2018.08.017
7. Rawla P, Sunkara T, Barsouk A. Epidemiology of colorectal cancer: Incidence, mortality, survival, and risk factors. Prz Gastroenterol. 2019;14(2):89-103. doi: 10.5114/pg.2018.81072
8. American Institute for Cancer Research. Diet, Nutrition, Physical Activity and Cancer: a Global Perspective. World Cancer Research Fund International [Internet].
9. Dos Santos Guedes MT, De Jesus JP, De Souza Filho O, Fontenele RM, Sousa AI. Clinical and epidemiological profile of cases of deaths from stomach cancer in the National Cancer Institute, Brazil. Ecancermedicalscience. 2014;8(1):445. doi: 10.3332/ecancer.2014.445
10. Sharkas GF, Arqoub KH, Khader YS, Tarawneh MR, Nimri OF, Al-zaghal MJ, et al. Colorectal Cancer in Jordan: Survival Rate and Its Related Factors. J Oncol. 2017;2017:1-6. doi: 10.1155/2017/3180762
11. ACS. Colorectal cancer, early detection, diagnosis, and staging. American Cancer Society [Internet].
12. Bhattacharya S. Colorectal Cancer: A Study of Risk Factors in a Tertiary Care Hospital of North Bengal. J Clin Diagnostic Res. 2014;8(11):FC08-10. doi: 10.7860/JCDR/2014/8844.5166
13. Daniel WW. Determination of sample size for estimating proportions. Biostatistics A foundation for analysis in the health sciences. 1999;8:189-90.
14. BDSS Corp . Released 2020. coGuide Statistics software, Version 1.0, India: BDSS corp.
15. Vieira AR, Abar L, Chan DSM, Vingeliene S, Polemiti E, Stevens C, et al. Foods and beverages and colorectal cancer risk: a systematic review and meta-analysis of cohort studies, an update of the evidence of the WCRF-AICR Continuous Update Project. Ann Oncol. 2017;28(8):1788-802. doi: 10.1093/annonc/mdx171
16. Siegel RL, Jakubowski CD, Fedewa SA, Davis A. Colorectal Cancer in the Young: Epidemiology, Prevention, Management. Am Soc Clin Oncol Educ B. 2020;40:1-14.
17. Wong MCS, Ching JYL, Chiu H-M, Wu KC, Rerknimitr R, Li J, et al. Risk of Colorectal Neoplasia in Individuals With Self-Reported Family History: A Prospective Colonoscopy Study from 16 Asia-Pacific Regions. Am J Gastroenterol. 2016;111(11):1621-9. doi: 10.1038/ajg.2016.52
18. Shin CM, Han K, Lee DH, Choi YJ, Kim N, Park YS, et al. Association Among Obesity, Metabolic Health, and the Risk for Colorectal Cancer in the General Population in Korea Using the National Health Insurance Service–National Sample Cohort. Dis Colon Rectum. 2017;60(11):1192-200. doi: 10.1097/DCR.0000000000000876
19. Almatroudi A. The incidence rate of colorectal cancer in Saudi Arabia: An observational descriptive epidemiological analysis. Int J Gen Med. 2020;13:977-90. doi: 10.2147/IJGM.S277272
20. Mafiana RN, Al Lawati AS, Waly MI, Al Farsi Y, Al Kindi M, Al Moundhri M. Association between Dietary and Lifestyle Indices and Colorectal Cancer in Oman: A Case-Control Study. Asian Pac J Cancer Prev. 2018;19(11):3117-22. doi: 10.31557/APJCP.2018.19.11.3117
21. Sinha R, Doval DC, Hussain S, Kumar K, Singh S, Basir SF, et al. Lifestyle and sporadic colorectal cancer in India. Asian Pacific J Cancer Prev. 2015;16(17):7683-8. doi: 10.7314/APJCP.2015.16.17.7683
22. Chapelle N, Martel M, Zoutendijk ET-, Barkun AN, Bardou M. Recent advances in clinical practice : colorectal cancer chemoprevention in the average- - risk population. 2020;(September 1980):2244-55. doi: 10.1136/gutjnl-2020-320990
23. Suryadevara S, Veerendra Kumar KV, Pampanagouda SKM, Arjun R, Deshmani V, Mukherjee G. Colorectal cancer profile in a tertiary care centre, Bangalore, India. Online J Heal Allied Sci. 2014;13(1):1-4.
24. Yang Y, Han Z, Li X, Huang A, Shi J, Gu J. Epidemiology and risk factors of colorectal cancer in China. 2020;32(6):729-41. doi: 10.21147/j.issn.1000-9604.2020.06.06.

This paper has been checked for language accuracy by JOSAM editors.
The National Library of Medicine (NLM) citation style guide has been used in this paper.

J Surg Med. 2021;5(12):1198-1201.
DOI: 10.28982/josam.957229

Journal of Surgery and Medicine
e-ISSN=2602-2079

A comparison of the harmonic scalpel, coblation, bipolar, and cold knife tonsillectomy methods in adult patients

Bugra Subasi, Fatih Oghan, Hamdi Taslı, Nesibe Esra Karaman, Seckin Akbal

Kutahya Health Sciences University, Faculty of Medicine, Department of Otorhinolaryngology, Kutahya, Turkey

ORCID ID of the author(s)

BS: 0000-0002-7666-612X
FO: 0000-0002-7967-2189
HT: 0000-0003-2186-5006
NEK: 0000-0002-3084-2618
SA: 0000-0002-2123-2180

Corresponding Author
Bugra Subasi
Kutahya Health Sciences University, Faculty of Medicine, Department of Otorhinolaryngology, Kütahya, Turkey
E-mail: drbugrasubasi@hotmail.com

Ethics Committee Approval
The study was approved by the Clinical Research Ethics Committee of Kutahya Health Sciences University, Faculty of Medicine (approval number: 2020-01/03).
All procedures in this study involving human participants were performed in accordance with the 1964 Helsinki Declaration and its later amendments.

Conflict of Interest
No conflict of interest was declared by the authors.

Financial Disclosure
The authors declared that this study has received no financial support.

Published
2021 November 28

Abstract

Background/Aim: Tonsillectomy is one of the widely performed surgical procedures by otolaryngologists. Today, many new surgical instruments are used in tonsil surgery to reduce postoperative morbidity. This study aimed to compare intraoperative blood loss, operating time, postoperative pain, and bleeding between harmonic scalpel tonsillectomy, coblation tonsillectomy, bipolar tonsillectomy, and cold dissection tonsillectomy in adult patients.

Methods: This prospective cohort study population comprised 96 adult patients aged 18-60 years (mean age: 34.9 (10.7) years) who were operated on for chronic tonsillitis. The amount of bleeding and the operation time were calculated intraoperatively. Postoperative pain level was evaluated using a Visual Analogue Scale (VAS) at the sixth postoperative hour and on postoperative days 1, 2, 3, and 7.

Results: In the harmonic scalpel group, the mean volume of intraoperative bleeding (2.7 (1.5) ml) and the mean operation time (8.8 (3.0) min) were significantly lower compared to the other groups ($P<0.001$, $P<0.001$ respectively). Secondary bleeding was detected in 10 patients but there was no significant difference in the post-tonsillectomy bleeding rates between the four groups ($P=0.86$). Pain scores at the sixth postoperative hour were similar and significantly lower in the harmonic scalpel, coblation, and bipolar groups compared with the cold dissection group ($P<0.001$). The postoperative pain scores were significantly higher in the harmonic scalpel group compared to the cold dissection group on postoperative days 3 and 7 ($P=0.03$, $P=0.02$ respectively).

Conclusion: Less bleeding during surgery, shorter operation time, and less pain in the early postoperative period are the advantages of Harmonic scalpel tonsillectomy. Also, it does not increase the rate of secondary bleeding but its benefit for late period pain is lower compared to the cold knife method. The harmonic scalpel is a practical and reliable method in adult tonsil surgery.

Keywords: Tonsillectomy, Harmonic scalpel, Coblation, Cold knife tonsillectomy, Bipolar dissection, Postoperative pain

How to cite: Subasi B, Oghan F, Taslı H, Karaman NE, Akbal S. A comparison of the harmonic scalpel, coblation, bipolar and cold knife tonsillectomy methods in adult patients. J Surg Med. 2021;5(12):1198-1201.

Introduction

Tonsillectomy is one of the most common surgeries which has been performed for over 3000 years. Various surgical devices were invented to increase the reliability and efficacy of tonsil surgery. Tonsillectomy, ligature, galvanocautery, electrocautery, cold steel dissection, NdYag and KTP lasers, bipolar diathermy, microdissection needle, coblation, and harmonic scalpel tonsillectomy methods are currently used [1]. The harmonic scalpel (HS) devices have a generator, a handpiece, a blade system, and a foot pedal. The high frequency (55.5 Hz) vibration of the hand-piece blades generates a heat of 50-100^{0}C that cuts and coagulates the tissue simultaneously. This low temperature causes minimal tissue damage. The HS transfers mechanical energy to the tissue, causing protein denaturation, which results in coagulum that seals small blood vessels, thereby providing hemostasis [2, 3]. The Coblation technique involves passing radiofrequency energy through a saline solution. The intercellular bonds of tissues are broken by sodium ions at a low temperature (60°C), which causes less postoperative pain [4]. Bipolar diathermy scissors cut and coagulate the tissue simultaneously [5]. The temperature of the cautery can reach 300-400 degrees; therefore, it may cause more pain and inconvenience after the surgery [6].

The cold dissection method is considered the gold standard. This technique causes mechanical injury and preserves maximum oral mucosa when compared to thermal injury. Postoperative healing is quicker, with less postoperative pain and delayed bleeding, but the operation time and the amount of intraoperative bleeding increase because of the lack of simultaneous homeostasis [7].

This study aimed to compare intraoperative (operating time, blood loss) and postoperative (bleeding and pain) important parameters of the harmonic scalpel, coblation, bipolar, and traditional cold knife tonsillectomy methods in adult patients.

Materials and methods

This prospective cohort study was carried out per the Declaration of Helsinki and approved by the Kutahya Health Sciences University Clinical Research Ethics Committee (decision no: 2020-01/3, dated: 08.01.2020). Among 96 patients who had tonsillectomy for a diagnosis of chronic tonsillitis during January 2020 to June 2021, 58 patients (60.4%) were male, 38 (39.6%) patients were female, and the mean age was 34.9 (10.7) years (range: 18-60 years). The study only included adult patients who were operated on under general anesthesia. The study exclusion criteria were being aged <18 years, having acute tonsillitis, coagulopathy, previous peritonsillar abscess, tonsil neoplasms, and craniofacial anomalies. All operations were performed by two surgeons using a harmonic scalpel on 26 patients (27.1%), the cold knife technique on 25 (24%), the bipolar tonsillectomy method on 23 (22.9%), and coblation tonsillectomy on 22 (26%). Operation time was calculated from the incision to the end of complete hemostasis. Intraoperative bleeding was calculated from the surgical aspirator, blood suction bottle, and by weighing gauze packing. Sterile 0.9% NaCl solution was used for irrigation and NaCl was excluded when bleeding was calculated. Bipolar electrocautery was used in 5 of 26 (19.2%) patients in the harmonic scalpel group and 7 of 22 (31.8%) patients in the coblation group for further hemostasis. Bipolar diathermy was used in all patients in the cold dissection group and the bipolar dissection group. The VAS (0=no pain and 10=most severe pain) was given to the patients to express their pain levels at postoperative 6 h, and on postoperative days 1, 2, 3, and 7. They were asked to bring it with them during the 1st-week controls. All patients stayed in the hospital overnight for observation and 50 mg/kg amoxicillin and 10 mg/kg paracetamol were started for 1 week. All patients were followed up closely for postoperative bleeding.

Statistical analysis

The data were statistically analyzed with SPSS for Windows, vn.23.0 software (Statistical Package for Social Sciences for Windows; IBM, Armonk, NY, USA). The results were shown as mean (standard deviation (SD)) and number (n) and percentage (%). Categorical variables were compared with a paired t-test. Variation analysis test (ANOVA) was used to compare multiple subgroups. A value of $P<0.05$ was considered statistically significant.

Results

Ninety-six adult patients, 58 (60.4%) males, 38 (39.6%) females, with a mean age of 34.9 (10.7) years, were evaluated for intraoperative bleeding, operative time, postoperative bleeding, and postoperative pain. The four groups were matched in terms of age and gender distribution.

Intraoperative bleeding

The mean volume of intraoperative bleeding was 2.7 (1.5) ml (range, 0-5 ml) in the harmonic scalpel group, 40.3 (22.5) ml (range, 20-90 ml) in the cold dissection group, 53.2 (38.5) ml (range, 1-150 ml) in the coblation group, and 24.3 (9.7) ml (range, 10-45 ml) in the bipolar dissection group (Table 1). The amount of bleeding was significantly lower in the harmonic scalpel group compared to the cold dissection, bipolar dissection, and coblation groups ($P<0.001$, $P<0.001$, $P<0.001$ respectively), and in the bipolar dissection group compared to the cold dissection and coblation groups ($P=0.03$, $P=0.01$ respectively). There was no significant difference between the coblation and the cold dissection groups in terms of mean intraoperative bleeding volume ($P=0.16$).

Table 1: Mean and standard deviation variables of four tonsillectomy techniques

	Harmonic Scalpel tonsillectomy mean (SD) (n=26)	Coblation tonsillectomy mean (SD) (n=22)	Bipolar Dissection tonsillectomy mean (SD) (n=23)	Cold Dissection tonsillectomy mean (SD) (n=25)	*P*-value
Operation time (min)	8.8(3.0)	23.7(4.6)	31.6(11.5)	26.1(6.1)	<0.001
Intraoperative bleeding (cc)	2.7(1.5)	53.2(38.5)	24.3(9.7)	40.3(22.5)	<0.001
Postoperative bleeding rate	7.7%	13.6%	13%	8%	0.86

SD: standard deviation. $P<0.05$: Statistically significant

Postoperative pain

VAS was used to determine postoperative pain levels. The mean VAS scores at the 6th postoperative hour and the first, second, third, and seventh postoperative days were 4.3 (2.5), 4.7 (2.1), 4.6 (2.4), 4.1 (1.8), and 4.0 (2.9), respectively, in the harmonic scalpel group, 5.8 (2.7), 4.5 (2.5), 3.6 (1.9), 3.0 (2.2), and 2.7 (2.6), respectively, in the coblation group, 5.0 (2.2), 4.2 (2.1), 3.9 (2.3), 3.5 (1.7), and 2.6 (3.0), respectively, in the

bipolar dissection tonsillectomy group, 7.5 (1.5), 5.2 (1.5), 4.0 (1.2), 2.6 (1.5), and 1.6 (1.7), respectively, in the cold dissection group.

Postoperative pain scores of the harmonic scalpel, coblation, and bipolar dissection groups were similar (Table 2).

Table 2: Pain levels after tonsillectomy (mean (SD))

	Pain score 6 h	Pain score day 1	Pain score day 2	Pain score day 3	Pain score day 7
Harmonic Scalpel tonsillectomy	4.3(2.5)	4.7(2.1)	4.6(2.4)	4.1(1.8)	4.0(2.9)
Coblation tonsillectomy	5.8(2.7)	4.5(2.5)	3.6(1.9)	3.0(2.2)	2.7(2.6)
Bipolar Dissection tonsillectomy	5.0(2.2)	4.2(2.1)	3.9(2.3)	3.5(1.7)	2.6(3.0)
Cold Dissection tonsillectomy	7.5(1.5)	5.2(1.5)	4.0(1.2)	2.6(1.5)	1.6(1.7)
P-value	<0.001	0.41	0.38	0.02	0.02

SD: standard deviation. $P<0.05$: Statistically significant

The postoperative pain scores were significantly lower in the harmonic scalpel, bipolar and coblation groups compared to the cold dissection group at the 6th postoperative hour ($P<0.001$, $P<0.001$, $P=0.01$ respectively), and in the cold dissection group compared to the harmonic scalpel group on postoperative days 3 and 7 ($P=0.03$, $P=0.02$ respectively).

The mean operation times

The mean operating time was 8.8 (3.0) min (range, 4-17 min**)** in the harmonic scalpel group, 26.1 (6.1) min (range, 15-40 min) in the cold dissection group, 23.7 (4.6) min (range, 13-30 min) in the coblation group, and 31.6 (11.5) min (range, 19-60 min) in the bipolar dissection group (Table 1). It was significantly shorter in the harmonic scalpel group compared to the cold dissection, bipolar dissection, and coblation groups ($P<0.001$ for all), and in the coblation and cold dissection groups compared to the bipolar dissection group ($P<0.001$, $P=0.04$ respectively), while it was similar between the coblation group and the cold dissection group ($P=0.14$).

Postoperative bleeding

Primary bleeding was not observed after tonsillectomy. Secondary bleeding was observed at a rate of 7.7% (2/26) in the harmonic scalpel group, 13.6% (3/22) in the coblation group, 8% (2/25) in the cold dissection group, and 13% (3/23) in the bipolar dissection group (Table 1). There was no significant difference between the groups in terms of bleeding rates after tonsillectomy.

Discussion

Tonsillectomy is one of the most frequently performed surgeries in both children and adults all over the world. Absolute indications for tonsillectomy are tonsillar cancer, tonsillar hypertrophy due to severe airway obstruction, and persistent tonsillar hemorrhage. The relative indications include chronic tonsillitis, recurrent acute tonsillitis, phlegmon, or repetitive peritonsillar abscess [8]. Unlike pediatric tonsillectomy, chronic infection is the most common indication for adult tonsillectomy [9]. In the present study, all adult patients underwent tonsillectomy with complete removal of all tonsillar tissue, due to chronic tonsillitis.

A few studies are comparing the harmonic scalpel and cold knife tonsillectomy methods in adults. In a single-blinded randomized clinical trial, Karimi et al. [10] compared cold dissection and harmonic scalpel tonsillectomy and reported that the mean volume of intraoperative bleeding was significantly lower with 9.59 ml on the harmonic scalpel side compared to 74.38 ml on the cold dissection side. The mean operation time was significantly shorter when using the harmonic scalpel, with 427.63 (196.32) secs compared to 747.84 (271.88) secs. On the first day after surgery, the mean pain level was significantly lower on the harmonic scalpel side and similar on the seventh postoperative day. There was no significant difference in terms of postoperative bleeding rates.

Similarly, in the current study, the mean volume of intraoperative bleeding and the mean operation time were significantly lower in the harmonic scalpel group compared to the cold dissection group. There was no primary bleeding after tonsillectomy and there was no significant difference between the groups in terms of secondary bleeding rates. Akural et al. [11] compared the harmonic scalpel and blunt dissection methods to find that perioperative blood loss was significantly lower on the side where the harmonic scalpel was used. Electrocoagulation was used in all cases on the dissection side, but it was required in only half of the cases on the harmonic scalpel side. Pain scores were significantly higher on the blunt dissection side at the 10th postoperative hour, but in the second postoperative week, the pain scores and level of otalgia were significantly higher on the harmonic scalpel side. They suggested that increased pain intensity and otalgia during the second week after Harmonic scalpel tonsillectomy may be due to a slower healing rate on the Harmonic scalpel. Similarly, the mean VAS scores of our patients in the harmonic scalpel tonsillectomy group were lower in the early postoperative period and higher during the late postoperative period, compared to the patients in the cold knife group.

Harmonic scalpel simultaneously cuts and coagulates the tissue. Less thermal damage occurs, and less electrocautery is required for hemostasis, thereby, it causes less pain during the early postoperative period. Also, the harmonic scalpel provides a clearer surgical field because of less intraoperative bleeding, so the surgery can be performed in a shorter time.

In a single-blinded prospective study of both adult and pediatric patients, Kamal et al. [3] compared the harmonic scalpel and conventional steel tonsillectomy and reported a mean operation time of 15 min for tonsillectomy with the harmonic scalpel and 20 min for the conventional steel tonsillectomy with no significant differences between the groups. However, intraoperative blood loss was 6.2 cc in the harmonic scalpel group, significantly less than the 49.4 ml in conventional steel tonsillectomy. Postoperative pain was lower and there was no major hemorrhage after tonsillectomy that required surgical attention in the harmonic scalpel group. In the current study, the amount of bleeding in the harmonic scalpel group was significantly lower than those in the cold dissection, coblation, and bipolar dissection groups.

Parsons et al. [12] reported less pain over 10 days in the coblation group compared to the harmonic scalpel and electrocautery groups. In the current study, postoperative pain scores were similar between the harmonic scalpel, coblation, and bipolar dissection groups. Basu et al. [13] reported that the postoperative secondary hemorrhage rate (7.8% vs. 1.5%) and intraoperative blood loss (125.62 (25.56) vs. 42.43 (5.31) ml) were significantly higher in the coblation group compared with the harmonic scalpel group. The diet recovery period was

insignificantly shorter and postoperative pain scores were insignificantly lower in the harmonic scalpel group. The mean operation time was significantly longer with 36.96 (4.83) min in the coblation group compared to 20.15 (4.49) min in the harmonic scalpel group. In the current study, the mean operation time was shorter, and the mean volume of intraoperative bleeding was significantly lower in the harmonic scalpel group than in the other groups.

Few publications in the literature compare the harmonic scalpel and bipolar tonsillectomy methods. A prospective randomized multi-unit study by Arbin et al. [14] reported that no significant differences were found in terms of post-tonsillectomy pain scores and the consumption of pain medication between the bipolar dissection and harmonic scalpel tonsillectomy techniques in both pediatric and adult patients. Sheahan et al. [15] compared the harmonic scalpel and bipolar diathermy methods and observed no significant differences in the post-tonsillectomy pain scores between the groups. On the harmonic scalpel side, an alternative technique of hemostasis was used to control bleeding in 14 of the 21 sides. They concluded that the use of harmonic scalpel tonsillectomy is a safe, effective technique, but substantial costs and difficulties of hemostasis may cause limited use of this instrument in tonsillectomy. In our study, postoperative pain scores were similar in the harmonic scalpel and bipolar dissection groups. Rescue electrocautery was used in 5 of 26 (19.2%) patients in the harmonic scalpel group.

The blade part of the Harmonic scalpel device is disposable. Thus, this method is expensive but reduces the transmission of Cruetzfield-Jacob disease [3]. While it can easily stop bleeding from the superficial veins during surgery, additional coagulation methods may be needed. Another disadvantage of harmonic scalpel tonsillectomy is that there is more pain on the 3rd and 7th postoperative days compared to the cold knife method. This may be due to a slower healing rate after harmonic scalpel tonsillectomy [11]. Short operation time reduces the duration of anesthesia and less pain in the early period may cause early discharge, therefore, surgery costs can be reduced. In addition, it does not increase the postoperative primary and secondary bleeding rates.

Limitations

The limitations of our study were the small number of patients and the lack of randomization. Additionally, all patients were operated on by two surgeons. Therefore, further randomized controlled trials with a larger number of patients should be performed by a single surgeon experienced in the current surgical techniques.

Conclusion

This study showed that harmonic scalpel tonsillectomy, easily learned and quickly applied by surgeons, provides a comfortable surgery with low intraoperative bleeding. Harmonic scalpel tonsillectomy is an effective, safe, and promising method in adult tonsil surgery.

References

1. McClelland L, Jones NS. Historical article tonsillectomy: hemorrhaging ideas. J Laryngol Otol. 2005;119(10):753-8.
2. Dutta NN, Bordoloi BM. Tonsillectomy using harmonic scalpel. Indian J Otolaryngol Head Neck Surg. 2002;54(1):74-6.
3. Kamal SA, Basu S, Kapoor L, Kulandaivelu G, Talpalikar S, Papasthatis D. Harmonic scalpel tonsillectomy: a prospective study. Eur Arc Otorhinolaryngol. 2006;263(5):449-54.
4. Timms MS, Temple RH. Coblation tonsillectomy, a double blind randomized controlled study. J Laryngol Otol. 2002;116(6):450-2.
5. Pang YT, El-Hakim H, Rothera MP. Bipolar diathermy tonsillectomy. Clin Otolaryngol Allied Sci. 1994;19(4):355-7.
6. Verma R, Verma RR, Verma RR. Tonsillectomy-comparative study of various techniques and changing trend. Indian J Otolaryngol Head Neck Surg. 2017;69(4):549-58.
7. Sayın I, Cingi C. Recent medical devices for tonsillectomy. Hıppokratia. 2012:16(1):11-6.
8. Galindo Torres BP, Miguel Garcia FD, Orozco JW. Tonsillectomy in adults: Analysis of indications and complications. Auris Nasus Larynx. 2018;45(3):517-21.
9. Hoddeson EK, Gourin CG. Adult tonsillectomy: current indications and outcomes. Otolaryngol Head Neck Surg. 2009;140(1):19-22.
10. Karimi E, Safaee A, Bastaninejad S, Dabiran EM, Salehi FM. A comparison between cold dissection tonsillectomy and harmonic scalpel tonsillectomy. Iran J Otorhinolaryngol. 2017;29(95):313–7.
11. Akural EI, Koivunen PT, Teppo H, Alahuhta SM, Löppönen HJ. Post-tonsillectomy pain: a prospective, randomized and double blinded study to compare an ultrasonically activated scalpel technique with the blunt dissection technique. Anaesthesia. 2001;56(1):1045-50.
12. Parsons SP, Cordes SR, Comer B Comparison of posttonsillectomy pain using the ultrasonic scalpel, coblator, and electrocautery. Otolaryngol Head Neck Surg. 2006;134(1):106-13.
13. Basu S, Sengupta A, Dubey AB, Sengupta A. Harmonic scalpel versus coblation tonsillectomy a comparative study. Indian J Otolaryngol Head Neck Surg. 2019;71(4):498-503.
14. Arbin L, Enlund M, Knutsson J. Post-tonsillectomy pain after using bipolar diathermy scissors or the harmonic scalpel: a randomised blinded study. Eur Arch Otorhinolaryngol. 2017;274(5):2281-85.
15. Sheahan P, Miller I, Colreavy M, Sheahan JN, McShane D, Curran A. The ultrasonically activated scalpel versus bipolar diathermy for tonsillectomy: a prospective, randomized trial. Clin Otolaryngol Allied Sci. 2004;29(5):5330-44.

This paper has been checked for language accuracy by JOSAM editors.
The National Library of Medicine (NLM) citation style guide has been used in this paper.

J Surg Med. 2021;5(12):1202-1205.
DOI: 10.28982/josam.1008359

Journal of Surgery and Medicine
e-ISSN=2602-2079

The predictive role of neutrophil-lymphocyte ratio, platelet lymphocyte ratio, and other complete blood count parameters in eclampsia and HELLP syndrome

Feyza Bayram [1], Süleyman Serkan Karaşin [2]

[1] Obstetrics and Gynecology, Health Sciences University Bursa Yüksek İhtisas Training and Research Hospital, Bursa, Turkey
[2] Obstetrics and Gynecology, Health Sciences University Bursa Yüksek İhtisas Training and Research Hospital, Bursa, Turkey

ORCID ID of the author(s)
FB: 0000-0003-1735-6997
SSK: 0000-0003-4025-9343

Corresponding Author
Süleyman Serkan Karaşin
Obstetrics and Gynecology, Health Sciences University Bursa Yüksek Ihtisas Training and Research Hospital, Bursa, Turkey
E-mail: sskarasin@icloud.com

Ethics Committee Approval
Bursa Yüksek Ihtisas Training and Research Hospital Ethics Committee approved the study with numbered 2011-KAEK-25 2021/03-06. All procedures in this study involving human participants were performed in accordance with the 1964 Helsinki Declaration and its later amendments.

Conflict of Interest
No conflict of interest was declared by the authors.

Financial Disclosure
The authors declared that this study has received no financial support.

Published
2021 November 28

Abstract

Background/Aim: Previous studies declared the neutrophil-to-lymphocyte ratio (NLR), platelet-to-lymphocyte ratio, and other routine complete blood count (CBC) components as sensitive preeclampsia biomarkers. We speculated that the same associations existed with eclampsia and HELLP syndrome.
Methods: This retrospective case-control study was conducted on 120 pregnant women between the ages of 18 and 40 years. Forty-nine patients with HELLP syndrome, 40 patients with eclampsia/preeclampsia, and 40 healthy pregnant women were included in the study. All groups were evaluated in terms of clinical characteristics and first-trimester hematological parameters. The primary outcomes were neutrophil-lymphocyte ratio (NLR), platelet-lymphocyte ratio (PLR), and the secondary results were hemoglobin, red blood distribution width, mean platelet volume, platelet count, neutrophil count, and lymphocyte count.
Results: The median gestational age was 34 weeks (ranging between 23 and 41), with a median birth weight of 2300 grams. The median NLR was 3.9 (1.3-25.1), and the median PLR was 113.6 (20.7-693). The NLR and PLR values were significantly different between the three groups (P=0.014, P=0.002, respectively). NLR was different between normotensive and eclamptic pregnant women. PLR values were higher in normotensive pregnant women than in pregnant women with a history of HELLP. The median red cell distribution width was 44.6 in normotensive women, 41.5 in women with eclampsia, and 44.3 in women with a history of HELLP (P=0.017).
Conclusion: TLR value was higher in pregnant women who had eclampsia. Platelet count and MPV were significantly lower in the HELLP group.

Keywords: Eclampsia, HELLP syndrome, Neutrophil-lymphocyte ratio (NLR), Platelet-lymphocyte ratio (PLR)

How to cite: Bayram F, Karaşin SS. The predictive role of neutrophil-lymphocyte ratio, platelet lymphocyte ratio, and other complete blood count parameters in eclampsia and HELLP syndrome. J Surg Med. 2021;5(12):1202-1205.

Introduction

Pregnancy-induced hypertensive (PIH) disorders include chronic hypertension, gestational hypertension, preeclampsia, severe preeclampsia and hemolysis, high liver enzymes and low platelet (HELLP) syndrome, and eclampsia. Hypertensive disorders of pregnancy occur in 5-11% of all pregnancies [1]. Preeclampsia (PE) is a pregnancy-specific disease characterized by arterial hypertension and significant proteinuria after 20 weeks of gestation. It complicates approximately 2-8% of pregnancies worldwide [2, 3].

Preeclampsia is a multifactorial obstetric pathology with high morbidity and mortality rates, the pathogenesis of which has not been clearly clarified. There is insufficient placentation due to the absence of trophoblastic invasion, which causes placental hypoxia followed by proinflammatory cytokine secretion, increased neutrophil counts, thrombocyte activation, systemic inflammation and endothelial dysfunction [4].

Eclampsia, the major neurological complication of preeclampsia, is defined as a convulsive episode or any other sign of altered consciousness that occurs in the setting of preeclampsia and cannot be attributed to any pre-existing neurological condition [5]. We hypothesized that there is a similar relationship in the pathogenesis between PE and eclampsia in the first trimester of pregnancy.

HELLP syndrome was first reported by Weinstein in 1982 as hemolysis (H), elevated liver enzymes (EL) and low platelet count (LP) in the third trimester of pregnancy [6]. The presence of hemolysis and microangiopathy is one of the basic criteria of the HELLP syndrome triad, seen in 80-85% of these patients. The incidence of HELLP syndrome is 0.1-0.8%, and it occurs after the 20th week of pregnancy [7]. Although the exact etiopathogenesis is not known, genetic predisposition, abnormal placentation, immunological pathologies, and maternal vascular endothelial dysfunction may play a role. Seventy percent of the cases were detected in the antenatal period, and 30% were detected postpartum (usually in the first 48 hours). There is still debate about whether HELLP is a severe form of preeclampsia or a separate condition [8].

HELLP syndrome is part of the hypertensive disorders of pregnancy, but the inflammatory reaction is more intense than in preeclampsia, and the immune system specifically attacks the liver and coagulation cascade [9]. In addition, while hypertension is the definitive diagnostic criterion in preeclampsia, it is not always present in HELLP syndrome [8–10].

There are no known diagnostic markers that can predict the development of HELLP syndrome or eclampsia in the early trimester of pregnancy. Recently, neutrophil-to-lymphocyte ratio (NLR) and platelet-lymphocyte ratio (PLR) were recognized as novel markers of systemic inflammation. It is also noteworthy that these indices obtained from peripheral blood cells are easily measurable and accessible. There are many studies that found the rate of NLR and PLR in the first trimester to be higher in preeclampsia than in healthy pregnancies [11, 12].

However, there is limited data in the literature regarding the effectiveness of these markers in HELLP syndrome and eclampsia. Currently, the predictive roles of NLR, PLR and other hemogram parameters in HELLP and eclampsia are still unclear. This study aims to determine the predictive value of routine hemogram parameters in the first trimester for early diagnosis of HELLP syndrome and eclampsia.

Materials and methods

This retrospective case-control study was conducted in Bursa Yüksek İhtisas Training and Research hospital. For sample calculation, the study "Neutrophil-to-lymphocyte ratio and platelet indices in pre-eclampsia" (DOI: 10.1002/ijgo.12701) was used [13]. As a result of the sample calculation made according to the Neutrophil/Lymphocyte Ratio parameter in Table 2 of this study, a total of 130 volunteers were needed for 95% confidence interval, 0.05 type 1 error, 0.44 effect size and 80% power. A total of 129 pregnant women between the ages of 18 and 40 years, who delivered in our obstetrics clinic were included in the study. Bursa Yüksek İhtisas Training and Research Hospital Ethics Committee approved the study numbered 2011-KAEK-25 2021/03-06. The patients had visited our obstetrics department in the first trimester (between 7 to 14 weeks of gestation) of their pregnancy and undergone a routine complete blood count (CBC) test. The participants were divided into three groups: There were 49 patients with HELLP syndrome, 40 patients with eclampsia/preeclampsia and 40 healthy pregnant women. All groups were evaluated in terms of clinical characteristics and first trimester hematological parameters.

American College of Obstetrics and Gynecology 2013 guidelines were used to diagnose HELLP and eclampsia [2]. HELLP syndrome indicated the presence of thrombocytopenia (<150,000/mm3), hepatic dysfunction (aspartate aminotransferase (AST) >40 IU/L, alanine aminotransferase (ALT) >40 IU/L, or both, and lactate dehydrogenase (LDH) level >600 IU/L), and hemolysis (increased LDH level, progressive anemia) [14].

PE was diagnosed with the following criteria: Systolic blood pressure (SBP) ≥140 mm Hg and/or diastolic blood pressure (DBP) ≥90 mm Hg on two occasions at least 4 hours apart and proteinuria (>0.3 g per day) after the 20th gestation week. Eclampsia was defined as the presence of new-onset grand mal seizures in a woman with preeclampsia. The control group included healthy pregnant women with matching gestational age. Women with a history of membrane rupture, anemia, infection, multiple pregnancy, history of drug use or systemic disease (such as diabetes mellitus, thyroid disorders, chronic hypertension, cardiac disease, collagen vascular disease, epilepsy and hypercoagulopathy) were excluded from the study.

The noted demographic and clinical information included age, body mass index (BMI), gravidity, parity, race, birthweight, gestational age at delivery, and gestational age at CBC collection. Venous blood samples were drawn into 2 mL EDTA tubes. CBC values were analyzed with the automated hematology analyzer (ABX Micros ES 60; Horiba Medical, Kyoto Japan). The main outcomes were NLR, PLR and MLR, and the secondary outcomes were hemoglobin, RDW, MPV, platelet count, neutrophil, and lymphocyte values.

Statistical analysis

Windows-based SPSS 24.0 program was used (SPSS Inc., USA) for statistical analyses. We used visual (histograms, probability plots) and analytical methods (Shapiro-Wilk's test

and Kolmogorov Smirnov tests.) to determine whether the variables were normally distributed. Variables were descriptively specified as mean (standard deviation) (X(SD)), median (minimum-maximum (min-max)), frequency (n) and percentage (%). One-way ANOVA compared the normally distributed data and the Kruskal Wallis test was used to compare the non-normally distributed variables. Post-hoc Tukey test was used for the binary analysis of significant results. A value of $P<0.05$ was considered statistically significant.

Results

In this retrospective study, we analyzed 89 pregnant women diagnosed with eclampsia and HELLP in the last 3 years (2018-2021) and 40 pregnant randomized women with normal pregnancies.

The demographic and obstetric characteristics of the patients are shown in Table 1. The median age of the patients was 28 (17-43) years. The median gestational age was 34 weeks (ranging between 23 and 41) with a median birth weight of 2300 grams. The median systolic and diastolic blood pressure values were 140 mmHg and 90 mmHg, respectively. The mean hemoglobin value was 12 (1.5) g/dl, the mean platelet value was 218 in the microliter. The median NLR was 3.9 (1.3-25.1) and the median PLR was 113.6 (20.7-693). The rest of the analysis is shown in Table 1.

Table 1: Demographic and obstetric characteristics of the patients

Characteristics (n=94)	Mean (standard deviation)* Median (Minimum – maximum)
Age (years)	28 (17-43)
Gravidity	2 (1-6)
Parity	1 (0-5)
BMI (kg/m^2)	29.3 (21.4-46.6)
Gestational age (weeks)	34 (23-41)
Birth weight (gr)	2300 (475-4500)
APGAR 1st min.	8 (0-9)
APGAR 5th min.	10 (0-10)
Systole (mmHg))	140 (100-240)
Diastole (mmHg)	90 (60-120)
Dipstick proteinuria	1 (0-3)
Hemoglobin (g/dl)*	12 (1.5)*
Neutrophil (10^6/ml)	8000 (2150-24000)
Lymphocyte (10^6/ml)	1970 (400-5080)
Platelets (mcl)*	218 (73.1)*
Monocyte (10^6/ml)	500 (50-1600)
Neutrophil/Lymphocyte ratio	3.9 (1.3-25.1)
Platelet/Lymphocyte ratio	113.6 (20.7-693)
Monocyte/Lymphocyte ratio	4.9 (0.4-9.1)
Mean platelet volume (fl)	10.5 (6.6-16.4)
Red cell distribution width (%)	43.7 (12.6-72.4)
Diagnosis (n, %)	Normal pregnancy (40, %31) Eclampsia (40, %31) HELLP (49, %38)

gr: gram, kg: kilogram, mcl: microliter, fl: femtolitre, min: minute, n: frequency, %: percentage. Descriptive analyses were presented using mean (X(SD)) and median (min-max) for normally distributed* and non-normally distributed data, respectively

The analysis results of the maternal and fetal characteristics of all 3 groups are detailed in Table 2. The median ages of normotensive and eclampsia groups were 26 years, and that of the HELLP group was 30 years. The median gestational age of Groups 1, 2 and 3 were 38 weeks, 32 weeks, and 33 weeks, respectively ($p<0.05$). The median birth weights in the same order were 3300 grams, 1690 grams, and 1600 grams ($p<0.05$). Infants' 1st and 5th minute APGAR scores, mothers' systolic and diastolic blood pressures, and dipstick protein values also significantly differed between the three groups (Table 2).

Table 2: Comparison of maternal and fetal characteristics

RF	Group 1 (n=40) X (SD)/Median (min–max)	Group 2 (n=40) X (SD)/Median (min–max)	Group 3 (n=49) X (SD)/Median (min–max)	*P*-value
Age (years)	26 (19-40)	26 (17-43)	30 (19-41)	0.066
Gravidity	2 (1-6)	1 (1-6)	2 (1-6)	0.005
Parity	2 (1-5)	1 (0-5)	1 (1-5)	<0.001
BMI (kg/m^2)	29.3 (23.4-36)	28.5 (21.4-40)	30.4 (21-8-46.6)	0.230
Gestational age (weeks)	38 (34-41)	32 (24-41)	33 (23-40)	<0.001
Birth weight (gr)	3300 (2380-4070)	1690 (500-3480)	1600 (475-4500)	<0.001
APGAR 1st min.	9 (5-9)	8 (0-9)	8 (0-9)	<0.001
APGAR 5th min.	10 (9-10)	9 (0-10)	9 (0-10)	<0.001
Systole (mmHg)	110 (100-120)	150 (100-240)	150 (130-220)	<0.001
Diastole (mmHg)	70 (60-80)	100 (80-120)	90 (80-110)	<0.001
Dipstick proteinuria	0 (0-1)	2 (0-3)	3 (0-3)	<0.001

gr: gram, kg: kilogram, min: minimum, max: maximum. Descriptive analyses were presented using mean (X(SD)) and median (min-max) for normally distributed* and non-normally distributed variables, respectively. $P<0.05$ was considered significant for Kruskal Wallis and one way ANOVA tests

Table 3 shows the laboratory parameters of all groups. The median neutrophil counts in the normotensive, eclampsia and HELLP groups were 6830 (2630-11950) (10^6/ml), 9715 (2150-24000) (10^6/ml), and 8040 (3400-22500) (10^6/ml), respectively ($P<0.001$). The NLR and PLR values were significantly different between three groups ($P=0.014$, $P=0.002$, respectively). Post-hoc analyses were performed to evaluate the groups that created the difference. Accordingly, NLR significantly differed between the normotensive and the eclamptic pregnant women. The median NLR values in the first and second groups were 3.3 (1.3-6.3), and 4.3 (1.3-25.1), respectively ($P=0.007$). PLR values significantly differed between the normotensive pregnant women and those with a history of HELLP (128.3 (75.5-693) vs. 100.6 (20.7-280) ($P=0.026$), respectively) (Table 3).

Table 3: Comparison of laboratory parameters

RF	Group 1 (n=40) X (SD)/Median (min–max)	Group 2 (n=40) X (SD)/Median (min–max)	Group 3 (n=49) X (SD)/Median (min–max)	*P*-value
Hemoglobin (g/dl)*	11.7 (1.2)	11.7 (1.6)	12.5 (1.6)	0.026
Neutrophil (10^6/ml)	6830 (2630-11950)	9715 (2150-24000)	8040 (3400-22500)	<0.001
Lymphocyte (10^6/ml)	1925 (1000-5080)	2090 (700-4200)	1920 (400-4670)	0.892
Platelets (mcl)*	234.9 (64.6)	228.6 (74.2)	195.5 (75.5)	0.021
Monocyte (10^6/ml)	460 (240-1240)	520 (100-1000)	530 (50-1600)	0.289
Neutrophil/Lymphocyte ratio	3.3 (1.3-6.3)	4.3 (1.3-25.1)	3.9 (1.5-17.3)	0.014
Platelet/Lymphocyte ratio	128.3 (75.5-693)	107.9 (44.2-644)	100.6 (20.7-280)	0.002
Monocyte/Lymphocyte ratio	5 (3.2-7.9)	5.2 (0.4-7.6)	4.7 (0.6-9.1)	0.619
Mean platelet volume (fl)	10 (7.9-16.4)	10 (6.6-12.4)	11.3 (7.1-15.9)	<0.001
Red cell distribution width (%)	44.6 (36-72.4)	41.5 (12.6-64)	44.3 (13.2-69.6)	0.017
Post-Hoc analyze		*P*-value * Group 1 vs. 2	*P*-value * Group 1 vs. 3	*P*-value * Group 2 vs. 3
Hemoglobin (g/dl)*		0.999	0.052	0.057
Neutrophil (10^6/ml)		<0.001	0.047	0.020
Platelets (mcl)*		0.918	0.029	0.080
Neutrophil/Lymphocyte ratio		0.007	0.168	0.324
Platelet/Lymphocyte ratio		0.336	0.026	0.492
Mean platelet volume (fl)		0.782	0.001	<0.001
Red cell distribution width (%)		0.001	0.500	0.025

gr: gram, dl: deciliter, min: minimum, max: maximum. Descriptive analyses were presented using mean (X(SD)) and median (min-max) for normally distributed* and non-normally distributed variables, respectively. $P<0.05$ was considered significant for Kruskal Wallis and one way ANOVA tests. The Tukey test was used for the double group comparison of the results that were significant in multiple analysis. Homogeneity of variances was evaluated with Levene's test.

The median red cell distribution width was 44.6 in normotensive women, 41.5 in women with eclampsia, and 44.3 in women with a history of HELLP ($P=0.017$). The first and the second groups ($P=0.001$), and the second and the third groups significantly differed from one another ($P=0.025$) (Table 3).

Discussion

Preeclampsia indicates either new-onset hypertension and significant end-organ dysfunction (with or without proteinuria) occurring in a previously normotensive woman after 20 weeks of gestation. HELLP is the acronym that suggests a syndrome in pregnant women characterized by hemolysis with a microangiopathic blood smear, elevated liver enzymes, and a low platelet count [15].

In this study, both NLR and PLR were significantly different between three groups. Post-hoc analysis revealed that the NLR differed between the normal pregnant women and those with preeclampsia, while PLR differed between the normal pregnant women and those with HELLP. Hemoglobin, Neutrophil, Mean Platelet Volume and Red Cell Distribution Width were also significantly different between the three groups. Lymphocyte and Monocyte/Lymphocyte ratio were similar.

Although the standard course of pregnancy is associated with oxidative stress, factors such as vascular endothelial damage, placental ischemia, oxidative damage, coagulation anomalies, inflammation are predisposing factors to preeclampsia [16].

Hyperactivation of inflammatory cells in preeclampsia causes inflammatory cytokines and autoantibodies to be released and higher superoxide production, resulting in endothelial dysfunction [4]. The NLR, PLR, and other routine CBC components are sensitive early markers of preeclampsia and other inflammatory obstetric conditions. Gogoi et al. [13] found that NLR, PLR, RDW, and MPV values were all higher in women with pre- eclampsia compared to healthy pregnant women. Sachan et al. [17] showed that first-trimester NLR could predict preeclampsia and severe preeclampsia in the third trimester. Mannaertset et al. [12] found that NLR was higher, and PLR was lower in preeclamptic patients compared to healthy controls. On the other hand, Sisti et al. [18] did not report a direct association of NLR, PLR, and other complete blood parameters with HELLP syndrome.

Measuring NLR and PLR is easy and inexpensive. These markers were studied in inflammatory disorders such as diabetes mellitus, coronary artery disease, ulcerative colitis, and cancer [19]. Since NLR and PLR suggest the presence of an increased inflammatory state, they can be used to predict preeclampsia [13, 18].

PLR plays a role in cytokine-dependent immune response and is associated with severe ischemia, end-organ damage, and preeclampsia. Raised C-reactive protein and impaired flow-mediated vasodilation precede preeclampsia [20].

In this study, NLR was significantly higher in pregnant women diagnosed with eclampsia compared to the normotensive control group. However, PLR did not differ between the normotensive group and pregnant women with eclampsia. In women who developed HELLP findings, NLR did not differ significantly compared to the eclampsia group. Of course, considering the low platelet count, which is one of the HELLP diagnostic criteria, PLR was significantly lower in those with HELLP than in normotensive pregnant women. Although RDW was reportedly associated with preeclampsia in some studies, we found that the RDW value was significantly higher among normotensive pregnant women than in pregnant women with eclampsia [13, 21]. The reason for the increase in RDW levels in preeclampsia has not been fully determined in these studies.

The main limitation of this study is the lack of a comparison group of preeclamptic patients and the small sample size. This study should be performed in a large geographical area, with more patients. In addition, the correlation with other radiological and biochemical markers was not researched in this study.

One of the strengths of our study is the evaluation of pregnant groups diagnosed with HELLP syndrome and eclampsia. We were able to characterize two hypertensive diseases that threaten maternal and fetal life and observe the difference between healthy controls and hypertensive pregnant patients.

Conclusion

This study found that NLR was higher in pregnant women with eclampsia. Platelet count and MPV were significantly lower in the HELLP group. NLR and PLR may be useful in predicting the risk of eclampsia prenatally or during delivery. Multicenter studies with large numbers of patients and long-term follow-up are needed to confirm these findings.

References

1. Ferrazzi E, Stampalija T, Monasta L, Di Martino D, Vonck S, Gyselaers W. Maternal hemodynamics: a method to classify hypertensive disorders of pregnancy. American journal of obstetrics and gynecology. 2018;218:124-e1.
2. Gynecologists AC of O and. Hypertension in pregnancy. Report of the American College of Obstetricians and Gynecologists' task force on hypertension in pregnancy. Obstetrics and gynecology. 2013;122:1122.
3. Steegers EAP, Von Dadelszen P, Duvekot JJ, Pijnenborg R. Pre-eclampsia. The Lancet. 2010;376:631–44.
4. Laresgoiti- Servitje E. A leading role for the immune system in the pathophysiology of preeclampsia. Journal of leukocyte biology. 2013;94:247–57.
5. Duley L. The global impact of pre-eclampsia and eclampsia. In: Seminars in perinatology. Elsevier; 2009. p. 130–7.
6. Weinstein L. Syndrome of hemolysis, elevated liver enzymes, and low platelet count: a severe consequence of hypertension in pregnancy. American journal of obstetrics and gynecology. 1982;142:159–67.
7. Sibai BM. Diagnosis, controversies, and management of the syndrome of hemolysis, elevated liver enzymes, and low platelet count. Obstetrics & Gynecology. 2004;103:981–91.
8. Kınay T, Küçük C, Kayıkçıoğlu F, Karakaya J. Severe preeclampsia versus HELLP syndrome: maternal and perinatal outcomes at< 34 and≥ 34 weeks' gestation. Balkan medical journal. 2015;32:359.
9. Vigil-de Gracia PE, Tenorio-Maranon FR, Cejudo-Carranza E, Helguera-Martinez A, Garcia-Caceres E. Difference between preeclampsia, HELLP syndrome and eclampsia, maternal evaluation. Ginecologia y obstetricia de Mexico. 1996;64:377–82.
10. Benedetto C, Marozio L, Tancredi A, Picardo E, Nardolillo P, Maria Tavella A, et al. Biochemistry of HELLP syndrome. Advances in clinical chemistry. 2011;53:85.
11. Gezer C, Ekin A, Ertas IE, Ozeren M, Solmaz U, Mat E, et al. High first-trimester neutrophil-to-lymphocyte and platelet-to-lymphocyte ratios are indicators for early diagnosis of preeclampsia. Ginekologia polska. 2016;87:431–5.
12. Mannaerts D, Heyvaert S, De Cordt C, Macken C, Loos C, Jacquemyn Y. Are neutrophil/lymphocyte ratio (NLR), platelet/lymphocyte ratio (PLR), and/or mean platelet volume (MPV) clinically useful as predictive parameters for preeclampsia? The Journal of Maternal-Fetal & Neonatal Medicine. 2019;32:1412–9.
13. Gogoi P, Sinha P, Gupta B, Firmal P, Rajaram S. Neutrophil- to- lymphocyte ratio and platelet indices in pre- eclampsia. International Journal of Gynecology & Obstetrics. 2019;144:16–20.
14. Martin Jr JN, Rinehart BK, May WL, Magann EF, Terrone DA, Blake PG. The spectrum of severe preeclampsia: comparative analysis by HELLP (hemolysis, elevated liver enzyme levels, and low platelet count) syndrome classification. American journal of obstetrics and gynecology. 1999;180:1373–84.
15. Stone JH. HELLP syndrome: hemolysis, elevated liver enzymes, and low platelets. Jama. 1998;280:559–62.
16. Karaşin SS, Çift T. The role of ischemia-modified albumin as a biomarker in preeclampsia. Revista Brasileira de Ginecologia e Obstetrícia. 2020;42:133–9.
17. Sachan R, Patel ML, Sachan P, Shyam R. Diagnostic accuracy of neutrophil to lymphocyte ratio in prediction of nonsevere preeclampsia and severe preeclampsia. Journal of Current Research in Scientific Medicine. 2017;3:79.
18. Sisti G, Faraci A, Silva J, Upadhyay R. Neutrophil-to-lymphocyte ratio, platelet-to-lymphocyte ratio and complete blood count components in the first trimester do not predict HELLP syndrome. Medicina. 2019;55:219.
19. Imtiaz F, Shafique K, Mirza SS, Ayoob Z, Vart P, Rao S. Neutrophil lymphocyte ratio as a measure of systemic inflammation in prevalent chronic diseases in Asian population. International archives of medicine. 2012;5:1–6.
20. Garciéa RG, Celedón J, Sierra-Laguado J, Alarcón MA, Luengas C, Silva F, et al. Raised C-reactive protein and impaired flow-mediated vasodilation precede the development of preeclampsia. American journal of hypertension. 2007;20:98–103.
21. Kurt RK, Aras Z, Silfeler DB, Kunt C, Islimye M, Kosar O. Relationship of red cell distribution width with the presence and severity of preeclampsia. Clinical and Applied Thrombosis/Hemostasis. 2015;21:128–31.

This paper has been checked for language accuracy by JOSAM editors.
The National Library of Medicine (NLM) citation style guide has been used in this paper.

J Surg Med. 2021;5(12):1206-1209.
DOI: 10.28982/josam.1009432

Journal of Surgery and Medicine
e-ISSN=2602-2079

Smartphones for evaluation of computerized tomography scan of patients with suspected skull fractures and intracranial hemorrhage in emergency medicine

Hasan Aldinc, Cem Gun

Department of Emergency Medicine, School of Medicine, Acibadem Mehmet Ali Aydinlar University, Istanbul, Turkey

ORCID ID of the author(s)
HA: 0000-0002-4734-5319
CG: 0000-0001-5907-5056

Corresponding Author
Hasan Aldinc
Department of Emergency Medicine, School of Medicine, Acibadem Mehmet Ali Aydinlar University, Istanbul, Turkey
E-mail: drhasana@hotmail.com

Ethics Committee Approval
The Acibadem Mehmet Ali Aydinlar University Ethics Committee approved the study protocol on 5.5.2015 with approval number 2015/6.
All procedures in this study involving human participants were performed in accordance with the 1964 Helsinki Declaration and its later amendments.

Conflict of Interest
No conflict of interest was declared by the authors.

Financial Disclosure
The authors declared that this study has received no financial support.

Published
2021 November 28

Abstract

Background/Aim: It is generally not probable to employ a radiologist or an experienced physician for interpreting radiological images at emergency services**.** The importance of telemedicine has grown, especially during the coronavirus 2019 pandemic. There are a few studies on cranial tomography image transfer and correct evaluation rate with smartphones in the literature. This study aims to evaluate the effectiveness of smartphones for diagnosing mortal pathologies such as skull fractures and intracranial hemorrhages compared to the original images on LED displays of radiology terminals.
Methods: This methodological study was designed to validate smartphones' usefulness in assessing cranial computerized tomography scans in emergency cases. Four sets of CT scans, each containing 10 case samples in four diagnostic groups, subarachnoid hemorrhage, subdural hemorrhage, epidural hemorrhage, and bone fractures, and a set of 10 non-pathological CT scans were evaluated first on 6.1-inches smartphone display for 1 minute, and then on the 17-inches LED display again for 1 minute. The internal camera of the smartphone was used to capture the image before assessments.
Results: A total of 12 neurosurgeons evaluated 50 CT scan images both on smartphones and LED displays. The overall accuracy between both methods ranged between 80%-100% for subarachnoid and epidural hemorrhage and bone fractures, and between 90%-100% for subarachnoid hemorrhage and non-pathological CT scans. The individual kappa coefficients of neurosurgeons ranged between 0.725 to 1.0 (P<0.001).
Conclusion: The overall accuracy of smartphone CT readings with computer LED displays was satisfactory. Our results showed that smartphones are useful for rapid communication between neurosurgeons and emergency department doctors, contributing to timely and accurate patient management in emergency situations.

Keywords: Smartphone, Computerized tomography, Intracranial hemorrhages, Emergency medicine, Telemedicine, Teleradiology

How to cite: Aldinc H, Gun C. Smartphones for evaluation of computerized tomography scan of patients with suspected skull fractures and intracranial hemorrhage in emergency medicine. J Surg Med. 2021;5(12):1206-1209.

Introduction

Intracranial hemorrhage is a significant medical emergency with an estimated incidence of 25 per 100,000 person-years [1]. The underlying pathology may vary widely, including but not limited to trauma, hypertension, aneurysms, thrombosis, and other causes [2]. Particularly traumatic intracranial injuries are significant public health problems that affect millions of people worldwide annually, which cause significant mortality and morbidity that can affect all domains of human life [3-5].

The admissions due to cranial injuries also possess a significant burden on emergency health services. The assessment of a patient with a suspected intracranial event includes appropriate imaging modalities, which are indispensable for the initial management of such a patient at the emergency room. The imaging studies contribute both to the diagnosis and the treatment [6]. Nevertheless, it is generally not probable to employ a radiologist or an experienced physician for interpreting radiological images at emergency services. An accurate and timely diagnosis of intracranial status is essential for reducing mortality, and mobile health, or telemedicine, in other words, may aid emergency service staff in such conditions.

The World Health Organization defines the concept of telemedicine as the communication or consultation between health professionals about patients using voice, text, data, imaging or video functions of a mobile device [7]. The time and lifesaving access to expert advice by using any means of technology draw attention in recent years, and numerous studies are being conducted to evaluate the different methods for such purposes. Smartphones and tablets helped assess radiological images for diagnosing fractures remotely in several recent studies [8-12].

The importance of this issue has grown during the coronavirus 2019 pandemic [13]. A unique advantage of telemedicine is that during the pandemic, even quarantined doctors can continue to provide teleconsultations.

Besides its advantages, the accuracy of the remote assessments is strictly associated with the quality of the images transferred. Nevertheless, there might not always be a chance to transmit high-quality radiological images, particularly the sequential sections like computerized tomography (CT) images. A quick way of image transfer is taking a photograph of the image on the computer screen and sending it to an expert over messaging applications, which may significantly affect the expert's decision.

Based on this background, this study aimed to evaluate the usefulness of CT images captured by smartphones compared to the original images on LED displays of computers for diagnosing skull fractures and intracranial hemorrhages, which are a significant burden of mortality and morbidity at the emergency rooms.

Materials and methods

This prospective study was performed between May 2018 and September 2018 with the radiology unit of a university hospital and 12 neurosurgeons working in İstanbul. The local institutional ethics board approved the study protocol on 5.5.2015 with the approval number 2015/6. The STROBE checklist was used in the study design and drafting of the manuscript [14].

Five sets of CT scans, each containing ten image sets, were randomly selected from the radiological repository of the hospital. The image sets included non-pathological radiological views, plus CT images of patients in four diagnostic groups, namely, subarachnoid hemorrhage, subdural hemorrhage, epidural hemorrhage, and skull fractures only. The CT scans were already assessed and diagnosed by the radiologists before the study.

A total of 12 neurosurgeons participated in the study. The participants were not informed about which pathologies were included. In addition, it was ensured that the participants did not know about the other participants participating in the study. Before the participants' assessments, the CT images were initially captured using the internal camera of a smartphone (6.1 inches display and 828x1792 pixels display resolution, and 12 MP camera) from a 30 cm distance of the 17-inches LED display (1920x1080 pixels of screen resolution). Each participant assessed the same CT images first on a 6.1-inches smartphone display for 1 minute and then on the 17-inches LED display again for 1 minute. The participants' diagnoses were recorded after assessing of each image, and evaluated by the authors based on the radiologists' reports as correct or not.

Statistical analysis

The descriptive analyses were presented as percentages throughout the study. During the analyses, first, the accuracy of the assessments was evaluated for each diagnostic group and each participant. The overall accuracy for each diagnostic group was defined as the proportion of the total number of correct and wrong diagnoses in both smartphone and LED displays divided by the total assessments (calculated as (A+D)/10; Table 1). Second, the level of agreement between smartphone and LED display assessments was analyzed using Kappa statistics for each participant. The results were interpreted considering the distribution range of the agreement levels. Third, the proportion of only correct diagnoses was calculated for each sample image and diagnostic subgroup (calculated as A/10; Figure 1). SPSS21 software (IBM Inc., Armonk, NY, USA) was used to build the tables and statistical analyses of the study. A value of $P<0.05$ was considered statistically significant.

Results

A total of 12 neurosurgeons evaluated 50 CT scan images both on smartphones and LED displays. The overall accuracy of the assessments and the kappa coefficients of agreement were presented in Table 2. If a participant made the correct diagnosis or made the same mistake on the same image on both displays, this was recorded as an accurate answer. Accordingly, the overall accuracy ranged between 80%-100% for subarachnoid and epidural hemorrhage and bone fractures, and between 90%-100% for subarachnoid hemorrhage and non-pathological CT scans. The individual kappa coefficients of agreement between the smartphone and LED display assessments of each participant ranged between 0.725 to 1.0. All were significant ($P<0.001$) and corresponded to good to very good agreement between both methods.

Table 1: Formulation of the accuracy analyses

		LED display Correct	False	
Smartphone display	Correct	A	B	∑ correct on smartphone display
	False	C	D	∑ false on smartphone display
		∑ correct on LED display	∑ false on LED display	∑ images assessed (10 images per diagnostic group)

Table 2: Overall accuracy of CT image assessments

Participants	Subarachnoid hemorrhage %	Subdural hemorrhage %	Epidural hemorrhage %	Bone fractures %	Normal CT scan %	Overall kappa (Tel-LED)	*P*-value
#1	90	90	100	100	100	0.905	<0.001
#2	90	100	100	100	90	0.947	<0.001
#3	100	100	100	100	100	1.000	<0.001
#4	100	100	100	100	100	1.000	<0.001
#5	100	90	80	100	100	0.848	<0.001
#6	100	100	80	100	100	0.875	<0.001
#7	90	90	100	80	100	0.817	<0.001
#8	100	90	100	100	100	0.940	<0.001
#9	100	100	100	100	100	1.000	<0.001
#10	100	100	90	90	100	0.905	<0.001
#11	90	100	100	100	90	0.891	<0.001
#12	80	90	90	90	90	0.725	<0.001

The correct diagnosis rates were presented in Table 3. The assessments revealed that the lowest levels of correct diagnoses were 80% for subarachnoid hemorrhage, 87.5% for subdural and epidural hemorrhage, 83.3% for bone fractures, and 88.9% for non-pathological CT scans.

Table 3: Correct diagnosis proportions

	Subarachnoid hemorrhage %	Subdural hemorrhage %	Epidural hemorrhage %	Bone fractures %	Normal CT scan %
Image #1	100	100	100	83.3	100
Image #2	80	87.5	100	100	100
Image #3	100	100	100	100	100
Image #4	100	100	100	100	100
Image #5	87.5	100	91.7	100	100
Image #6	100	100	87.5	100	88.9
Image #7	100	100	100	100	88.9
Image #8	91.7	87.5	100	100	100
Image #9	100	100	90.9	100	100
Image #10	100	100	100	100	100

Discussion

In this study, we evaluated the usability of smartphones for assessing CT images to diagnose skull fractures and intracranial hemorrhages. Our analyses revealed that the images captured by an internal smartphone camera could provide adequate quality to a neurosurgeon on a 6.1-inch display for accurate diagnosis of a skull fracture or intracranial injury. Accuracy of diagnoses on a smartphone display compared to computer LED screen was satisfactory, and both displays showed significant overall accordance to aid neurosurgeons in diagnosing the correct pathology.

Today, physicians' consulting the radiological images over mobile messaging applications became a common practice [15]. This is particularly important in emergency medicine, since accurate and timely diagnosis and appropriate interventions are lifesaving in this vulnerable patient group. Unfortunately, there is limited availability of experienced health professionals to evaluate the radiological images in most emergency services. At this point, a practical solution is consulting the images over messaging applications [16]. To date, several studies evaluated the usability of smartphones for the diagnosis of musculoskeletal traumas and bone fractures over radiological images and reported that this was a safe and accurate way for skeletal trauma consultation that can significantly decrease the lags in emergency services [8, 17].

One of the very first reports about using mobile devices for CT evaluation was published by Yamamoto and Williams [18] in 2000, which reported that a wireless pocket computer can download the CT scan images from a wireless modem in 4 to 6 minutes and provide adequate quality for reviewing on display. Three years later, another study by Yaghmai et al. [19] evaluated the feasibility of a personal digital assistant (PDA) device for interpreting the cranial CT scans of trauma patients, which were directly transferred into the device from a picture archiving and communications system (PACS). The authors reported that this handheld device can reliably interpret the CT scans of patients with suspected intracranial hemorrhage. In a recent study from Sakai et al. [20], using a telemedicine application to transfer images on smartphone, there was a high degree of inter-device and inter-rater agreement in terms of the vascular neurologists' neuroimaging findings between the smartphone and the desktop PC monitor in patients with acute stroke. Unlike this study, we used manually captured images by the smartphone, which made the quality of the images more dependent on the manual capturing and the technical specifications of the smartphone. Nevertheless, we confirmed the accuracy of the manually captured images.

Another study by Waran et al. [21] evaluated the utility of sending short video clips of an entire scan series between junior and senior doctors in a neurosurgery unit after office hours and reported that this method is very effective for emergency consultations, which should otherwise only depend on verbal descriptions, which is more susceptible to errors. In our study, we did not send images as video clips because the resolution of photos taken with the smartphone is higher than the resolution of the video clips.

In 2013, Shivapathasundram et al. [22] evaluated the utility of transferring entire series of patient neuroimaging using the video application of the smartphones to the consultant neurosurgeons over only one patient's three video recordings. They reported that this was a valuable and rapid way to communicate with the neurosurgeons in emergency situations. Mobile devices were evaluated in numerous studies for radiological assessment in many situations other than traumatic emergencies. In one of those, Park et al. [23] evaluated the diagnostic performance of smartphones in the assessment of coronary CT angiography of patients with acute chest pain in the emergency services. The authors reported that smartphone readings by the cardiac radiologist were more similar to the angiography results and in-house radiologists' reports than the reading of on-call residents, which was considered a promising result for further evaluations of the real-time mobile consultations to achieve an improved diagnostic competency. Unlike Park et al.'s study, in our study, the same physicians evaluated the images from smartphones and LED displays.

As currently available evidence in the literature suggests, mobile technologies are becoming more integrated in healthcare practice, especially in situations in which rapid communications with colleagues are most needed. Traumatic injuries are examples of these emergencies. Our results also confirmed the previous reports on this topic and showed that smartphones are useful for consulting the CT scans of patients

with a probable skull fracture, intracranial injury, and hemorrhage with off-site neurosurgeons.

There are some limitations in our study. Monitoring of the same CT image by the participants right after the first evaluation may cause them to look more carefully at the suspicious place in the initial assessment. Another limitation is that clinicians are likely to use phones with different resolutions and sizes in real life. In the future, the minimum phone features that can be used to evaluate images correctly can be determined with comprehensive studies to be carried out with phones with different resolutions and sizes.

Conclusions

This study showed that the overall accuracy of smartphone CT readings with computer LED displays was satisfactory, suggesting that CT images captured with smartphones can provide an adequate quality to the neurosurgeons for accurate diagnosis. This rapid communication between the neurosurgeons and the emergency department doctors can contribute much to patient management in emergency situations.

References

1. Van Asch CJ, Luitse MJ, Rinkel GJ, van der Tweel I, Algra A, Klijn CJ. Incidence, case fatality, and functional outcome of intracerebral haemorrhage over time, according to age, sex, and ethnic origin: a systematic review and meta-analysis. Lancet Neurol. 2010 Feb;9(2):167-76. doi: 10.1016/S1474-4422(09)70340-0. Epub 2010 Jan 5. PMID: 20056489.
2. Heit JJ, Iv M, Wintermark M. Imaging of Intracranial Hemorrhage. J Stroke. 2017 Jan;19(1):11-27. doi: 10.5853/jos.2016.00563. Epub 2016 Dec 12. PMID: 28030895; PMCID: PMC5307932.
3. Daneshvar DH, McKee AC. Traumatic Brain Injury. Neurobiology of Brain Disorders 2015. p. 219-235. doi: 10.1016/B978-0-12-398270-4.00016-1
4. Chakraborty S, Skolnick BE, Alves WM, Marshall LF, Narayan RK. Traumatic Brain Injury. Handbook of Neuroemergency Clinical Trials 2018. p. 85-109. doi: 10.1016/B978-0-12-804064-5.00005-9
5. Ouellet M-C, Beaulieu-Bonneau S, Morin CM. Traumatic Brain Injury. Handbook of Sleep Disorders in Medical Conditions 2019. p. 221-252.
6. Rincon S, Gupta R, Ptak T. Imaging of head trauma. Neuroimaging Part I. Handbook of Clinical Neurology 2016. p. 447-477.
7. World Health Organization. mHealth - New horizons for health through mobile technologies. 2011. accessable on: https://www.who.int/goe/publications/goe_mhealth_web.pdf.
8. Naqvi GA, Daly M, Dawood A, Kurkuri A, Kutty S. Smart consultation for musculoskeletal trauma: accuracy of using smart phones for fracture diagnosis. Surgeon. 2014 Feb;12(1):32-4. doi: 10.1016/j.surge.2013.09.001. Epub 2013 Oct 3. PMID: 24090680.
9. Tennant JN, Shankar V, Dirschl DR. Reliability and validity of a mobile phone for radiographic assessment of ankle injuries: a randomized inter- and intraobserver agreement study. Foot Ankle Int. 2013 Feb;34(2):228-33. doi: 10.1177/1071100712466849. Epub 2013 Jan 11. PMID: 23413062.
10. Ferrero A, Garavaglia G, Gehri R, Maenza F, Petri GJ, Fusetti C. Analysis of the inter- and intra-observer agreement in radiographic evaluation of wrist fractures using the multimedia messaging service. Hand (N Y). 2011 Dec;6(4):384-9. doi: 10.1007/s11552-011-9362-4. Epub 2011 Sep 23. PMID: 23204964; PMCID: PMC3213258.
11. Eranki V, Munt J, Lim MJ, Atkinson R. Consultation of orthopaedics cases using multimedia messaging services. Open Orthop J. 2010 Apr 23;4:164-8. doi: 10.2174/1874325001004010164. PMID: 21249168; PMCID: PMC3023093.
12. Chandhanayingyong C, Tangtrakulwanich B, Kiriratnikom T. Teleconsultation for emergency orthopaedic patients using the multimedia messaging service via mobile phones. J Telemed Telecare. 2007;13(4):193-6. doi: 10.1258/135763307780908049. PMID: 17565775.
13. Yang XJ, Wei W, Zhang Y, Wang YN, Zhang N, Li TQ, et al. What Is the Best Way for Patients to Take Photographs of Medical Images (Radiographs, CT, and MRI) Using a Smartphone? Clin Orthop Relat Res. 2021 Oct 1;479(10):2228-2235. doi: 10.1097/CORR.0000000000001731. PMID: 33787525; PMCID: PMC8445547.
14. Vandenbroucke JP, von Elm E, Altman DG, Gøtzsche PC, Mulrow CD, Pocock SJ, et al. Strengthening the Reporting of Observational Studies in Epidemiology (STROBE): explanation and elaboration. Epidemiology 2007;18(6):805-35
15. Paryavi E, Schwartz BS, Meyer CL, Herman MJ, Abzug JM. Reliability and Effectiveness of Smartphone Technology for the Diagnosis and Treatment Planning of Pediatric Elbow Trauma. J Pediatr Orthop. 2016 Jul-Aug;36(5):483-7. doi: 10.1097/BPO.0000000000000477. PMID: 25851688.
16. Stahl I, Katsman A, Zaidman M, Keshet D, Sigal A, Eidelman M. Reliability of Smartphone-Based Instant Messaging Application for Diagnosis, Classification, and Decision-making in Pediatric Orthopedic Trauma. Pediatr Emerg Care. 2019 Jun;35(6):403-406. doi: 10.1097/PEC.0000000000001211. PMID: 28697157.
17. Giordano V, Koch HA, Mendes CH, Bergamin A, de Souza FS, do Amaral NP. WhatsApp Messenger is useful and reproducible in the assessment of tibial plateau fractures: inter- and intra-observer agreement study. Int J Med Inform. 2015 Feb;84(2):141-8. doi: 10.1016/j.ijmedinf.2014.11.002. Epub 2014 Nov 11. PMID: 25468642.
18. Yamamoto LG, Williams DR. A demonstration of instant pocket wireless CT teleradiology to facilitate stat neurosurgical consultation and future telemedicine implications. Am J Emerg Med. 2000 Jul;18(4):423-6. doi: 10.1053/ajem.2000.6316. PMID: 10919531.
19. Yaghmai V, Kuppuswami S, Berlin JW, Salehi SA. Evaluation of personal digital assistants as an interpretation medium for computed tomography of patients with intracranial injury. Emerg Radiol. 2003 Oct;10(2):87-9. doi: 10.1007/s10140-003-0300-9. Epub 2003 Aug 22. PMID: 15290513.
20. Sakai K, Komatsu T, Iguchi Y, Takao H, Ishibashi T, Murayama Y. Reliability of Smartphone for Diffusion-Weighted Imaging-Alberta Stroke Program Early Computed Tomography Scores in Acute Ischemic Stroke Patients: Diagnostic Test Accuracy Study. J Med Internet Res. 2020 Jun 9;22(6):e15893. doi: 10.2196/15893. PMID: 32515744; PMCID: PMC7312257.
21. Waran V, Bahuri NF, Narayanan V, Ganesan D, Kadir KA. Video clip transfer of radiological images using a mobile telephone in emergency neurosurgical consultations (3G Multi-Media Messaging Service). Br J Neurosurg. 2012 Apr;26(2):199-201. doi: 10.3109/02688697.2011.605482. Epub 2011 Oct 4. PMID: 21970777.
22. Shivapathasundram G, Heckelmann M, Sheridan M. Using smart phone video to supplement communication of radiology imaging in a neurosurgical unit: technical note. Neurol Res. 2012 Apr;34(3):318-20. doi: 10.1179/1743132812Y.0000000006. Epub 2012 Mar 12. PMID: 22449291.
23. Park JH, Kim YK, Kim B, Kim J, Kwon H, Kim K, et al. Diagnostic performance of smartphone reading of the coronary CT angiography in patients with acute chest pain at ED. Am J Emerg Med. 2016 Sep;34(9):1794-8. doi: 10.1016/j.ajem.2016.06.009. Epub 2016 Jun 7. PMID: 27396538.

This paper has been checked for language accuracy by JOSAM editors.
The National Library of Medicine (NLM) citation style guide has been used in this paper.

J Surg Med. 2021;5(12):1210-1213.
DOI: 10.28982/josam.1033128

Journal of Surgery and Medicine
e-ISSN=2602-2079

The effect of Covid-19 pandemic on gastric cancer surgery

Nidal İflazoğlu, Ömer Yalkın

Bursa City Hospital, Department of Surgical Oncology, Bursa, Turkey

ORCID ID of the author(s)
Nİ: 0000-0001-7727-602X
ÖY: 0000-0003-0311-5885

Corresponding Author
Nidal İflazoğlu
Bursa City Hospital, Department of Surgical Oncology, Sağlık Bakanlığı Bursa Şehir Hastanesi, Doğanköy Mahallesi, 16110, Bursa, Turkey
E-mail: nidal1933@yahoo.com

Ethics Committee Approval
The study was conducted after approval was granted by Bursa city hospital clinical research ethics committee (Date: September 08, 2021, and No: 2021.16/3-08.09.21).
All procedures in this study involving human participants were performed in accordance with the 1964 Helsinki Declaration and its later amendments.

Conflict of Interest
No conflict of interest was declared by the authors.

Financial Disclosure
The authors declared that this study has received no financial support.

Published
2021 December 30

Abstract

Background/Aim: The global spread of the COVID-19 pandemic has led to difficulties in the prevention of other diseases and especially in the maintenance of cancer treatment, along with the attempts to control the pandemic. The present study aims to investigate the clinical, oncological, and financial effects of COVID-19 on patients undergoing radical gastric cancer surgery.

Methods: This retrospective cohort study included 46 patients and the clinical, epidemiological, radiological, and laboratory data of these patients were analyzed. Inclusion criteria were patients who were diagnosed with gastric cancer, who underwent radical surgical resection in pre-COVID-19 and during COVID-19 periods. Appropriate surgical options were used by taking precautions against viral transmission.

Results: Of the study patients, 56.5% were males, the median age was 69 (42–83) years, and the median length of stay was 9 (7–34) days. The rate of thoracic computed tomography (CT) taken was statistically significantly higher in during-COVID-19 period (P=0.008). The length of the surgery was statistically significantly longer and the estimated blood loss (cc) was lower in during-COVID-19 period (P<0.001, P=0.043, respectively). From a financial point of view, the cost was statistically significantly higher during-COVID-19 period (P=0.038).

Conclusion: The use of thoracic CT in the surgical management of gastric cancer patients was increased, the surgery was prolonged, and the estimated blood loss was reduced along with the pandemic. In addition, the cost of patient treatment increased due to increasing amount of the routine examination and surgical materials used.

Keywords: Gastric cancer, Surgery, COVID-19

How to cite: İflazoğlu N, Yalkın Ö. The effect of covid-19 pandemic on gastric cancer surgery. J Surg Med. 2021;5(12):1210-1213.

Introduction

Gastric cancer is one of the most common cancer types worldwide [1]. The global spread of the COVID-19 pandemic has led to difficulties in the prevention of other diseases and especially in the maintenance of cancer treatment, along with the attempts to control the pandemic. In this regard, health authorities have changed their strategies around the world and COVID-19 has resulted in the postponement or delay of oncological treatments, as in gastric cancer. To ensure that gastric cancer patients are minimally affected by the current situation, traditional treatment approaches has to be left to adapt to the new circumstances brought into our lives by the COVID-19 pandemic [2].

As gastric cancer is a tumor with well-known immunosuppression and cachexia, it is obvious that COVID-19 is likely to be more mortal in these patients than in the normal population [3]. The extent to which the COVID-19 pandemic has affected gastric cancer surgery is yet to be clarified. The potential effects of the COVID-19 pandemic on healthcare service delivery, outpatient follow-up, surgical strategy, and healthcare workers are not clear [4].

The present study aims to investigate the clinical, oncological, and financial effects of COVID-19 on patients undergoing radical gastric cancer surgery, before and from the onset of the COVID-19 pandemic to the present.

Materials and methods

Study design

Our hospital's surgical oncology clinic was and still is a tertiary cancer center before and during the COVID-19 pandemic. In addition, a part of our hospital and some intensive care units serve as the admission and treatment center for COVID-19 in our region. In our country, the first COVID-19 case was detected on March 1, 2020, followed by a rapid spread, resulting in health measures as well as changes in oncological patient management according to systemic facts. It is possible to state that there have been three major waves of COVID-19 in our country since the pandemic. Within those periods, the health authority adopted the relevant course of action based on short-interval assessments of the status to ensure that cancer therapy services would not be disrupted.

Our study defined the time from August 2019 to February 2020 as the pre-COVID-19 period, and the time from March 2020 to August 2021 as the COVID-19 period. The cases undergoing radical gastric cancer surgery in both periods were compared for demographic characteristics, main characteristics, clinicopathological characteristics, and health economics. The sub-items of the financial burden of COVID-19 on the surgical period-related health economics in these patients were also evaluated.

Financial calculations were calculated in Turkish lira and USD dollars according to the exchange rate at the time of surgery. The time to surgery was defined as the time from the finalization of the pathology to the day of the surgical intervention. Complications were evaluated according to the Clavien-Dindo classification system [5], using a grading of 1 to 5. Preoperative mouth and nose swabs were collected from gastric cancer patients undergoing surgery in the COVID-19 period and the patients were found to be COVID-19-free.

The study included 46 patients who were operated by two surgical oncologists. The clinical, epidemiological, radiological, and laboratory data of these patients were retrospectively retrieved from the hospital information management system. Inclusion criteria were patients who were diagnosed with gastric cancer, who underwent radical surgical resection, and who hadfully accessible records. Patients who had emergency surgery and who had palliative surgery instead of radical surgery were excluded. Additionally, appropriate surgical options (laparoscopic/open surgery etc.) were used by taking precautions against viral transmission during Covid-19 period.

Ethical statement

The study was conducted after approval was granted by Bursa city hospital clinical research ethics committee (Date: September 08, 2021, and No: 2021.16/3-08.09.21). All phases of the study were carried out under the principles established in the Declaration of Helsinki (World Medical Association Declaration of Helsinki "Ethical Principles for Medical Research Involving Human Subjects", amended in October 2013, www.wma.net).

Statistical analysis

The SPSS version 26.0 was used for statistical analysis. The assumption of data normality for all quantitative variables was verified by the Shapiro-Wilk test. For the normally distributed variables, the data were expressed as mean (standard deviation). The non-normally distributed measurement data, in turn, were expressed as median and interquartile range. The count data were expressed using frequency and percentage (%). The Student's t-test was used to compare the means for normally distributed variables and the Mann-Whitney U test for non-normally distributed variables. The count data were statistically analyzed using Pearson's Chi-square test or Fisher's exact probability method. A *P*-value less than 0.05 was considered significant.

Results

Of the study patients, 56.5% were males, the median age was 69 (42–83) years, and the median length of stay was 9 (7–34) days. The rate of the patients receiving neoadjuvant chemotherapy was 21.7%. Early gastric cancer was detected in 21.7%. Laparoscopic surgery was performed in 50% of the patients. The mean length of surgery was 239 minutes. Complications were identified in 36.9% (n = 46) of the patients. The mean intraoperative blood loss was 220 cc. Additional organ resection was performed in 13% of the patients.

Within the scope of the study, one patient (3.3%) who was perioperatively infected by COVID-19 virus during COVID-19 period, needed intubation upon pulmonary involvement and was discharged after 14 days of hospitalization with anti-COVID-19 and supportive therapies. None of the patients died due to COVID-19.

The comparison of pre-COVID-19 and COVID-19 periods revealed no statistically significant difference in age, sex, length of hospital stay, time from diagnosis to surgery, tumor localization, T-stage, TNM stage, rates of early gastric cancer detection, and rates of neoadjuvant therapy ($P>0.05$, Table 1). The rate of thoracic Computed Tomography (CT) was

statistically significantly higher during COVID-19 period than in the pre-COVID-19 period (*P*=0.008, Table 1).

Table 1: Comparison of demographic and clinical features of Pre-Covid-19 and Covid-19 periods

	Pre-Covid-19 n=16	Covid-19 n=30	*P*-value
Age median(min-max)	75(42-82)	66(44-83)	0.362
Gender n(%)			
F	6(37.5)	14(46.7)	0.550
M	10(62.5)	16(53.3)	
Length of stay (day)	10(7-26)	9(7-34)	0.889
Time to surgery(day)			
Neoadjuvant (SD)	105.6 (3)	118.2 (67)	0.639
Non-neoadjuvant	31(11-165)	24(6-225)	0.874
Tumor site			
Cardia	2(12.5)	4(13.3)	0.666
Corpus	6(37.5)	15(50)	
Antrum	8(50)	11(36.7)	
T stage**			
1	4(25)	6(20)	0.331
2	0(0)	3(10)	
3	9(56.3)	11(36.7)	
4	3(18.8)	10(33.3)	
TNM Stage**			
1	3(18.8)	7(23.3)	0.276
2	8(50)	8(926.7)	
3	5(31.3)	15(50)	
Early Gastric Cancer (T1NxM0)*	4(25)	6(20)	0.712
Neoadjuvanttreatment	3(18.8)	7(23.3)	0.720
Number of Thorax CT	1(0-2)	2(1-5)	0.008

**According to NCCN guidelines, *According to Japanese guidelines, SD: standard deviation

The comparison of pre-COVID-19 and COVID-19 periods revealed no statistically significant difference in the type of the intervention, type of gastrectomy, additional organ resection (and splenectomy), degree of the complications (Clavien&Dindo Classification), tumor size (cm), number of total lymph nodes, number of metastatic lymph nodes, the closest surgical margin (mm), and perioperative mortality rates (*P*>0.05, Table 2). The rates of conversion to open surgery could not be statistically analyzed due to the inappropriate number of cases. The length of the surgery was statistically significantly longer and the estimated blood loss (cc) was lower during COVID-19 period than in the pre-COVID-19 period (*P*<0.001, *P*=0.043, respectively, Table 2).

Table 2: Comparison of postoperative clinical and oncopathological features of Pre-Covid-19 and Covid-19 periods

	Pre-Covid-19 n=16	Covid-19 n=30	*P*-value
Type of the intervention			
Laparoscopic	9(56.3)	15(50)	0.686
Open	7(43.8)	15(50)	
Type of the gastrectomy			
Total	7(43.8)	(20)66.7	0.133
Subtotal	9(56.3)	10(33.3)	
Length of the surgery	220(140-410)	348(220-525)	0.001
Conversion to open surgery	1 (6.25%)	0 (0%)	*
Estimated blood loss (cc)	280 (90-430)	190 (50-230)	0.043
Additional organ resection	2(12.5)	4(13.3)	0.936
Splenectomy	1(6.3)	2(6.7)	0.957
Complications**			
1-2	5(62.5)	4(50)	0.614
3-4	3(37.5)	4(50)	
Tumor diameter (cm)	4(0.5-10)	4(0.5-11)	0.870
Number of total lymph nodes (SD)	26 (9.8)	23 (10.5)	0.482
Number of metastatic lymph nodes	2(0-25)	2(0-17)	0.972
The closest surgical board (mm)	20(2-90)	25(2-50)	0.508
Perioperative mortality	1(6.3%)	2(6.7%)	0.957

*Statistical analysis could not be performed due to insufficient numbers**According to Clavien&Dindo Classification, SD: standard deviation

From a financial point of view, the cost was statistically significantly higher during COVID-19 period, both in Turkish Lira and USD (*P*<0.001, *P*=0.038, respectively, Table 3). The analysis of the cost sub-items revealed that drugs and treatment services, surgical material costs, radiological examinations and interventions, and laboratory services costs were statistically significantly more during COVID-19 period (Table 3).

Table 3: Distribution of invoice expenses in US dollars ($)

Invoice items	Pre-Covid-19 n=16	Covid-19 n=30	*P*-value
Medicines and treatment services	732 (336-1116)	1098 (659-2112)	0.018
Surgical material costs	594(256-877)	909 (475-1714)	0.038
Surgery Packages	461 (194-653)	565 (420-1070)	0.215
Hospitality expenses	199 (91-302)	301 (187-350)	0.173
Radiological examinations and interventions	120 (54-182)	198 (113-365)	0.14
Blood product transfusions	40 (17-60)	53 (38-69)	0.648
Laboratory services	39 (16-52)	66 (36-117)	0.029
Pathological examinations	28 (12-43)	46 (27-54)	0.525
Total cost	2217(1021-3399)	3236(1955-6305)	0.038

Discussion

Patients undergoing major surgery may die when faced with serious respiratory tract infections. Liang et al. [3] stated that gastric cancer patients would die if infected with COVID-19. Our study had one patient who contracted COVID-19 during gastric cancer surgery. Despite the need for intubation, intensive care, and close follow-up, this patient did not die.

The Eastern literature indicates that the time to gastric cancer progression is approximately 36–44 months [6]. For most patients, a wait time of a few months does not have a significant impact on the prognosis [7]. Our study observed that the non-neoadjuvant CT group had a similar time to surgery in the pre-COVID-19 and during COVID-19 periods, which was approximately 3 months. Ma et al.[8] showed that a waiting time of six months in early gastric cancer and three months in locally advanced cancer did not affect the prognosis. Lui et al. [9] concluded that the time to surgery did not impact overall survival or disease-free survival, but a time to surgery over six weeks improved the pathological complete response. However, Moraiset al. [10] reported a higher short-term mortality rate in the patient group with mostly gastrointestinal cancer cases.

Studies in the literature have suggested postponing the surgical treatment of gastric cancer and initiating the patient on chemotherapy during such delay [9,11,12]. On the other hand, Aznab [13] stated that conventional cancer chemotherapies could be administered by taking preventive health measures. It is known that chemotherapy, like surgical interventions, has an immunosuppressive effect [14]. However, chemotherapy cannot be used at all in older adult patients, making surgery the only curative treatment option [15]. Our study established similar waiting times and neoadjuvant therapy rates in both study groups, suggesting that the COVID-19 pandemic has not delayed the surgical treatment of gastric cancer and not increased the tendency to neoadjuvant therapy. We believe that this may be due to the patient's and the physician's concerns about tumor progression. In fact, stress has increased in oncological patients during the pandemic [16]. The increased stress might have triggered the psychological idea of "being closer to recover from the disease via surgery" in our society. In addition, the strict management of our center's surgical oncology clinic, intensive care units, and operating rooms under the pandemic restrictions might have contributed to the prioritization of surgery by giving confidence to the physician and the patient. Furthermore, the recent increase in vaccination and a better understanding of the transmission of the virus and characteristics of the disease might have created an environment of self-confidence and brought surgeons closer to their old clinical behaviors.

The retrospective study by Li et al. [17] examining the effects of the COVID-19 pandemic on gastric cancer treatment reported that the COVID-19 cost per patient was higher, which was attributed to the prolonged hospital stay. Our study also established increased cost per patient during COVID-19 period. However, this was not due to the prolonged hospital stay. Because the length of stay was similar in both groups of our study. The subgroup cost analysis showed that laboratory and radiological examinations were more common during COVID-19 period. It further revealed that more surgical materials were used during COVID-19 period. The increased cost observed in our study might be because the surgeons wanted to perform more examinations and used more surgical materials, due to the sensitive clinical approach of surgeons, and perhaps due to the pandemic, during COVID-19 period.

Li et al. [17] found that the time of surgery and estimated blood loss were the same before and after the pandemic. Our study observed prolonged surgeries and lower amounts of blood loss in the COVID-19 group. Along with the pandemic, it is seen that social distancing principles and strict hygienic behaviors have made our surgical interventions slower, more careful, and less bleeding while prolonging the surgery. From surgeons to nurses, all of the health professions, need to protect themselves against COVID-19 virus transmission. So, we think it is the reason of longer surgical time and lower amount of blood loss during surgery.

The main organ involvement in COVID-19 that causes mortality is the lungs, for which thoracic CT is used primarily in diagnosis. It is an expected result that this examination is used more in the COVID-19 group in our study. However, compared to the early days of the pandemic, we observed that the use of thoracic CT in our center has been increasingly reserved for patients with severe respiratory problems and low saturation. We also observe that this behavior has been affected by the decisions and recommendations of the scientific advisory board of the Ministry of Health.

Limitations

First of all, this is the first study that described the effect of this outbreak on gastric cancer in our region. This highlights the importance of the study. Despite that, since the outbreak of COVID-19 did not occur so long ago, the number of participants was relatively low. Although the surgical team was the same in this study, we couldn't evaluate the periodic effects of the outbreak on the healthcare team according to the fluctuations. Prospective studies may contribute to understand changes in fluctuations.

Conclusion

According to our study, the use of thoracic CT in the surgical management of gastric cancer patients was increased, the surgery was prolonged, and the estimated blood loss was reduced along with the pandemic. In addition, the cost of patient treatment was increased due to the examinations and surgical materials used. Future studies will clarify these issues.

Considering the effects of the COVID-19 pandemic on cancer surgery in the short term experienced, precautions should be taken and healthcare professionals should be prepared for possible situations in the light of scientific research on its long-term effects. In addition, given the fluctuating course of the pandemic, we believe that individualized treatment options should be considered more according to the treatment period (time, place, and patient's condition).

References

1. Yusefi A, BagheriLankarani K, Bastani P, RadinManesh M, Kavosi Z. Risk factors for gastric cancer: a systematic review. Asian pac j cancer prev. 2018;19(3):591–03.
2. Jindal V, Sahu KK, Gaikazian S, Siddiqui AD, Jaiyesimi I. Cancer treatment during COVID-19 pandemic. Med Oncol. 2020;37(7):58.
3. Liang W, Guan W, Chen R, Wang W, Li J, Xu K, et al. Cancer patients in SARS-CoV-2 infection: a nationwide analysis in China. Lancet Oncol. 2020;21(3):335-7.
4. Rosa F, Alfieri S. Possible impact of COVID-19 on gastric cancer surgery in Italy. Minerva Chir. 2020;75(5):380-1.
5. Clavien PA, Barkun J, de Oliveira ML, Vauthey JN, Dindo D, Schulick RD, et al. The Clavien-Dindo classification of surgical complications: five-year experience. Ann Surg. 2009;250(2):187-96.
6. Li Y, Qin JJ, Wang Z, Yu Y, Wen YY, Chen XK, et al. Surgical treatment for esophageal cancer during the outbreak of COVID-19. ZhonghuaZhong Liu ZaZhi. 2020;42(4): 296-300
7. Kang WZ, Zhong YX, Ma FH, Liu H, Ma S, Li Y, et al. Treatment strategies for gastric cancer during the COVID-19 pandemic. World J Clin Cases. 2020;8(21):5099-03.
8. Ma FH, Hu HT, Tian YT. Surgical treatment strategy for digestive system malignancies during the outbreak of novel coronavirus pneumonia. ZhonghuaZhong Liu ZaZhi. 2020;42(3):180-3.
9. Liu Y, Zhang KC, Huang XH, Xi HQ, Gao YH, Liang WQ et al.Timing of surgery after neoadjuvant chemotherapy for gastric cancer: Impact on outcomes. World J Gastroenterol. 2018;24(2):257-65.
10. Morais S, Antunes L, Rodrigues J, Fontes F, Bento MJ, Lunet N. The impact of the COVID-19 pandemic on the short-term survival of patients with cancer in Northern Portugal. Int J Cancer. 2021;149(2):287-96.
11. Chen YH, Peng JS. Treatment strategy for gastrointestinal tumor under the outbreak of novel coronavirus pneumonia in China. Zhonghua Wei Chang WaiKeZaZhi. 2020;23(2):1-4.
12. Tuech JJ, Gangloff A, Di Fiore F, Michel P, Brigand C, Slim K, et al.Strategy for the practice of digestive and oncological surgery during Covid-19 epidemic. J ViscSurg. 2020;153(3):7-12
13. Aznab M. Evaluation of COVID 19 infection in 279 cancer patients treated during a 90-day period in 2020 pandemic. Int J ClinOncol. 2020;25(9):1581-6.
14. Carmona-Bayonas A, Jiménez-Fonseca P, VirizuelaEchaburu J, Antonio M, Font C, Biosca M, et al. Prediction of serious complications in patients with seemingly stable febrile neutropenia: validation of the Clinical Index of Stable Febrile Neutropenia in a prospective cohort of patients from the FINITE study. J Clin Oncol. 2015;33(5):465-71.
15. Polkowski WP, Sędłak K, Rawicz-Pruszyński K. Treatment of Gastric Cancer Patients During COVID-19 Pandemic: The West is More Vulnerable. Cancer Manag Res. 2020;12:6467-76.
16. Pigozzi E, Tregnago D, Costa L, Insolda J, Turati E, Rimondini M, et al. Psychological impact of Covid-19 pandemic on oncological patients: a survey in Northern Italy. PLoS One. 2021;16(3): e0248714.
17. Li YX, He CZ, Liu YC, Zhao PY, Xu XL, Wang YF, et al. The impact of COVID-19 on gastric cancer surgery: a single-center retrospective study. BMC Surg. 2020;20(1):222.

This paper has been checked for language accuracy by JOSAM editors.
The National Library of Medicine (NLM) citation style guide has been used in this paper.

J Surg Med. 2021;5(12):1214-1217.
DOI: 10.28982/josam.1024568

Journal of Surgery and Medicine
e-ISSN=2602-2079

Acute and chronic invasive fungal sinusitis and imaging features: A review

Hacı Taner Bulut [1], Ela Kaplan [2], Mahmut Çoraplı [2]

[1] Adıyaman University, Medicine Faculty, Department of Radiology, Adıyaman, Turkey
[2] Adıyaman Education and Research Hospital, Department of Radiology, Adıyaman, Turkey

ORCID ID of the author(s)
HTB: 0000-0002-8152-2497
EK: 0000-0001-5039-9070
MÇ: 0000-0002-4223-7845

Abstract

Fungal sinusitis is an infrequent disease that happens in immunosuppressed patients. Although acute and chronic invasive fungal sinusitis are pathologies with different clinical features and radiological imaging findings, mortality and morbidity rates are similarly high in patients. Therefore, early identification and offensive treatment are crucial. The use of diagnostic methods and the correct interpretation of imaging findings help to prevent fatal outcomes.

Keywords: Fungal sinusitis, Magnetic resonance imaging, Computed tomography

1. Introduction

1.1) Background

Inflammation of the paranasal sinuses (PNS) is called sinusitis. Sinusitis is most commonly caused by viral agents. Usually, the symptoms are mild and temporary (<4 week) [1]. Sinusitis with nonspecific symptoms and imaging findings for four weeks or longer is called chronic sinusitis [2]. An infrequent type of acute or chronic sinusitis is fungal sinusitis. Fungal sinusitis usually does not happen in people with normal immune functions [3]. However, chronic immunosuppression is one of the primary sinusitis factors that should be considered in people undergoing steroid use or malignancy treatment [4]. Fungal sinusitis can be divided into two groups as acute and chronic. However, its clinical progression is divided into invasive and non-invasive fungal sinusitis [5]. Invasive fungal sinusitis may result in destruction of mucosa, bone, adjacent neurovascular structures and surrounding soft tissues [6]. In this way, it may spread to the bone, intracranial structures, orbit and facial structures [7]. This study is aimed to review the imaging modalities and imaging findings of fungal sinusitis.

1.2) Imaging Methods

Computed tomography (CT) and magnetic resonance imaging (MRI) are performed to evaluate the presence of fungal sinusitis and its complications. CT is the first preferred method in the evaluation of fungal sinusitis [8, 9]. Non-contrast CT provides detailed bone structure visualization. Inflammatory secretions appear hypodense on CT. As the inflammatory process prolongs, the secretion density becomes more hypodense than the muscular structures. In addition, in the presence of fungal sinusitis, calcium salts accumulate in these secretions and appear hyperdense [10]. In addition, CT is very useful in determining the spread of fungal sinusitis to the intraorbital area and other compartments [11].

The soft tissue signal changes in MRI are based on the amount of protein in the contents of the sinuses, the viscosity of the content or the presence of calcifications. In fungal sinusitis with increased protein content, hypointense appearance on T1-weighted images and hypointense areas and/or loss of signal void can be observed on T2-weighted images [10]. MRI is better than CT in evaluating invasion and spread in adjacent tissues, including areas such as the orbit, intracranial compartment, vascular structures, neck and facial soft tissues, and pterygomaxillary fissure in fungal sinusitis [10]. MRI presents better soft tissue contrast resolution and is helpful in describing the spread of disease in more detail [12].

Corresponding Author
Hacı Taner Bulut
Adıyaman University Medical Faculty, Department of Radiology, Adıyaman, Turkey
E-mail: taner.bulut02@gmail.com

Conflict of Interest
No conflict of interest was declared by the authors.

Financial Disclosure
The authors declared that this study has received no financial support.

Published
2021 December 20

How to cite: Bulut HT, Kaplan E, Çoraplı M. Acute and chronic invasive fungal sinusitis and imaging features: A review. J Surg Med. 2021;5(12):1214-1217.

2) Acute Invasive Sinusitis

Acute invasive fungal sinusitis is a fatal paranasal sinus infection caused by fungal factors in less than four weeks, occurring in immunosuppressed patients and uncontrolled diabetes patients [13, 14]. Zygomycetes type fungus such as Rhizopus, Mucor, Absidia are the most widespread reasons of invasive fungal sinusitis. Infections caused by these agents are called zygomycosis. It is frequently encountered in patients with diabetic ketoacidosis, patients receiving systemic chemotherapy, patients receiving steroid therapy, patients with hematological malignancies, and patients receiving immunosuppression therapy, such as after transplantation, and the mortality is high in these patients [13]. For this reason, the information provided by radiologists about the diagnosis and the complications that develop or may develop are very important in determining the treatment approaches of the clinicians.

2.1) Clinical features

In invasive fungal sinusitis, there are symptoms such as nasal congestion, facial pain, fever, nasal discharge and numbness that can be seen in other sinusitis rather than specific symptoms. Hematogenous spread is frequently observed with angioinvasion and epistaxis symptoms occur accordingly. The mucosa-submucosa is completely involved and ulceration and necrosis develop [15]. Depending on the degree of invasion and spread, intracranial and maxillofacial enlargement, visual disturbances, headache, and seizures may occur. Nasal cavity involvement occurs frequently [16].

2.2) Acute Invasive Fungal Sinusitis Imaging Features

Non-contrast CT particularly helps to evaluate the paranasal sinuses, nasal cavity and turbinates. The presence of mucosal thickening and soft tissue density at this level is the most common first CT imaging finding, though it isn't specific [17]. An unilateral involvement is observed in the ethmoid sinuses and especially in the sphenoid sinus. The maxillary and ethmoid sinuses are frequently affected, and the presence of full or partial soft tissue density in this sinus is a typical imaging feature (Figure 1A). One of the important factors that will indicate fungal infection is the presence of hyperdense areas in the soft tissue on CT.

The presence of these hyperdense areas specifically indicates vascular invasion. The structures to be evaluated in this type of invasive fungal sinusitis ought to be evaluated in the nasal cavity adjacent to the sinus, bone structures forming the nasal cavity and paranasal sinuses, structures next to the maxillary sinuses such as premaxillary and pterygopalatine fossa [14] (Figure 1B). The presence of erosion in bone structures is a marker for invasion, especially (Figure 1A-1B-1C). In addition, the presence of obliteration and enlargement in the periantral fatty tissue are very important (Figure 1A). This finding is an indication of intraorbital invasion and should be evaluated in patients with invasive fungal sinusitis [18].

MRI ought to be the first-choice imaging modality to detect bone erosion and visualize the orbital compartment, adjacent soft tissues and vascular structures, and the cavernous segment in case of periantral fatty tissue obliteration. The most important findings showing adjacent tissue invasion on MRI are the involvement of fatty tissue adjacent to the sinuses and signal changes similar to soft tissue on T1W images, and the presence of increased signal secondary to edema on T2-weighted images and the presence of enhancement in contrast-enhanced series (Figure 2B, Figure 2C). Contrast enhancement in the nasal mucosa, turbinates, and levels of soft tissue signaling is the typical finding of invasive fungal infection (Figure 2C). However, the absence of contrast enhancement in the turbinates in these areas where invasive soft tissue is evaluated is called the black turbinate sign and is a precursor of conchal necrosis [14] (Figure 2C). In orbital compartment imaging, signal changes in orbital fatty tissue and extraocular muscle groups and volume increase secondary to inflammation, prominence in retroorbital fatty tissue, and accordingly proptosis is indicators of intraorbital invasion [14] (Figure 2B). In the patient with these changes, the cavernous sinus and intracranial structures adjacent to the orbit should be evaluated rapidly (Figure 2A). Especially the presence of leptomeningeal enhancement, cerebritis, intracranial granuloma development should be evaluated. Intracranial well-circumscribed lesions with hypointense in T1W and T2W series that show minimal enhancement on contrast-enhanced images are indicative of intracranial granulomas.

Figure 1: 1A: CT images of a 46-year-old female patient. Soft tissue density filling the maxillary sinus: black arrow. Erosion of the posterior wall of the maxillary sinus and fullness of the periantral fat tissue: white arrow. Increase in skin thickness and decrease in edematous density: Red arrow. 1B: Soft tissue density filling the nasal cavity: Black Arrow. Bone density cannot be discerned due to invasion of the orbital lateral wall: White arrow. Soft tissue edematous changes in the anterior orbit: Red arrow. Bone structures secondary to invasion in the ethmoidal sinuses could not be discerned: White arrow

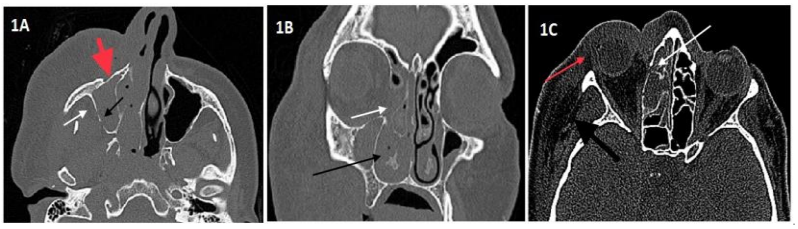

Figure 2: 2A: Contrast enhancement of internal carotid artery at the level of carotid canal on MRI T1W images: white arrow 2B: In a 46-year-old female patient, contrast enhancement in the bones in the conchae and nasal cavity with soft tissue invasion and enhancement in the adjacent soft tissue on MRI T1W contrast images: white arrows 2C: Areas of enhancement in the premaxillary area (red arrow) and nasal cavity (black arrow) and unenhanced areas secondary to soft tissue necrosis in the maxillary sinus cavity on MRI T1W images: White arrow

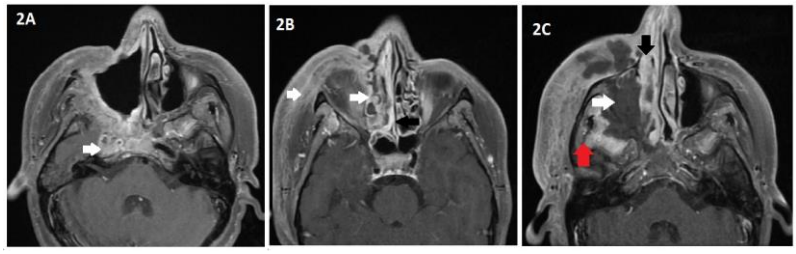

Thrombosis in the cavernous sinus, presence of thrombophlebitis, dissection in the cavernous artery segment and pseudoaneurysm are some of the advanced complications that can be observed due to the hematogenous spread and angioinvasion characteristics of fungal agents.

2.3) Treatment

Treatment in acute invasive fungal sinusitis is aggressive antifungal therapy and surgical debridement. However, it is very important to detect and control the situation that causes immunosuppression in the patient. Management and correction of this process in diabetic ketoacidosis patients affect the response to treatment. However, the mortality rate in acute invasive fungal sinusitis is 50-80%, and it is quite high despite all treatment methods [19].

3) Chronic Invasive Fungal Sinusitis

It is an inflammation caused by respiratory fungal agents in the sinuses between 4 and 12 weeks, andshows an angioinvasive structure just like the acute form by holding the mucosa, submucosa and bone structures. The process is slower than acute inflammation and can be limited. However, it is a significant reason of morbidity and mortality rates are high in case of delayed diagnosis and treatment [20].

3.1) Clinical features

Individuals diagnosed with chronic fungal invasive sinusitis are also immunosuppressed and poorly controlled diabetes patients, just like those diagnosed with acute invasive fungal sinusitis. Symptoms include sinusoidal and facial pain, epistaxis, and fever. These symptoms are resistant to treatment. Orbital pain and limitation of motion in the orbit may also be observed in patients due to invasion into the orbital compartment. Polypoid mucosa may be observed and mass-like appearances may be present in the soft tissue on nasal examination [21].

3.2) Chronic Invasive Fungal Sinusitis Imaging Methods

Chronic invasive fungal sinusitis is less common than acute invasive fungal sinusitis [21]. Accurate diagnosis may not be made due to radiological variances [22, 23]. Therefore, the imaging features should be well known. The first preferred method in imaging for diagnosis should be CT without contrast. On imaging, findings are the same as acute invasive fungal sinusitis, with the presence of hypodense soft tissue density in the sinuses (Figure 3A). The destruction of the sinus wall and the mass appearance in this soft tissue and the expansion caused by the adjacent nasal cavity and structures are distinctive for chronic invasive fungal sinusitis (Figure 3A). One of the most important indicators of invasion is the presence of infiltration in the periantral soft tissue around the maxillary sinus [10]. In addition, as the process becomes chronic, hyperdense calcified areas can be detected within the defined mass soft tissue density (Figure 3A-3B). In MRI, soft tissue filling the sinus is seen as hypointense on T1-weighted images, while the signal may vary on T2-weighted images. Signal void loss of calcification in hypointense content can be observed in T2-weighted (Figure 4A-Figure 4B). Irregular bone destruction in the paranasal sinus walls and sclerotic changes in the affected sinus wall can also be seen on CT (Figure 3B). Due to the accumulation of calcium, a rough appearance is observed in the adjacent bone structures [24]. Irregularities and changes occur in adjacent tissues secondary to invasion. In this process, if no treatment is applied and immunosuppression is not controlled, extension to orbital structures, adjacent soft tissues and intracranial structures can be observed as in acute invasive sinusitis. Due to long-term invasive changes in the cavernous compartment, it may lead to complications such as mycotic aneurysm and cavernous sinus transformation in vascular structures [10].

Figure 3: 3A: Soft tissue density filling the maxillary sinus unilaterally: red arrow, calcified content in soft tissue density: thin white arrow; Bone structures in the medial wall of the maxillary sinus could not be distinguished due to invasion: thick white arrow 3B: Density increase of calcification in the anterior of the polypoid soft tissue mass filling the maxillary sinus: White arrow

Figure 4: 4A: In the MRI T2W image of a 67-year-old patient diagnosed with chronic invasive fungal sinusitis, increase in soft tissue thickness in the maxillary sinus, concentrated hypointense content (black arrow) and loss of signal void of calcification (white arrow). 4B: Maxillary soft tissue intensity with high viscosity on MRI T2W images: White arrow

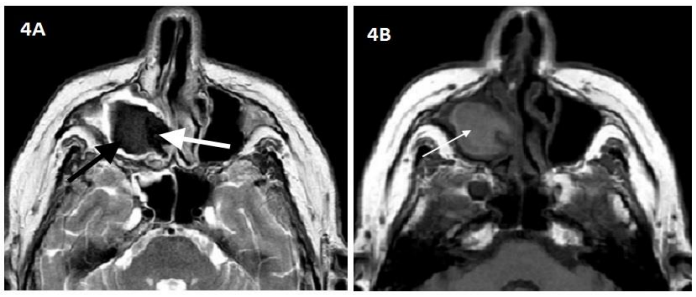

3.3) Treatment

Surgical removal of infected tissues and the use of systemic antifungal agents are the main treatment. Although the process is chronic, aggressive treatment such as acute invasive fungal sinusitis should be applied especially in cases with intracranial compartment and cavernous sinus invasion due to high morbidity and mortality [19].

4) Conclusion

Fungal sinusitis is a significant clinical trouble with different symptoms and imaging findings. It ought to be taken in to consideration in the differential diagnosis in the presence of chronic sinusitis in diabetic patients, especially in immunosuppressed patients. In the presence of acute invasive fungal sinusitis, orbital and intracranial invasion often occur due to the rapid progression of complications, with the development of destruction and necrosis in the sinuses and nasal cavity. Although the imaging features in CT and MRI are more subtle initially, radiologists have a significant role in assessing the presence of invasion, especially in the early stages. In addition, it is important not only to diagnose, but also to show the spread of the disease and to recognize the findings of possible complications. Although chronic invasive fungal sinusitis differs from acute fungal sinusitis with its slow course, its symptoms and imaging findings are similar. If left untreated and undifferentiated, morbidity and mortality rates are as high as acute fungal sinusitis. It is especially important to distinguish it

from aggressive neoplastic lesions or benign soft tissue masses such as nasal polyps.

In order for radiologists to guide the clinician to the appropriate diagnosis and treatment, it is necessary to know the imaging findings of different types of fungal sinusitis and to evaluate possible complications with appropriate imaging methods. Early diagnosis and initiation of appropriate treatment are important to avoid a delayed and fatal outcome.

References

1. Fokkens WJ, Lund VJ, Mullol J, Bachert C, Alobid I, Baroody F, et al. EPOS 2012: European position paper on rhinosinusitis and nasal polyps 2012. A summary for otorhinolaryngologists. Rhinology. 2012 Mar;50(1):1-12. doi: 10.4193/Rhino12.000. PMID: 22469599.
2. Nocon CC, Baroody FM. Acute rhinosinusitis in children. Curr Allergy Asthma Rep. 2014 Jun;14(6):443. doi: 10.1007/s11882-014-0443-7. PMID: 24700347; PMCID: PMC7088858.
3. Bazan C 3rd, Rinaldi MG, Rauch RR, Jinkins JR. Fungal infections of the brain. Neuroimaging Clin N Am 1991;1:57–88.
4. Watkinson JC, Clarke RW. Scott-Brown's Otorhinolaryngology and Head and Neck Surgery: Volume 1: Basic Sciences, Endocrine Surgery, Rhinology; CRC Press: Boca Raton, FL, USA, 2018.
5. Montone KT. Pathology of Fungal Rhinosinusitis: A Review. Head Neck Pathol. 2016 Mar;10(1):40-6. doi: 10.1007/s12105-016-0690-0. Epub 2016 Feb 1. PMID: 26830404; PMCID: PMC4746136.
6. Watkinson, J.C.; Clarke, R.W. Scott-Brown's Otorhinolaryngology and Head and Neck Surgery: Volume 1: Basic Sciences, Endocrine Surgery, Rhinology; CRC Press: Boca Raton, FL, USA, 2018.
7. Reid JR. Complications of pediatric paranasal sinusitis. Pediatr Radiol. 2004 Dec;34(12):933-42. doi: 10.1007/s00247-004-1252-2. Epub 2004 Jul 27. PMID: 15278322.
8. Cornelius RS, Martin J, Wippold FJ 2nd, Aiken AH, Angtuaco EJ, Berger KL, et al. ACR appropriateness criteria sinonasal disease. J Am Coll Radiol. 2013 Apr;10(4):241-6. doi: 10.1016/j.jacr.2013.01.001. Epub 2013 Feb 16. PMID: 23420025.
9. Fatterpekar G, Mukherji S, Arbealez A, Maheshwari S, Castillo M. Fungal diseases of the paranasal sinuses. Semin Ultrasound CT MR. 1999 Dec;20(6):391-401. doi: 10.1016/s0887-2171(99)90023-9. PMID: 10634589.
10. Aribandi M, McCoy VA, Bazan C 3rd. Imaging features of invasive and noninvasive fungal sinusitis: a review. Radiographics. 2007 Sep-Oct;27(5):1283-96. doi: 10.1148/rg.275065189. PMID: 17848691.
11. Zeifer B. Pediatric sinonasal imaging: normal anatomy and inflammatory disease. Neuroimaging Clin N Am. 2000 Feb;10(1):137-59, ix. PMID: 10658159.
12. Iida E, Anzai Y. Imaging of Paranasal Sinuses and Anterior Skull Base and Relevant Anatomic Variations. Radiol Clin North Am. 2017 Jan;55(1):31-52. doi: 10.1016/j.rcl.2016.08.009. Epub 2016 Oct 25. PMID: 27890187.
13. Gillespie MB, O'Malley BW Jr, Francis HW. An approach to fulminant invasive fungal rhinosinusitis in the immunocompromised host. Arch Otolaryngol Head Neck Surg. 1998 May;124(5):520-6. doi: 10.1001/archotol.124.5.520. PMID: 9604977.
14. Groppo ER, El-Sayed IH, Aiken AH, Glastonbury CM. Computed tomography and magnetic resonance imaging characteristics of acute invasive fungal sinusitis. Arch Otolaryngol Head Neck Surg. 2011 Oct;137(10):1005-10. doi: 10.1001/archoto.2011.170. PMID: 22006778.
15. Yakirevitch A, Barg AA, Bedrin L, Primov-Fever A, Wolf M, Migirov L. Acute Invasive Fungal Rhinosinusitis in Children With Hematologic Malignancies: Outcome of Surgical Treatment. Pediatr Hematol Oncol. 2015;32(8):568-75. doi: 10.3109/08880018.2015.1092058. Epub 2015 Nov 11. PMID: 26558653.
16. Ni Mhurchu E, Ospina J, Janjua AS, Shewchuk JR, Vertinsky AT. Fungal Rhinosinusitis: A Radiological Review With Intraoperative Correlation. Can Assoc Radiol J. 2017 May;68(2):178-86. doi: 10.1016/j.carj.2016.12.009. PMID: 28438285.
17. DelGaudio JM, Swain RE Jr, Kingdom TT, Muller S, Hudgins PA. Computed tomographic findings in patients with invasive fungal sinusitis. Arch Otolaryngol Head Neck Surg. 2003 Feb;129(2):236-40. doi: 10.1001/archotol.129.2.236. PMID: 12578456.
18. Silverman CS, Mancuso AA. Periantral soft-tissue infiltration and its relevance to the early detection of invasive fungal sinusitis: CT and MR findings. AJNR Am J Neuroradiol. 1998 Feb;19(2):321-5. PMID: 9504486; PMCID: PMC8338170.
19. Craig JR. Updates in management of acute invasive fungal rhinosinusitis. Curr Opin Otolaryngol Head Neck Surg. 2019 Feb;27(1):29-36. doi: 10.1097/MOO.0000000000000507. PMID: 30585877.
20. Thompson 3rd GR, Patterson TF. Fungal disease of the nose and paranasal sinuses. J Allergy Clin Immunol. 2012;129(2):321–6.
21. Stringer SP, Ryan MW. Chronic invasive fungal rhinosinusitis. Otolaryngol Clin North Am 2000; 33(2):375–87.
22. Reddy CE, Gupta AK, Singh P, Mann SB. Imaging of granulomatous and chronic invasive fungal sinusitis: comparison with allergic fungal sinusitis. Otolaryngol Head Neck Surg. 2010 Aug;143(2):294-300. doi: 10.1016/j.otohns.2010.02.027. PMID: 20647138.
23. Gavito-Higuera J, Mullins CB, Ramos-Duran L, Sandoval H, Akle N, Figueroa R. Sinonasal Fungal Infections and Complications: A Pictorial Review. J Clin Imaging Sci. 2016 Jun 14;6:23. doi: 10.4103/2156-7514.184010. PMID: 27403401; PMCID: PMC4926542.
24. Yoon JH, Na DG, Byun HS, Koh YH, Chung SK, Dong HJ. Calcification in chronic maxillary sinusitis: comparison of CT findings with histopathologic results. AJNR Am J Neuroradiol. 1999 Apr;20(4):571-4. PMID: 10319962; PMCID: PMC7056005.

This paper has been checked for language accuracy by JOSAM editors.
The National Library of Medicine (NLM) citation style guide has been used in this paper.

J Surg Med. 2021;5(12):1218-1220.
DOI: 10.28982/josam.933280

Journal of Surgery and Medicine
e-ISSN=2602-2079

An overview about galectin-3 and its relationship with cardiovascular diseases

Lutfu Askin [1], Husna Sengul Askin [2], Okan Tanriverdi [1], Ali Gokhan Ozyildiz [3], Siho Hidayet [4]

[1] Department of Cardiology, Adiyaman Education and Research Hospital, Adiyaman, Turkey
[2] Department of Infectious Disease, Adiyaman Education and Research Hospital, Adiyaman, Turkey
[3] Department of Cardiology, Rize University Medicine Faculty, Rize, Turkey
[4] Department of Cardiology, Inonu University, Medicine Faculty, Malatya, Turkey

ORCID ID of the author(s)
LA: 0000-0001-7768-2562
HSA: 0000-0001-9997-9447
OT: 0000-0002-3508-2048
AGÖ: 0000-0003-0679-9434
SH: 0000-0002-4103-9345

Corresponding Author
Lutfu Askin
Adiyaman Education and Research Hospital, Department of Cardiology, Adiyaman, Turkey
E-mail: lutfuaskin23@gmail.com

Conflict of Interest
No conflict of interest was declared by the authors.

Financial Disclosure
The authors declared that this study has received no financial support.

Published
2021 December 28

Abstract

Inflammation is one of the cornerstones of atherosclerosis. Galectin-3 (Gal-3) acts on the stages of the inflammatory process. Gal-3 is a candidate for being a valuable marker for heart failure (HF) and coronary artery disease (CAD). Further studies are needed for the diagnosis and follow-up of CAD. In the literature, the relationship between Gal-3 and CAD has not been researched sufficiently. We aimed to write a review by referring to recent studies about Gal-3 in the etiopathogenesis of CAD, its prognostic significance, and its contribution to the treatment regimen.

Keywords: Atherosclerosis, Galectin-3, İnflammation, Heart failure, Coronary artery disease

Introduction

Inflammation is one of the cornerstones of atherosclerosis and an important cause of stroke and cardiovascular disease (CVD) [1]. Galectin-3 (Gal-3), one of the soluble galactoside-binding lectins, induces phagocytosis and proliferation of vascular smooth muscle cells and accelerates atherogenesis [2]. Gal-3 is a predictor of mortality in coronary artery disease (CAD) [3]. Elevated Gal-3 expression causes the development of cardiovascular diseases. We aimed to review Gal-3's impact on CAD.

Fibroblasts, endothelial cells, neutrophils, monocytes/macrophages, dendritic cells, and inflammatory cells are involved in the release of Gal-3. Gal-3 affects inflammation stages such as neutrophil adhesion, monocyte/macrophage chemoattraction, apoptotic neutrophils opsonization, and activation of mast cells [4, 5]. It has a significant correlation with CAD, and it is an important bioxmarker to predict heart failure and CV events [6, 7].

The Gal-3 expression is low in the myocardial cells, but some pathological conditions notably upregulate this expression. Gal-3 influences the entry of macrophages into myocardial cells in hypertrophy. In the hypertrophic rat heart, Gal-3 is a potent mitogenic agent for active myocardial macrophages and fibroblasts with binding sites in the fibroblasts and extracellular matrix. This finding shows that Gal-3 acts in tissue fibrogenesis. Also, it increases the production of collagen by contributing to the differentiation of cardiac fibroblasts to myofibroblasts [5, 8, 9].

How to cite: Askin L, Askin HS, Tanriverdi O, Ozyildiz AG, Hidayet S. An overview about galectin-3 and its relationship with cardiovascular diseases. J Surg Med. 2021;5(12):1218-1220.

Gal-3 in heart failure (HF)

Increasing Gal-3 levels may reflect the degree of myocardial fibrosis, determined by cardiac magnetic resonance (CMR). Increased Gal-3 levels may indicate left ventricular (LV) diastolic dysfunction (Figure 1) [10, 11]. Gal-3 has recently been added to the class of useful prognostic markers as an important predictor of HF [12]. Hashmi and Al-Salam et al. reported transcriptional translational Gal-3 expression in the early stage of the ischemic left ventricular myocardium [13].

Figure 1: Galectin-3 and myocardial fibrosis

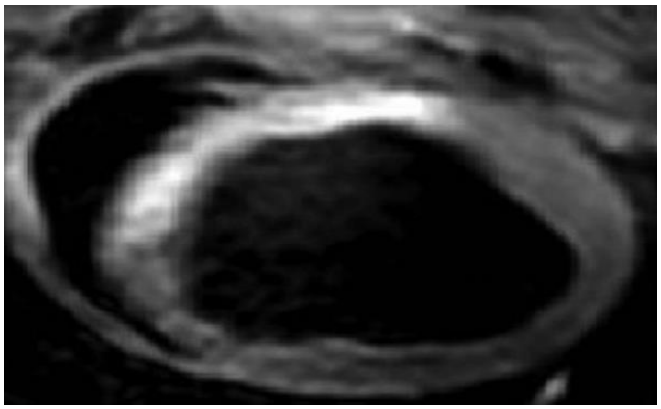

Coromilas et al. [14] demonstrate that Gal-3 can be used as a useful biomarker to assess prognosis in patients with HF with a left ventricular assist device. Gal-3 is a marker of inflammation that is not affected by acute cardiac volume or pressure increase compared to BNP. The role of Gal-3 in heart transplant follow-up may be better understood through more studies. In a cohort study, Rieth et al. [15] found a positive correlation between high Gal-3 and systolic dysfunction.

Gal-3 was highly detected in myofibroblasts as an independent determinant of myocardial fibrosis [16]. Liu et al. [17] showed that the inhibition of the transforming growth factor-β (TGF-β)/signal protein 3 (Smad3) pathway by AC-SDKP also regressed the Gal-3-activated profibrotic process and improved cardiac remodeling. Thus, the interaction of gal-3 and TGF-β/Smad3 protein signal transduction pathway proved to cause myocardial remodeling. Another study showed that suppression of Gal-3 reduces type I collagen synthesis and accumulation [18]. Decreasing Gal-3 expression effectively reduces oligomyositis fibrinolysis. In addition, Gal-3 triggers cardiac fibroblast proliferation, collagen deposition, and ventricular dysfunction [19].

The reliability of this result was confirmed after the elimination of various confounding variables affecting the prognosis in patients with normal ejection fraction (EF). Gal-3 may cause LV hypertrophy in hypertrophic cardiomyopathy (HCM) [20]. It may be useful for identifying major adverse cardiac events (MACE) in HCM.

Gal-3 in diabetes mellitus (DM)

Gal-3 levels may increase in type 2 DM [21]. Despite insufficient evidence, Gal-3 is thought to cause microvascular and macrovascular complications in type 2 DM [22]. It may be a potential biomarker for myocardial and structural lesions in patients with Type 2 DM complicated with hypertension [23]. Gal-3 was also proven to have an important role in the physiopathogenesis of diabetic nephropathy [24]. It was negatively correlated with glycosylated hemoglobin levels, and its level was significantly decreased with metformin treatment. Thus, it may play a role in the development and progression of diabetes [25].

Experiments showed that recombinant Gal-3 given exogenously may cause insulin resistance *in vitro*. Its mechanism may rely on a possible inhibition of insulin signaling by binding of gal-3 to the insulin receptor [26]. The induction of insulin resistance by gal-3 may also be related to its proinflammatory role in lipid-related metabolic disorders [27]. Pang et al. [28] claimed that gal-3 has an active role in glucose intolerance and obesity in mice.

Gal-3 in myocardial infarction (MI)

Some researchers assumed that Gal-3 has an active role in the formation of atherogenesis. Furthermore, it transports modified lipoproteins in the proinflammatory pathway in atherosclerosis [29]. Gal-3 levels may increase in MI. A higher Gal-3 was proven to be a strong predictor of MACE at 30 days follow-up [30].

Gal-3 is an essential marker for determining atherosclerotic plaque burden and stability [31]. Higher Gal-3 levels were observed in macro-calcified plaques [32]. The inhibition of gal-3 probably prevents the atherosclerotic process. The inhibition of Gal-3 may be a new therapy regimen in atherosclerosis by providing plaque stabilization [33].

Mayr et al. [34] demonstrated the relationship between post-MI left ventricular dysfunction and Gal-3. The association of Gal-3 with increased formation of oxidized low-density lipoprotein cholesterol (LDL-C) and vascular smooth muscle cell activation was demonstrated. This relationship predisposes to atherosclerotic plaque formation and MI [35].

Winter et al. [36] argued that increased Gal-3 is a potent factor for MI recurrence. Also, Aksan et al. [37] demonstrated that Gal-3 is a successful agent in determining the severity of CAD. Gleissner et al. [38] showed that increased levels of the Gal-3 binding protein (Gal-3BP) were related to long-term mortality. Based on these findings, it may be assumed that Gal-3BP levels could be a marker of inflammatory and metabolic stress rather than a reflection of coronary atherosclerotic plaque instability.

Gal-3 in atrial fibrillation (AF)

In the Framingham Heart Study (FHS), 3450 patients were followed 10 years. In a 10-year follow-up, it was observed that the incidence of AF increased with high serum Gal-3 [39]. Gal-3 value was higher in patients with AF than those with sinus rhythm [40]. Gal-3 was also correlated with AF duration and left atrial diameter [41], and significantly higher in the presence of spontaneous echo contrast (SEC) and left atrial thrombus [42].

After radiofrequency ablation, Gal-3 and left atrial diameter were independent risk factors for recurrent AF [43]. The interaction of Gal-3 with AF is thought to be via atrial remodeling and myocardial fibrosis. This mechanism could shed light on future research [44].

Gal-3 in Kawasaki disease (KD)

Numano et al. [45] found high Gal-3 in KD with a giant coronary aneurysm. Gal-3 may be a clinical marker for myocardial and vascular fibrosis in KD, with precise imaging techniques and measurement of procollagen fragments. Gal-3 therapy may provide functional improvement in myocardial cells in KD.

Conclusion

The role of Gal-3 in determining atherosclerotic plaque burden and CAD severity is still debated in the current scientific world. Increased Gal-3 levels in CAD suggest that it is part of the atherosclerotic inflammatory process. Today, Gal-3 is considered as a new marker associated with HF and other CV events according to different clinical trials. Presumably, the inhibition of Gal-3 will be useful in preventing atherosclerosis. Strategies to diminish the gal-3 function may provide a different perspective in the treatment of atherosclerotic diseases.

References

1. Askin L, Tanrıverdi O. An Overview of Clinical Studies on Endocan and Cardiovascular Disease. Erciyes Med J. 2021;43(3):233-6. doi: 10.14744/etd.2020.09699.
2. Blanda V, Bracale UM, Di Taranto MD, Fortunato G. Galectin-3 in Cardiovascular Diseases. Int J Mol Sci. 2020;21(23):9232. doi: 10.3390/ijms21239232.
3. Maiolino G, Rossitto G, Pedon L, Cesari M, Frigo AC, Azzolini M, et al. Galectin-3 predicts long-term cardiovascular death in high-risk patients with coronary artery disease. Arterioscler Thromb Vasc Biol. 2015;35(3):725-32. doi: 10.1161/ATVBAHA.114.304964.
4. Henderson NC, Sethi T. The regulation of inflammation by galectin-3. Immunol Rev. 2009;230(1):160-71. doi: 10.1111/j.1600-065X.2009.00794.x.
5. Sharma UC, Pokharel S, van Brakel TJ, van Berlo JH, Cleutjens JP, Schroen B, et al. Galectin-3 marks activated macrophages in failure-prone hypertrophied hearts and contributes to cardiac dysfunction. Circulation. 2004;110(19):3121-8. doi: 10.1161/01.CIR.0000147181.65298.4D.
6. Kusaka H, Yamamoto E, Hirata Y, Fujisue K, Tokitsu T, Sugamura K, et al. Clinical significance of plasma galectin-3 in patients with coronary artery disease. Int J Cardiol. 2015;201:532-4. doi: 10.1016/j.ijcard.2015.08.099.
7. Chen A, Hou W, Zhang Y, Chen Y, He B. Prognostic value of serum galectin-3 in patients with heart failure: a meta-analysis. Int J Cardiol. 2015;182:168-70. doi: 10.1016/j.ijcard.2014.12.137.
8. Reifenberg K, Lehr HA, Torzewski M, Steige G, Wiese E, Küpper I, et al. Interferon-gamma induces chronic active myocarditis and cardiomyopathy in transgenic mice. Am J Pathol. 2007;171(2):463-72. doi: 10.2353/ajpath.2007.060906.
9. Yu L, Ruifrok WP, Meissner M, Bos EM, van Goor H, Sanjabi B, et al. Genetic and pharmacological inhibition of galectin-3 prevents cardiac remodeling by interfering with myocardial fibrogenesis. Circ Heart Fail. 2013;6(1):107-17. doi: 10.1161/CIRCHEARTFAILURE.112.971168.
10. Lepojärvi ES, Piira OP, Pääkkö E, Lammentausta E, Risteli J, Miettinen JA, et al. Serum PINP, PIIINP, galectin-3, and ST2 as surrogates of myocardial fibrosis and echocardiographic left venticular diastolic filling properties. Front Physiol. 2015;6:200. doi: 10.3389/fphys.2015.00200.
11. McCullough PA. Practical experience using galectin-3 in heart failure. Clin Chem Lab Med. 2014;52(10):1425-31. doi: 10.1515/cclm-2014-0278.
12. Meijers WC, Januzzi JL, deFilippi C, Adourian AS, Shah SJ, van Veldhuisen DJ, et al. Elevated plasma galectin-3 is associated with near-term rehospitalization in heart failure: a pooled analysis of 3 clinical trials. Am Heart J. 2014;167(6):853-60.e4. doi: 10.1016/j.ahj.2014.02.011.
13. Hashmi S, Al-Salam S. Galectin-3 is expressed in the myocardium very early post-myocardial infarction. Cardiovasc Pathol. 2015;24(4):213-23. doi: 10.1016/j.carpath.2014.12.001.
14. Coromilas E, Que-Xu EC, Moore D, Kato TS, Wu C, Ji R, et al. Dynamics and prognostic role of galectin-3 in patients with advanced heart failure, during left ventricular assist device support and following heart transplantation. BMC Cardiovasc Disord. 2016;16:138. doi: 10.1186/s12872-016-0298-z.
15. Rieth AJ, Jung C, Gall H, Rolf A, Mitrovic V, Hamm CW, et al. Association of galectin-3 with changes in left ventricular function in recent-onset dilated cardiomyopathy. Biomarkers. 2019;24(7):652-658. doi: 10.1080/1354750X.2019.1642959.
16. Ho JE, Liu C, Lyass A, Courchesne P, Pencina MJ, Vasan RS, et al. Galectin-3, a marker of cardiac fibrosis, predicts incident heart failure in the community. J Am Coll Cardiol. 2012;60(14):1249-56. doi: 10.1016/j.jacc.2012.04.053.
17. Liu YH, D'Ambrosio M, Liao TD, Peng H, Rhaleb NE, Sharma U, et al. N-acetyl-seryl-aspartyl-lysyl-proline prevents cardiac remodeling and dysfunction induced by galectin-3, a mammalian adhesion/growth-regulatory lectin. Am J Physiol Heart Circ Physiol. 2009;296(2):H404-12. doi: 10.1152/ajpheart.00747.2008.
18. Calvier L, Miana M, Reboul P, Cachofeiro V, Martinez-Martinez E, de Boer RA, et al. Galectin-3 mediates aldosterone-induced vascular fibrosis. Arterioscler Thromb Vasc Biol. 2013;33(1):67-75. doi: 10.1161/ATVBAHA.112.300569.
19. Lax A, Sanchez-Mas J, Asensio-Lopez MC, Fernandez-Del Palacio MJ, Caballero L, Garrido IP, et al. Mineralocorticoid receptor antagonists modulate galectin-3 and interleukin-33/ST2 signaling in left ventricular systolic dysfunction after acute myocardial infarction. JACC Heart Fail. 2015;3(1):50-58. doi: 10.1016/j.jchf.2014.07.015.
20. Yakar Tülüce S, Tülüce K, Çil Z, Emren SV, Akyıldız Zİ, Ergene O. Galectin-3 levels in patients with hypertrophic cardiomyopathy and its relationship with left ventricular mass index and function. Anatol J Cardiol. 2016;16(5):344-8. doi: 10.5152/AnatolJCardiol.2015.6191.
21. de Boer RA, Edelmann F, Cohen-Solal A, Mamas MA, Maisel A, Pieske B. Galectin-3 in heart failure with preserved ejection fraction. Eur J Heart Fail. 2013;15(10):1095-101. doi: 10.1093/eurjhf/hft077.
22. Pugliese G, Iacobini C, Ricci C, Blasetti Fantauzzi C, Menini S. Galectin-3 in diabetic patients. Clin Chem Lab Med. 2014;52(10):1413-23. doi: 10.1515/cclm-2014-0187.
23. Seferovic JP, Lalic NM, Floridi F, Tesic M, Seferovic PM, Giga V, et al. Structural myocardial alterations in diabetes and hypertension: the role of galectin-3. Clin Chem Lab Med. 2014;52(10):1499-505. doi: 10.1515/cclm-2014-0265.
24. Tan KCB, Cheung CL, Lee ACH, Lam JKY, Wong Y, Shiu SWM. Galectin-3 is independently associated with progression of nephropathy in type 2 diabetes mellitus. Diabetologia. 2018;61(5):1212-1219. doi: 10.1007/s00125-018-4552-z.
25. Weigert J, Neumeier M, Wanninger J, Bauer S, Farkas S, Scherer MN, et al. Serum galectin-3 is elevated in obesity and negatively correlates with glycosylated hemoglobin in type 2 diabetes. J Clin Endocrinol Metab. 2010;95(3):1404-11. doi: 10.1210/jc.2009-1619
26. Li P, Liu S, Lu M, Bandyopadhyay G, Oh D, Imamura T, et al. Hematopoietic-Derived Galectin-3 Causes Cellular and Systemic Insulin Resistance. Cell. 2016;167(4):973-984.e12. doi: 10.1016/j.cell.2016.10.025.
27. Johnson AMF, Hou S, Li P. Inflammation and insulin resistance: New targets encourage new thinking: Galectin-3 and LTB4 are pro-inflammatory molecules that can be targeted to restore insulin sensitivity. Bioessays. 2017;39(9):10.1002/bies.201700036. doi: 10.1002/bies.201700036.
28. Pang J, Rhodes DH, Pini M, Akasheh RT, Castellanos KJ, Cabay RJ, et al. Increased adiposity, dysregulated glucose metabolism and systemic inflammation in Galectin-3 KO mice. PLoS One. 2013;8(2):e57915. doi: 10.1371/journal.pone.0057915.
29. Iacobini C, Menini S, Ricci C, Scipioni A, Sansoni V, Cordone S, et al. Accelerated lipid-induced atherogenesis in galectin-3-deficient mice: role of lipoxidation via receptor-mediated mechanisms. Arterioscler Thromb Vasc Biol. 2009;29(6):831-6. doi: 10.1161/ATVBAHA.109.186791.
30. Tsai TH, Sung PH, Chang LT, Sun CK, Yeh KH, Chung SY, et al. Value and level of galectin-3 in acute myocardial infarction patients undergoing primary percutaneous coronary intervention. J Atheroscler Thromb. 2012;19(12):1073-82. doi: 10.5551/jat.12856.
31. Gullestad L, Ueland T, Kjekshus J, Nymo SH, Hulthe J, Muntendam P, et al. The predictive value of galectin-3 for mortality and cardiovascular events in the Controlled Rosuvastatin Multinational Trial in Heart Failure (CORONA). Am Heart J. 2012;164(6):878-83. doi: 10.1016/j.ahj.2012.08.021.
32. Falcone C, Lucibello S, Mazzucchelli I, Bozzini S, D'Angelo A, Schirinzi S, et al. Galectin-3 plasma levels and coronary artery disease: a new possible biomarker of acute coronary syndrome. Int J Immunopathol Pharmacol. 2011;24(4):905-13. doi: 10.1177/039463201102400409.
33. Menini S, Iacobini C, Ricci C, Blasetti Fantauzzi C, Salvi L, Pesce CM, et al. The galectin-3/RAGE dyad modulates vascular osteogenesis in atherosclerosis. Cardiovasc Res. 2013;100(3):472-80. doi: 10.1093/cvr/cvt206.
34. Mayr A, Klug G, Mair J, Streil K, Harrasser B, Feistritzer HJ, et al. Galectin-3: relation to infarct scar and left ventricular function after myocardial infarction. Int J Cardiol. 2013;163(3):335-337. doi: 10.1016/j.ijcard.2012.06.087.
35. Gao Z, Liu Z, Wang R, Zheng Y, Li H, Yang L. Galectin-3 Is a Potential Mediator for Atherosclerosis. J Immunol Res. 2020;2020:5284728. doi: 10.1155/2020/5284728.
36. Winter MP, Wiesbauer F, Alimohammadi A, Blessberger H, Pavo N, Schillinger M, et al. Soluble galectin-3 is associated with premature myocardial infarction. Eur J Clin Invest. 2016;46(5):386-91. doi: 10.1111/eci.12605.
37. Aksan G, Gedikli Ö, Keskin K, Nar G, İnci S, Yıldız SS, et al. Is galectin-3 a biomarker, a player-or both-in the presence of coronary atherosclerosis? J Investig Med. 2016;64(3):764-70. doi: 10.1136/jim-2015-000041.
38. Gleissner CA, Erbel C, Linden F, Domschke G, Akhavanpoor M, Doesch AO, et al. Galectin-3 binding protein plasma levels are associated with long-term mortality in coronary artery disease independent of plaque morphology. Atherosclerosis. 2016;251:94-100. doi: 10.1016/j.atherosclerosis.2016.06.002.
39. Ho JE, Yin X, Levy D, Vasan RS, Magnani JW, Ellinor PT, et al. Galectin 3 and incident atrial fibrillation in the community. Am Heart J. 2014;167(5):729-34.e1. doi: 10.1016/j.ahj.2014.02.009.
40. Sonmez O, Ertem FU, Vatankulu MA, Erdogan E, Tasal A, Kucukbuzcu S, et al. Novel fibro-inflammation markers in assessing left atrial remodeling in non-valvular atrial fibrillation. Med Sci Monit. 2014;20:463-70. doi: 10.12659/MSM.890635.
41. Gurses KM, Yalcin MU, Kocyigit D, Canpinar H, Evranos B, Yorgun H, et al. Effects of persistent atrial fibrillation on serum galectin-3 levels. Am J Cardiol. 2015;115(5):647-51. doi: 10.1016/j.amjcard.2014.12.021.
42. Kocyigit D, Gurses KM, Yalcin MU, Canpinar H, Canpolat U, Evranos B, et al. Serum galectin-3 level as a marker of thrombogenicity in atrial fibrillation. J Clin Lab Anal. 2017;31(6):22120. doi: 10.1002/jcla.22120.
43. Clementy N, Benhenda N, Piver E, Pierre B, Bernard A, Fauchier L, et al. Serum Galectin-3 Levels Predict Recurrences after Ablation of Atrial Fibrillation. Sci Rep. 2016;6:34357. doi: 10.1038/srep34357.
44. Clementy N, Piver E, Bisson A, Andre C, Bernard A, Pierre B, et al. Galectin-3 in Atrial Fibrillation: Mechanisms and Therapeutic Implications. Int J Mol Sci. 2018;19(4):976. doi: 10.3390/ijms19040976.
45. Numano F, Shimizu C, Jimenez-Fernandez S, Vejar M, Oharaseki T, Takahashi K, et al. Galectin-3 is a marker of myocardial and vascular fibrosis in Kawasaki disease patients with giant aneurysms. Int J Cardiol. 2015;201:429-37. doi: 10.1016/j.ijcard.2015.07.063.

This paper has been checked for language accuracy by JOSAM editors.
The National Library of Medicine (NLM) citation style guide has been used in this paper.

J Surg Med. 2021;5(12):1221-1223.
DOI: 10.28982/josam.981762

Journal of Surgery and Medicine

Closed reduction with external fixation and percutaneous screwing in talus neck fractures with severe soft tissue edema: A case report

Emre Teksan [1], Sercan Karadeniz [2]

[1] Giresun University, Prof. Dr. Ilhan Ozdemir Training and Research Hospital, Department of Orthopedic and Traumatology, Giresun, Turkey
[2] Bulancak State Hospital, Department of Orthopedic and Traumatology, Giresun, Turkey

ORCID ID of the author(s)

ET: 0000-0001-9389-504X
SK: 0000-0003-2802-4816

Abstract

We herein report a patient with a Hawkins type 3 talus neck fracture because of a traffic accident. A 21-year-old male patient had excessive soft tissue edema in his ankle and suspicious COVID-19 findings in thorax chest computed tomography. Therefore, spinal anesthesia was administered to the patient for the operation, in addition to intravenous midazolam for sedation. Under external fixation, the ankle joint was distracted, and the fracture was reduced. The fracture was fixed percutaneously with two cannulated screws. The operation was completed with two one-centimeter incisions. There was no postoperative edema. The patient was discharged with an external fixator one day later. Percutaneous screwing after closed reduction with external fixation can be a successful method in patients with soft tissue edema.

Keywords: Talus neck fracture, Covid-19, Percutaneous screw

Introduction

Talus plays a key role in a significant part of foot and ankle movements. However, intraosseous blood supply is insufficient in the talus, which is fed by the tibialis posterior and peroneal arteries extraosseously [1, 2]. The blood supply of this bone is significantly affected by the fracture displacement ratio and the dislocation of the subtalar-navicular joint [3, 4].

Talus neck fractures are uncommon and are mostly caused by high-energy trauma. Soft tissue lesions, other bone fractures and life-threatening injuries may accompany this condition [5]. Diagnosis is usually made with AP and lateral x-rays. Computed tomography (CT) can also be used to better understand the presence of other accompanying bone pathologies and fracture morphology.

The treatment of talus neck fracture is one of the orthopedic emergencies. While casting may be sufficient in type 1 fractures that are not displaced, fixation with compression screws after open reduction is required in types 2, 3, and 4.

Due to the presence of severe ankle edema in our case, closed reduction and percutaneous screwing were preferred.

Corresponding Author
Emre Teksan
Giresun University, Prof. Dr. Ilhan Ozdemir Training and Research Hospital, Department of Orthopedic and Traumatology, Giresun, Turkey
E-mail: emreteksan@yahoo.com

Informed Consent
The authors stated that the written consent was obtained from the patient presented with images in the study.

Conflict of Interest
No conflict of interest was declared by the authors.

Financial Disclosure
The authors declared that this study has received no financial support.

Published
2021 November 15

How to cite: Teksan E, Karadeniz S. Closed reduction with external fixation and percutaneous screwing in talus neck fractures with severe soft tissue edema: A case report. J Surg Med. 2021;5(12):1221-1223.

Case presentation

A 21-year-old male patient was brought into the emergency department after an in-vehicle traffic accident. His left ankle was tender, painful, and edematous. There was pain in the left hip upon examination. Trauma series and chest tomography were obtained. Radiographs showed a left Hawkins type 3 talus neck fracture and a non-displaced fracture posterior to the left acetabulum (Figure 1). The ankle was splinted and elevated after an immediate closed reduction. The patient was admitted to the Covid hospital for surgery after his lung tomography revealed suspicious Covid-19 findings.

Because the patient was suspected of having Covid-19, it was decided to give him spinal anesthesia. Closed reduction and percutaneous pinning were aimed due to excessive edema in the ankle. A triangular system external fixator was placed with two screws, one on the proximal tibia and one on the calcaneus distally. The distal screw was locked. The proximal one was released, and straight traction was performed by holding the distal screws. Meanwhile, intravenous midazolam was administered by the anesthesiologist for muscle relaxation to aid the reduction. After a strong straight traction, the proximal gears were locked so that the ankle remained in distraction. The proximal screws were locked after a strong straight traction to keep the ankle distracted. Following foot dorsiflexion, reduction was completed by pressing from the medial side with plantar flexion. Fluoroscopy control confirmed that the fracture was completely reduced. Following that, two mini-incisions were made from the distal, lateral and medial parts anterior to the talus, and guide k wires were placed under fluoroscopy. The fracture was fixed with two 5.0 headless compression screws (Figure 2, 3, 4). Then the distraction of the external fixator was neutralized, but the fixator was not removed for soft tissue healing (Figure 5). He was discharged on the first postoperative day. There was no additional edema. Informed consent was obtained from the patient's family for scientific presentation.

Figure 1: Preoperative lateral ankle x-ray shows a Hawkins type 3 talus fracture (arrow)

Figure 2: Postoperative lateral x-ray shows two cannulated screws

Figure 3: Postoperative antero-posterior X-ray

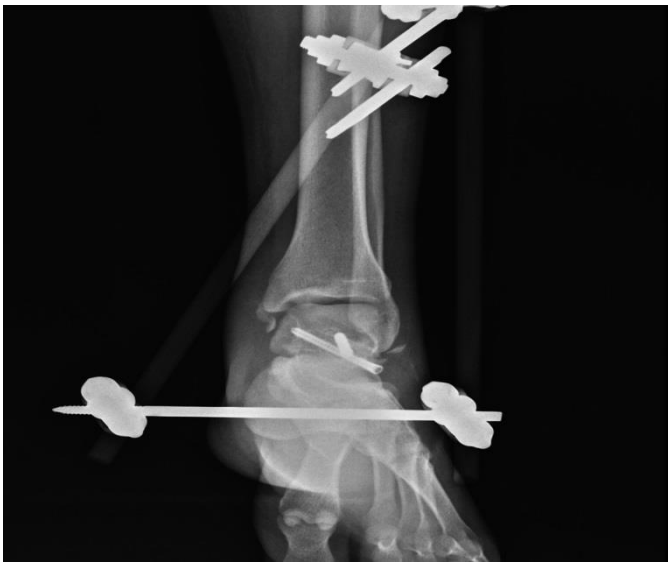

Figure 4: Postoperative CT scan sequence shows the joint

Figure 5: 15th day after the operation. Ankle before the removal of the external fixator

Discussion

Talus neck fractures usually occur as a result of axial loading while the foot is in dorsiflexion [6, 7]. This mechanism was classified by Hawkins according to the degree of displacement of the fractures.

Hawkins [7] published the surgical results of 57 talus fractures in 55 cases in his study in 1970. Avascular necrosis (AVN) did not develop in non-displaced fractures (type 1) and all fractures united without problems. In type 2 fractures with subtalar joint dislocation, nonunion was not observed, but AVN was observed at a rate of 42%. In type 3 fractures accompanied by both subtalar and tibiotalar joint dislocations, the rates of nonunion and AVN were 11% and 91%, respectively. Due to the high rates of nonunion and AVN, the treatment of talus neck fractures should be performed urgently, and anatomic fixation should be aimed to the best.

Canale and Kelly [8] evaluated 71 talus neck fractures clinically and radiologically in 70 patients followed for a mean of 12.7 years. In this study, cases with type 1 fracture with AVN were also reported, but the clinical results of these cases were evaluated as very good. In type 3 fractures, the clinical outcome was closely related to the reduction of the subtalar dislocation and fractured fragments. Based on this, the main goals must be to evaluate all talus neck fractures carefully, avoid leaving subluxated joints after the operation, and ensure that all fracture parts have as much anatomical alignment as possible. It should also be kept in mind that clinical results may be good following fracture union, independent of AVN.

No matter how perfect the fracture fixation is, the accompanying soft tissue lesion can always bring along progressive additional problems. Due to the advanced soft tissue edema in our case, we performed a closed reduction by the percutaneous pinning technique, which is not actually preferred in type 3 fractures. Sherif Mohamed Abdelgaid and Farid Fouad Ezzat [5] reduced 16 talus neck fractures, mostly type 2 and 3, with a t-handle in 2012, then reported an 87% success rate with percutaneous screwing. We performed this reduction with an external fixator, which we believe allows to approach the broken talus fragments and soft tissue more carefully. However, we think that extensive case series are needed to comment on the results.

While general anesthesia is preferred in such cases, in patients with suspected Covid-19 infection, spinal anesthesia and a sedative agent may be sufficient for the surgeon to achieve closed reduction. The fractures of the talus neck may highly likely develop AVN, and urgent intervention is required. Therefore, the recovery of soft tissue edema should not be waited. Closed reduction with an external fixator and percutaneous pinning may be an alternative to open reduction in ankles with soft tissue problems in talus neck fractures. In addition, we think that the external fixator we placed may contribute to soft tissue healing.

References

1. Murphy GA. Fractures and dislocations of the foot. Champbell‘s Operative Orthopaedics 2003; pp. 1136-1138.
2. Sean EN, David PB. Orthopaedic Knowledge Update 9, AAOS, 2008; p : 499-502.
3. Inokuchi S, Ogawa K, Usami N, Hashimoto T. Long-term follow up of talus fractures. Orthopedics. 1996;19:477-81.
4. Pajenda G, Vécsei V, Reddy B, Heinz T. Treatment of talar neck fractures: clinical results of 50 patients. J Foot Ankle Surg. 2000;39:365-75.
5. Abdelgaid SM, Ezzat FF. Percutaneous reduction and screw fixation of fracture neck talus. Foot Ankle Surg. 2012;18(4):219-28.
6. Smith NP, Ziran BH. Fractures of the talus. Operative Techniques Orthopaedics. 1999;9:229-38.
7. Hawkins LG. Fractures of the neck of the talus. J Bone Joint Surg [Am]. 1970;52:991-1002.
8. Canale ST, Kelly FB Jr. Fractures of the neck of the talus. Long-term evaluation of seventy-one cases. J Bone Joint Surg [Am]. 1978;60:143-56.

This paper has been checked for language accuracy by JOSAM editors.
The National Library of Medicine (NLM) citation style guide has been used in this paper.

J Surg Med. 2021;5(12):1224-1226.
DOI: 10.28982/josam.947606

Journal of Surgery and Medicine

Phalloplasty – Sensate radial forearm free flap for creation of neourethra and neophallus in gender affirmation surgery: A case report

George Taliat [1], Kumaraswamy Mohan Kumar [1], Arjun Nagaraj [2]

[1] Department of Plastic Surgery, MS Ramaiah Hospital, Bangalore, India
[2] Department of Urology, MS Ramaiah Hospital, Bangalore, India

ORCID ID of the author(s)

GT: 0000-0002-9152-8358
KMK: 0000-0003-3039-9350
AN: 0000-0002-5573-0065

Corresponding Author
George Taliat
Department of Plastic Surgery, MS Ramaiah Medical College Hospital MSR Nagar, 80 feet Road, Bengaluru, India
E-mail: georgetaliat@gmail.com

Informed Consent
The authors stated that written consent was taken from the patient for the procedure and publication of data including clinical photographs

Conflict of Interest
No conflict of interest was declared by the authors.

Financial Disclosure
The authors declared that this study has received no financial support.

Published
2021 December 23

Abstract

With an increase in gender affirmation surgery requirements, it is imperative to understand the procedure for phalloplasty. The Radial Forearm Free Flap is one of the most commonly used flaps for the same. We present this case of a 29-year-old patient who underwent phalloplasty by means of a radial artery forearm free flap. Surgical technique has been described including flap design, harvest, recipient site preparation, anastomosis of vessels and nerves, and post-operative care. The patient developed a small area of partial necrosis which was the dorsoulnar border of the flap. The rest of the neophallus and neourethra were viable, sensate and the patient was able to void urine through the neourethra while standing. The radial forearm free flap is a good option for phalloplasty in gender affirmation surgeries. However, surgeons need to be wary of the possibility of necrosis of the dorsoulnar aspect which may be exceeding the radial artery territory.

Keywords: Phalloplasty, Gender affirmation surgery, Radial forearm flap, Neophallus, Penile reconstruction

Introduction

The radial forearm free flap (RFFF) originated in 1978 in China and was developed and reported to the rest of the world by Ruyao Song [1]. It was used for construction of penis in transgenders by Biemer [2] in the early 1980s who fabricated skin graft within the flap for the neourethra. Chang and Hwang [3] reported tube within a tube by folding the flap in order to for a vascularized neourethra within the neophallus in 1984. With a growing number of requests for gender affirmation surgery, it is imperative to understand the intricacies of the same. The aim of phalloplasty is to construct an aesthetically acceptable neophallus, ability to void urine while standing, tactile and erogenous sensation and rigidity sufficient for sexual activity [4]. The RFFF is considered a good option as it can achieve these goals. For these reasons, we chose the RFFF with certain modifications for our case. Several modifications have been made to the flap design as described by Chang [5]. We have fashioned it with a centrally placed urethra with distal extension to create a neoglans. Including coaptation of sensory nerve would also provide good tactile and erogenous sensation.

How to cite: Taliat G, Kumar KM, Nagaraj A. Phalloplasty – Sensate radial forearm free flap for creation of neourethra and neophallus in gender affirmation surgery: A case report. J Surg Med. 2021;5(12):1224-1226.

Case presentation

A 29-year-old patient presented after appropriate evaluation and therapy as per guidelines by World Professional Association for Transgender health [6]. Allens test was done to confirm patency of ulnar artery. Written consent was taken from the patient for the procedure and publication of data including clinical photographs. Patient underwent general anesthesia. Simultaneous vaginal hysterectomy was done. Flap was marked with maximum dimensions being 18x14 cm. The distal incision was performed first and the radial artery and cephalic vein were identified and they were ligated and divided distally after confirming patency of ulnar artery. Tourniquet was applied. Around the centrally planned neourethra 1 cm of skin was de-epithelialized on either side (Figure 1).

Flap incisions was harvested suprafascially taking care to include the cephalic vein, basilic vein, the lateral and medial antebrachial cutaneous nerve. Radial artery and its venae comitantes were included in the flap all along its length including the proximal communicating vessel between the cephalic vein and the venae comitantes. A 12 french foleys catheter was placed on the central portion of the flap and was wrapped by the flap by suturing the de-epithelized portions onto each other in multiple layers forming a tube in tube technique of phallus (Figure 2).

The rest of the flap was then wrapped around itself to create a neophallus. The distal portion of the flap was incised and folded on itself to fashion a neoglans and sutures placed to itself to create a corona. The neophallus is left on the forearm while being perfused by the vascular pedicle until it is ready for transfer (Figure 3).

Figure 1: Flap marked, incised, area around central urethra de-epithelized and raised

Figure 2: Central neourethra creation (tube in tube) with catheter in situ

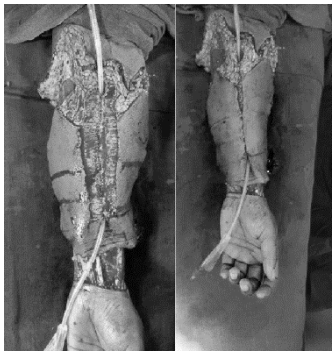

Figure 3: Flap wrapped to form neophallus and distal portion fashioned to neoglans

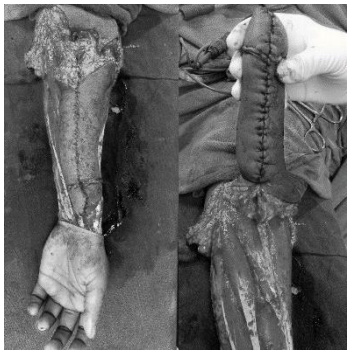

M shaped incision was made over the labia majora and displaced inferiorly. An incision was made on the left thigh and femoral artery and vein identified. The long saphenous vein was dissected and divided at 20 cm distal to its attachment to femoral vein. A temporary A-V Loop fistula was created by anastomosing the bisected part of the saphenous vein to the superficial femoral artery in an end to side manner.

After ligating and dividing the pedicle, the neophallus was detached and brought to recipient site. Urethral anastomosis was done between native and neourethra with the catheter in situ. The sapheno-femoral AV loop was divided and anastomosed to radial artery and cephalic vein respectively to arterial and venous limbs with microvascular technique. Basilic vein was anastamosed to a tributary of saphenous vein (Figure 4).

Figure 4: Arterial and venous anastomosis

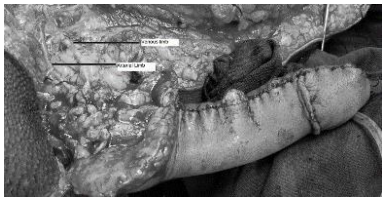

The left ilioinguinal nerve was coapted with the lateral antebrachial cutaneous nerve. The clitoris was de-epithelized and placed at the root of the neophallus. The flap inset was completed and the vagina closed (Figure 5).

The forearm donor site was covered with skin graft. Drain was placed in the left thigh and dressing was done using cylindrical saline bottle to support the neophallus (Figure 6).

Figure 5: Flap inset completed

Figure 6: Dressing of neophallus

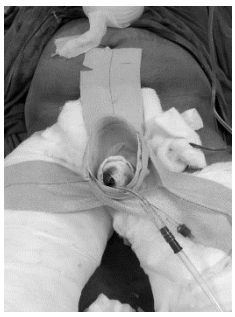

Post-operative care

The flap was monitored regularly. Small portion of skin that was the dorso-ulnar aspect of forearm was found to undergo necrosis (Figure 7). Hence patient was taken up for debridement of that portion and secondary suturing was done after 14 days (Figure 8). At 1 month follow up, the neophallus was intact and a retrograde urethrogram was done which showed a patent urethral anastomosis and catheter was removed. Patient was able to void urine through the neourethra. Erogenous sensation was present at the root of neophallus. Gross tactile sensation was gained at 4 months postoperatively. The planning for penile prosthesis was discussed with the patient to be done at a later stage.

Figure 7: Partial necrosis of dorsoulnar portion of flap

Figure 8: One month postoperatively after debridement and secondary suturing

Discussion

Patient prsented to plastic surgery department as a biological female after hormone therapy and psychological consultations for penile construction and the authors chose RFFF for the same. The RFFF has been used for penile reconstruction with several modifications added later on. It has been divided into two stages with phalloplasty and urethroplasty separately [7]. The neourethra has also been fashioned by pre lamination with skin graft and catheter to the forearm [8]. This may in authors opinion cause ulceration and stenosis. We folded the flap on itself to form neourethra provides a well vascularized neourethra. Nerve coaptation of has provided tactile and erogenous sensation in the neophallus up to 98.4% and 71.4% respectively according to a review done by Morrison et al. [9]. In our case, tactile sensation was achieved with the lateral antebrachial cutaneous nerve coapted to the ilioinguinal nerve. The dorsal clitoral nerve could not be identified hence the clitoral skin was de-epithelized and placed at the root of penis which would provide erogenous sensation upon its stimulation. Common complications that can occur in the procedure are partial necrosis, urethrocutaneous fistula and urethral stenosis [10]. We encountered partial necrosis at the dorsoulnar aspect which was excised and secondary suturing was done. Hence it is in authors opinion to conduct further studies to estimate the exact extent of radial artery territory for this flap which may exclude the dorsoulnar border.

Conclusion

With increasing number of transgender patients requesting for gender affirmation surgery, it is vital to understand intricacies of phalloplasty. Among the various options we believe the radial artery forearm free flap is a good option as was demonstrated in our case report where creation of a viable, sensate neophallus and neourethra was possible with this flap. However extent of radial artery territory may require exclusion of the dorsoulnar border.

References

1. Song R, Gao Y, Song Y, et al. The forearm flap. Clin Plast Surg. 1982;9:21.
2. Biemer E. Penile construction by the radial arm flap. Clin Plast Surg. 1988;15:425.
3. Chang T-S, Hwang WY. Forearm flap in one-stage reconstruction of the penis. Plast Reconstr Surg. 1984;74:251.
4. Kim S, Dennis M, Holland J, Terrell M, Loukas M, Schober J. The Anatomy of forearm free flap phalloplasty for transgender surgery. Clinical Anatomy. 2018;31:145-51
5. Gottlieb LJ, Levine LA. A new design for the radial forearm free flap phallic construction. Plast Reconstr Surg. 1993;92:276.
6. Lawrence A. editor. The Harry Benjamin International Gender Dysphoria Association's Standards Of Care For Gender Identity Disorders, Sixth Version. [Internet]. World Professional Association For Transgender Health. Available from: http://wpath.org/Documents2/socv6.pdf [cited 2009 Apr16].
7. Garcia MM, Christopher NA, De Luca F, Spilotros M, Ralph DJ. Overall satisfaction, sexual function, and the durability of neophallus dimensions following staged female to male genital gender confirming surgery: The institute of urology, London U.K. experience. Transl Androl Urol. 2014;3:156–62.
8. Song C, Wong M, Wong CH, Ong YS. Modifications of the radial forearm flap phalloplasty for female-to-male gender reassignment. J Reconstr Microsurg. 2011;27:115–20.
9. Morrison SD, Shakir A, Vyas KS, Kirby J, Crane CN, Lee GK. Phalloplasty: A review of techniques and outcomes. Plast Reconstr Surg. 2016;138:594–615.
10. Trombetta C, Liguori G. Management of gender dysphoria: A multidisciplinary approach. Italia: Springer. 2015; p. 249–256

This paper has been checked for language accuracy by JOSAM editors.
The National Library of Medicine (NLM) citation style guide has been used in this paper.

J Surg Med. 2021;5(12):1227-1229.
DOI: 10.28982/josam.871142

Journal of Surgery and Medicine

Intravenous regional anesthesia (IVRA) with forearm tourniquet for short-term hand surgery: A case report

Ergun Mendes [1], Mehmet Cesur [2], Elzem Sen [2], Huseyin Gocergil [1]

[1] Anesthesiology and Reanimation, Kilis State Hospital, Kilis, Turkey
[2] Department of Anesthesiology and Reanimation, School of Medicine, Sahinbey Research and Education Center, Gaziantep University, Gaziantep, Turkey

ORCID ID of the author(s)
EM: 0000-0003-4350-6055
MC: 0000-0002-7482-6353
ES: 0000-0003-3001-7324
HG: 0000-0001-5265-6405

Corresponding Author
Ergun Mendes
Kilis State Hospital, Kilis, Turkey
E-mail: erg.mendes@gmail.com

Informed Consent
The authors stated that written consent was taken from the patient for the procedure and publication of data including clinical photographs

Conflict of Interest
No conflict of interest was declared by the authors.

Financial Disclosure
The authors declared that this study has received no financial support.

Published
2021 December 25

Abstract

Intravenous Regional Anesthesia (IVRA) was modified many times since its first use and these changes continue according to the type of surgery. A 36-year-old male patient was operated for trigger finger in the fascia of the first and second carpal bones. Because of the short operation time and for early detection of possible vascular or nerve damage after surgery, the IVRA method was used with the forearm tourniquet containing contrast agent. Forearm tourniquet can be preferred in short-term hand surgeries due to its advantages such as easy application, low side effect profile and early block recovery.

Keywords: IVRA, Forearm tourniquet, Contrast agent, Intraosseous passage, Local anesthetic toxicity

Introduction

The type of anesthesia achieved by adding a local anesthetic agent to the venous system of the extremity isolated from the general circulation using a tourniquet is called Intravenous Regional Anesthesia (IVRA). Although it was first used in 1908 by Karl August Bier for anesthesia of the area between two tourniquets, it is now used with the double-cuff tourniquet method, which is placed on the proximal part of the extremity after several modifications [1].

Because the use of local anesthetics is limited in the extremities, the aim of IVRA is to further reduce this area to cut the risk of toxicity in the case of a possible leak. Although tourniquet modification was used first in IVRA, this approach is no longer preferred due to toxicity concerns related to intraosseous leak. It is now reported that the use of a forearm tourniquet is as safe as the proximal tourniquet and that it can be reused in surgical practice [2].

In this case, we aimed to evaluate the adequacy of a reduced amount of local anesthetic using a forearm tourniquet for hand surgery and to detect a possible leak early.

How to cite: Mendes E, Cesur M, Sen E, Gocergil H. Intravenous regional anesthesia (IVRA) with forearm tourniquet for short-term hand surgery: A case report. J Surg Med. 2021;5(12):1227-1229.

Case presentation

After obtaining written consent for the procedure and future publishing, a 36-year-old and 96 kg ASA II male patient was operated on from the first and second carpal bone fascia for trigger finger. Because the patient did not want general anesthesia, regional approaches were given priority. The need for a tourniquet for a bloodless surgical field was determined by the surgical team. IVRA was preferred for early control of vascular and nerve injury after surgery. The use of IVRA with a forearm tourniquet was planned to reduce the amount of local anesthetic and for early tourniquet deflation. A contrast agent was added to the local anesthetic solution to detect possible leakage. The tourniquet was kept ready in the proximal region for early intervention in the case of a possible leak.

Electrocardiogram, saturation, and non-invasive blood pressure monitoring of the patient were performed in the supine position. Ringer's Lactate infusion was started at 10 mL/kg after a 20-gauge venous cannula was placed on the dorsum of the contralateral extremity. Midazolam was administered at 0.02 mg/kg for sedation. A single-cuff pneumatic tourniquet was placed on the proximal of the extremity to be operated on, and a 21-gauge venous cannula was inserted from the dorsum of the hand. A manually adjustable tension cuff was placed on the forearm 10 cm above the wrist. The cuff was inflated to 250 mmHg after the extremity was properly wrapped using the Esmarch bandage and elevated for two minutes. A local anesthetic mixture containing 5 mL contrast agent (iohexol 3mg/mL, Omnipaque, GE Healthcare, USA), 5 mL of 2% lidocaine and 10 mL of 0.9% NaCl was administered. Serial radiological images were obtained to determine the distribution of local anesthetics and possible leaks.

Radiological images of the patient after the local anesthetic injection revealed that the solution did not pass above the cuff. A distal movement of the solution was observed without any intraosseous leaks. Sensory and motor block were achieved in the 5th minute pin-prick test, and the surgical procedure began (Figures 1, 2).

Pain was monitored using the Visual Analogue Scale (VAS). The VAS score was 2 in the first five minutes. The patient, who did not have pain in the surgical incision area, felt discomfort due to the compression around the tourniquet, and this was evaluated as tourniquet discomfort. Tourniquet discomfort resolved after the addition of fentanyl (1 mcg/kg) in the 10th minute. The z-plasty incision was performed along the contracture band, corresponding to the natural palmar and digital folds. After the neurovascular structures were identified, restrictive fasciae were excised. The finger circulation and nerve innervation of the patient were checked after the tourniquet was deflated. The total tourniquet time was 35 minutes.

The patient was taken to PACU in the postoperative period and observed for one hour. He was hemodynamically stable and did not show any toxic symptoms. His postoperative VAS scores were less than 2, and rescue analgesics were not required.

Figure 1: Injection of the local anesthetic solution

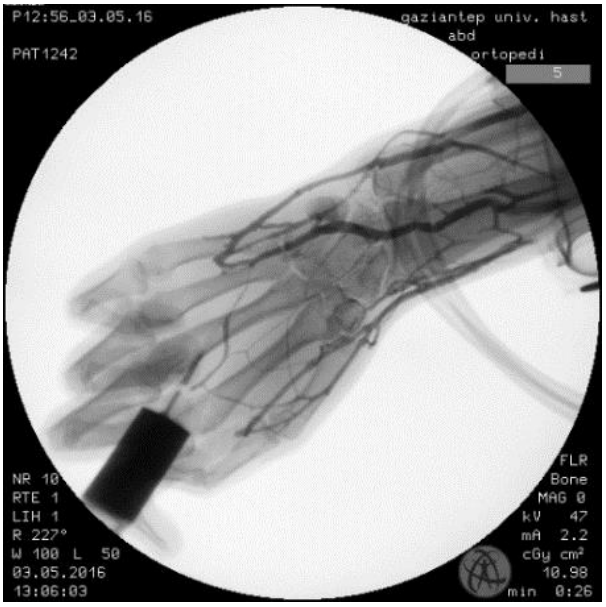

Figure 2: No intraosseous leak was observed

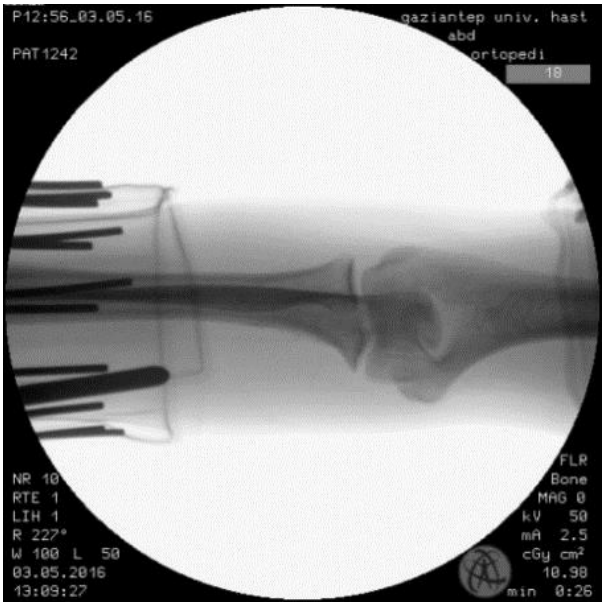

Discussion

IVRA is currently rarely preferred because of the increasing use of ultrasound-guided regional methods. Due to the long motor recovery time after peripheral nerve block, it is not preferred in the evaluation of possible nerve damage. However, it also has various advantages, such as easy application, a lower side effect profile and early block recovery time and can be a priority in cases such as the one presented [3].

The proximal double-cuff tourniquet method is the most widely used IVRA approach. To manage tourniquet pain, the distal cuff is inflated, and the proximal cuff is deflated [4]. More local anesthetic agents and sedo-analgesia are used after tourniquet pain develops; however, this approach may pose a risk in terms of early tourniquet deflation in distal region operations and short surgeries. Risks during surgery can be minimized by limiting the ischemic area and reducing the amount of local anesthetic with the forearm tourniquet even in the event of possible leakage [5].

The aim of this procedure was to reduce the amount of local anesthetic used with a forearm tourniquet, and leaks were assessed with a contrast agent. Tourniquet discomfort was

controlled with intravenous rescue analgesics. There was no leakage due to the use of the forearm tourniquet. There were no toxic symptoms.

Conclusion

IVRA can be optimized with alternative adaptations in extremity surgery. The forearm tourniquet can be preferred in short-term hand surgeries because it is easy to apply, has a low risk of toxicity and provides an early block recovery time.

References

1. Loser B, Petzoldt M, Loser A, Bacon DR, Goerig M. Intravenous Regional Anesthesia: A Historical Overview and Clinical Review. J Anesth Hist. 2019;5(3):99-108.
2. Cousins GR, Gill SL, Tinning CG, Johnson SM, Rickhuss PK. Arm versus forearm tourniquet for carpal tunnel decompression - Which is better? A randomized controlled trial. J Hand Surg Eur Vol. 2015;40(9):961-5.
3. Arslanian B, Mehrzad R, Kramer T, Kim DC. Forearm Bier block: a new regional anesthetic technique for upper extremity surgery. Ann Plast Surg. 2014;73(2):156-7.
4. Chiao FB, Chen J, Lesser JB, Resta-Flarer F, Bennett H. Single-cuff forearm tourniquet in intravenous regional anaesthesia results in less pain and fewer sedation requirements than upper arm tourniquet. Br J Anaesth. 2013;111(2):271-5.
5. Vaughn N, Rajan N, Darowish M. Intravenous Regional Anesthesia Using a Forearm Tourniquet: A Safe and Effective Technique for Outpatient Hand Procedures. Hand (NY). 2020;15(3):353-9.

This paper has been checked for language accuracy by JOSAM editors.
The National Library of Medicine (NLM) citation style guide has been used in this paper.

J Surg Med. 2021;5(12):1230-1232.
DOI: 10.28982/josam.919650

Journal of Surgery and Medicine

A rare cause of upper extremity deep venous thrombosis: Paget Schroetter syndrome

Fatih Erdem [1], Bahar Yanık [1], Bahadır Çağlar [2], Süha Serin [2], Erdoğan Bülbül [1]

[1] Department of Radiology, Balikesir University Research Hospital, Balikesir, Turkey
[2] Department of Emergency Medicine, Balikesir University Research Hospital, Balikesir, Turkey

ORCID ID of the author(s)
FE: 0000-0001-9228-2866
BY: 0000-0003-3358-7330
BÇ: 0000-0002-4164-393X
SS: 0000-0003-0654-8061
EB: 0000-0002-1136-9407

Corresponding Author
Fatih Erdem
Department of Radiology, Balikesir University Research Hospital, Balikesir, Turkey
E-mail: mdfatiherdem@gmail.com

Informed Consent
The authors stated that written consent was taken from the patient for the procedure and publication of data including clinical photographs

Conflict of Interest
No conflict of interest was declared by the authors.

Financial Disclosure
The authors declared that this study has received no financial support.

Published
2021 December 28

Abstract

Paget-Schroetter syndrome is a rare clinical entity, which is characterized by the thrombosis of the axillary and/or subclavian vein resulting from the activation of the coagulation cascade due to vigorous and repetitive activity of the arm and the external compression related microtrauma to the venous intima. The first imaging modality for diagnosis should be color Doppler ultrasonography. Thrombolysis and surgical decompression of the thoracic outlet are focused on relieving the external compression of the veins. In this case report, we aimed to present the greyscale ultrasonography and dynamic Doppler ultrasonography findings of a patient with upper extremity deep venous thrombosis.

Keywords: Paget-Schroetter Syndrome, Effort thrombosis, Color Doppler ultrasonography, Upper extremity deep venous thrombosis

Introduction

Paget-Schroetter syndrome (PSS) or ‘effort’ thrombosis is the thrombosis of the subclavian vein due to its compression at the thoracic outlet level by variation or deformities of adjacent anatomic structures with excessive physical activity in otherwise healthy individuals [1]. PSS corresponds to approximately 10-20% of all upper extremity deep venous thrombosis cases [2]. It is suggested that coagulation cascade activation, which is triggered by intimal microtrauma in the vein, is responsible for the pathogenesis of PSS [3]. Plain radiography, ultrasonography (US), color Doppler US (CDUS), computerized tomography (CT)/magnetic resonance imaging (MRI) venography, and catheter venography can be used for diagnosis [4].

In this case report, we aimed to present the US and dynamic CDUS findings of a 46-year-old female patient who was admitted to our emergency room with discoloration and swelling in the right arm and diagnosed with PSS.

How to cite: Erdem F, Yanık B, Çağlar B, Serin S, Bülbül E. A rare cause of upper extremity deep venous thrombosis: Paget Schroetter syndrome. J Surg Med. 2021;5(12):1230-1232.

Case presentation

A 46-year-old female patient with discoloration, swelling, and increasing pain in the right arm for 1 week was admitted to our emergency department. In her medical history, there were no related traumas, chronic diseases, no regular drug use such as oral contraceptives, and no history of insect bites. She had been working with repetitive and excessive arm movements in a chicken processing factory. In physical examination, slight blue-purple discoloration and edema were present in her dominant arm, forearm, and hand, compared to the contralateral one. The range of motion in her joints was normal. The peripheric pulses were normal in the neutral position. Her lab test results and posteroanterior chest radiography showed no clinical significance. Together with all those findings, CDUS was requested for the right arm to confirm the preliminary diagnosis of right upper extremity deep venous thrombosis. US and CDUS examinations were performed with a 6-12 MHz band range, linear, high-frequency transducer (Toshiba Aplio MX SSA-780A, Tokyo, Japan). In greyscale US examination, hypoechoic thrombus material filling the whole lumen of the right subclavian vein was observed and the vein was non-compressible. In color mode and spectral mode, no flow signal or recanalization finding was observed (Figure 1 a-b).

Figure 1 a-b: Color Doppler Ultrasonography (CDUS) examination showed hypoechoic, uncompressed thrombus and an absence of flow in the right subclavian vein lumen in the a-long axis and b-transverse plane.

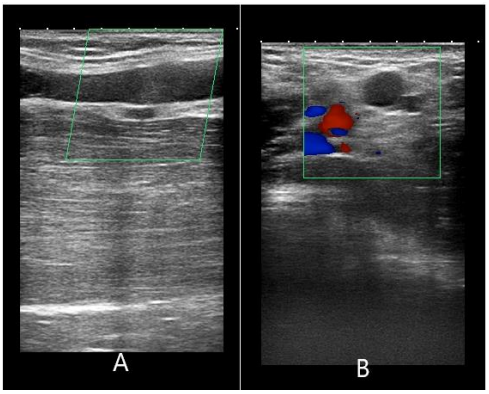

More distal veins showed mild dilatation and slow flow findings. The findings were consistent with acute/subacute thrombosis of the right subclavian vein. The patient was given anticoagulant medication and called for control evaluation 2 weeks later. Control examinations revealed that the blue-purple discoloration and edema in her right arm had regressed. Also, thrombus material had resolved and recanalized flow was observed in the neutral position in greyscale US and CDUS imaging. The recanalized flow ceased by dynamic CDUS examination, which was combined with Adson's test (the arm was abducted to the level of the head and the head was rotated to the contralateral side during deep inspiration). Because all those findings pointed to the external compression to the subclavian vein at the thoracic outlet, the diagnosis was venous thoracic outlet syndrome (TOS) (Figure 2 a-b). When the patient was questioned about the activities, such as hanging clothes or curtains, she stated that she had difficulties when performing activities that required raising her arm above her head. During the Adson maneuver, normal flow and the waveform of the right subclavian artery were gradually dampened then completely ceased (Figure 3 a-b). Hence, the patient also had arterial TOS apart from PSS. After anticoagulant treatment, the patient did not have any further examinations or surgical treatment during the pandemic. Written informed consent was obtained from the patient.

Figure 2 a-b: In the dynamic control examination of CDUS performed two weeks later, a-prominent recanalized flow in the subclavian vein was seen in the neutral position, especially in the posterior part of the lumen, b- cessation of the recanalized flow during the provocation test.

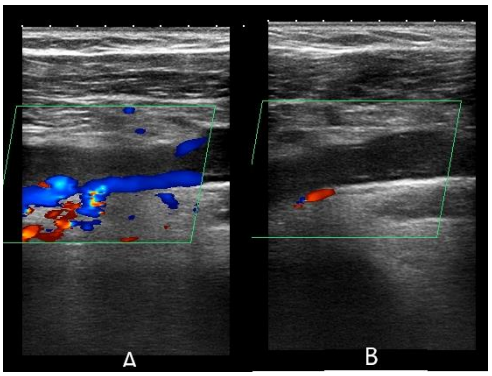

Figure 3 a-b: In dynamic CDUS examination, a- color mode and spectral mode in the neutral position showed normal flow velocity and waveform in the subclavian artery; b- color mode and spectral mode during the provocation test showed complete cessation of flow (blue arrow).

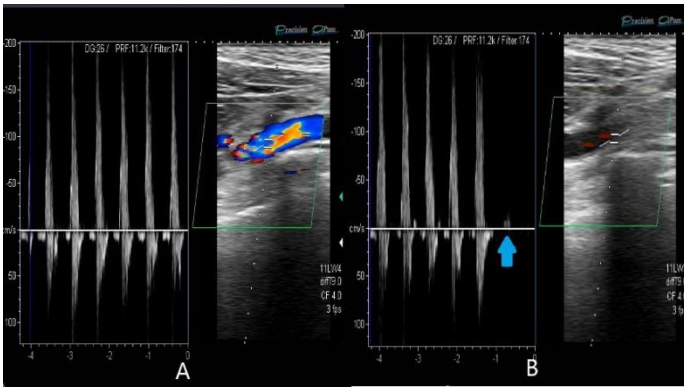

Discussion

This entity was first described by Paget in 1875 and Von Schroetter in 1884, and Hughes named it "PSS" in 1949 [1]. PSS is seen in approximately 2-11/100,000 people and constitutes 1-4% of all venous thrombosis [5,6]. In PSS, there is primary thrombus development without any traumatic injury that may cause secondary thrombosis in the subclavian vein or an iatrogenic cause such as a pacemaker, or central venous catheter insertion [3, 4]. Approximately 60-80% of PSS cases are due to excessive physical activity and are seen in the dominant arm. It is often seen in males, athletes, and in the 3rd decade of life. The entity, which is named "strain thrombosis", was thought to be related to dominant use; however, external compression can also contribute. For this reason, compression of vascular structures due to narrowing in the thoracic outlet region may also be one of the causes of PSS [4]. Microintimal trauma in the subclavian vein caused by excessive shoulder-arm movement and the external compression at the thoracic outlet level causes intimal hyperplasia and fibrosis in the connective tissue around the vein [7]. In recent years, studies reported a thrombophilia incidence in PSS patients, but there has been no consensus to screen these patients for hypercoagulability disorders [4,8]. In our case, because the patient had no family history or a similar history of thrombosis, no further investigation was conducted.

Vascular compressions may be caused by abnormal subclavius or anterior scalene muscles, cervical vertebrae with long transverse processes, cervical ribs, congenital fibromuscular bands, 1st rib deformations due to trauma, osteodegeneration, or narrow costoclavicular space [3, 4, 9]. External compression of the subclavian vein (venous thoracic outlet syndrome - venous TOS) in the thoracic outlet that may cause PSS is a rare condition with an annual incidence of 1/100,000 [3]. The clinical picture in which symptoms related to venous TOS is seen without evidence of thrombosis is called intermittent obstruction or McCleery's syndrome [4]. In this process, diagnosis and treatment with 1st rib resection or scalenectomy may prevent the formation of PSS. Clinically, it may be difficult to distinguish between McCleerly's syndrome and neurogenic TOS due to compression on the brachial plexus. Pain, numbness, and tingling are common symptoms in both entities [4]. CDUS and electromyography can be used to distinguish between the two. Our patient repeatedly used her arm due to her job, which may have triggered thrombus formation. Chest radiography of the patient allowed us to exclude possible bone pathologies. However, etiological factors related to soft tissues such as anomalies or hypertrophic changes in the muscle and ligament structures in this region might have triggered thrombus formation. Due to the pandemic period, this suspicion could not be confirmed by cross-sectional imaging methods, such as a CT or an MRI.

Clinical symptoms, blood tests, and radiological imaging methods should be evaluated together when diagnosing PSS. The clinical findings alone have a specificity of less than 50% [12, 13]. Since partial venous drainage will be provided, especially due to the collateral network that develops after a while, clinical findings regress, and diagnosis may be difficult [4]. Although the Plasma D dimer test is relatively highly sensitive, its specificity is very low as it can be increased in many inflammatory processes [14]. Bone anomalies or pathologies can be evaluated radiologically on cervical vertebrae or chest radiographs. With dynamic CDUS, CT venography, MRI venography, and catheter venography examinations combined with dynamic maneuvers, the exact location and degree of vascular compression can be revealed. Among them, CDUS stands out as the first choice because it is non-invasive, non-ionizing, inexpensive, and ubiquitous [6, 9]. Besides, as an advantage against CT and MRI, high false-negative results that may occur in the supine position can be avoided by performing the CDUS in a sitting position [10]. With dynamic CDUS examination, both the subclavian vein and subclavian artery can be examined in the same session. There are publications about both arterial and venous TOS association in the literature, reporting a rate of 13.7% [10, 11]. Different provocation tests can be performed during the examination. The most common one is the Adson test. A dynamic examination can also be performed with EAST (elevated arm stress test) or ULTT (upper limb tension test) [15]. With the dynamic CDUS examination performed during the test, the venous flow, which normally changes with respiration, is disrupted. Infraclavicular enlargement can be observed in the vein together with loss of respiratory changes, increased velocity due to narrowing of the vein, or complete cessation of flow [4, 10]. In detecting thrombosis in the subclavian vein, CDUS has a sensitivity of 78-100% and a specificity of 82-100% [6]. Although CT and MRI venography are expensive compared to CDUS examinations, they are alternative radiological imaging methods because they can give better anatomical details about the surrounding structures for the etiology of thrombosis. However, since this detail does not affect the initial treatment management for thrombosis, they are not the first choice of radiological imaging [14]. Catheter venography examination, on the other hand, is preferred in catheter thrombolytic treatment rather than in making the diagnosis because it is invasive and ionizing [10].

Conclusion

PSS is a rare, primary deep vein thrombosis of the upper extremity, which is more common in the young population and is caused by repetitive excessive arm activity and vascular compression. The diagnosis of PSS should be considered especially when there is no trauma to the subclavian vein or any iatrogenic procedures in the patient's history. CDUS examination is the imaging method that can detect thrombosis with high accuracy and should be the first choice in diagnosis. This method also gives an idea about the etiological factors because it is easily suitable for dynamic examination.

References

1. Sharma H, Tiwari A. Recurrent Upper Extremity Thrombosis Associated with Overactivity: A Case of Delayed Diagnosis of Paget-Schroetter Syndrome. Case Rep Vasc Med. 2017;2017:8764903. doi: 10.1155/2017/8764903. Epub 2017 Jul 10. PMID: 28775908; PMCID: PMC5523535.
2. Bernardi E, Pesavento R, Prandoni P. Upper extremity deep venous thrombosis. Semin Thromb Hemost. 2006 Oct;32(7):729-36. doi: 10.1055/s-2006-951458. PMID: 17024601.
3. Illig KA, Doyle AJ. A comprehensive review of Paget-Schroetter syndrome. J Vasc Surg. 2010 Jun;51(6):1538-47. doi: 10.1016/j.jvs.2009.12.022. Epub 2010 Mar 20. PMID: 20304578.
4. Moore R, Wei Lum Y. Venous thoracic outlet syndrome. Vasc Med. 2015 Apr;20(2):182-9. doi: 10.1177/1358863X14568704. PMID: 25832605.
5. Vijaysadan V, Zimmerman AM, Pajaro RE. Paget-Schroetter syndrome in the young and active. J Am Board Fam Pract. 2005 Jul-Aug;18(4):314-9. doi: 10.3122/jabfm.18.4.314. PMID: 15994479.
6. Butros SR, Liu R, Oliveira GR, Ganguli S, Kalva S. Venous compression syndromes: clinical features, imaging findings and management. Br J Radiol. 2013 Oct;86(1030):20130284. doi: 10.1259/bjr.20130284. Epub 2013 Aug 1. PMID: 23908347; PMCID: PMC3798333.
7. Aziz S, Straehley CJ, Whelan TJ Jr. Effort-related axillosubclavian vein thrombosis. A new theory of pathogenesis and a plea for direct surgical intervention. Am J Surg. 1986 Jul;152(1):57-61. doi: 10.1016/0002-9610(86)90141-8. PMID: 3728818.
8. Hendler MF, Meschengieser SS, Blanco AN, Alberto MF, Salviú MJ, Gennari L, et al. Primary upper-extremity deep vein thrombosis: high prevalence of thrombophilic defects. Am J Hematol. 2004 Aug;76(4):330-7. doi: 10.1002/ajh.20131. PMID: 15282664.
9. Mall NA, Van Thiel GS, Heard WM, Paletta GA, Bush-Joseph C, Bach BR Jr. Paget-schroetter syndrome: a review of effort thrombosis of the upper extremity from a sports medicine perspective. Sports Health. 2013 Jul;5(4):353-6. doi: 10.1177/1941738112470911. PMID: 24459553; PMCID: PMC3899898.
10. Baz AA. An overview of the findings of dynamic upper limbs' arterial and venous duplex in cases of vascular thoracic outlet syndrome. Egypt J Radiol Nucl Med 50, 76 (2019). doi: 10.1186/s43055-019-0100-1
11. Wadhwani R, Chaubal N, Sukthankar R, Shroff M, Agarwala S. Color Doppler and duplex sonography in 5 patients with thoracic outlet syndrome. J Ultrasound Med. 2001 Jul;20(7):795-801. doi: 10.7863/jum.2001.20.7.795. PMID: 11444739.
12. Alla VM, Natarajan N, Kaushik M, Warrier R, Nair CK. Paget-schroetter syndrome: review of pathogenesis and treatment of effort thrombosis. West J Emerg Med. 2010 Sep;11(4):358-62. PMID: 21079709; PMCID: PMC2967689.
13. Glavich G, Gourley J, Fong V. Paget-Schroetter syndrome with bilateral pulmonary emboli. Radiol Case Rep. 2017 Oct 31;13(1):28-31. doi: 10.1016/j.radcr.2017.10.006. PMID: 29552239; PMCID: PMC5851115.
14. Desjardins B, Rybicki FJ, Kim HS, Fan CM, Flamm SD, Gerhard-Herman MD, Kalva SP, Koss SA, Mansour MA, Mohler ER 3rd, Narra VR, Schenker MP, Tulchinsky M, Weiss C. ACR Appropriateness Criteria® Suspected upper extremity deep vein thrombosis. J Am Coll Radiol. 2012 Sep;9(9):613-9. doi: 10.1016/j.jacr.2012.05.021. PMID: 22954541.9:613-9;2012.
15. Jones MR, Prabhakar A, Viswanath O, Urits I, Green JB, Kendrick JB, et al. Thoracic Outlet Syndrome: A Comprehensive Review of Pathophysiology, Diagnosis, and Treatment. Pain Ther. 2019 Jun;8(1):5-18. doi: 10.1007/s40122-019-0124-2. Epub 2019 Apr 29. PMID: 31037504; PMCID: PMC6514035.

This paper has been checked for language accuracy by JOSAM editors.
The National Library of Medicine (NLM) citation style guide has been used in this paper.